Aerosol–Cloud–Precipitation Interactions

Edward Gryspeerdt

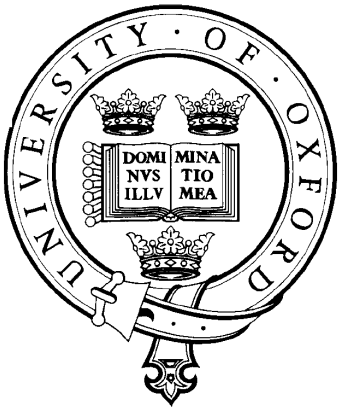

Submitted for the degree of Doctor of Philosophy in Physics
Michaelmas Term 2013

Atmospheric, Oceanic and Planetary Physics
Department of Physics
University of Oxford

Aerosol–Cloud–Precipitation Interactions

Edward Gryspeerdt, Linacre College
Submitted for the degree of Doctor of Philosophy in Physics, Michaelmas Term 2013

Abstract

Aerosols are thought to have a large effect on the climate, especially through their interactions with clouds. The magnitude and in some cases the sign of aerosol effects on cloud and precipitation are highly uncertain. Part of the uncertainty comes from the multiple competing effects that aerosols have been proposed to have on cloud properties. In addition, covariation of clouds and aerosol properties with changing meteorological conditions has the ability to generate spurious correlations between cloud and aerosol properties.

This work presents a new way to investigate aerosol-cloud-precipitation interactions while accounting for the influence of meteorology on cloud and aerosol. The clouds are separated into cloud regimes, which have similar retrieved cloud properties, to investigate the regime dependence of aerosol-cloud-precipitation interactions. The strong aerosol optical depth (AOD)- cloud fraction (CF) correlation is shown to have the ability to generate spurious correlations. The AOD-CF correlation is accounted for by investigating the frequency of transitions between cloud regimes in different aerosol environments. This time-dependent analysis is also extended to investigate the development of precipitation from each of the regimes as a function of their aerosol environment.

A modification of the regime transition frequencies consistent with an increase in stratocumulus persistence over ocean is found with increasing AI (aerosol index). Increases in transitions into the deep convective regime and in the precipitation rate consistent with an aerosol invigoration effect are also found over land. Comparisons to model output suggest that a large fraction of the observed effect on the stratocumulus persistence may be due to aerosol indirect effects. The model is not able to reproduce the observed effects on convective cloud, most likely due to the lack of parametrised effects of aerosol on convection. The magnitude of these effects is considerably smaller than correlations found by previous studies, emphasising the importance of meteorological covariation on observed aerosol-cloud-precipitation interactions.

Acknowledgements

I would like to thank the many people have helped with this work over the last few years. Philip Stier has been a brilliant supervisor and has provided a lot of useful guidence over my time in Oxford. Daniel Partridge and Nick Schutgens, have been incredibly helpful as advisors, reading over drafts at various stages during my studies. Natalie Weigum has been a great officemate, providing helpful advice throughout the last three years as well as reading a draft of this thesis. I would also like to thank the other occupants of 'the fridge', Bethan White and Steffen Lohrey, for putting up with me over the last three years. The occupants of the other office, Benjamin Grandey, Zak Kipling, Rosalind West and Sarah Taylor have also provided a lot assistance to my work, either through the running of models or general discussions about datasets. Thanks also to the members of the atmospheric science groups at the Max Planck Institute of Meteorology for making my stay so enjoyable, especially Bjorn Stevens and Louise Nuijens who organised my visit and were very helpful in deciphering some of my results.

I am very grateful for many lunches with Peter Watson, Hannah Arnold, James Sinclair and Lauren Fletcher - among others. They definitely made me more productive over the last three years. My family have also provided a lot of support, together with welcome breaks from work, which has been invaluable while writing this thesis. Finally, I am particularly grateful for the help and support Emma has given me over the last few years, without which this thesis would have taken much longer to complete.

Edward Gryspeerdt, October 2013, Oxford

‘There are perfectly logical explanations for everything that happened. The bonfire sent soot into the air which created rain, and with all the trees cut down a flood was inevitable.’

Lisa Simpson, The Simpsons.

Contents

Chapter 1

Introduction

1.1 Aerosols, precipitation and the climate system

Clouds and precipitation play vital roles in the earth's atmosphere, transporting water and energy in the atmosphere through evaporation and condensation. Clouds are important components of the earth's energy budget, cooling the planet by reflecting solar radiation and warming it by absorbing outgoing longwave radiation. Small changes in cloud or precipitation properties can have large effects on the climate.

The influence of atmospheric aerosols (small particulate matter) on cloud and precipitation, both inadvertent (Warner, 1968) and deliberate (Fleming, 2006) has been studied since the 1940s, with early experiments on the effects of aerosols on precipitation taking place in 1946 (Vonnegut, 1947). Subsequent experiments confirmed that pollution could also modify cloud properties - Gunn and Phillips (1957) showed that cloud droplets in polluted air are smaller than those in cleaner air. Further evidence for a pollution effect on clouds comes from studies of clouds over clean continental regions, which share similarities with clouds over clean oceanic regions. This suggests that it is pollution and not some other difference between continental and maritime environments which is important (Andreae et al., 2004).

It is difficult to quantify the effect of aerosols on clouds, and the effect of aerosols on precipitation is still disputed (Levin and Cotton, 2009). Whilst some modification of cloud properties by deliberate introduction of aerosols has been shown, the effect on total precipitation is still uncertain due to the difficulty of obtaining comparable data for clouds that have not had aerosols introduced

(National Research Council, 2003; Garstang et al., 2005). This often requires the use of larger scale statistical studies when looking at precipitation changes, but these studies can suffer from spurious correlations. These spurious correlations are generated by covariation of cloud and aerosol retrievals with meteorological properties - that is without aerosols causing a change in cloud properties (eg. Quaas et al., 2010).

Major uncertainties are also generated by difficulties in determining aerosol number concentration from space (Kapustin et al., 2006) and in the attribution of cause and effect. Due to the many feedbacks and possible pathways for aerosols to influence cloud systems, it can be difficult to determine the results of aerosol perturbations (Stevens and Feingold, 2009). Additionally, different cloud types are thought to respond in different ways to increased aerosol concentrations, which makes the quantification of separate effects difficult (Khain, 2009).

The main aim of this thesis is to gain an improved understanding of how aerosols affect cloud and precipitation. Due to the large influence of meteorological factors in generating spurious correlations between aerosol and cloud properties, accounting for meteorological factors forms an important part of this work. Satellite data and global models will be used to study these interactions and investigate how aerosols influence cloud and precipitation properties.

1.1.1 Aerosols

In the context of atmospheric sciences, aerosols are suspended particles which range in diameter from molecular clusters of approximately $\sim$1 nm to giant particles around 20 μm in diameter (Seinfeld and Pandis, 1998). The radiative imbalance at the top of the atmosphere, or radiative forcing, is a measure of how strongly an effect impacts the energy budget of the atmosphere. The forcing due to aerosol effects is thought to be the largest anthropogenic radiative forcing after greenhouse gases (Forster et al., 2007), although the uncertainty in the forcing from aerosols is much larger than that from greenhouse gases. Part of this uncertainty is due to the complexity of their interactions with clouds (Stevens and Feingold, 2009) and their short lifetime (Textor et al., 2006), which introduces large spatio-temporal inhomogeneities.

There are a variety of sources of atmospheric aerosols. Natural sources include sea spray forming sea salt (Gantt and Meskhidze, 2013), desert dust, and sulphates emitted by phytoplankton (Ayers and Gillet, 2000). Biogenic particles (e.g. bacteria, pollen and biological debris) are an important

source of natural aerosol (Schnell and Vali, 1976). Secondary organic aerosols (SOA), are formed by the condensation of organic vapours from primarily biogenic sources such as terpenes and isoprene (Henze and Seinfeld, 2006). SOA rarely forms directly; it usually forms by condensation onto pre-existing aerosol (Kerminen et al., 2000). Aerosols formed from biomass burning (vegetation fires and domestic biofuel use) contain a very large proportion of carbonaceous material, both organic carbon and 'soot-like' black carbon (Bond et al., 2013). There are also many anthropogenic sources of aerosols, such as sulphates, nitrates and other absorbing aerosols. These can come from similar sources to natural aerosols, although a large contribution to anthropogenic aerosol comes from the burning of fossil fuels. The sources of aerosols are such that aerosols are usually emitted into the troposphere, with the notable exception of aerosol generated by explosive volcanic eruptions, which can be directly injected into the stratosphere. The removal processes of aerosol in the troposphere are dominated by wet scavenging, giving them a mean lifetime of around one week (Textor et al., 2006).

Satellites retrieve a property known as aerosol optical depth (AOD), which is related to the column amount of aerosol. Is it unclear as to whether a global AOD trend exists (Zhao et al., 2008; Thomas et al., 2010), although regional trends may exist, particularly over India (Zhang and Reid, 2010; Krishna Moorthy et al., 2013). Satellite studies estimate the anthropogenic component of the current atmospheric aerosol at between 10 and 20% of the total AOD over ocean (Kaufman et al., 2005; Yu et al., 2009) although the uncertainty in the anthropogenic contribution is still high. For a more detailed summary of the differing species of aerosols and how the emissions of each have evolved with time, see Andreae and Rosenfeld (2008).

Aerosols have the ability to aid the condensation of water vapour when forming cloud droplets. These aerosols are known as cloud condensation nuclei (CCN), but not all aerosols are effective CCN. The classical Köhler theory describes the 'activation' of aerosol particles as CCN, emphasising the importance of particle size as an indication of droplet nucleating ability. Köhler theory predicts larger particles to be much more effective as CCN (Kohler, 1936). The size of aerosol particles has been shown to be a better predictor of nucleating ability than the chemistry (Dusek et al., 2006), although the chemistry and mixing state of the aerosols cannot be ignored (Roesler and Penner, 2010; Cappa et al., 2012).

Soluble and wettable particles are much more effective CCN than hydrophobic particles such as fresh soot (Pruppacher and Klett, 1978; Seinfeld and Pandis, 1998), although insoluble particles

may provide good ice nuclei (IN) (Hoose and Möhler, 2012). For example, desert dust is known to provide good IN (DeMott et al., 2003).

Aerosols are rarely found as a single type; for example the burning of fossil fuel often creates soot, but it also creates sulphates via sulphur dioxide from the burning of the sulphur in the fuel (Andreae and Rosenfeld, 2008). As noted earlier, organic vapours condensing onto aerosol particles are a particularly large source of mixing. This mixing of the aerosol types acts to modify the aerosol properties, a few percent in mass of sulphate can modify a poor CCN soot particle into a much more efficient CCN particle by making it slightly soluble (Zhang et al., 2008).

1.1.2 Clouds and Precipitation

Clouds can form once air becomes saturated with respect to water or ice. This typically happens in the atmosphere as the result of rising air cooling during its ascent, although mixing can also result in airmasses reaching saturation. Cloud droplets do not necessarily form once saturation is achieved, usually requiring the presence of sufficient CCN or IN. To form droplets, aerosol must be activated, requiring saturations in excess of 100% (Kohler, 1936). Once cloud droplets form, they grow by the condensation of water vapour onto the droplet. Condensational growth slows down with size (due to a reduction in the surface area/volume ratio) resulting in a narrowing of the droplet size distribution with time. A typical cloud droplet of 10 μm has to grow to around 1 mm to form a raindrop (a increase in volume of 1 million times), but condensational growth proceeds too slowly to form precipitation in warm clouds (Reynolds, 1878). The primary processes by which precipitation is formed are determined by the structure of the cloud, with a major distinction being whether the cloud contains ice (Rogers and Yau, 1989).

The collision-coalescence mechanism can occur in any clouds containing liquid water droplets. Once droplets reach around 20 μm, they begin to fall through the cloud, undergoing rapid growth through coalescence with the cloud droplets they collide with. The efficiency of this process depends on the droplet size. Droplets below 20 μm have a poor collection efficiency, but the collection efficiency increases with size, resulting in a fast increase in droplet size for larger droplets. Comparisons of satellite observations with radar measurements indicate that when the cloud top effective radius reaches 14 μm, precipitation sized particles can be detected inside clouds (Rosenfeld and Gutman, 1994). In addition to the droplet size spectrum, the liquid water content (LWC) is an important con-

trol on the coalescence rate of the droplets. For clouds with low LWC such as tropical stratocumulus, the droplet growth rate is low, resulting in low precipitation rates (Stephens and Kummerow, 2007).

Whilst the collision-coalescence process is still important in clouds containing ice, as the cloud top temperature decreases, ice processes rapidly become important to precipitation initiation. Above the freezing level, the supersaturation over ice is higher than that over water, so ice crystals will grow at the expense of water droplets (Pruppacher and Klett, 1978). The crystals can form either homogeneously or on a suitable IN. Below around -35 °C the freezing of cloud droplets is almost certain through homogeneous freezing. The presence of IN can raise the droplet freezing temperature by allowing heterogeneous freezing.

In mixed phase clouds (with both ice crystals and supercooled droplets), the ice crystals can grow by colliding with the droplets or with each other (processes known as riming and aggregation respectively), producing precipitation sized particles. The size of the precipitation produced by these processes is dependent on the internal cloud dynamics and cloud updraughts. If the temperature near the ground is high enough, the precipitating ice crystals may fall as rain (Franklin, 1789).

1.1.3 Aerosol influences on clouds and precipitation

The properties of aerosols give rise to several effects on the earth's climate. The aerosols themselves interact with solar radiation, both scattering and absorbing incoming radiation depending on the type of aerosol, in an effect known as the direct effect (Myhre et al., 2013). To first order, the direct effect is proportional to the mass of aerosol in the path of the radiation (Murphy, 2013), but also depends on the albedo of the underlying surface. The direct effect usually results in a negative radiative forcing, as radiation is scattered back into space, but if the aerosol is above a surface with an albedo larger than the single-scattering albedo of the aerosol, such as aerosol over snow or ice, the aerosol reduces the planetary albedo resulting in a positive radiative forcing and a net warming (Haywood and Shine, 1995). Absorbing aerosols such as black carbon can also reduce the planetary albedo resulting in warming, but this warming effect is currently thought to be smaller that the cooling effect of scattering aerosols (Chung et al., 2012). The total direct effect of aerosols is estimated as -0.27 $\mathrm{W\,m^{-2}}$ with a range of -0.58 $\mathrm{W\,m^{-2}}$ to -0.02 $\mathrm{W\,m^{-2}}$ (Myhre et al., 2013).

In their role as CCN, aerosols also modify cloud properties, processes known as 'indirect' effects. By providing more condensation nuclei, aerosols can increase the cloud droplet number concentra-

tion (CDNC), which at constant LWC results in smaller cloud droplets. Small droplets are more efficient scatterers of radiation, so this effect results in an increase in cloud albedo and is known as the 'cloud albedo effect' (Twomey, 1974, 1977). The effect of increased CCN decreasing cloud droplet size is supported by laboratory studies (Gunn and Phillips, 1957); however the strength of the cloud albedo effect in the atmosphere is difficult to quantify due to interactions with other cloud processes. Observations of ships tracks (narrow bands of optically thicker marine stratocumulus in otherwise thinner regions) (Coakley et al., 1987) with both satellite and aircraft suggest that there are indeed higher droplet number concentrations in these ship tracks (Radke et al., 1989), and that the tracks reflect more solar energy than the surrounding clouds (King et al., 1993). Measurements during the Monterray ship–track experiment (MAST) suggested that changes in CCN due to ship exhaust are the cause of these changes in cloud properties (Durkee et al., 2000). Whilst ship tracks illustrate the effect aerosols can have on clouds, their small extent results in a small overall forcing of around 50 mW m^{-2} (Schreier et al., 2007). The total radiative forcing due to the cloud albedo effect is thought to be between -0.5 and -1.9 W m^{-2}. When combined with the estimates of the direct effect forcing of approximately -0.27 W m^{-2}, the radiative forcing from aerosol is comparable in magnitude to current estimates of the radiative forcing from anthropogenic CO_2 at +1.7 W m^{-2} (Forster et al., 2007).

These changes to the microphysical properties of clouds, and to their radiative environment can feed-back on the clouds, creating further changes in cloud properties. Many different feedbacks and indirect aerosol effects have been proposed (Lohmann and Feichter, 2005), often acting in opposition, so the net effect of aerosols on cloud properties is unclear. For example, the reduction in cloud droplet radius is thought to decrease precipitation efficiency, which may in turn result in an increased cloud lifetime (Albrecht, 1989). However, such clouds may entrain more dry air (Ackerman et al., 2004) and smaller cloud droplets also evaporate faster, which can reduce cloud water content (Sandu et al., 2008). Wood (2007) suggests that marine stratocumulus with higher bases (>400 m) might experience cloud thinning in higher aerosol environments, resulting in a cancellation of the aerosol indirect effect on shorter timescales. It is also possible that aerosols influence the transition between open and closed-celled stratocumulus by influencing precipitation rates (Rosenfeld et al., 2006). Whether a cloud is producing surface precipitation may be important, with Lee et al. (2009) suggesting that for thin stratocumulus clouds, aerosols increase the cloud liquid water path (LWP)

only in precipitating clouds. As changes in the LWP of a cloud via lifetime effects also influence the strength of the cloud albedo effect, the different effects of aerosols on clouds cannot be completely separated.

Strong relationships have been found between satellite retrieved cloud fraction (CF) and AOD in low clouds (Kaufman et al., 2005), varying with aerosol types and dynamic regimes (Small et al., 2011) and also in higher altitude ice clouds (Mahowald and Kiehl, 2003; Koren et al., 2010b). An increase in CF may be connected with the suppression of precipitation in some cloud types, although aerosols may not result in a suppression of precipitation in all cloud types. Rosenfeld et al. (2002) suggest sea salt, acting as giant CCN (GCCN), increases rainfall and may help to clean the atmosphere of pollutants. These GCCN can nucleate droplets which are above the collision-coalescence threshold and so can immediately form rain. Recent work has suggested that relationships between AOD and CF may be the result of factors other than aerosol-cloud interactions (Quaas et al., 2010; Grandey et al., 2013b).

Convective clouds

The suppression of precipitation in shallow clouds may lead to invigoration of deeper clouds (Williams et al., 2002; Rosenfeld et al., 2008). The suppression of warm rain in the initial phases of the convective cloud lifecycle may lead to precipitation only forming once cloud droplets freeze. This would increase the buoyancy of cloud parcels, which in turn invigorates the cloud dynamics (Fig. 1.1). This microphysical effect may be offset by a radiative effect, with a reduction of shortwave (SW) radiation at the surface and a heating of the atmosphere leading to a reduction in convective available potential energy (CAPE) and decrease in the strength of convection at very high aerosol concentrations (Rosenfeld et al., 2008; Koren et al., 2008).

Stevens and Feingold (2009) propose another method for convective invigoration of clouds. They suggest that the increase in CCN should delay the onset of precipitation, allowing hydrometeors to be advected to higher levels. This would increase cooling by evaporation at the cloud top, destabilising the cloud top region. The destabilised cloud top could invigorate updraughts, increasing the cloud top height and increasing precipitation. These effects are likely to be more complicated in systems with multiple clouds due to competition and interactions between the clouds (Lee and Feingold, 2010). The invigorated convection is likely to result in an increase in precipitation, although this is

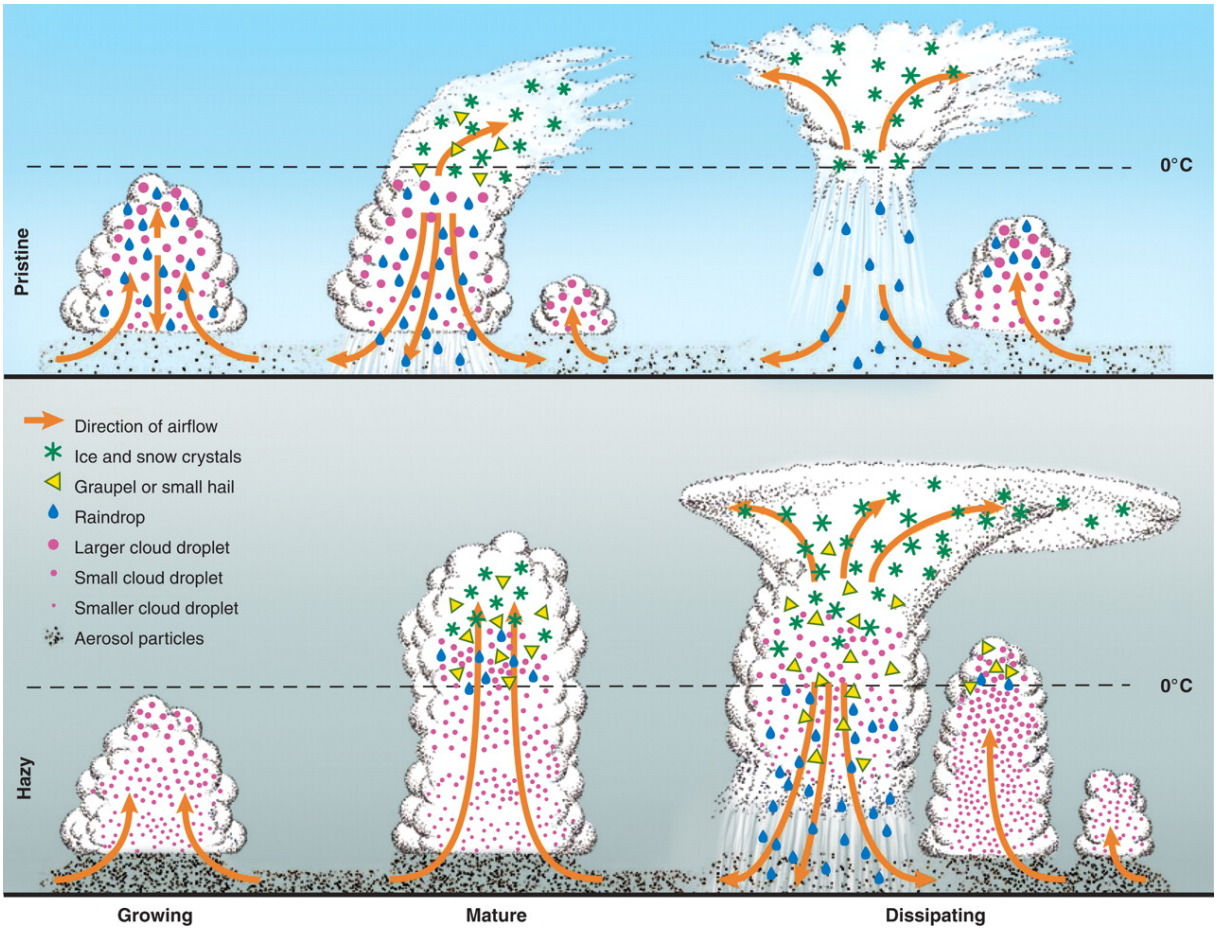

Figure 1.1: Comparison of the development of deep convective clouds in pristine (top) and polluted atmospheres. The reduction in precipitation in the early stages of cloud development in the polluted atmosphere results in water reaching the freezing level, where it freezes forming precipitation which then falls through the cloud melting in the lower levels. The suppression of precipitation until the droplets reach the freezing level increases the buoyancy of the cloud parcels, invigorating the cloud dynamics. [From Rosenfeld et al. (2008), © AAAS, Reproduced with permission.]

not certain and model studies suggest it depends strongly on the environmental conditions (Khain, 2009).

Semi direct effect

Different aerosols are suspected to play varying roles in the atmosphere. Black carbon (BC) is an efficient absorber of solar radiation. In very polluted atmospheres, reductions in cloud fraction have been observed with increasing aerosol. Ackerman et al. (2000) suggest that this might be due to absorbing aerosols heating the atmosphere at higher altitudes, reducing the relative humidity. These aerosols can also cool lower altitudes, stabilising the atmosphere. This stabilisation acts to reduce cloud fraction and precipitation due to convective clouds, a process known as the semi-direct ef-

fect. Reductions in cloud fraction over the Amazon with increasing AOD have been observed (Koren et al., 2008) and attributed to the semi-direct effect. This same process could also result in absorbing aerosols heating the tops of cloud, increasing evaporation and thereby decreasing cloudiness. More subtle effects have also been proposed, such as absorbing aerosol weakening wind shear in the Arabian Sea, intensifying tropical cyclones in that region (Evan et al., 2011).

Over stratocumulus regions, absorbing aerosols can also have other effects on cloud through modification of the atmospheric temperature structure (Koch and Del Genio, 2010). By enhancing a temperature inversion over stratocumulus cloud, absorbing aerosols above a cloud layer can cause a thickening of the cloud layer, enhancing its reflectivity and resulting in a negative radiative forcing (Wilcox, 2010; Peters et al., 2011).

Total effect

Aerosols modify the planetary energy balance, both directly and through their influence on cloud properties. They are generally assumed to lead to an increase in the planetary albedo, leading to a reduction in absorbed solar radiation that could also lead to a reduction in global mean precipitation. Allen and Ingram (2002) show that general circulation models (GCMs) produce an increase in precipitation with an increase in surface temperature due to greenhouse gases of $\sim$2-3 % K^{-1} resulting from an increase in latent heating compensating for stronger radiative cooling of the atmosphere. A corresponding cooling effect from aerosols would result in a reduction in precipitation, with aerosols perhaps being effective at modifying precipitation rates as they have a larger influence on shortwave radiation (Wild and Liepert, 2010). Absorbing aerosols can also have an effect on the global mean precipitation by altering the planetary energy budget (Frieler et al., 2011), but the sign of the precipitation change is dependent on the level in the atmosphere at which they are located (Ming et al., 2010; O'Gorman et al., 2011). The global energy balance is less useful for constraining regional changes in precipitation. The dry static energy flux divergence has been shown to be important for regional precipitation changes due to greenhouse gases in GCMs, but the local water vapour budget becomes more important on smaller scales (Muller and O'Gorman, 2011).

1.2 Observations of aerosols, clouds and precipitation

There are a variety of different ways to retrieve aerosol, cloud and precipitation properties from space. These are described below.

1.2.1 Aerosol properties

Aerosols are highly variable, so whilst there are many accurate in-situ measurements of aerosols and ground based remote sensing datasets (eg. AERONET (Holben et al., 1998)), the lack of spatial coverage and representativeness afforded by these datasets can present a problem in determining a global picture of aerosol–cloud–precipitation interactions. The most common solution is the use of satellite measurements, which can retrieve aerosol optical depth (AOD), a quantitative measurement of aerosol extinction along a path between the satellite and the ground.

The AOD provides a measure of the attenuation of solar radiation due to aerosols, which has been proposed as an estimate of the CCN concentration (Andreae, 2009). There are several difficulties in retrieving AOD that should be considered when using it for aerosol-cloud interaction studies. AOD is generally only retrieved in cloud free pixels. As the AOD (around 0.1) is much less than typical cloud optical depths (usually >5), cloud contamination of the AOD retrieval can result in increases in the retrieved AOD. Although cloud contamination was initially thought to be small for retrievals using the Moderate Resolution Imaging Spectrometer (MODIS) instrument (Kaufman et al., 2005), other studies suggest that it is more significant (Zhang et al., 2005).

Even in the case of perfect cloud-aerosol identification, the AOD retrieval can still be influenced by the presence of clouds. Light escaping from the edges of clouds or '3D effects' (Wen et al., 2007; Várnai and Marshak, 2009) can also give rise to increased AOD retrievals up to 15 km away from a cloud without an increase in CCN. The enhancement of relative humidity near clouds can cause aerosols to swell, increasing the AOD in a systematic effect known as the 'twilight zone' (Koren et al., 2007; Twohy et al., 2009).

The size variation of aerosols introduces biases in the AOD-CCN relationship depending on the type of aerosol being studied, as larger particles typically have a larger cross sectional area and a higher Mie scattering efficiency (Liou, 2002). For example, aerosols are known to swell in humid environments, increasing the AOD with little change to the CCN concentration (eg. Liu and Li, 2013).

As the humid swelling of aerosols increases the AOD without modifying the CCN concentration, this can lead to an artificial correlation between AOD and CF (eg. Chand et al., 2012). The processing of aerosol by clouds, where aerosol is dissolved and re-evaporated can also modify the aerosol size distribution, resulting in a larger AOD for a given CCN concentration (Pruppacher and Jaenicke, 1995).

The AOD can be retrieved at different wavelengths - in this work the 550 nm AOD is used. The Angström exponent is derived from the AOD at two separate wavelengths and is inversely proportional to the mean aerosol size. The aerosol index (AI - AOD $\times$ Angström exponent) (Nakajima et al., 2001; Bréon et al., 2002) uses Angström exponent to provide a size dependent parameter and provides a better estimate of CCN than the AOD, although it is still influenced by local effects and uncertainties in the aerosol optical properties (Kapustin et al., 2006).

There are two main ways of retrieving aerosol properties from space, using active instruments such as the LIDAR CALIOP (Cloud Aerosol Lidar with Orthogonal Polarisation) (Winker et al., 2007), or passive radiometer type instruments, operating in the visible and infra-red (eg. MODIS) or UV (eg. the Ozone Monitoring Instrument - OMI).

Radiometers typically have much larger swaths (eg. MODIS has an $\sim$2300 km swath) enabling greater spatial coverage than LIDARs, which only view a single strip in the nadir under 100 m wide. Radiometers do come with some disadvantages; being passive instruments they can only retrieve AOD during daylight hours and they suffer more from thin cirrus contamination, with thin clouds being classified as aerosol or vice-versa (Huang et al., 2011). Whilst some progress has been made in retrieving aerosol properties over clouds (eg. Torres et al., 2012), radiometers are generally unable to retrieve aerosol and cloud properties from the same pixel, only in cloud-free pixels will an aerosol retrieval be attempted resulting in aerosol and cloud retrievals not being perfectly co-located. LIDARs are able to perform retrievals of aerosol properties for aerosol layers above cloud, allowing the retrievals to be horizontally co-located. Their active nature makes LIDARs less sensitive to 3D effects, where light exiting the side of a cloud can cause an apparent increase in the AOD. LIDARs have problems determining the AOD as they require knowledge of the extinction to backscatter ratio, resulting in possible errors of 40%, although CALIOP retrievals compare well to MODIS AOD retrievals (Kittaka et al., 2011). CALIOP can also be used to determine the height of aerosol layers relative to cloud (Costantino and Bréon, 2013).

This study primarily uses aerosol retrievals from MODIS (Remer et al., 2005), which has a high swath giving near-complete global coverage each day. The high instrument resolution (250 m in certain visible channels (King et al., 1992)) minimises cloud contamination. MODIS is flown onboard both the Terra and Aqua satellites, Aqua is part of the A-Train constellation (L'Ecuyer and Jiang, 2010), enabling easy comparisons with data from other instruments in the constellation. The MODIS dataset has been heavily studied and evaluated against AERONET and CALIOP (Zhang and Reid, 2006; Schaap et al., 2008; Levy et al., 2010; Shi et al., 2011; Kittaka et al., 2011), generally showing good agreement with the other datasets. It is thought to have some issues over land (Xia, 2006) and in broken cloud regimes (Zhang et al., 2005), although it generally shows a good correlation with AERONET (Chu et al., 2002). Aqua and Terra MODIS compare well against each other, and there is minimal difference between the sensors (Remer et al., 2006; Xiong et al., 2008).

GlobAerosol AOD data from the Advanced Along-Track Scanning Radiometer (AATSR) (Thomas et al., 2010), flown onboard ENVISAT, is also used. AATSR makes use of dual views of the same scene, with a changing atmospheric path length. Whilst the MODIS AOD retrieval assumes a relationship between the IR and visible surface reflectances (Kaufman et al., 1997, 2002), the AATSR retrieval assumes the angular dependence of the surface reflectance (Thomas et al., 2013). Using different assumptions, the AATSR AOD retrieval provides an independent aerosol retrieval for comparison.

As aerosol retrievals are generally only performed in cloud free locations, AOD from the ECMWF Monitoring Atmospheric Composition and Climate (MACC) product is used to sample the aerosol in cloud covered regions (Inness et al., 2013). The MACC product involves the assimilation of MODIS 550 nm AOD retrievals into a version of the ECMWF IFS model which is running an aerosol scheme. The modelled aerosol component allows an estimate of the AOD in cloudy conditions where MODIS and AATSR cannot retrieve AOD.

1.2.2 Cloud properties

As with aerosols, cloud properties are highly variable in space and time, exhibiting a strong diurnal cycle. This gives polar orbiting satellites and geostationary satellites distinct advantages and disadvantages.

Geostationary satellites are able to sample the entire diurnal cycle, but they are limited in ge-

ographic sampling and spatial resolution (eg. SEVIRI on Meteosat Second Generation has a peak resolution of around 3 km (Schmetz et al., 2002), compared to the peak MODIS resolution of about 250 m). Polar orbiting satellites typically provide a higher spatial resolution, better geographic coverage and more varied instruments at the expense of a reduction in temporal coverage. Sun-synchronous satellites are the most common variety. With a single overpass time they do not sample the diurnal cycle, but are able to investigate day-to-day variations in cloud properties. The MODIS instrument is flown on two different sun-synchronous satellites, with daytime overpasses at 1030 and 1330 local solar time (LST), giving it a limited ability to investigate the diurnal cycle. Non sun-synchronous satellites, such as the Tropical Rainfall Measurement Mission (TRMM) (Kummerow et al., 1998, 2000), are able to sample the entire diurnal cycle as their overpass time varies. However, as they rarely have more than two overpasses per day, they are limited in their ability to investigate individual clouds.

The International Satellite Cloud Climatology Project (ISCCP) (Rossow and Schiffer, 1991, 1999) collects weather satellite radiance measurements which are then used to retrieve cloud properties (including cloud top pressure, cloud optical depth and cloud fraction). ISCCP determines the cloud top height using temperature based methods. As this can result in the retrieval of mid-layer clouds where thin high cloud overlies low cloud, a visible retrieval is used to adjust the retrieved values where it can be determined that this situation has occurred. The ISCCP retrievals are aggregated to a 3 hourly basis, generating near-complete global coverage every three hours (Rossow and Schiffer, 1999). The ISCCP products rely on geostationary satellites for much of their data, and this reliance has been shown to bias some of the cloud properties with respect to the satellite zenith angle, making long term trends in the data unreliable (Evan et al., 2007).

Whilst MODIS does not have the temporal resolution of ISCCP, it operates at a higher spatial resolution, allowing better separation between cloud types (Marchand et al., 2010). MODIS uses a CO_2 slicing based technique for determining the cloud top pressure (CTP) of high clouds and a cloud top temperature based method similar to ISCCP for low clouds (Menzel et al., 2008). Cloud top temperature based methods can lead to errors determining the height of thin clouds (Marchand et al., 2010) and low level broken cloud (Zuidema et al., 2009).

Cloud fraction (CF) is important not just for the physical properties of a cloud field, but also for cloud retrievals, which are only performed where a cloud is detected. In this work, the CF of a region

is defined as the area fraction of that region covered by cloud. The sensitivity of the instrument and the vertical structure of the cloud field can affect cloud detection, so that varying observation angles can change the apparent CF (Maddux et al., 2010). Cloud fraction also depends on resolution, with large over-estimations of the CF being found at low instrument resolutions (Shenk and Salomonson, 1972). The resolution that CF is determined at also affects the CF distribution, with the distribution being also binary at scales much smaller than the typical cloud scale, but showing a larger variation when determined at larger spatial scales.

MODIS can have difficulties in retrieving cloud properties in high aerosol environments, especially where there is aerosol above clouds. High aerosol concentrations can be mis-classified as cloud (eg. Hubanks et al., 2008), which leads to an increased AOD-CF correlation. This is a less important factor than cloud contamination of the AOD retrieval and is generally mitigated by picking a conservative cloud retrieval, or by discarding pixels with an AOD above 0.6 (Brennan et al., 2005). In situations where there is aerosol above cloud, MODIS can underestimate the LWP due to an apparent reduction in visible cloud brightness and droplet effective radius (Haywood et al., 2004). Microwave instruments can also retrieve cloud properties, using the brightness at GHz frequencies to determine the profile of water vapour and cloud water (Stephens and Kummerow, 2007). They may be more reliable than MODIS in very high aerosol regions when retrieving liquid water path, but they generally operate at a lower spatial resolution (Seethala and Horvath, 2010).

Active instruments (which transmit radiation as well as receiving it), including radars and LIDARs can also be used to investigate cloud properties. Whilst LIDARs are attenuated quickly by clouds, they can be suitable for the study of cloud tops or thin clouds (Borg et al., 2011). Radars generally cannot detect thin clouds, but their ability to penetrate thicker clouds enables the vertical resolution of cloud properties (Austin and Stephens, 2001). This high vertical resolution comes with a reduced horizontal swath. The CloudSat Cloud Profiling Radar (CPR) (Stephens et al., 2008) operates only in the nadir and the TRMM Precipitation Radar (PR) (Kummerow et al., 1998, 2000) has a swath of around 200 km, but cannot detect cloud.

In the majority of this work, cloud retrievals from MODIS (Platnick et al., 2003) are used, due to their high spatial resolution, near-coincident aerosol retrievals and multiple daylight overpasses each day. The ISCCP retrievals are used to provide a second independent set of cloud property retrievals. Zenith angle dependencies are also present in the MODIS dataset (Maddux et al., 2010), with thin

cloud and aerosol more likely to be detected at the edge of the swath. The use of the ISCCP dataset allows the influence of varying scattering angles to be considered, as they vary between the viewing geometries of MODIS and ISCCP.

1.2.3 Precipitation

Precipitation is even more variable than clouds or aerosol, making it very difficult to get an accurate measurement of the areal precipitation accumulation with limited measurements. Local rain gauge data can be accurate for well maintained and well sited gauges ($\pm 10\%$), but precipitation estimates are often required over a larger area, resulting in errors due to the lack of representativeness of rain gauges (Groisman and Legates, 1994). Measurements are also available from ship based sensors, improving the spatial coverage, but as ships are rarely stationary, they require careful use (Woodruff et al., 2011).

Ground based weather radars are able to provide precipitation retrievals over larger regions and at higher temporal frequency than rain gauges. However, their coverage is still limited globally, especially over the ocean and over regions with complex topography. They are often dependent on bias corrections provided by local rain gauges, making comparisons between radars difficult.

Passive microwave instruments such as the Special Sensor Microwave/Imager (SSM/I) can retrieve precipitation estimates as well as cloud properties. Over ocean, lower frequency measurements (10-20 GHz) are typically used to determine the precipitation rate. Below 20 GHz, absorption by water modifies the upwelling surface radiation, increasing the brightness temperature. This increase is small, so precipitation retrievals using this method are limited to regions where the surface brightness temperature is low, such as the ocean. Over land, absorption by precipitation is typically smaller than can be detected given the uncertain surface properties. In this case, precipitation is usually retrieved using higher frequency channels (higher than 60 GHz). At these frequencies, the brightness temperature is determined primarily by scattering from ice particles rather than surface emission. As they are related to ice scattering, high frequency retrievals are less directly related to surface precipitation rates than the lower frequency retrievals, which are more sensitive to liquid precipitation (Bauer et al., 2005).

To convert these measurements of column properties into surface precipitation, either empirical relationships between brightness temperature and precipitation, or cloud profiles based on cloud

models are used. The empirical methods require many assumptions to be made regarding the separation of cloud water from precipitation (Stephens and Kummerow, 2007). As they are known to have difficulties in separating precipitation and cloud water, an increase in LWC could cause a passive microwave instrument to see an increase in precipitation (Berg et al., 2006; O'Dell et al., 2008; Bennartz et al., 2011). The GPROF retrieval (Kummerow et al., 2001) makes use of modelled precipitation and cloud water profiles to retrieve the vertical distribution of cloud properties from microwave brightness temperatures, separating cloud and precipitation properties. More recent retrievals extend this method to use hydrometeor profiles from radar rather than models (Kummerow et al., 2011). Microwave instruments can be subject to retrieval errors based on assumptions about the underlying surface, whether it is due to the the ocean surface emissivity model and its relation to windspeed, or the effect of soil moisture on surface emissivity. They are also subject to beam-filling errors due to their low resolution (Greenwald et al., 2007), although they compare well to higher resolution active instruments (Berg et al., 2006).

Active microwave instruments, or radars, such as the TRMM PR and the CloudSat CPR can provide complementary measurements of precipitation properties. To first order, radar reflectivity is proportional to the sixth power of droplet radius. This makes radars more sensitive to the large precipitation droplets, but also introduces a dependency on the assumed droplet size spectrum (Iguchi and Meneghini, 1994). Radar instruments also have to contend with attenuation by clouds and especially precipitation. The CloudSat CPR suffers from this more than the TRMM PR, being severely attenuated by any rainfall over $40\,\mathrm{mm\,hr^{-1}}$ which can cause it to underestimate tropical rainfall (Ellis et al., 2009). The TRMM PR operates at a lower frequency and so is less susceptible to attenuation, although this comes with a reduced sensitivity to light rain and drizzle compared to the CloudSat CPR (Haynes et al., 2009).

Given the variability of precipitation, individual instruments are unable to capture the full nature of precipitating systems. Geostationary IR instruments are also used to estimate precipitation, such as in the PERSIANN (Hsu et al., 1997; Sorooshian et al., 2000) and CMORPH (Joyce et al., 2004) datasets. These can be combined with other satellite and surface gauge data to generate a better precipitation estimate (Adler et al., 2001). Comparisons between the datasets indicate that pure IR retrievals most likely overestimate precipitation (Tompkins and Adebiyi, 2012).

The Global Precipitation Climatology Project (GPCP) (Huffman et al., 2001; Adler et al., 2003;

Huffman et al., 2009) uses rain gauge data, satellite microwave and IR information to produce a global picture of precipitation. A global precipitation estimate is generated by using rain gauge data to calibrate satellite microwave instruments, and these in turn to calibrate geostationary IR measurements. This method is also used for the TRMM Multisatellite Precipitation Analysis (TMPA or TRMM 3B42) (Huffman et al., 2007). This uses the TRMM Microwave Imager (TMI) and PR to provide a calibration against which other microwave satellite instruments are matched. Any gaps in this record are filled using a geostationary IR precipitation dataset. This purely satellite dataset is then corrected monthly using rain gauges, producing a tropical precipitation estimate every three hours. This product captures both the regional distribution of precipitation as well as the diurnal cycle in the tropics (Bowman, 2005). This study uses the TRMM 3B42 product as the main precipitation dataset, augmented by vertically resolved satellite radar products where possible.

1.3 Atmospheric models

The complex nature of clouds and the atmospheric system makes determination of cause and effect from purely observational studies difficult. Randomised control experiments are difficult and expensive when investigating the effect of aerosols on clouds. Atmospheric models provide one possible solution.

Global climate projections often make use of general circulation models (GCMs), which are used to simulate the atmosphere-ocean-land system. These models often contain a dynamic atmosphere that covers the entire globe. Due to computational cost, these models are usually run at resolutions lower than 1° by 1° degree. As this is too coarse to resolve many atmospheric processes, the small scale processes are parametrised (eg. Arakawa, 2004). A wide range of parametrisations can be employed, generating uncertainties in the response of the climate system to perturbations. Whilst global models can capture the main features of accumulated global precipitation, they still have some unrealistic features, such as a double Intertropical Convergence Zone (ITCZ) over the central Pacific (Dai, 2006) and they produce precipitation approximately twice as often and much lighter than observations (Stephens et al., 2010).

These atmospheric models can be coupled to aerosol modules (eg. ECHAM-HAM (Stier et al., 2005) and HadGEM3-UKCA (Bellouin et al., 2013)), which represent the effect of aerosols on

clouds. These aerosol modules include large uncertainties, particularly in their influence of aerosols on cloud properties. Large compensating errors can be hidden inside parametrisations, generating similar magnitudes for an aerosol effect on clouds in different models, but via different pathways (Penner et al., 2006). However, models are expected to reproduce meteorological covariations between cloud and aerosol properties, allowing these covariations to be investigated as possible causes for aerosol cloud correlations (eg. Lohmann et al., 2006; Quaas et al., 2010). Coupled with the ability to remove atmospheric processes, global models are a powerful tool for testing hypotheses about aerosol-cloud interactions.

Models run at a higher resolution are able to resolve individual clouds and cloud processes, removing the need for parametrisations of larger scale processes. As the resolution of these models is increased, fewer processes need to be parametrised. Convection resolving (or permitting) models run at a resolution of around 1 km can resolve convective processes. Large eddy simulations (LES), run between around 10 m and 100 m resolution, can resolve large scale turbulence. Direct numerical simulations (DNS) resolve all turbulence and dissipating eddies (Jacobson, 2005). These high resolution models often include sophisticated models of aerosols as CCN, maintaining number and size distributions in multiple size bins. As they operate at high resolution they are often used to examine the effects of convection and microphysics on the individual clouds (eg. Khain et al., 2008). As they are expensive to run, they are not generally used for climate modelling on a global scale, but they can help analyse possible interactions between aerosols and individual clouds.

1.4 Studies of aerosol–cloud–precipitation interactions

Many studies have been conducted on the effect of aerosols on precipitation. The effect of aerosols on cloud fraction and cloud top pressure are also strongly related.

1.4.1 Cloud fraction

Correlations between aerosol and cloud fraction (CF) have been observed using many different instruments in a variety of different cloud regimes. Global studies with satellite datasets show an increase in CF with increasing aerosol number (Sekiguchi et al., 2003) and over the Atlantic, Kaufman et al. (2005) find an increase in CF with AOD in several separate regions, each dominated by

different aerosol types. Studies using aircraft also suggest an increase in CF with increasing aerosol; Heymsfield and McFarquhar (2001) find increased CF with increased aerosol during the INDOEX experiment. High resolution studies with the ASTER instrument (15 m resolution) also show an increase in CF, suggesting that errors in the CF retrieval are unlikely to be the cause of the AOD-CF correlation (Dey et al., 2011).

Whilst increases in CF are observed in ship-tracks in stratocumulus clouds (Taylor et al., 2000), there can be a decrease in cloud optical depth in regions close to the tracks (Chen et al., 2012). However, this decrease is small compared to the overall increase in cloud reflectivity, and the changes in cloud properties can persist over large distances after the initial shiptrack is no longer obvious (Goren and Rosenfeld, 2012). Baker and Charlson (1990) suggest the existence of two stable states of shallow cloud depending on the aerosol environment. This is expanded upon by Rosenfeld et al. (2006), who suggest that aerosol influences precipitation properties and so the transition between open and closed celled stratocumulus. Simple theoretical models (Koren and Feingold, 2011) and cloud resolving models of stratocumulus clouds support this interpretation (Wang and Feingold, 2009a,b). Studies using windspeed as a proxy for sea salt aerosol have shown a decrease in stratocumulus CF at high aerosol (high windspeed), suggesting that GCCN may have a different effect on stratocumulus through their different impact on precipitation (Lehahn et al., 2011).

Decreases in CF with increasing aerosol are also found at high AODs over land (Koren et al., 2008). Using AERONET sunphotometers, Kaufman and Koren (2006) show an increase in CF with increasing AOD in smoke dominated regions, with the change in CF with AOD becoming negative at large AOD. A similar effect is found by Small et al. (2011) in smoke dominated regions, with a strong increase in CF with AOD at low AODs but a decrease in CF at high AODs. In these studies, the increase in CF is hypothesised to be due to a suppression of precipitation with increasing AOD. At high AODs, the increased absorption is thought to suppress CF via the semi-direct effect.

Model studies have also found increases in CF with increased AOD. The GCM parametrisation of precipitation suppression (which may then lead to an increase in CF) is usually simple, with aerosols modifying the autoconversion rate, resulting in reduced precipitation in higher aerosol environments (eg. Beheng, 1994; Wilson and Ballard, 1999). The AeroCom indirect effect experiment showed an increase in CF and LWP with increased AOD in almost all of the models, although the magnitude of the sensitivities of CF and LWP to AOD showed large variation (Quaas et al., 2009).

High resolution models provide varying results as to an aerosol influence on CF. A reduction in cloud fraction in high aerosol environments is seen by Xue and Feingold (2006), who attribute it to increased evaporation of small cloud droplets. They suggest that CF may only increase for larger clouds that are less susceptible to increased evaporation. Jiang et al. (2006) find in their model that while individual clouds may experience a modification of their lifetime, the mean lifetime of shallow cumulus clouds was unchanged with increasing aerosol.

Correlations between CF and AOD have also been observed in other cloud types. Mahowald and Kiehl (2003) show small changes in thin cirrus cloud amount with increased aerosol. Koren et al. (2010a) find an increase in cloud anvil area with increased AOD, although this increase is likely to proceed by different mechanisms to the studies emphasised above. Models also show an increase in CF at the anvil height, even with no explicit influence of aerosols on ice processes (Grabowski, 2003). This increase may be related to convective invigoration and the suppression of precipitation in the early stages of the cloud development.

There are large uncertainties in observed AOD-CF relationships. CF and AOD are known to both vary with meteorological parameters, such that large AOD-CF correlations may be generated by meteorological covariation. Model studies indicate that the majority of the AOD-CF correlation may be generated by the swelling of aerosols increasing the AOD in humid, high CF environments (Quaas et al., 2010; Grandey et al., 2013a). These meteorological covariations have to be considered in any study of possible aerosol effects on CF.

1.4.2 Cloud top height

Convective invigoration by aerosols is thought to increase cloud top height as well as increasing the precipitation from these clouds (Williams et al., 2002). Strong correlations have been observed between aerosol and cloud top height properties using multiple different instruments. Increases in cloud top height have been seen in satellite data, using both passive radiometers (Koren et al., 2005) and active radars (Niu and Li, 2012). In-situ measurements of CCN coupled with ground based remote sensing measurements of cloud properties show similar increases in cloud top height with increased aerosol (Li et al., 2011), suggesting retrieval errors are not the primary reason for correlation between AOD and cloud top height.

It is thought that meteorology is likely to play a large role in generating correlations between

aerosol and cloud properties. Koren et al. (2010b) suggest that meteorological covariation cannot explain the AOD-CTP correlation in MODIS data. They find that although NOAA NCEP-GDAS reanalysis data is correlated to cloud and aerosol properties, there are no variables which are sufficiently correlated to both cloud and aerosol properties. Increased cloud top height with increasing AOD has been observed in regions dominated both by dust and by pollution from North America, suggesting that both types of aerosol play a role in this process (Koren et al., 2005).

The relationship between aerosol and cloud top height in models is not as strong as in observations. Very few global models have parametrised effects of aerosols on convective clouds or ice processes, which are likely to be important when modelling aerosol effects on convective clouds. Of the models in the AeroCom indirect effect experiment, only one model showed a significant overall correlation between AOD and CTP (Quaas et al., 2009).

Cloud top height and precipitation rate are correlated, a correlation important in IR based satellite precipitation retrievals (eg. Arkin and Meisner, 1987). The relationship between cloud top height and surface precipitation is good at monthly and daily timescales, but breaks down at higher temporal resolutions and may not be constant under changes in convective cloud microphysics. For example, smaller and lighter precipitation particles forming in polluted clouds may fall outside of the cloud in the presence of background wind-shear, evaporating faster than droplets from a clean cloud, which are typically larger and fall from lower levels (Khain, 2009). However, increases in cloud top height with increasing aerosol could be a result of convective invigoration and may indicate an increase in precipitation in convective clouds.

1.4.3 Precipitation

Observations of warm rain from shallow cumulus show a suppression of rainfall with increasing aerosol (Rosenfeld, 1999) and in some cases, pollution has been shown to completely inhibit precipitation (Rosenfeld, 2000). These case-study results have been expanded to more global studies of oceanic shallow cumulus clouds (Sorooshian et al., 2009), and all maritime clouds (Lebsock et al., 2008). Changes in the annual cycle of precipitation over the tropical Atlantic (Huang et al., 2009b) and decadal trends of precipitation and aerosol properties over the China Sea (Bennartz et al., 2011) also indicate a suppression of precipitation over large regions with many varying cloud types. Krüger and Graßl (2011) also find a decrease in precipitation with increased aerosol, although they avoid

measuring aerosol directly, inferring it from ocean colour and phytoplankton concentration.

Stratocumulus clouds also show suppression characteristics (Sorooshian et al., 2010); flights as part of the MASE-II experiment across ship tracks note a reduction in the precipitation measured by CloudSat in regions where the aircraft found high aerosol concentrations (Lu et al., 2009). Direct observations of precipitation from stratocumulus clouds are uncommon, as the low precipitation rates are below the detection limit for many spaceborne radars - only the CloudSat CPR can directly detect drizzle from stratocumulus clouds. Comparisons between the CPR and the AMSR-E microwave radiometer show that the precipitation rate is a strong function of LWP, and that this function changes in response to aerosol. These observations also suggest that sea-salt may increase precipitation in marine stratocumulus, compared to sulphate and other pollution aerosols which suppress drizzle (L'Ecuyer et al., 2009).

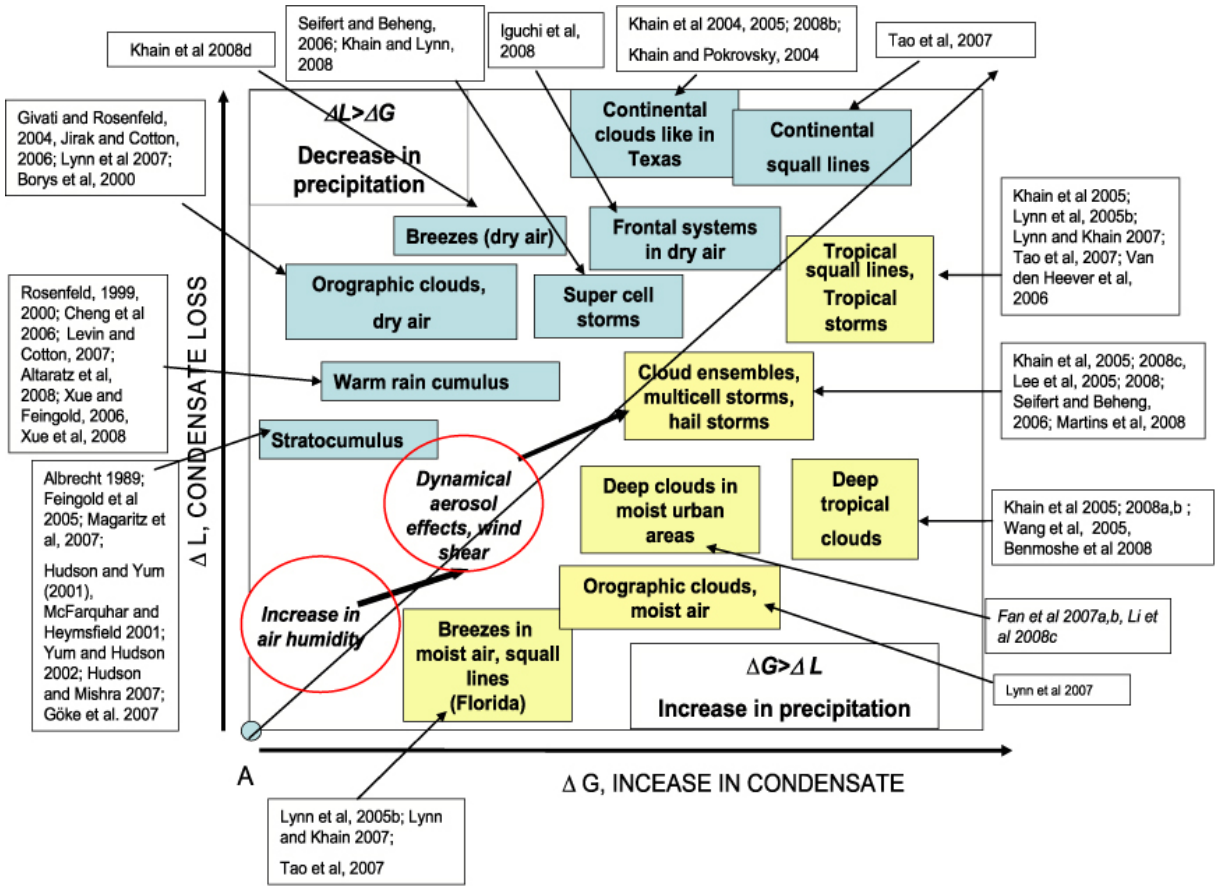

Figure 1.2: Summary of modelling studies of aerosol effects on precipitation from Khain (2009) showing the variety of different effects produced by cloud resolving models. Studies in the lower right of the figure show an increase in precipitation with increasing aerosol [© IOP Publishing Ltd. Reproduced under the CC BY-NC-SA 3.0 license].

Modelling studies have highlighted the importance of the competition between condensate growth processes (e.g. collision-coalescence) and condensate loss processes (e.g. evaporation) in determin-

ing the sign of the precipitation change (Khain, 2009) (Fig. 1.2). Studies using cloud resolving models have suggested that increased evaporation at the cloud top can result in a reduction of precipitation from shallow cumulus clouds (Altaratz et al., 2008).

The importance of ambient relative humidity (RH) is also highlighted using models. Fan et al. (2007) show a small aerosol effect in dry air, becoming much larger at more significant RH (>70%). This strong dependence on RH is also found in orographic clouds, where aerosols act to suppress precipitation in dry air, but increase it in humid air. This is attributed to the increased CCN resulting in smaller cloud droplets which evaporate easily in dry air, but in humid air this evaporation enhancement due to aerosols is much smaller (Lynn et al., 2007). Khain et al. (2008) use multiple model studies of different clouds to show increased evidence for a change in sign of the aerosol effect on precipitation in different RH environments (Fig. 1.2).

Low level marine clouds are particularly important for the planet's radiation balance and are the main source of uncertainty in climate models (Bony and Dufresne, 2005). However, they are not the main source of rain, with convective clouds and systems accounting for a larger fraction of total rainfall (Schumacher and Houze, 2003). Observations of deep convective clouds often show an increase in precipitation with increasing aerosol. Lin et al. (2006) find an enhancement of precipitation with increased AOD over the Amazon during the biomass burning season. They also see an increase in cloud cover and cloud top height with increasing AOD, perhaps suggesting an invigoration effect. Similar increases of precipitation with increased satellite retrieved AOD are found globally by Koren et al. (2012) and Niu and Li (2012).

These effects are not only observed with satellite measurements of cloud and aerosol properties. Using in-situ CCN measurements, Li et al. (2011) find an increase in cloud top height with increased aerosol. Aircraft measurements of the droplet size distribution in similar clouds (Andreae et al., 2004) also see a reduction in droplet size in polluted environments, forcing the cloud droplets to reach greater heights before precipitating, despite the substantial reduction in surface heating due to the aerosol. This would suggest that although aerosol retrieval errors may be important, it is likely other effects play a role in generating these correlations.

Modelling studies find a varying importance of ice processes in possible convective invigoration. Tao et al. (2007) suggest that evaporative cooling in the lower atmosphere is important for the aerosol invigoration of convective clouds. However, Phillips et al. (2007) demonstrate the impor-

tance ice melting processes in convective clouds, suggesting that aerosol modify these processes to invigorate clouds. Studies using an aquaplanet also show invigoration of convective clouds, finding a maximum at the convective anvil height (Grabowski, 2003), similar to the observational studies of Koren et al. (2010a). The dependence of models on the parametrisation of small scale processes has been suggested to have undesirable consequences for models. Lebo and Seinfeld (2011) show little change in precipitation in a cloud resolving model when using a bulk microphysics scheme (the type used in many global climate models) but a slight reduction in precipitation when using a more sophisticated scheme.

Some studies avoid using aerosol retrievals, making use of changes in aerosol properties over time to investigate aerosol influences on clouds and precipitation. One possible method of looking for aerosol effects involves searching for weekly cycles in cloud properties. Weekly cycles in aerosol properties have been observed (Xia et al., 2008), and it has been suggested that weekly cycles found in cloud properties are due to these weekly cycles in aerosols, as no other atmospheric phenomenon has a cycle tied to the 7-day week (Bell et al., 2008; Bell and Rosenfeld, 2008). Weekly cycles in more complex properties, such as tornado frequency (Rosenfeld and Bell, 2011) and lightning (Bell et al., 2009) have also been observed, suggesting that aerosols may invigorate convective storms. However, the existence of weekly cycles in atmospheric phenomena is disputed with some studies finding a weekly cycle in aerosol/visibility but not in precipitation properties (Schultz et al., 2007; Stjern, 2011). For a more complete overview of the use of weekly cycles, see Sanchez-Lorenzo et al. (2012).

1.4.4 Circulation changes

Global scale models are particularly useful for their ability to study non-local aerosol effects on clouds and precipitation. Changes in the large scale circulation and non-local change in cloud properties and precipitation due to aerosols cannot be observed through instantaneous observations of cloud and aerosol properties, requiring long-term trend analysis to determine the magnitude of these effects in observations.

The cooling effect of some aerosols can also result in changes to the large scale circulation. Due to their short atmospheric lifetime, there is a large hemispheric asymmetry in aerosol concentrations, with higher concentrations in the northern hemisphere due to stronger emissions. This asymmetry

results in a cooling of the northern hemisphere, which in turn shifts the ITCZ south, an effect which may have contributed to the Sahelian drought of the 1970s and 1980s (Rotstayn and Lohmann, 2002).

The total aerosol effect on precipitation in the IPCC AR4 models varies from no change to -0.13 mm day^{-1}, with the changes being larger where the atmospheric model is coupled to a mixed layer ocean, allowing evaporation to vary (Denman et al., 2007). As global evaporation must balance precipitation a reduction in solar heating due to aerosols would be expected to cause a decrease in global mean precipitation (Liepert et al., 2004). This is in contrast to precipitation measurements over the last century, perhaps suggesting an overestimate in the effects of aerosols on global mean precipitation. Changes in global precipitation patterns are still likely to be important, given the regional nature of aerosol effects (Denman et al., 2007). The effect of aerosols on the South Asian summer monsoon is of particular interest (Ramanathan et al., 2005). Recent work suggests that a drying trend over India is likely the result of increases in aerosols over the 20th century (Bollasina et al., 2011).

1.5 Possible influences on aerosol-cloud correlations

This work primarily considers relationships between cloud and aerosol properties in observational data. Whilst aerosol effects on clouds are one possible explanation of the observed correlations between retrieved aerosol and cloud properties, there are many other effects which have been shown or hypothesised to influence the strength of the correlations between aerosol and cloud properties (Tab. 1.1). Even if these effects cannot be accounted for, it is vital to identify sources of possible error to gain an accurate understanding of the uncertainty in any estimate of aerosol effects on clouds and precipitation.

Meteorological biases on the correlations between AOD and other cloud properties can be separated into two types. The first type of meteorological covariations are due to errors in the determination of the CCN concentration. For example, when AOD is used as a proxy for CCN, humidification of aerosol results in an increase in AOD without a change in the underlying CCN. Effects where the cloud properties and the CCN proxy are modified without a change in CCN are referred to as type one meteorological covariations throughout this thesis. They include effects such as cloud contamination and 3D effects, and can be completely accounted for by a perfect CCN retrieval/measurement. Type

Cause	Type	Effect
AOD retrieval errors		
- Cloud Contamination	1	
- 3D effects	1	Increased correlation between AOD and CF
- Aerosol humidification in the vicinity of clouds	1	
AOD-CCN relationship breakdown		
- Cloud processing	1	Change of the aerosol size distribution
- Aerosol humidification due to large scale RH	1/2	
Meteorological covariations (Type 2)		Meteorological covariations should be reproduced in models.
- Covariation of AOD/CCN and cloud with windspeed	1/2	Increased AOD - CF or AOD - CTP correlations, can result in AOD retrieval errors due to uncertainties in surface properties
- Covariation of CCN and cloud with air-mass properties	2	
- Wet scavenging of aerosol	2	Increased correlation between aerosol and rainfall suppression, decreases correlation between AOD and CF
Aerosol effects on clouds		
- Influence on CF		Increase in CF with aerosol
- Cloud invigoration		Increase in CTP and precipitation with aerosol
- Semi-direct effect		Reduction in CF and perhaps CTP with increased aerosol

Table 1.1: Possible effects in observations that might result in correlations between aerosol and cloud properties.

two covariations are the result of the cloud and CCN properties varying in response to an external controlling factor and cannot be accounted for by a perfect CCN retrieval, perhaps requiring a control experiment of a modelling study.

Type one covariations typically result in the enhancement of AOD in high CF regions, generating a spurious AOD-CF correlation. Some of these covariations (3D effects, cloud contamination) depend on the existence of clouds, enhancing AOD in high CF regions to create an AOD-CF correlation. These covariations create conditions which affect the AOD retrieval, but not the CCN. They can be further split into two types, errors in the AOD retrieval, and deviations from a simple AOD-CCN relationship.

The swelling of aerosols in the vicinity of clouds (the twilight zone), cloud contamination of the AOD retrieval and 3D effects cause errors in the retrieval of the AOD and are not explicitly modelled in current GCMs. The difference between observed and model relationships can give an idea of the magnitude of these AOD biases, suggesting that they may be responsible for around a third of the observed correlation between AOD and CF (Quaas et al., 2010).

The swelling of aerosol (and the corresponding increase in AOD) in response to large scale RH is modelled in modern GCMs. As CF is a strong function of RH, regions with high RH are likely to show both high AOD and high CF, generating a strong AOD-CF correlation. Using the ECHAM model (Roeckner et al., 2003), Quaas et al. (2010) find that this swelling of aerosols is responsible for the majority of the correlation between AOD and CF. Not all studies of the effect of RH on aerosol-cloud correlations come to the same conclusion; Koren et al. (2010a) investigate the links between multiple meteorological fields from re-analysis data and find that none of them adequately explain the correlation between AOD and CTP.

Type two meteorological covariations are found when CCN properties are modified along with cloud properties. For example, dust outflow from the Sahara is often accompanied by warm dry air (Carlson and Prospero, 1972), which can increase the inversion strength over the north Atlantic stratocumulus regions. This correlation between low troposphere stability and AOD can result in stronger apparent correlations between AOD and CF. Mauger and Norris (2007) show that by accounting for this effect, the strength of the AOD-CF correlation is reduced by 30 %. Type two covariations are more subtle and still exist even in the case of a perfect CCN retrieval. This distinction is explored further in section 4.3.

Whilst meteorological properties directly related to moisture are important for cloud formation and aerosol properties, other meteorological properties have been shown to have strong influences in the strength of the AOD-CF correlation. Together with large scale RH, Engstrom and Ekman (2010) show a strong influence of windspeed on the strength of the AOD-CF correlation, finding that accounting for these meteorological effects reduces the correlation by 27 %. Synoptic systems in the mid-latitudes also generate high windspeeds and high AODs, as well as having high cloud fractions (Grandey et al., 2011). It has been suggested that these systems might influence the correlations between aerosol and cloud properties, however recent work suggests that their impact is minimal (Grandey et al., 2013a).

Removal processes of aerosols can also play a role in generating aerosol-cloud correlations, although they are likely to generate negative correlations. Wet deposition is the main method of removal of atmospheric aerosol, and generates the false impression that precipitation is higher where aerosol is lower. Some have attempted to reduce it by using the aerosol averaged over a large area (Huang et al., 2009a), but as wet scavenging introduces a systematic bias this method may not be very effective. Sorooshian et al. (2009) remove points where precipitation was retrieved in the previous 24 hours as a way of accounting for the effects of wet scavenging. Back-tracing of aerosol trajectories has also been used as a method for avoiding wet-scavenging biases by locating airmasses from high aerosol regions. This can introduce even more uncertainty in the result due to the difficulty of providing an accurate path for the aerosol. Huang et al. (2009b) back traced aerosol over West Africa for three days from different heights, and found possible sources from most of Africa and Europe. Bennartz et al. (2011) were more successful in locating the source of aerosol over the China Sea as industrial areas in China, but the length of the trajectory was much shorter and the source easier to confirm.

The expected negative effect of wet scavenging in the AOD-CF relationship may also be disguised by the use of cloud free points to retrieve the AOD. It has been argued that the aerosol beneath the cloud is more representative of the aerosol acting on the cloud. The aerosol in cloud free regions has not experienced the same degree of wet scavenging as that below the cloud, and so can have a larger AOD, increasing the strength of the AOD-CF correlation (Grandey et al., 2013b).

Errors can also be generated by geographical correlations. Grandey and Stier (2010) showed that Simpson's paradox (see Pearl, 2009) applies to aerosol-cloud interactions, where climatological

spatial gradients in cloud and aerosol properties may generate spurious correlations. Errors can also occur when considering the different scales of aerosol-cloud interactions and satellite data scales. These errors due to scale mismatches can be mitigated by accounting for variation in cloud properties (McComiskey and Feingold, 2012).

Some studies make use of natural experiments to account for the confounding effects of meteorology. Yuan et al. (2011a) make use of volcanic emissions from Hawaii during the summer of 2008, comparing these results to the climatology. Although these results may account for the influence of meteorology when determining the influence of aerosol on cloud, they are limited to a specific regime and location, so do not provide a global picture of these effects.

Individually, none of these processes (Tab. 1.1), including an aerosol effect on clouds and precipitation, can explain observed correlations between aerosols and cloud properties. They all have to be accounted for when considering possible aerosol-cloud-precipitation interactions.

1.6 Structure of thesis

The aim of this thesis is to improve the understanding of possible aerosol-cloud-precipitation interactions, in particular how aerosols interact with cloud fraction and precipitation. Given the importance of meteorological covariation in generating correlations between aerosol and cloud properties, this thesis will consider the role of these correlations and attempt to minimise them when investigating possible aerosol-cloud-precipitation interactions.

The remainder of this thesis is formed from the following chapters;

Chapter 2

This chapter investigates one possible cause of the AOD-CTP correlation, the strong AOD-CF correlation. The chapter examines what proportion of the AOD-CTP correlation can be explained by a combination of the AOD-CF and the CF-CTP correlations and how the effect varies globally.

Chapter 3

In chapter three, MODIS data is used to determine cloud regimes, which are then used to investigate the correlation between AOD and CDNC. This correlation is important in determining the magnitude of the cloud albedo effect. Two related issues are studied: how does the sensitivity of CDNC to AOD

vary by regime, and are there sampling issues when determining this correlation due to the lack of AOD retrievals in cloud covered pixels?

Chapter 4

In chapter four, the effect of the AOD-CF correlation is accounted for by investigating how aerosols are correlated with transitions between cloud regimes. This chapter presents a new method for investigating aerosol-cloud interactions while accounting for the influence of meteorological covariation. This chapter aims to determine whether there is a link between aerosol properties and the development of the cloud regimes.

Chapter 5

This chapter extends the work in the previous chapter to investigate the precipitation development of each of the cloud regimes. The principle aim of this chapter is to determine whether aerosols influence the precipitation development of the cloud regimes, whilst accounting for the influence of meteorological covariation.

Chapter 6

This chapter continues the work on cloud regime development, extending it to studies using models. This chapter poses two main questions. First, can a GCM reproduce the observed changes in cloud regime transitions and precipitation development? Second, can the results from a GCM be used to determine the influence of meteorological covariations on the results found in the satellite data?

Chapter 7

The conclusions from this thesis are presented and future avenues of research are discussed.

Chapter 2

Influence of the aerosol optical depth - cloud fraction correlation

A strong correlation between AOD and cloud top height is observed globally (Koren et al., 2005, 2010b; Yuan et al., 2011a; Niu and Li, 2012). Different measurements of cloud top height, both passive radiometer based (Koren et al., 2005, 2010b) and active radar based (Niu and Li, 2012) show an increase in cloud top height (decrease in CTP) with increased AOD.

A strong link is also observed between AOD and CF in both observations (Sekiguchi et al., 2003; Kaufman et al., 2005; Kaufman and Koren, 2006; Loeb and Schuster, 2008; Koren et al., 2008; Dey et al., 2011; Koren et al., 2010a; Small et al., 2011) and models (Myhre et al., 2007; Quaas et al., 2009; Grandey et al., 2013b). These correlations have been found in several different cloud regimes, such as stratocumulus (Costantino and Bréon, 2013) and convective anvils (Koren et al., 2010a), but they all show the same general form, a strong increase in CF with increasing AOD. Some studies find a decrease in CF at high AOD (eg. Koren et al., 2008), but a positive AOD-CF relationship is found in the majority of regions. Much of the AOD-CF correlation is thought to be due to effects other than aerosol-cloud interactions such as cloud contamination of the aerosol retrieval (Zhang et al., 2005), cloud 3D effects (Wen et al., 2007), aerosol humidification (Twohy et al., 2009; Quaas et al., 2010; Chand et al., 2012) and other meteorological influences (Engstrom and Ekman, 2010).

These previous studies of the AOD-CTP and AOD-CF correlations have shown strong correlations with many different observing systems, suggesting that retrieval errors or other measurement

This chapter is currently in preparation for publication. I have worked on it together with Benjamin Grandey (Singapore - MIT Alliance for Research and Technology) and Philip Stier. The analysis and manuscript are my own work, with comments and suggestions from co-authors.

effects are not the primary cause of these correlations between aerosol and cloud properties. However, due to effects such as aerosol humidification, AOD may not be a good proxy for CCN (eg. Nakajima et al., 2001).

The influence of the AOD-CF correlation on the AOD-CTP correlation has been considered previously (Myhre et al., 2007), but its importance for determining the AOD-CTP correlation was not fully considered. This chapter demonstrates how this strong AOD-CF relationship may explain the majority of the AOD-CTP relationship across the globe. This underscores the importance of accounting for CF when considering relationships between aerosol and cloud properties.

2.1 Method

Nine years (2003-2011) of MODIS Terra cloud (Platnick et al., 2003) and aerosol (Remer et al., 2005) daily level three data are used at a 1° by 1° resolution for the region 50°N-50°S. The cloud mask (MOD35) cloud fraction retrieval are used to provide the cloud fraction product from the level 3 (MOD08_D3) dataset, although these results are applicable when using other cloud fraction products. There is evidence of heavy aerosol being mis-classified as cloud by the MODIS cloud retrieval (Brennan et al., 2005; Hubanks et al., 2008). Restricting the maximum AOD to 0.6 partially accounts for the influence of aerosols on the CF retrieval, although not for cloud contamination of the aerosol retrieval. The aerosol retrieval used is the standard dark-target MODIS AOD retrieval, 'Optical Depth Land and Ocean Mean.' As MODIS cannot make co-located observations of aerosol and cloud properties, so the level 3 AOD is assumed to be representative of the entire gridbox. Gridboxes with no AOD retrieval are excluded from this analysis.

To investigate the strength of the relationships between ln(AOD), CF and ln(CTP), the sensitivity is defined as the slope of a linear regression between two quantities. To avoid errors from seasonal effects or climatological spatial gradients (Grandey and Stier, 2010), sensitivities are calculated locally, at a 1° by 1° scale and separately for each season, with the seasonal sensitivities being combined using a standard-error weighted mean.

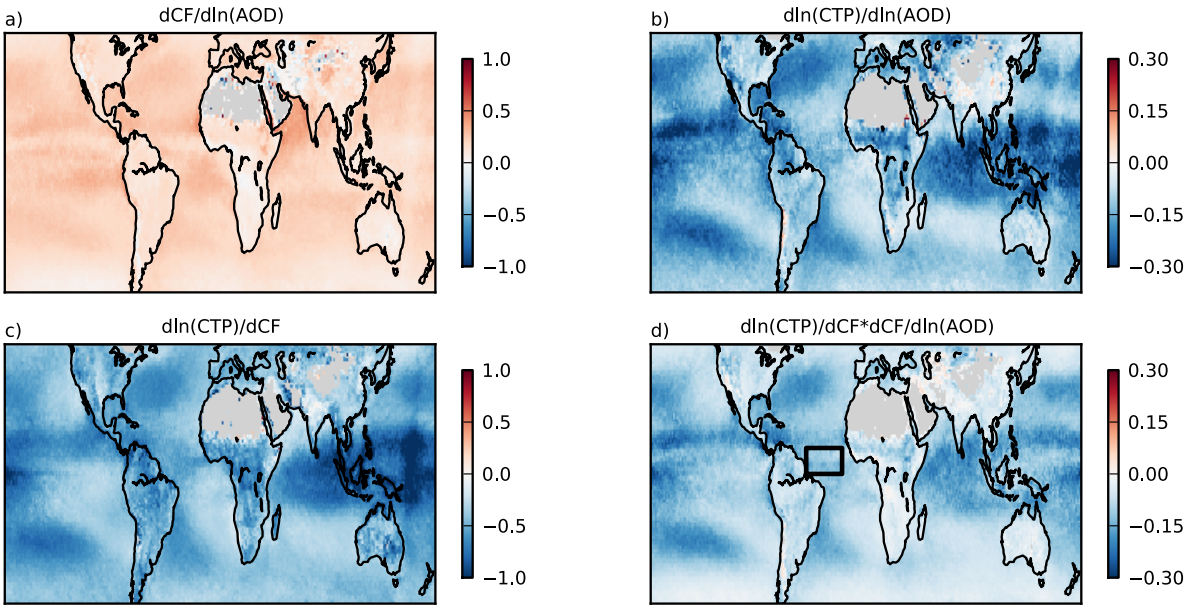

Figure 2.1: a) Sensitivity of cloud fraction to ln(AOD), b) sensitivity of ln(CTP) to ln(AOD), c) sensitivity of ln(CTP) to CF. d) The reconstructed ln(CTP) - ln(AOD) sensitivity generated assuming the relationship is mediated by CF. Grey regions indicate missing data. The highlighted region in (d) is studied further in Fig. 2.2

2.2 Results

Similar to the previous studies discussed in the introduction to this chapter, strong sensitivities of both CF (Fig. 2.1a) and CTP to AOD (Fig. 2.1b) are found over the majority of the globe. There is also a strong sensitivity of CF to CTP, (Fig. 2.1c), especially in convective regions. This is likely due to deep convective clouds having both a high CF and low CTP, but may also be due to retrieval errors in broken cloud regions, where cloud flagging is not perfect. In this case, radiances from the underlying surface can be included with radiances from clouds, resulting in a warmer apparent cloud top temperature and so a lower retrieved cloud top height. This is more common in low cloud fraction pixels and can result in a negative correlation between CF and CTP for low clouds (Zuidema et al., 2009). Other than possible retrieval errors, the changes in CTP may not be the result of changes in CF, so this may only represent a statistical rather than causal relationship between the cloud properties.

Using the sensitivity of CTP (p_{top}) to CF (f_c) and CF to AOD (τ), the sensitivity of CTP to AOD can be considered as in Eq. 2.1. The combination of the statistical relationships between CF, CTP and AOD can then be used to determine the residual term, the part of the sensitivty of CTP to AOD that is not mediated by the CF. The residual term includes the sensitivity of CTP to AOD at constant CF (and with constant meteorology) as well as other terms. Using the natural logarithm of the AOD

allows the use of linear regression to determine the sensitivies as the relationship between AOD and cloud properties is thought to be non-linear.

$$\frac{\mathrm{dln}(p_{top})}{\mathrm{dln}(\tau)} = \frac{\mathrm{dln}(p_{top})}{\mathrm{d}f_{\mathrm{c}}} \times \frac{\mathrm{d}f_{\mathrm{c}}}{\mathrm{dln}(\tau)} + \text{Residual} \tag{2.1}$$

When the negative relationship between CF and CTP in Fig. 2.1c is multiplied by the strong positive sensitivity of CF to AOD (as in Eq. 2.1), a pattern between AOD and CTP (Fig. 2.1d) can be generated that is similar to that found when calculating the sensitivity of CTP to AOD (Fig. 2.1b). Given the uncertainty surrounding the causes of the AOD-CF relationship (Quaas et al., 2010; Grandey et al., 2013b), this suggests that effects other than an aerosol influence on cloud processes may play an important role in determining the strength of the sensitivity of CTP to AOD.

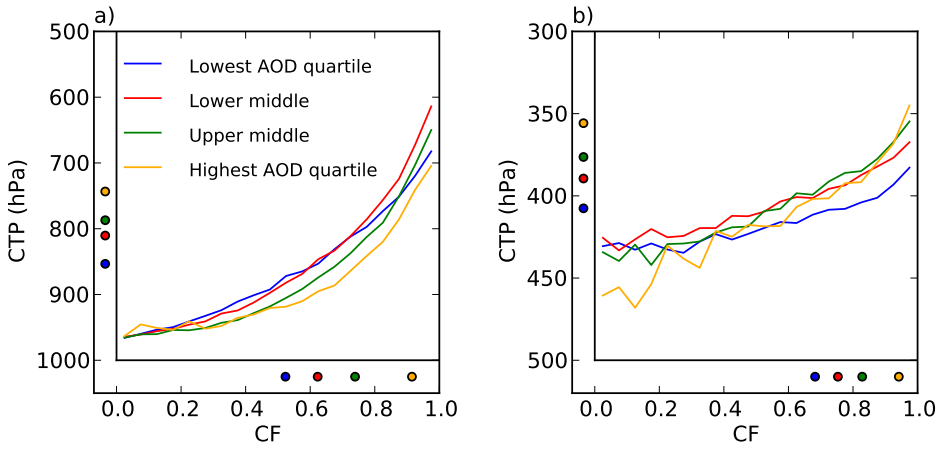

Figure 2.2: a) The dependence of mean CTP on CF for four AOD quartiles. The dots on the axes indicate the mean of the property for each AOD quartile. b) As (a) but restricting the CTP to those with a mean CTP above 600hPa.

A closer examination of clouds in the central tropical Atlantic (10°N-10°S,20°W-50°W), (the region marked in Fig. 2.1d, similar to that used in Koren et al. (2010a)) shows the relationship between CF and CTP has a weak dependence on AOD (Fig. 2.2a). This region has many convective clouds and is also in the outflow region for African aerosol, providing a good location for the study of potential aerosol influences on CTP.

For a given CF, the higher AOD populations have typically lower cloud tops (a higher CTP). Given the prevalence of low clouds, and the difficulty in retrieving the CTP for these clouds, it is possible that this negative relationship is due to the retrieval rather than an effect of aerosols on cloud properties. This dependence is opposite from that seen with the mean CTP (dots in Fig. 2.2a), where

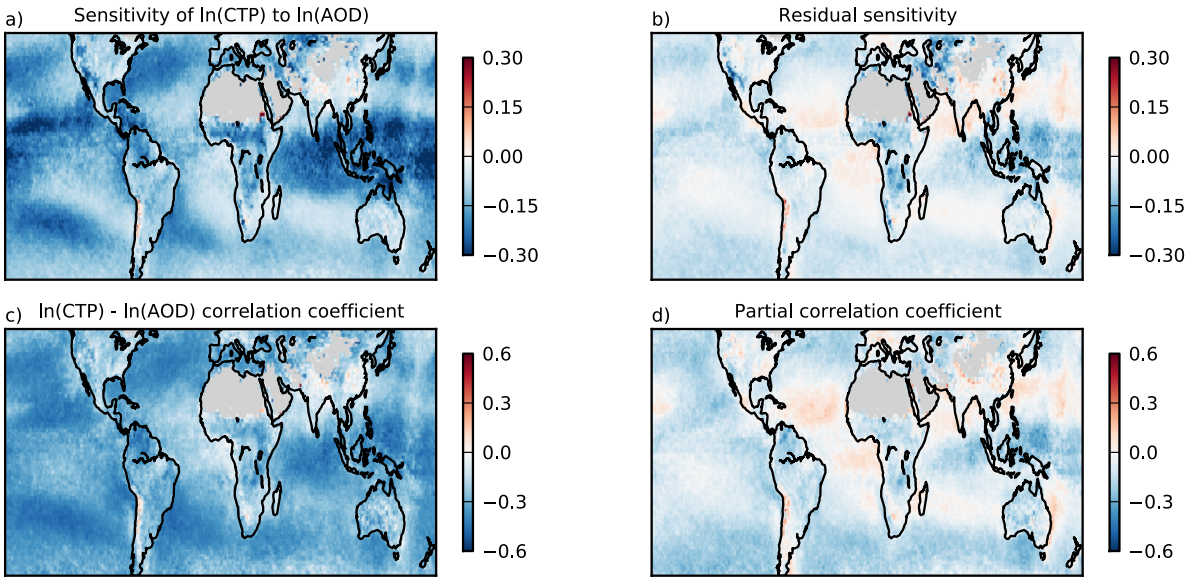

Figure 2.3: a) The sensitivity of ln(CTP) to ln(AOD) over 9 years of MODIS data (as in Fig. 2.1a). b) The residual sensitivity of ln(CTP) to ln(AOD) once the reconstructed AOD-CTP relationship (Eq. 2.1) is removed. c) The correlation of ln(CTP) and ln(AOD). d) The residual correlation (Eq. 2.2) of ln(CTP) to ln(AOD) accounting for CF as the co-varying variable.

increased AOD is correlated with a decrease in CTP. A strong AOD-CF relationship is found in this region, which when combined with the strong CF-CTP relationship, results in an decrease in CTP at increased AOD despite the AOD-CTP relationship having the opposite sign at fixed CF in this region.

As the convective invigoration hypothesis predicts effects mainly on high topped cloud, this analysis is repeated with the CTP retrievals restricted to only those above (CTP less than) 600 hPa (Fig. 2.2b). The mean CTP for retrievals above 600 hPa is determined using the CTP histogram in the level 3 MODIS product. This has the added benefit of being in the altitude region where MODIS determines CTP using CO_2 slicing rather than IR temperatures, resulting in a more accurate determination of the CTP (Menzel et al., 2008). For these high clouds, CTP is not such a strong function of CF. There is also a weak dependence of CTP on AOD for fixed CF, displaying higher clouds at higher AOD. However, the combination of the AOD-CF and the CTP-CF relationships are still acting to increase the observed AOD-CTP relationship.

The strength of the CF correlation and its ability to generate a strong relationship between CTP and AOD then leads to the question of what proportion of the AOD-CTP relationship is not attributable to the AOD-CF relationship (in this framework) and thus may be due to an aerosol influence on cloud properties?

The sensitivity of ln(CTP) to ln(AOD) is shown in Fig. 2.3a. Assuming that the dependence of

the CF-CTP relationship on AOD is small, the 'reconstructed' relationship can be subtracted from Fig. 2.1d, to leave the residual sensitivity (Fig. 2.3b). Compared to the total sensitivity, the residual sensitivity is much smaller, in some regions it becomes positive, indicating an increase in CTP (decrease in cloud top height) with increasing AOD. These decreases in height are located in regions with large amounts of low-lying cloud, indicating that low stratiform cloud may not respond to aerosol perturbations in the same way as convective clouds. Not all of the regions with large amounts of low level cloud show this positive sensitivity, with the east coast of South America showing a noticeably different residual sensitivity to regions in the Atlantic and the North-West Pacific. This may indicate the possibility of a semi-direct effect (eg. Koren et al., 2008; Koch and Del Genio, 2010), as these regions also have significant amounts of absorbing aerosol.

There is also a possibility of meteorological covariation generating the observed relationship. Meteorological covariations have not explicitly accounted for here, and although the removal of the CF influence on the AOD-CTP sensitivity accounts for some (due to the large influence of meteorology on the AOD-CF correlation), it is likely that they are still important in the residual sensitivity.

The correlation between ln(CTP) and ln(AOD) (Fig. 2.3c) is strongly negative over the majority of the tropics, with a decrease in the strength of the correlation on the eastern edge of the Atlantic ocean. To account for the effect of CF as a controlling variable, the residual correlation coefficient is computed by using the partial correlation coefficient (Hazewinkel, 2002). The partial correlation (Eq. 2.2) is designed to measure the linear dependence of one variable (CTP) on another (AOD), with the effect of the controlling variable (CF) removed.

$$r_{CTP-AOD\cdot CF} = \frac{r_{CTP-AOD} - r_{CTP-CF}r_{CF-AOD}}{\sqrt{1-r^2_{CTP-CF}}\sqrt{1-r^2_{CF-AOD}}} \tag{2.2}$$

The partial correlation (Fig. 2.3d) displays a similar pattern to the residual sensitivity. There is a negative correlation over the majority of the globe; however, in certain regions there is a positive correlation between CTP and AOD, indicating a reduction in cloud height with increasing AOD. These regions are characterised by stratocumulus clouds, which would not be expected to respond to aerosol perturbations according to the aerosol invigoration hypothesis (Williams et al., 2002).

2.3 Discussion and conclusions

The results suggest that a large part of the AOD-CTP relationship is an artifact of the strong AOD-CF sensitivity. As in previous work, strong ln(AOD)-ln(CTP) and ln(AOD)-CF sensitivities are observed globally. There is also a strong CF-ln(CTP) sensitivity. When the ln(AOD)-CF sensitivity is multiplied by the sensitivity of CF to ln(CTP), a similar pattern and magnitude to the sensitivity of ln(CTP) to ln(AOD) is found. The residual ln(AOD)-ln(CTP) sensitivity suggests that in some cases ln(AOD) is correlated with decreases in cloud height (increases in CTP), an effect that is obscured when CF variations are not considered.

A large part of the AOD-CF correlation has been suggested to be due to effects other than aerosol-cloud interactions, such as meteorological covariation. This suggests that the residual ln(AOD)-ln(CTP) sensitivity and correlation might be closer to the true effect of aerosols on CTP. There are two major caveats to the calculation of this residual. The first is that it is likely that there are other meteorological effects which could generate the observed AOD-CTP correlation. Accounting for these would likely reduce the residual sensitivity and correlation further.

Secondly, the potential effect of aerosols on CF is ignored here. An aerosol influence on CF would, through the CTP-CF relationship, produce a AOD-CTP relationship. This would act to increase the residual sensitivity and possibly the residual correlation. However, the proportion of the AOD-CF relationship that is due to the effect of aerosol on CF is thought to be small. Whilst there may be specific regimes where a large increase in CF is coupled to an decrease in CTP (such as convective anvils (Koren et al., 2010b)), estimates of the aerosol induced fraction of the total measured effect are usually much smaller. Mauger and Norris (2007) set an upper limit to the aerosol induced fraction at around 70% of the total; some estimates (Zhang et al., 2005; Quaas et al., 2010; Engstrom and Ekman, 2010) attribute a much smaller proportion of the total AOD-CF correlation to aerosol effects. This would suggest that including aerosol effects on CF would not result in a large increase in the residual sensitivity of CTP to AOD.

This chapter shows that a significant fraction of the observed relationship between AOD and CTP can be attributed to spurious correlations related to CF, disguising the magnitude, and in some cases the sign of the relationship between AOD and CTP. This spurious correlation does not account for the entire ln(AOD)-ln(CTP) relationship, the residual sensitivity is around 20% of the total ln(AOD)-ln(CTP) sensitivity. In regions where low-lying stratiform clouds are common, the residual ln(AOD)-

ln(CTP) sensitivity is positive, perhaps indicating a different response of these regimes to increases aerosol. This emphasises the importance of accounting for both cloud regimes and the AOD-CF correlation when investigating aerosol-cloud correlations.

Restricting CF when determining cloud properties also removes the ability to investigate an aerosol effect on CF. Although the aerosol effect on CF is expected to be small, even a small effect on low level CF could have large implications for the reflected SW radiation. As the AOD-CF relationship needs to be removed to account for the influence of CF on AOD, a different method has to be used to investigate the influence of aerosols on CF. The remainder of this thesis investigates improved ways to account for the AOD-CF relationship and other meteorological covariations whilst allowing the study of possible effects of aerosol on CF and other cloud properties.

Chapter 3

Regime–based analysis of the cloud albedo effect

Satellite studies on the cloud albedo effect have concentrated on the sensitivity of cloud droplet effective radius (r_{e}) and cloud droplet number concentration (CDNC) to AOD. Kaufman et al. (2005) found a decrease in r_{e} in shallow clouds over the Atlantic ocean with increasing AOD. A corresponding increase in CDNC with increasing AOD was found by (Quaas et al., 2008), who used the CERES science team retrieval of data from the MODIS instrument (Minnis et al., 2011) over large regions to determine the correlation between CDNC and AOD. Such satellite correlations are based on the assumption that AOD is a suitable proxy for cloud condensation nuclei (CCN) (Andreae, 2009).

These studies confine their data to specific regions for the purposes of determining the sensitivity of cloud properties to AOD, based on the assumption that the aerosol and cloud properties are largely similar across each region. However, Grandey and Stier (2010) showed that this assumption is not valid over regions larger than about 4° by 4°, due to the possibility of climatological spatial gradients of aerosol and cloud properties across the region generating spurious correlations. They also note that the sensitivity of CDNC to AOD is negative over land when using MODIS collection 5 data, which would result in a positive indirect radiative forcing from the cloud albedo effect over land, in contrast to model results (Quaas et al., 2009).

Whilst these, and other studies based on the CERES retrieval take into account spatial variations of cloud properties, they do not consider how different cloud types vary in their responses to AOD

The text and figures in this chapter based on those from Gryspeerdt and Stier (2012). (E Gryspeerdt and P. Stier, Regime-based analysis of aerosol-cloud interactions. *Geophys. Rev. Lett.*, 39, L21802, doi:10.1029/2012GL053221. The analysis and manuscript are my own work, with comments and suggestions from co-authors.

changes. Stratifying by pressure vertical velocity has previously been used to separate out different cloud regimes (Bony et al., 2004), with stratocumulus clouds being much more likely to form in regions of positive pressure vertical velocity. Jones et al. (2009) consider the indirect effect using data stratified by 850 hPa pressure vertical velocity but find very little change in the indirect forcing between regions of ascending and descending air. However, these large scale properties may not be suitable for determining cloud regimes locally. Rossow et al. (2005) suggest that satellite cloud properties provide a better description of the local state of the atmosphere.

This chapter uses cloud and aerosol data from the MODIS instrument to study the sensitivity of CDNC to AOD perturbations. By using the objective clustering method of Williams and Webb (2009) to determine tropical cloud regimes, this sensitivity for different liquid cloud regimes is calculated, determining which regimes are most important to the indirect forcing and ultimately bringing this type of statistical satellite approach closer to the physically relevant process scale. In addition, this regime based method also investigates the contribution made by sampling biases to the observed relationships.

3.1 Methods

The data is separated into different cloud regimes using the method of Williams and Webb (2009). This method uses a k-means clustering process (Anderberg, 1973) on the MODIS cloud top pressure-cloud optical depth (CTP-COD) collection 5.1 daily level 3 histogram at $1^\circ \times 1^\circ$ resolution. The k-means clustering algorithm requires the number of clusters as an input, which is determined following the method of Rossow et al. (2005). Starting at four clusters, the number of clusters is increased and the clusters are judged by whether they fulfil the following conditions: 1) The cluster centroid histograms do not change significantly when the clustering process is re-run with different starting centroids; 2) The resulting cluster centroid patterns should differ from each other such that the correlations between them are low (usually <0.6); 3) The spatial and temporal correlations between the frequency of occurrence patterns of the regimes should be low. Strong correlations between the centroid histograms or the frequency of occurrence patterns may indicate that a cluster is being repeated. In a similar fashion to Williams and Webb (2009), the additional condition that the total relative frequency of occurrence (RFO) of each of the regimes should be above 3.5 % is also imposed, as these

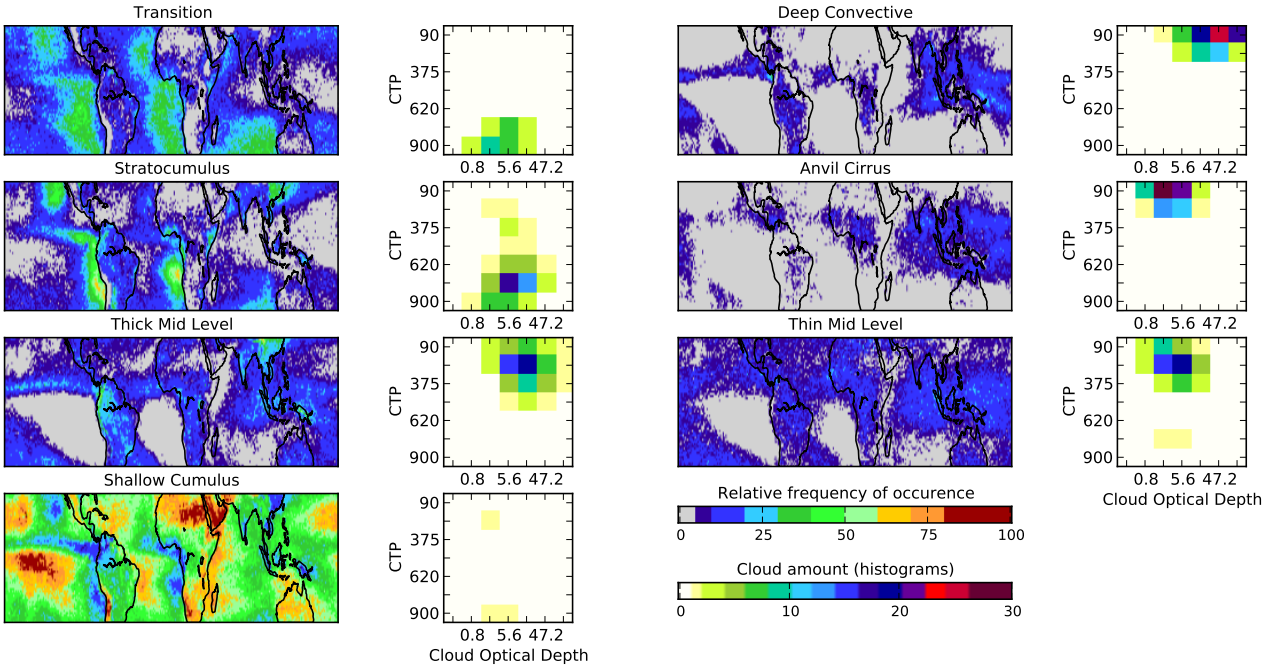

Figure 3.1: Maps of the relative frequency of occurrence (RFO) and joint cloud top pressure – cloud optical depth histograms of each cloud regime between 30°N and 30°S.

low frequency clusters tend to be sensitive to the initial seeding of the clusters. The final number of clusters used is the largest number of clusters which satisfies these criteria.

Seven clusters are found in the tropics (30°N - 30°S) (Tab. 3.1) when using 1 year of MODIS Aqua data. When dealing with the full set of data from 2003-2011, each level 3 pixel is assigned to the regime with the closest mean properties (CF, CTP and albedo). Each of these variable is normalised to the range 0-1. This assignment method improves the speed of the assignment while having a negligible effect on the regime histograms. Fig. 3.1 shows the relative frequencies of occurrence of the different regimes. The transition regime refers to the transition between the shallow cumulus and the stratocumulus regimes.

MODIS Aqua collection 5.1 level 3 daily data at 1° by 1° resolution is used for aerosol (Remer et al., 2005) and cloud (Platnick et al., 2003) property retrievals, with 'Optical Depth Land And Ocean Mean' as the AOD product. The adiabatic approximation (Eq. 3.1) (Brenguier et al., 2000) is used to estimate CDNC (N_d), where τ_c is the cloud optical depth, and $\gamma = 1.37 \times 10^{-5}\,\mathrm{m}^{-\frac{1}{2}}$ (Quaas et al., 2006).

$$N_d = \gamma \tau_c^{\frac{1}{2}} r_e^{-\frac{5}{2}} \tag{3.1}$$

This relationship assumes that the liquid water content and droplet radius increase monotonically

Table 3.1: Properties of the regimes centroids used in this study. including regime relative frequency of occurrence (RFO) and the contribution to the total mean sensitivity (Sens). The mean GPCP rainrate (Huffman et al., 2009) and the initial height used for the HYSPLIT trajectory analysis (see chapter 5) are also included.

Regime	Albedo	CTP hPa	CF %	RFO %	Sens %	Rain mm d^{-1}	HYSPLIT alt. m
Shallow Cumulus	0.452	551	24.7	50.0	11	1.13	1000
Thick Mid. Level	0.628	261	97.6	9.5	11	10.56	3000
Thin Mid. Level	0.400	270	84.3	8.6	7	5.54	6000
Transition	0.405	856	58.3	14.3	18	0.99	1000
Anvil Cirrus	0.337	137	88.0	4.5	0	6.54	8000
Deep Convection	0.697	127	98.6	3.7	-2	23.68	6000
Stratocumulus	0.487	745	83.9	9.4	58	1.75	1000

with height in the cloud, and that r_{e} is representative of the true droplet radius at the top of the cloud.

Although the MODIS cloud property retrievals are not performed where overlapping cloud layers are detected, in cases with a undetected thin cirrus layer overlying a low liquid water cloud, the retrieval of cloud droplet radius can be compromised (Davis et al., 2009). The removal of clouds where overlapping layers are detected may also influence the statistics of regime occurrence, as high-topped regimes such as the deep convective regime are unlikely to have an issue with overlapping high cloud. In this work, the retrievals in regions where no overlapping cloud is detected are assumed to representative of the dominant cloud regime at each location. Previous work (Grandey and Stier, 2010) has suggested that restricting the study to regions where only single-layer clouds are detected does not make a large difference to the sensitivity of CDNC to AOD. Following Grandey and Stier (2010), N_d is calculated using the τ_{c}–r_{e} joint histogram in the MODIS level 3 product, excluding bins where $\tau_{\mathrm{c}} < 4$ and $r_{\mathrm{e}} < 4$.

The sensitivities is calculated following the method of Feingold et al. (2003), where the sensitivity (b_{N_d}), of N_d, to AOD (τ) is given by

$$b_{N_d} = \frac{\mathrm{d}\ln N_d}{\mathrm{d}\ln \tau} \tag{3.2}$$

The sensitivities are calculated separately for each season DJF, MAM, JJA and SON, and ignore pixels with fewer than five retrievals before calculating the one-sigma error-weighted mean.

The adiabatic approximation for the CDNC is valid in adiabatic liquid clouds, assuming that there is no precipitation or entrainment, that the CDNC is constant with height and that the liquid water

content increases monotonically with height. Marine stratocumulus clouds have been found that are very close to adiabatic (Zuidema et al., 2005). Although continental clouds are often found to be sub-adiabatic, the sensitivity is defined such that the absolute magnitude of γ is not important.

3.2 Results

When considering all the data for determining the sensitivity of droplet effective number concentration to AOD (Fig. 3.2e), a strong positive sensitivity is found over ocean, indicating that an increase in AOD is correlated with an increased CDNC. There is a predominantly negative relationship over land, which is not seen either in climate models, or when using cloud data from the CERES science team retrieval of cloud properties from MODIS (Quaas et al., 2009). This negative sensitivity is not consistent with conventional theories of the cloud albedo effect, which predict an increase in cloud albedo with increasing CCN. The pattern of negative sensitivities observed is not consistent with semi-direct effects expected to occur in regions with significant aerosol absorption (eg. Stier et al., 2007), as they would not be expected to show such a clear land–sea contrast.

As expected, the regimes dominated by mixed–phase clouds (deep convective and anvil cirrus) show no significant sensitivity of CDNC to AOD (Fig, 3.2). The regimes with high proportions of liquid clouds (shallow cumulus, transition and stratocumulus) show a positive sensitivity over ocean, indicating that a higher AOD is correlated with a higher CDNC. Negative sensitivities are also found over land in the shallow cumulus regime, which has a very similar sensitivity pattern to that found when considering all data, due to the high regime RFO. In regions where the correlation is significant at the 2-sigma level, both stratiform regimes show a larger sensitivity than the shallow cumulus regime. The stratocumulus regime shows a strong positive sensitivity over ocean, especially along the western edge of the Pacific, but also over land, in contrast to the negative relationship observed in the shallow cumulus regime.

Failure to consider regimes when calculating sensitivities leads to an under-representation of the high CF regimes, as aerosol and cloud cannot be retrieved at the same location (about 60 % of stratocumulus regime has no valid AOD retrieval, compared to only 30 % of the shallow cumulus regime). This is especially important given that these regimes have a high proportion of the total liquid cloud amount. To account for this, when the regime sensitivities are recombined to calculate

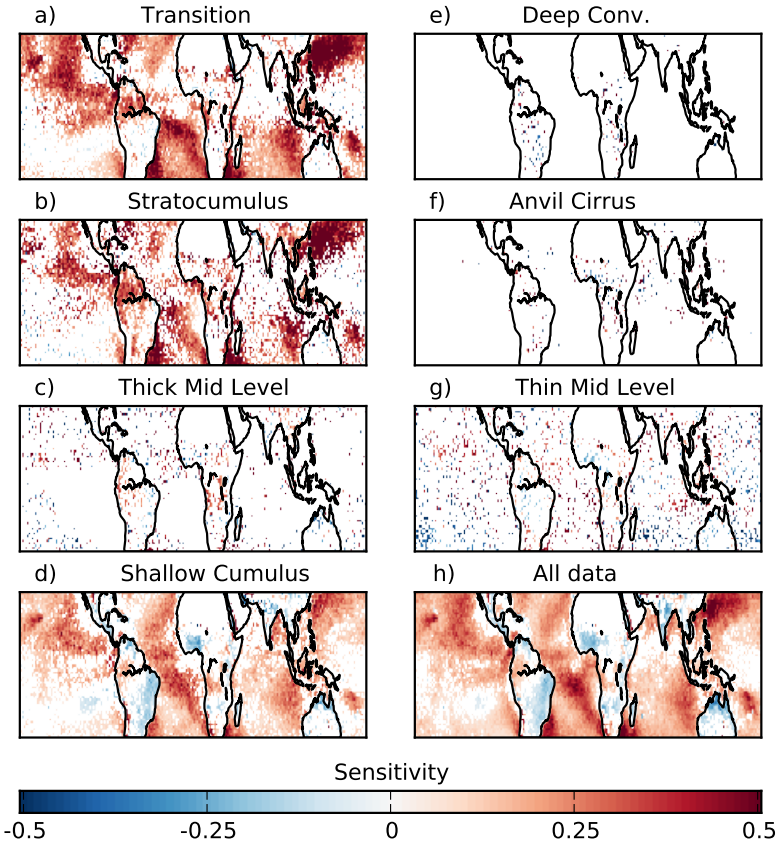

Figure 3.2: Sensitivity of cloud droplet effective number concentration (CDNC) to aerosol optical depth (AOD) for the separate regimes. This uses 9 years of Aqua-MODIS collection 5.1 cloud and aerosol products, from 2003-2011. Only relationships significant at the 2-sigma level are shown.

the total sensitivity, the regime sensitivities are weighted by the total regime RFO, which has no requirement for valid AOD retrievals. This assumes that the regimes behave similarly whether or not there is a co-located AOD retrieval. The regimes are also weighted by the regime mean liquid CF in each gridbox, on the basis that the indirect forcing from a regime/gridbox would scale with liquid CF.

Fig. 3.3 shows that the regime based method of calculating sensitivity (Fig.3.3b) results in similar sensitivities to those calculated without separating and weighting the regimes (Fig. 3.3a), but with some notable differences. The sensitivity over ocean decreases slightly, although there are increases in some regions, notably in the Western Pacific, on the edge of the stratocumulus region. In general, the sensitivity increases over land, becoming positive in some regions, compared to a negative sensitivity when regimes are not used. This is in better agreement with models and theory. Given that only the shallow cumulus regime experiences a negative sensitivity over land, this suggests that

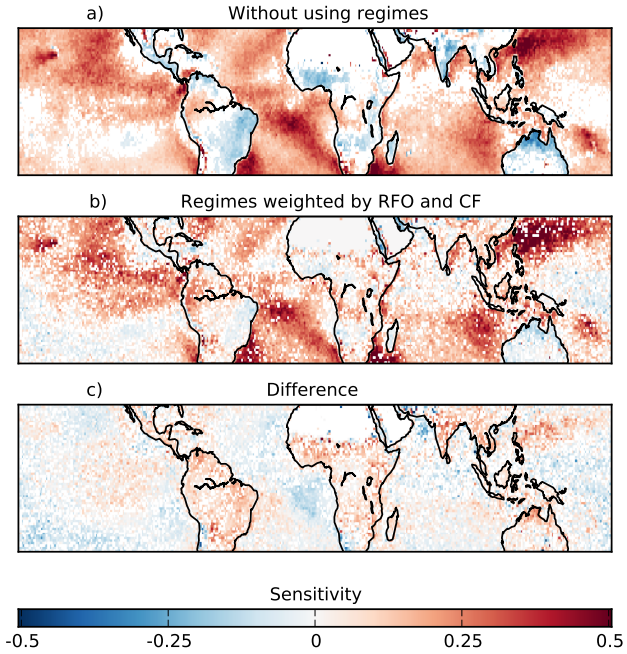

Figure 3.3: Comparison between the sensitivity of CDNC to AOD without splitting the data into cloud regimes (a), using a liquid cloud fraction and frequency of occurrence weighted mean (b), and the difference between the methods (c). Only relationships significant at the 2-sigma level are shown.

the negative sensitivity over land may be due to difficulty in retrieving CDNC in low cloud fraction pixels (Bennartz, 2007). However, these results show that the low CF pixels provide a relatively small contribution to the weighted total sensitivity (Tab. 3.1) even though they have a high frequency of occurrence, limiting the impact of this negative sensitivity. The majority of the total sensitivity comes from the stratocumulus regime, due to its high liquid CF compensating for its low frequency of occurrence.

It is also possible that the increase in sensitivity in the higher CF regimes is not a physical effect, but may be due to one of the numerous different effects which result in the strong relationship between CF and AOD (Quaas et al., 2010). However, the ability to pinpoint the source of the negative sensitivity over land to the low CF retrievals illustrates the importance of regime based analysis.

3.3 Conclusion

This chapter highlights the importance of regime–based studies of aerosol–cloud interactions, due to the differing interaction strengths of the different regimes.

Using a k-means clustering process on retrieved cloud properties, nine years of MODIS Aqua data are separated into seven tropical cloud regimes. These cloud regimes have differing sensitivities of CDNC to perturbations in AOD, with the stratiform regimes having the largest sensitivities. The shallow cumulus regime has very similar sensitivity to the total sensitivity determined without using regimes, due to its high relative frequency of occurrence.

Without accounting for the different cloud regimes, a negative sensitivity is found over land, in the location of the strongest anthropogenic aerosol perturbations. This negative sensitivity is produced by the low CF shallow cumulus regime and although this could be an aerosol effect, it does not agree with other satellite products, suggesting that it may be due to the difficulty of retrieving CDNC in low CF scenes.

Determining the sensitivity requires both AOD and cloud property retrievals at the same location. This requirement means that the high cloud fraction (CF) stratiform regimes are typically under-represented in sensitivity determinations due to a lower number of AOD retrievals reducing the apparent regime frequency of occurrence. To compensate for this sampling bias, the total regime frequency of occurrence, which is not dependent on AOD retrievals, is used to determine the regime frequency. In addition, each regime is weighted by its mean liquid CF to account for the extra contribution high CF regimes make to the forcing.

With these weightings, the stratocumulus regime contributes the most to the total sensitivity (58 % of the total) despite its low frequency of occurrence, due to high liquid CF and regime sensitivity. Due to a low liquid CF, the shallow cumulus regime only makes a small contribution to the total sensitivity (1 1% of the total), limiting the impact of the negative sensitivity of this regime. This weighting increases the total sensitivity of CDNC to AOD over land, in some regions changing the sign of the sensitivity to positive, putting it in better agreement with other studies.

This increased sensitivity of CDNC to AOD over land is particularly significant given that the short lifetime of many aerosol species leads them to be concentrated near sources, which are often over land. This increased sensitivity and the differing sensitivity of the regimes highlights the importance of regime based analysis for investigating the magnitude of the cloud albedo effect.

In the remaining chapters, the cloud regimes determined here are used to further examine the possible effects of aerosols on cloud, particularly cloud and precipitation development. Whilst the use of cloud regimes partially restricts the CF variance, reducing the influence of the AOD-CF cor-

relation, they do not fully account for it. The next chapter shows how the AOD-CF relationship can be accounted for whilst still allowing the study of possible aerosol effects on CF.

Chapter 4

Satellite observations of regime transitions

The majority of previous satellite studies of aerosol-cloud interactions are limited to a single overpass time, and so have to infer important elements of the cloud lifecycle, such as convective development and stratocumulus breakup. The use of 'snapshot' correlations, where both the aerosol and cloud properties are retrieved at the same time, limits the ability to distinguish real aerosol cloud interactions (especially aerosol influences on CF - see chapter 2) from meteorological covariation or retrieval errors.

Some previous studies have investigated the development of clouds in different aerosol environments using sub-daily time resolved satellite datasets. Matsui et al. (2006) used the Visible and Infrared Scanner (VIRS) instrument onboard TRMM to investigate the diurnal cycle of low clouds and used MODIS to provide an aerosol retrieval. However, they restrict their study to low clouds, and do not account for the different development of the cloud regimes, so may miss important effects. Lagrangian studies of marine boundary layer (MBL) clouds have also shown possible aerosol effects on cloud development. Mauger and Norris (2007) suggest that whilst there may be an aerosol effect, retrieval errors and meteorological covariations mean that a simple correlation between AOD and CF may be overestimating the influence of aerosol on CF by 30 %. They were able to study the evolution of MBL clouds over several days, using MODIS to provide the cloud and aerosol products. However, there may be important effects happening on a sub-daily timescale, such as the strong diurnal cycle of convection and stratocumulus breakup, that are missed by this approach. Meskhidze et al. (2009)

The text and figures in this chapter are based on Gryspeerdt, E.,P. Stier and D. G. Partridge, Satellite observations of cloud regime development: Links to aerosol processes, *Atmos. Chem. Phys. Discuss*, 13, 22931-22977, doi:10.5194/acpd-13-22931-20113, 2013. The analysis and manuscript are my own work, with comments and suggestions from co-authors.

attempted to reduce retrieval errors by examining the evolution of cloud properties between the Terra and Aqua MODIS overpasses as a function Terra MODIS AOD. They found an apparent increase in the breakup rate of stratocumulus clouds in high AOD environments, but they did not account for meteorological covariation or the strong AOD-CF relationship. As shown in chapter 2, not accounting for the AOD-CF relationship can lead to spurious correlations between aerosol and cloud properties.

This chapter addresses these issues with a regime based approach, using the regimes determined in chapter 3. The relationship between both the frequency of occurrence of cloud regimes and the probability of transitions between the regimes and satellite retrieved AI is investigated, with a strong emphasis placed on accounting for meteorological covariation. The development of CF is also investigated, due to the strong AOD-CF correlation making studies of aerosol effects on CF difficult. By studying transitions, the work in this chapter aims to reduce spurious correlations due to meteorological covariation and retrieval errors. It also shows how these studies of short term cloud development can be related to 'snapshot' studies, where the aerosol and cloud properties are retrieved at the same time.

4.1 Methods

MODIS L3 collection 5.1 data at 1° by 1° resolution is used for cloud property retrievals (Platnick et al., 2003), splitting data into separate cloud regimes over the period 2003-2011 inclusive. The same method as chapter 3 is used here to determine the regimes; details of the regimes are given in table 3.1. Fig. 4.2 shows the frequencies of occurrence of the different regimes in the tropics (30°N – 30°S, 150°W – 150°E) using Terra MODIS.

Only products from retrievals performed during daylight hours are used to ensure that the retrieval time within the study region is known. The region studied is restricted to 150°W – 150°E, avoiding the region around the international dateline where the overpass order of the satellites relative to UTC can be unclear.

In this chapter, the two separate MODIS instruments are used to investigate links between aerosol properties and the transitions between cloud regimes. The MODIS instruments are onboard Terra and Aqua, satellites in sun-synchronous orbits with equatorial crossing times of 1030 and 1330 LST respectively. The local overpass time can vary slightly due to the wide swath of MODIS, such that

the time between overpasses can vary from between one and a half to four and a half hours. These instruments are of the same design, minimising error due to instrument differences. There are some slight differences between the instruments, with Terra MODIS suffering from more significant optical sensor degradation than Aqua (Levy et al., 2010; Xiong et al., 2008). These differences do not affect the results of this study.

Whilst there are different possible MODIS CF products available, in this and following chapters, the MODIS cloud optical properties 'CF Combined' is used to determine the cloud regime, rather than the cloud mask CF used in chapter 2. This CF product is determined by the cloud optical properties retrieval, which ignores pixels not surrounded by cloudy pixels and pixels where the retrieval algorithm fails. This gives a lower CF than the cloud mask CF (hereafter referred to as CF Day), but it is directly related to the cloud optical properties retrieval and the ISCCP style CTP-optical depth histogram produced by MODIS and previously used for regime determination. It also reduces the probability of having heavy aerosol classified as cloud (Hubanks et al., 2008).

For atmospheric relative humidity at 850 hPa, 10 m wind speed, 500 hPa vertical velocity (ω_{500}) and low troposphere static stability (LTSS - calculated from the temperature profile (Klein and Hartmann, 1993)), data from the full resolution ECMWF ERA-Interim dataset is used, re-gridded to a 1° by 1° grid (Dee et al., 2011). The meteorological properties are re-sampled to 1030 LST by taking a weighted average of the properties at the two closest times provided by ERA-Interim.

The AOD was used in previous chapters for ease of comparison with earlier work. The aerosol index (AI) is used from this chapter onwards, generated from the MODIS AOD QA_mean and Angström exponent QA_mean products. The Angström exponent provides a size dependent measurement. The AI, as AOD multiplied by Angström exponent, is thought to provide a better estimate of CCN than the AOD alone (Nakajima et al., 2001).

To ensure that correlations caused by seasonal variations or climatological spatial gradients in cloud and aerosol properties are removed (Grandey and Stier, 2010), high and low aerosol are defined as the highest and lowest AI quartile for each 1° by 1° location, regime and season separately. This means that the difference between high and low AI varies by location and regime.

The ECMWF Monitoring Atmospheric Composition and Climate (MACC) AOD product is also used as an AOD dataset to investigate the possibility of sampling errors caused by the lack of AOD retrievals in high CF regimes (Sayer et al., 2010b). The MACC product uses assimilated MODIS

data, so while it does not account for cloud contamination or relative humidity issues, it does provide AOD estimates for cloud covered regions. As the performance of the MACC Angström exponent has not been evaluated, a MACC AI product is not created. Whilst this limits direct comparisons to results using MODIS AI, but the benefits of using AI from MODIS outweigh these drawbacks. Throughout the remainder of this thesis, the low AI population is the lowest AI quartile, and the high AI population is the highest AI quartile.

4.1.1 Transitions

The frequency of occurrence of the regimes is determined in part by the CF, so the strong AI-CF correlation would be likely to cause changes in the frequency of occurrence of the regimes with increasing AI. Changes in the mean properties of the regimes, such as precipitation rate, are less likely to be influenced by the strong AI-CF correlation, as they do not depend on the frequency of occurrence of the regimes (and hence regime CF). Such properties also include effective radius and cloud droplet number concentration as well as the probability of transitions between regimes.

The dual overpasses of the MODIS instruments allows the investigation the transitions between cloud types over the period between roughly 1030 – 1330 LST. This period is referred to as the timestep throughout this chapter. To minimise sources of variance, this study is restricted to the tropics (30°N to 30°S) where the strong diurnal cycle is the main driver of variability, rather that the synoptic systems of the mid-latitudes. Over ocean in the tropics, the diurnal cycle accounts for approximately 20% of the variability in brightness temperature. Over land the percentage variability explained by the diurnal cycle is larger, at 30 – 40%, representing a significant contribution to the total variability (Yang and Slingo, 2001).

Transitions are only defined when there is a valid retrieval and regime assignment at the start and the end of the timestep in the same location. Note that if there is no change in the regime type over the timestep, this is considered a transition between regimes of the same type. At a resolution of 1° by 1°, the scale of a single gridbox in the tropics is roughly 120 km, at the limit of whether advection should be considered over a three hour timestep. Throughout this chapter the effects of advection are neglected, as the cloud regimes are often similar over scales larger than 1° by 1°. The validity of neglecting advection over the three hour timestep is investigated in this chapter.

Statistical significance for the changes in the transition histograms is determined using a boot-

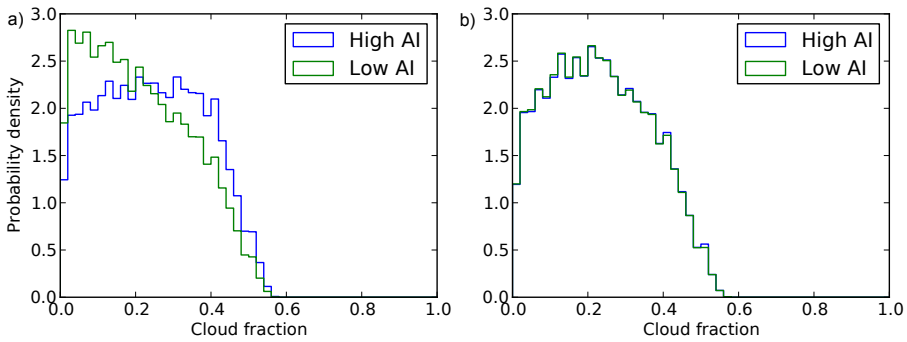

Figure 4.1: The shallow cumulus regime CF distribution for low and high AI populations. Before accounting for CF variations (a), there is a strong link between AI and CF, afterwards (b), this link is reduced. 500 hPa vertical velocity, low troposphere static stability, 850 hPa relative humidity and 10 m windspeed are also accounted for. This step is performed for each regime, separately over land and ocean.

strap method (Efron, 1979). A change in transition frequency is considered significant if the 95% confidence intervals of the transition frequency for the high AI and low AI populations do not intersect.

4.1.2 Meteorological covariations

Meteorological effects exert a strong influence on both cloud development and AI, and so must be accounted for in any study into aerosol-cloud interactions (Koren et al., 2010a). Even in the absence of other meteorological influences, the diurnal cycle results in transitions between cloud regimes. For example, the increase in convection over land during the day will result in transitions into the deep convective regime, and the breakup of stratocumulus clouds over the ocean during the day will result in transitions out of the stratocumulus regime. This study aims to determine whether separating the regimes into high and low AI populations modifies the regime transition probabilities.

Given the strong link between CF and AI, it is necessary to account for possible effects linking CF and AI at the time of the aerosol retrieval. This process is illustrated in Fig. 4.1. Normalised histograms of CF are made for the high and low AI populations. For each histogram bin, data-points are removed at random from the population with the larger frequency density in that bin until both normalised distributions match. This is performed independently for each bin, and the entire process is repeated until the populations have sufficiently similar normalised histograms. Investigations suggest that this process reduces the difference in the mean CF between the high and low AI populations to below 0.1% at the start of the timestep for each of the regimes. This process is performed for each

regime over land and ocean separately. It is not used when determining the frequency of occurrence of the regimes, only at the start of the timestep when investigating the frequency of the transitions between the regimes. While this process removes any effects of aerosol on CF, previous studies have shown that this represents a small fraction of the overall AI-CF correlation (Quaas et al., 2010). The main result of this process is to remove non-aerosol effects linking CF and AI.

Fig. 4.1 also demonstrates how the diurnal cycle may result in apparent aerosol effects on the transition frequencies if this correction is not performed. In a system made up of two regimes, defined only by high or low CF, clouds starting in the low CF regime will transition to the high CF regime if their CF is increased. As demonstrated in Fig. 4.1a, the high and low AI populations have different CF distributions. If this were an example of the low CF regime, an increase in CF of all the clouds equally, would generate more transitions for the high AI population, as it has more higher CF data-points. After the correction process (Fig. 4.1b), this effect no longer occurs, as both populations have the same CF distribution, so there would be no difference in the frequency of transitions between the high and low AI populations.

As the relationship between aerosol and cloud properties may also be influenced by relative humidity (Quaas et al., 2010), this step is repeated with ECMWF 850 hPa relative humidity. This technique is also used to ensure the high and low AI populations have the same distributions of divergence (which can be approximated by 500 hPa vertical velocity), 10 m windspeed (Engstrom and Ekman, 2010) and LTSS (Mauger and Norris, 2010), as these have all been suggested to influence aerosol-cloud correlations. It should be noted that the ECMWF RH may not provide a constraint on the actual RH (Boucher and Quaas, 2012) and the CF may be a more effective constraint on RH. It is included here as it appears to have an influence on the strength of the transitions between the regimes.

Other meteorological properties, such as sea surface temperature have been shown to have important influences on cloud evolution (Pincus et al., 1997), but they are thought to have less of an influence on the apparent strength of aerosol-cloud interactions. Not all meteorological parameters are considered here, the main focus is on parameters that have previously been shown to have strong correlations with aerosol and cloud properties (eg. Koren et al., 2010a). By ensuring the high and low AI populations have the same distribution of each of these meteorological variables within each regime, meteorological covariations controlled by these variables are reduced.

This process reduces the amount of data available for study by about half for all the regimes.

At the start of the timestep there are approximately 500,000 data-points in the shallow cumulus regime and 50,000 in the deep convective regime, the most and least numerous regimes respectively. Requiring a coincident MODIS AI retrieval removes the transitions from the deep convective regime, as there are not enough co-located MODIS AI retrievals in this regime due to the high CF. Transitions from the deep convective regime are still present when using MACC AOD, as it provides values for AOD in completely cloud covered regions.

The AI-CF relationship is removed at the time of the Terra (morning) overpass. To investigate the possible effect of aerosol on CF, the recovery of the AI-CF relationship over the three hour timestep is examined. To aid this, δ(CF) (Eq. 4.1) is defined as the difference between the mean change in CF (f_c) of the low and high AI populations over the timestep. If the AI used is retrieved at the start of the timestep and the CF sampling is performed as described in this section, δ(CF) is the difference in mean CF between the high and low AI populations at the end of the timestep. This is extended to different variables, for example, δ(LWP) would be the difference in mean liquid water path evolution between the high and low AI populations.

$$\delta(\text{CF}) = \overline{\Delta f_c\,[\text{High AI}]} - \overline{\Delta f_c\,[\text{Low AI}]} \tag{4.1}$$

4.2 Results

4.2.1 Regime RFO changes

Fig. 4.2 shows the change in regime relative frequency of occurrence (RFO) between the low and the high AI populations, the scale being the change in percentage frequency occurrence. A positive change indicates a regime becoming more common at higher AI. There is a clear decrease in the shallow cumulus regime at high AI (Fig. 4.2h), almost universally across the globe, although the decrease is less pronounced around the Atlantic coast of Africa, in the Arabian Sea and in Indonesia. There is a corresponding increase in the stratiform cloud types, with the increase in stratocumulus regime (Fig. 4.2n) being more confined to the edge of continents than the transition regime, which increases over most of the globe (Fig. 4.2k). The decreases in the RFO of the transition regime appear to be due to thickening of the cloud in that area, seen as an increase in the stratocumulus regime. The increases in stratiform cloud are consistent with an increase in AI being correlated with

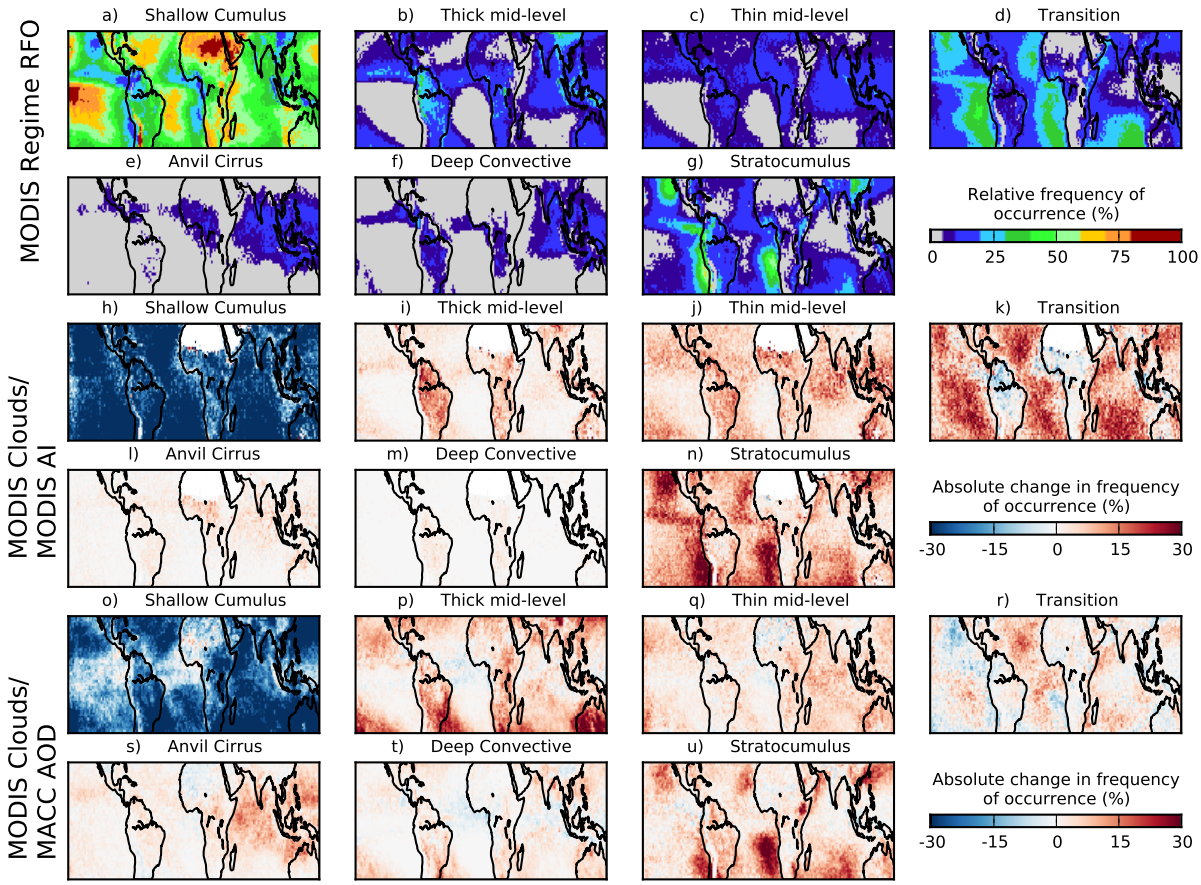

Figure 4.2: a-g)Relative frequency of occurrence (RFO) of each of the MODIS cloud regimes from Terra MODIS (2003-2011). The RFO is defined such that the sum of the RFOs for all of the regimes is 100%. h-n) The difference in frequency of occurrence of the regimes between the lowest and the highest MODIS AI quartiles. o-t) As (h-n) but using MACC AOD instead of MODIS AI as the aerosol product. Note that the effect of CF on the AI retrieval is not accounted for when determining changes in regime RFOs.

an increase in CF in the stratocumulus and transition regimes.

There is also an almost universal increase in the RFO of mid-level regimes with increasing AI. A small increase in the anvil cirrus type is also observed, confined to regions where it already commonly occurs (Fig. 4.2l). The increases in the convective types (anvil cirrus and thick mid-level) are consistent with the convective invigoration hypothesis of aerosol effects on convective clouds, resulting in an increased cloud top height. There is very little observed change in the deep convective regime RFO when using MODIS AI (Fig. 4.2m), most likely due to the low regime RFO and high cloud fraction restricting the number of locations where the Deep Convective regime exists with a valid AI retrieval.

Similar changes in regime frequency are observed when using the MACC AOD product, with

increases in deep convective (Fig. 4.2t) and stratocumulus regimes (Fig. 4.2u). The decrease in the deep convective RFO in some regions when using MACC, may be due to the effect of wet scavenging, which may not be sampled by the standard retrieval (Grandey et al., 2013b). This may also be linked to the smaller increase in the anvil cirrus regime in the same region, which also has a very high mean CF. The decrease in shallow cumulus RFO with increasing MACC AOD (Fig. 4.2o) is slightly less pronounced than when using MODIS AI. This may also be due to the effect of wet scavenging, with a reduced change in shallow cumulus clouds being easiest to see over the equatorial Atlantic and East Pacific, where the anvil cirrus and deep convective regimes are more common. The increase in the stratocumulus regime is also less pronounced, although it does occur in the same geographic locations as when using MODIS AI.

4.2.2 Transitions

To investigate the frequencies of transitions between the regimes during the three hour timestep, transition histograms similar to those of Lee et al. (2013) are used. These are two dimensional histograms, normalised such that the sum of all the transition probabilities for any given starting regime is 100% (a regime has to transition into another type). For this reason, situations where there is no change in regime over the timestep are also referred to as a transition. As an example, the top-right bin in each of the transition histograms indicates the strength of the stratocumulus (Strat.) to shallow cumulus (S.C.) transition. If this was 100%, all the stratocumulus regime clouds at the start of the timestep would end the timestep as the shallow cumulus regime.

The majority of the transitions between the regimes (Fig. 4.3a,b) occur between regimes of the same type (i.e. there is no change in the regime type over the timestep). The dominant off-diagonal elements of the transition histogram display the strong elements of the diurnal cycle. Over land (Fig. 4.3a) there are strong transitions between the shallow cumulus, thick mid-level (Thick M.L.) and deep convective (D. Conv.) regimes. The shallow cumulus – thick mid-level – deep convective pathway is referred to as the convective pathway in this thesis.

Over ocean, the transitions from the transition regime to shallow cumulus regime stand out, as do the ones from the stratocumulus regime to transition regime (Fig. 4.3b). These are a result of the breakup of stratocumulus clouds during the day (Wood, 2012). The breakup of stratocumulus is not so obvious over land, where the stratocumulus regime can be a precursor to convective cloud types,

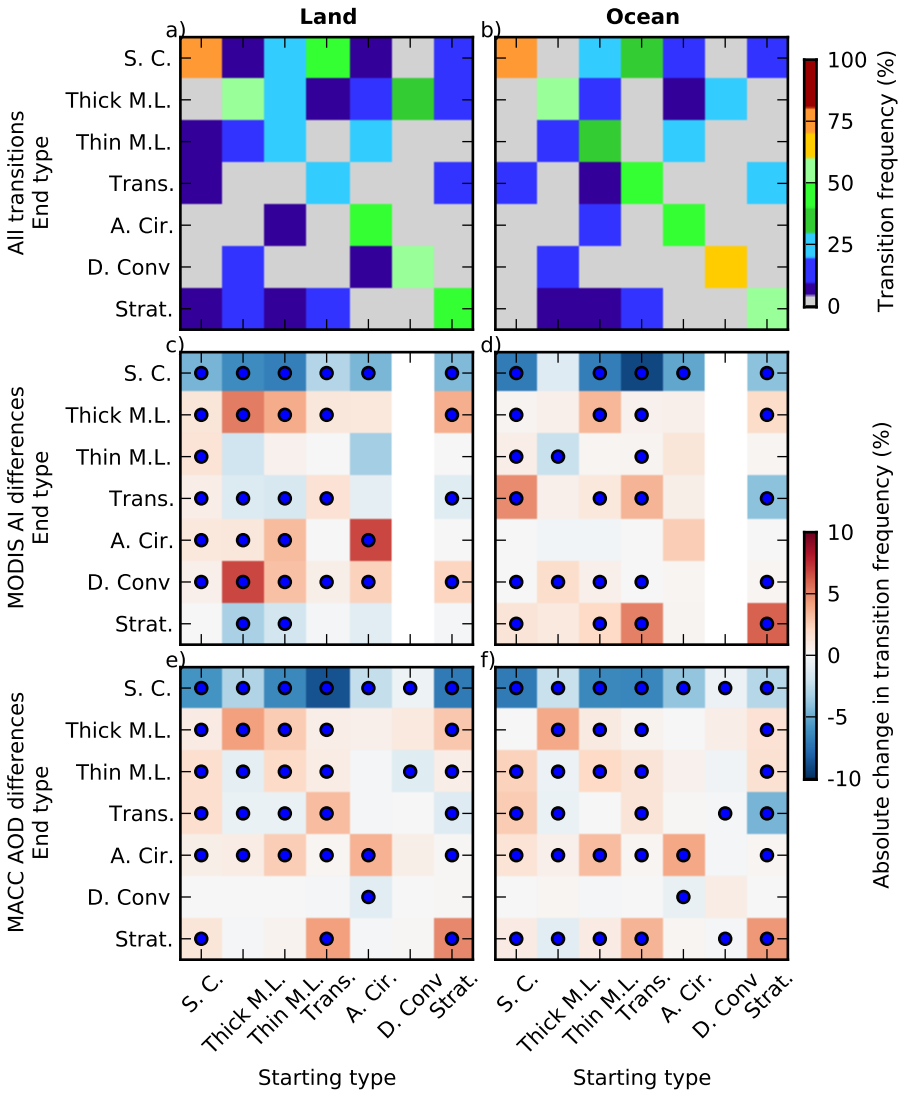

Figure 4.3: Regime transition histograms showing the conditional probability of a given transitions between regimes over (a) land and (b) ocean during the three hour period between 1030 and 1330 LST, given each starting regime. Each column sums to 100%. The difference in the histograms between the highest and lowest MODIS AI quartile days over c) land and d) ocean, and using MACC AOD over e) land and f) ocean. Positive values indicate an increase in the frequency of the transition with increasing AI. Note the non-linear colourbar in a) and b). The dots indicate 95% statistical significance. This plot covers regime transitions for the tropical region (30°N - 30°S).

in contrast to its behaviour over ocean. This is shown by the higher probability of the stratocumulus to thick mid-level transitions over land compared to over ocean. In this thesis, the shallow cumulus – transition – stratocumulus pathway is referred to as the stratiform pathway (the stratiform regimes in order of increasing CF).

When investigating the change in transition frequencies, the strong AI-CF correlation is accounted for using the method described in section 4.1.2. The difference between the regime transitions histograms for those transitions starting in the highest AI quartile and the lowest AI quartile

is less pronounced than the change in regime RFOs (Fig. 4.2b). This is partly because the transitions only consider the results of an effect over three hours, rather than the integrated effect considered by the 'snapshot' correlations present when determining the change in regime RFOs. The differing diurnal cycle over land and ocean generates different features in the difference histograms (Fig. 4.3c-f)over land and ocean. Due to the restricted number of deep convective regime clouds with a co-located MODIS AI retrieval, there are no observed changes in transitions from the deep convective regime (Fig. 4.3c,d) when using MODIS AI.

The transitions histograms over both land and ocean (Fig. 4.3c,d) show a distinct decrease in all of the transitions into the shallow cumulus regime with increasing AI. They also both show an increase in transitions out of the shallow cumulus regime, with the increase in transitions to the transition regime with increasing AI over ocean with being more pronounced.

Over land (Fig. 4.3c) the dominant effect is the increase in transitions into the thick mid-level and deep convective regimes, suggesting that the convective pathway transitions occur more frequently in the high AI population. There are also increases in transitions into the anvil cirrus regime (A. Cir.). The particular transitions to note for the convective pathway are the increase in thick mid-level to deep convective and the increase in stratocumulus to thick mid-level, as they are both important for the convective pathway over land.

These changes in convective pathway transition frequencies are consistent with the hypothesis of invigoration of convective clouds by aerosols. There are increases in transitions into the deep convective regime and the anvil cirrus regime, which are consistent with an invigoration hypothesis (Williams et al., 2002; Koren et al., 2005), and an increase in anvil area (Koren et al., 2010b). The increase in the stratocumulus to thick mid-level transition over land is also characteristic of an increase in convective activity with increasing AI. Convection over land in the tropics can develop from widespread low clouds with high CF (Machado et al., 2002), which appears here as the stratocumulus regime. The transitions from stratocumulus to thick mid-level represent the initiation of convection, while the thick mid-level to deep convective transition is a later state in the cloud lifecycle. The increase in thick mid-level to thick mid-level transitions is at the expense of transitions from thick mid-level to the shallow cumulus or stratocumulus regimes, and so can also be interpreted as a strengthening of convection with increasing AI.

There is very little increase in the convective pathway transitions over ocean. This may be due

to the smaller AI variance over ocean (smaller difference between high and low AI quartiles) and a lower frequency of occurrence of the deep convective regime over ocean (Fig. 4.5e). It is also possible that the diurnal cycle is playing a role. Convective systems over ocean are expected to be dissipating through the day (Chen and Houze, 1997), compared to convective systems over land, where they would be intensifying.

There are also changes to transitions involving the stratiform cloud types. The stratocumulus regime becomes more persistent over ocean (Fig. 4.3d), with both increases in the occurrence of stratocumulus to stratocumulus transitions and in transitions into the stratocumulus regime. There are also increases in the transitions into the transition regime from the shallow cumulus regime, and decreases in the occurrence of the stratocumulus–transition regime transition.

Although an increase in stratocumulus persistence with increasing AI is observed in this study, previous studies have observed an increase in the rate of stratocumulus breakup. They show increased AOD is correlated with a larger decrease in CF between the Terra and Aqua MODIS overpass times (1030 and 1330 LST respectively). They speculate that this decrease may be due to increased evaporation of the cloud at the cloud top, caused by increased evaporation of the smaller cloud droplets that are more common in polluted regions (Meskhidze et al., 2009). These results are supported by some modelling studies which show an increased rate of stratocumulus breakup in high aerosol environments (Sandu et al., 2008).

The analysis presented here shows the opposite effect (Fig. 4.3d), suggesting that stratocumulus breakup is suppressed in high AI regions. This is shown by the reduced probability of a stratocumulus to transition regime transition in higher AI environments, suggesting longer lived stratiform clouds and resulting in an increase in stratiform CF with increased AI. This slowing of the stratocumulus breakup may provide further evidence of aerosols influencing the transition from closed to open celled stratocumulus (Rosenfeld et al., 2006).

This difference is due to the more sophisticated accounting of meteorological properties, especially CF, at the start of the timestep in this study. In stratocumulus clouds, initial CF is correlated with the decrease in CF over the timestep, such that a high initial CF is correlated with a large CF decrease over the timestep. When coupled with the strong AI-CF relationship, this results in an apparent aerosol induced reduction in CF over the timestep. If the strong AI-CF relationship is accounted for, a slight increase in CF over the timestep with increasing AI is found, which exhibits itself in this

study as an increase in stratocumulus persistence with increasing AI.

The use of MACC AOD to provide aerosol properties co-located with MODIS cloud properties does suggest some possible sampling errors, although the main features of the transition histograms are the same. Whilst there is still an increase in the convective pathway transitions when using MACC AOD, there is no longer an increase in transitions into the deep convective regime (Fig. 4.3e). There is also a strengthening of the stratiform pathway over land compared to MODIS AI. Over ocean (Fig. 4.3f), there is a very slight decrease in the strength of the stratiform pathway compared to MODIS, which may also be due to sampling issues in the high CF stratocumulus regime. These differences are probably due to wet scavenging in cloud-covered scenes in the MACC product. These are under-sampled in the MODIS product, as aerosol properties can not be retrieved in cloud covered scenes. There is some uncertainty over whether the changes as a function of MODIS AI or MACC AOD are more reliable, as although MACC eliminates sampling issues, its accuracy in cloud covered scenes is not known (Grandey et al., 2013b). It is possible that as the aerosol in cloud covered scenes has been influenced by the cloud (such as by wet scavenging), it may not be suitable for determining the influence of aerosols on cloud.

The results for the changes in frequencies of transitions between the cloud regimes where a 'clear-sky' regime is included are shown in Fig. A.3. In general, the 'clear-sky' regime is not included in this study, as it almost exclusively only exchanges with the shallow cumulus regime. Having zero CF also means that the CF cannot be used to limit humidity variations. The exclusion of the 'clear-sky' regime does not impact the results in the remainder of this work.

4.2.3 Regional effects

Transitions from the shallow cumulus regime are investigated here, as the shallow cumulus regime has the largest frequency of occurrence across the tropics (Fig. 4.2a). To prevent regional variations in the AI-CF relationship from affecting the transition frequency spatial patterns, the method described in section 4.1.2 is applied to regions of 5° by 5°. This ensures that each location has the same CF distribution, rather than just each regime. This resolution gives enough data to determine the transition frequencies whilst still maintaining a reasonable spatial resolution and acceptable sampling errors (Grandey and Stier, 2010).

The changes in transition frequencies observed in Fig. 4.4 are well correlated with both increases

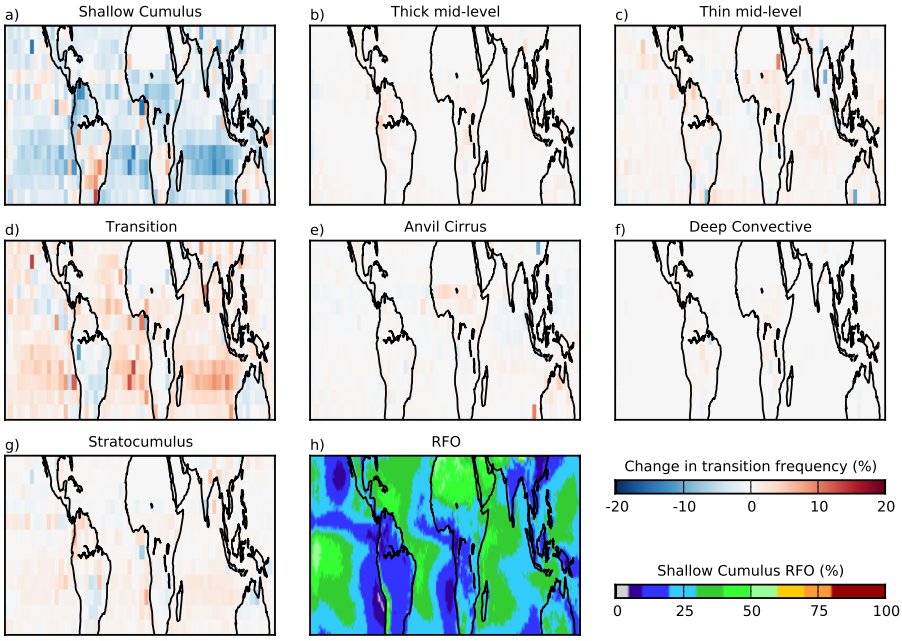

Figure 4.4: Difference in transition frequency between the low and high AI populations for transitions from the shallow cumulus regime. These maps correspond to the first column of Fig. 4.3d. The relative frequency of occurrence of the shallow cumulus regime is shown in the final plot. These plots all use MODIS Aqua and Terra data from 2003–2011, between 30°N and 30°S.

in δ(CF) and decreases in δ(CTP) (Fig. 4.5a,h). The increase in δ(CF) is much less pronounced in the Northern Hemisphere, although over land it is much larger, generating a corresponding larger decrease in the shallow cumulus to shallow cumulus transition (Fig. 4.4a). In this case, the decrease in CTP may be a consequence of the increase in CF due to the strong CF-CTP relationship (Chapter 2).

The liquid water path (LWP) for shallow cumulus clouds is larger in high AI environments than low AI environments across the tropical oceans, apart from the Atlantic (Fig. 4.5c,g). Over the timestep, δ(LWP) shows a pattern similar to but opposite in sign to that of δ(CF) (Fig. 4.5a). The increase in LWP at the start of the timestep is similar to model results, with most GCMs predicting a large increase in LWP with increasing AOD (Quaas et al., 2009). This study finds a negative δ(LWP) in the shallow cumulus regime, suggesting that increased AI is correlated with a reduction in LWP. This decrease in observed mean LWP is not due to a decrease in LWP of existing clouds at higher AI. It results from an increase in low LWP clouds, which generates an increase in CF in the high AI population. The CF weighted LWP increases over the timestep (not shown), suggesting that the total cloud water increases, while the mean in-cloud water decreases. LWP retrievals may not be reliable in high aerosol regions (Seethala and Horvath, 2010), and although changes in LWP rather

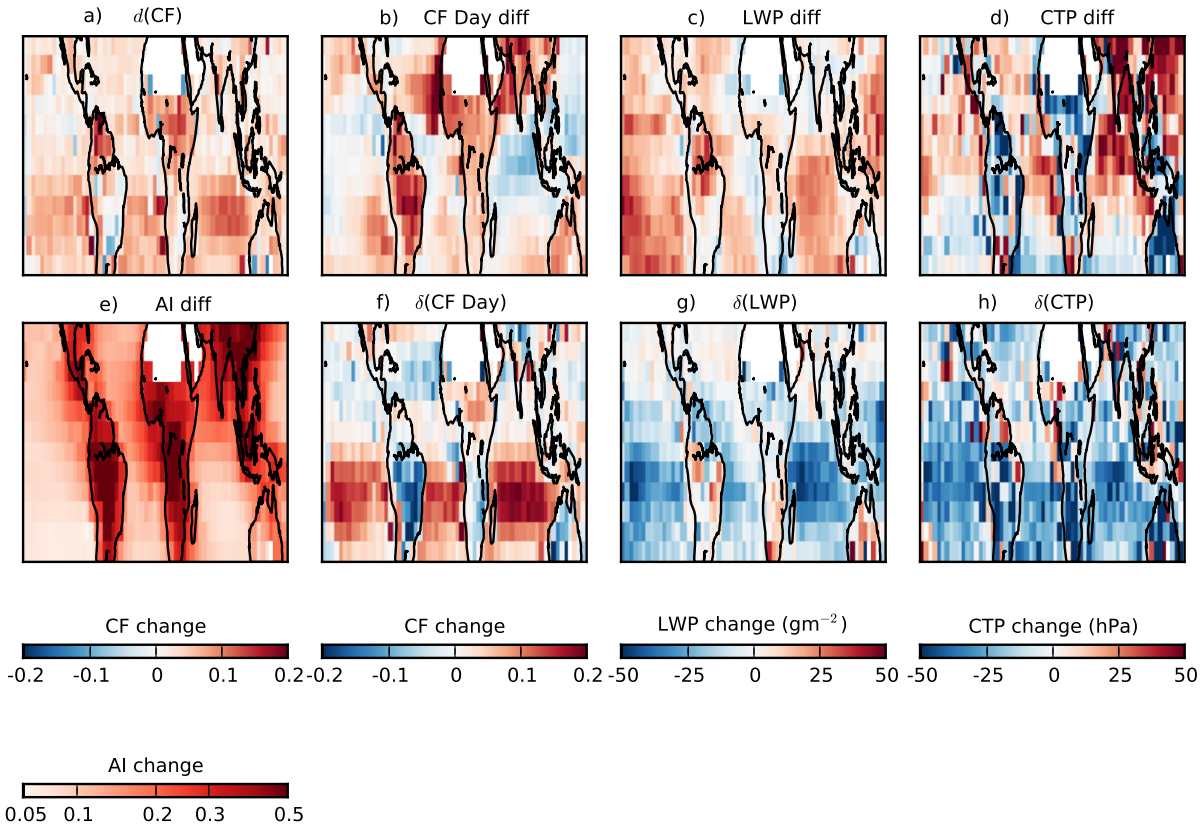

Figure 4.5: The difference in end of timestep CF and AI between the low and high AI populations (a) and the difference in AI between the highest and lowest AI quartiles (e) for the shallow cumulus regime. The difference in CF Day (MODIS cloud mask) (b), liquid water path - liquid clouds (c) and cloud top pressure at the start of the timestep (d), and the difference in the evolution of these quantities over the timestep (f,g,h) are also shown. These plots all use MODIS Aqua and Terra data from 2003–2011, between 30°N and 30°S.

than absolute magnitudes are investigated here, these changes may also be unreliable.

Given the strong relationship observed in δ(CF), changes in the MODIS CF Day product are also investigated. The CF Day product is created from the MODIS cloud mask (MOD35), rather than the cloud properties retrieval (MOD06, referred to as CF in this chapter). The cloud properties retrieval (CF) requires each pixel where the retrieval is performed to be surrounded by cloudy pixels and so it has a smaller cloud fraction than the total cloud mask (CF Day). The CF Day product may also include some heavy aerosol flagged as cloud (Hubanks et al., 2008), and for this reason is not used when assigning the regimes or when considering the effects of cloud on AI at the start of the timestep. The ratio between CF and CF Day can also be affected by the cloud shape, as it is dependent on the perimeter-to-area ratio of the clouds as well as the amount of heavy aerosol. CF Day is often higher in the higher AI population at the start of the timestep (Fig. 4.5b), especially in regions where the

primary source of aerosol is dust, such as the West coast of Africa and the Arabian Sea. This suggests that the larger CF Day is due to aerosol contamination of the cloud retrieval (Brennan et al., 2005), but it may also be due to a changing area to perimeter ratio in these regions. As CF Day is not the same for the high and low AI populations at the start of the timestep (Fig. 4.5b), the value of δ(CF Day) at the end of the timestep (Fig. 4.5f) may be affected by the difference in the initial state. δ(CF Day) shows some similarities to δ(CF), with increased δ(CF Day) over the ocean in the Southern Hemisphere. However, there is a decrease in δ(CF Day) over the Northern Hemisphere and over land. This is most likely due to the difference in CF Day between the high and low AI populations at the start of the timestep (Fig. 4.5b), possibly due to heavy aerosol being flagged as cloud in these regions (Brennan et al., 2005).

4.2.4 Meteorology

Considering δ(CF) of the shallow cumulus regime in a meteorological variable space instead of a latitude-longitude space, the dependence of the correlations between aerosol and the CF development as a function of meteorological variables can be investigated (Fig. 4.6).

As expected, the shallow cumulus regime tends to occur in regions of subsidence and low LTSS, although it is not exclusively confined to these locations (black lines in Fig. 4.6). The δ(CF) at the end of the three hour timestep is a not a strong function of ω_{500} for the shallow cumulus regime. LTSS shows a much clearer relationship, with δ(CF) increasing with increasing LTSS. The increase in δ(CF) is particularly clear over the range from 12 to 20 K, where δ(CF) increases linearly from around 0.02 to around 0.08. Outside of this range the relationship becomes harder to determine due to the reduction in data volumes and correspondingly larger errors.

Shallow cumulus clouds develop differently under strong inversions, spreading out and tending to be topped by a stratiform cloud layer (Stevens et al., 2001). This more stratiform character could lead to increases in δ(CF) in higher LTSS regions. The increase in δ(CF) with increasing LTSS matches well with the observation of increased δ(CF) in the high LTSS regions of the Southern Hemisphere (Fig. 4.5a) and may explain the hemispheric difference in δ(CF).

Across the majority of the range investigated for relative humidity, it appears to have a relatively poor relationship to δ(CF). There is perhaps an increase in δ(CF) with increasing relative humidity above around 70%, but given the smaller quantity of data and larger uncertainty in this range it is

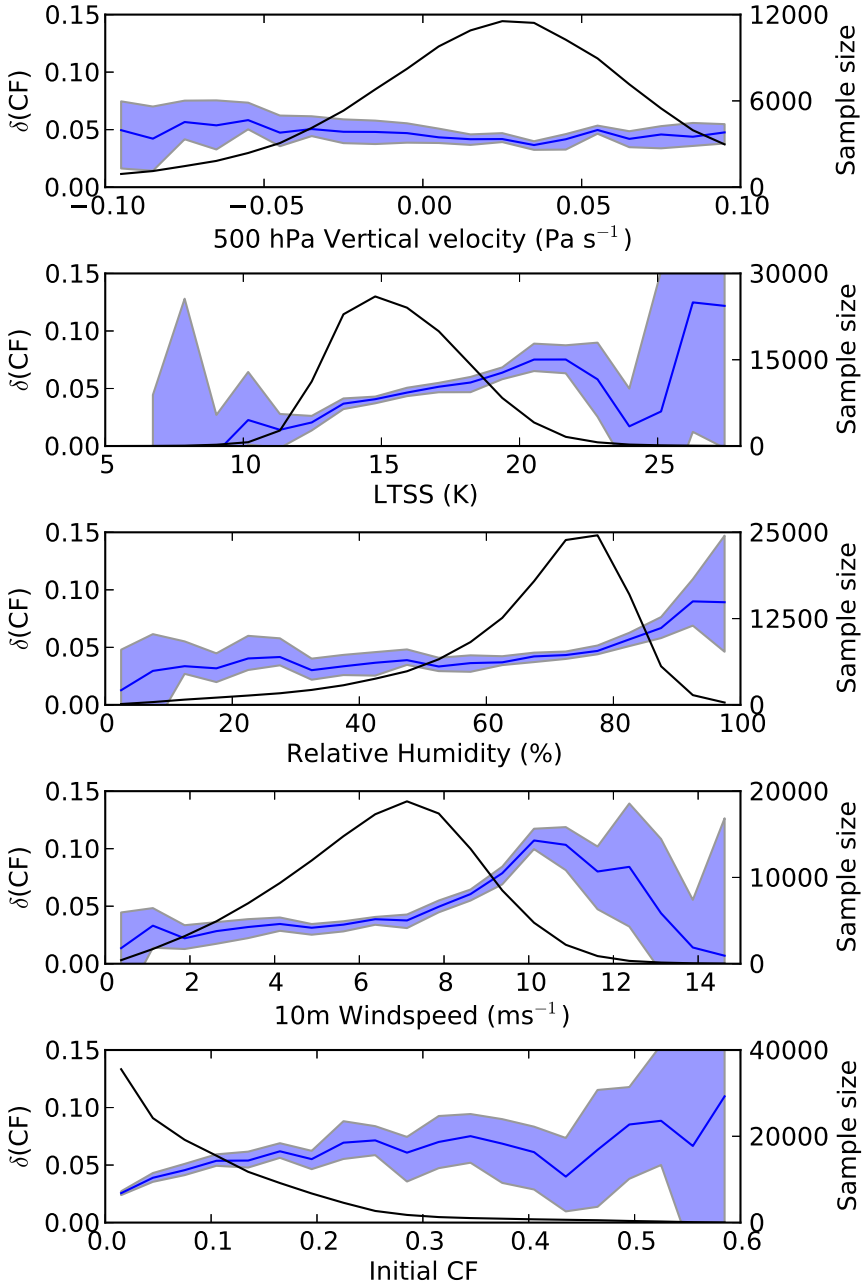

Figure 4.6: The dependence of δ(CF) (blue) on initial meteorological parameters for the oceanic shallow cumulus regime. The distribution of points as a function of meteorological parameter is also shown by the solid black line. This plot is composed from MODIS data at all the oceanic shallow cumulus points from July-August-September over the years 2003-2011.

hard to draw any conclusions.

Windspeed at 10 m appears to have a significant effect on δ(CF) above 8 m s^{-1}, where a large increase in δ(CF) can be seen, from around 0.04 to over 0.1. Below this range, there is a much less significant relationship between windspeed and δ(CF). The cause of the relationship between windspeed and δ(CF) is not clear. Sea spray is known to be related to windspeed (Woodcock, 1953),

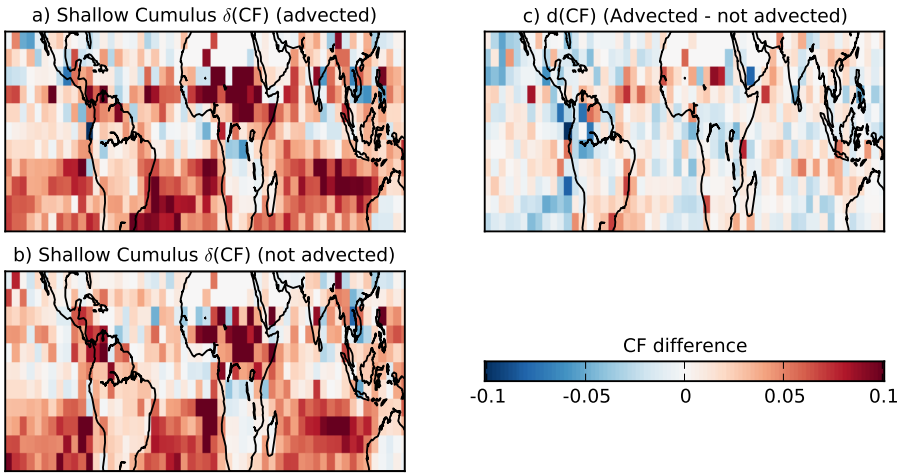

Figure 4.7: The difference in the CF at the end of the timestep between the high AI and low AI populations (δ(CF)). This figure shows the difference when advection is taken into account using HYSPLIT, when the effects of advection are neglected, and the difference between them. This plot covers the period July-September, 2003-2011.

where wind and waves force air bubbles to burst. When the 10 m wind reaches a threshold of around 7-11 m s^{-1}, 'spume' droplets are also formed, where droplets are separated from wave crests by the wind (eg. Kientzler et al., 1954; Andreas, 1998). If this increase in sea salt aerosol increases the variance in AI, this may result in an increase of δ(CF). Another possible explanation is the effect of whitecaps increasing the retrieved AI (Sayer et al., 2010a), as significant whitecaps begin to occur above about 5 m s^{-1}. How this would increase δ(CF) is unclear, as the high and low AI populations have the same distribution of 10 m windspeeds.

Whilst there is a small influence of initial CF on δ(CF) at very low values of CF, in general there is a very weak relationship between them, with a slight increase in δ(CF) at higher initial CF (Fig. 4.6).

4.2.5 Advection

The geographical pattern of δ(CF) for the shallow cumulus regime (Fig. 4.5) and the link to LTSS (Fig. 4.6), suggests the possibility of advection having an important role. The MODIS L3 resolution of 1° by 1° is at the limit of whether advection should be considered over the three hour timestep. Although advection has been neglected in this chapter, within a 3 hour timestep an airmass may well have left the 1° by 1° gridbox in which it started the timestep. This movement of airmasses

between gridboxes could generate transitions between the regimes, reducing the apparent strength of any aerosol effect on the transitions. Large scale meteorology may generate systematic errors. The tropical subsidence regions have a strong East-West gradient in CF, with the trade winds transporting air parcels down gradient. This results in higher CF air being advected into a gridbox during the timestep, an effect which may be important if advection is neglected. Advection may be generating the positive δ(CF) in the shallow cumulus regime in the trade wind cumulus regions, by advecting stratocumulus clouds into a gridbox during the timestep, apparently increasing the CF of the shallow cumulus regime.

The Hybrid Single Particle Lagrangian Integrated Trajectory Model (HYSPLIT) with a starting altitude of 1000 m is used to include the effect of advection on the observed changes in cloud fraction for the shallow cumulus regime. NCEP reanalysis data is used to determine trajectories from the centre of each 1° by 1° degree box over the period July-August-September 2003-2011. If this trajectory ends in a different gridbox after three hours, data from that gridbox is used to provide the end of timestep CF.

Comparing δ(CF) from the cases both with and without accounting for advection, the difference between them is generally much smaller than the magnitude of δ(CF) (Fig. 4.7). Taking into account advection does result in an increased δ(CF) over the north tropical Atlantic, as well as the east coast of South America. There is also a small increase over the Arabian Sea. In some cases neglecting advection reduces the observed δ(CF). In general the effect of advection on δ(CF) is much smaller than δ(CF), justifying the assumption that the effects of advection can be neglected.

4.2.6 Role of the retrieval product

To investigate the possibility that the particular retrievals used could be generating these results, this analysis is repeated using data from ISCCP (Rossow and Schiffer, 1999). In the tropics, ISCCP uses mainly geostationary satellites, allowing several views of the same region each day. This also minimises effects from instrument variation over the day and allows investigation of the region around 180° W as there is no uncertainty in the timing of the retrievals. The cloud regimes used are from Williams and Webb (2009), which restricts the analysis in this section to 20° N - 20° S as the regimes are not defined outside of this region. These are similar regimes to the ones used in this work, although there is not an exact correspondence due to differences between the instruments, retrievals

and regimes determined by the clustering processes. The GlobAerosol (Thomas et al., 2013) AOD retrieval from the AATSR instrument on the ENVISAT satellite is also used. This is similar to Terra MODIS in that it is sun-synchronous and has an overpass time of approximately 1030 LST. It has a smaller swath, meaning that it only covers the entire tropics approximately once every three days. All of the data in this section is regridded to a common resolution of 2.5° by 2.5°.

Similar results are found when using ISCCP and AATSR data (Figs. A.1, A.2) to those seen with MODIS data (Figs. 4.2, 4.3). With the AATSR AOD data, there is an increase in the strength of the convective pathway over land, which is also seen to a lesser extent over ocean. There is also a strong increase in the stratocumulus pathway over ocean, similar to the changes seen when using MODIS cloud and AI retrievals. When using MACC AOD, the increase in the convective pathway over land is not as prominent as when using AATSR AOD, similar to when using MODIS cloud retrievals. This provides further evidence that the observed results are not due to the details or resolution of either the cloud properties or aerosol retrievals.

4.2.7 Relationship to long term effects

The developmental studies presented here can only assess the possible effect of aerosol on CF over the period between the two cloud retrievals, approximately three hours in this case. 'Snapshot' studies, where the aerosol and cloud properties are retrieved at the same time, have the advantage that they represent the total time–integrated effect of aerosol on CF. However, developmental studies can be used to estimate the extent that a snapshot AI-CF correlation overestimates the influence of AI on CF.

Two AI retrievals are used, one AI retrieval with CF 'effects' on AI (such as humid swelling and cloud contamination) included (similar to a 'snapshot' study, Fig. 4.8c), and one where they are accounted for in the same way as the developmental studies in this thesis (Fig. 4.8b). δ(CF) is then compared for each of these retrievals to examine how CF 'effects' on the retrieved AI influence observed AI-CF correlations.

It is assumed here that the retrieved AI ($\mathrm{AI}_{\mathrm{retrieved}}$,$\alpha_{\mathrm{retrieved}}$) is composed of two parts, a part dependent on the actual AI ($\mathrm{AI}_{\mathrm{real}}$,$\alpha_{\mathrm{real}}$) and a scaling factor dependent on some function of the CF ($f\left(f_c\right)$) (Eq. 4.2). The developmental studies have the same CF distribution for both the high and low AI populations, and so the same CF contribution to the retrieved AI. This ensures the high AI

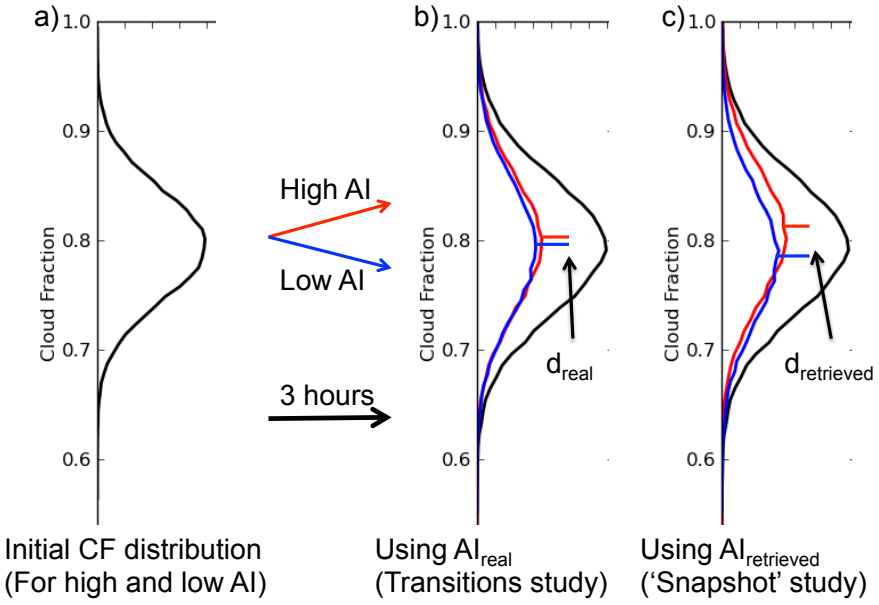

Figure 4.8: Schematic demonstrating how the time of the aerosol retrieval can affect δ(CF). At the start of the timestep (a), both the high and low AI populations have the same CF distribution. b) Despite starting with the same CF, these populations evolve differently, generating δ_{real}(CF) at the end of the timestep. c) Using the AI retrieval from the end of the timestep ($\text{AI}_{\text{retrieved}}$) gives a larger CF difference $\delta_{\text{retrieved}}$(CF), due to the effects of humid swelling and cloud contamination, which increase with CF.

population has a high AI_{real}, not just a higher CF. δ_{real}(CF) is the δ(CF) calculated in the developmental studies (Fig. 4.8b).

$$\alpha_{\text{retrieved}} = f\left(f_c\right) \times \alpha_{\text{real}} \tag{4.2}$$

The CF effects are accounted for at the start of the timestep, so the same instrument cannot be used at the same time to get an AI retrieval including CF effects for the same sample of clouds. However, at the end of the timestep, there is a second AI retrieval using Aqua MODIS. This retrieval is used as a 'contaminated' AI retrieval, as it includes the CF dependent part. This AI retrieval is referred to as $\text{AI}_{\text{retrieved}}$, and the corresponding δ(CF) as $\delta_{\text{retrieved}}$(CF) (Fig. 4.8c). Due to the included CF effects, $\delta_{\text{retrieved}}$(CF) is analogous to a 'snapshot' study.

Assuming that AI_{real} is constant across the timestep, the δ_{real}(CF) calculated using an AI retrieval that has CF effects accounted for (as in the studies of regime transitions) can be compared to one that does not account for CF effects on the AI retrieval (as in 'snapshot' studies). Comparing these for a single group of clouds shows the amount the AI-CF relationship is overestimated by studies using a

'snapshot' of the AI and CF properties.

It is important to note that the effects of CF on AI are not necessarily due to cloud contamination of the AI retrieval. Some studies of the MODIS aerosol retrieval have suggested that the residual cloud contamination effect is small (Kaufman et al., 2005), while others suggests that is plays a larger role (Zhang et al., 2005). Quaas et al. (2010) suggested that the largest contributors to the positive AI-CF relationship are retrieval errors and humid swelling of aerosols. They find that the effect of aerosols on CF in the GCM is smaller than retrieval errors or humid swelling, and may still be overestimated (Quaas et al., 2009). As the effect of AI on CF is a small fraction of the total AI-CF correlation, justifying the removal of the link between AI and CF at the start of the timestep.

Tab. 4.1 shows the different values of δ(CF) over the tropics. As expected, $\delta_{\text{retrieved}}$(CF) is larger than δ_{real}(CF) in all the regimes, over both land and ocean, in many cases by a significant margin. This shows that a snapshot AI-CF correlation will overestimate the magnitude of the possible aerosol effect on CF by at least a factor of two (Column $\delta_{\text{real}}(\text{CF})\text{Terra} / \delta_{\text{retrieved}}(\text{CF})$ in Tab. 4.1). This overestimation is slightly larger over land than over ocean, possibly due to the difficulty in retrieving aerosol over land.

So far, this work assumes that AI_{real} is constant across the timestep, considering variations in $\text{AI}_{\text{retrieved}}$ as due only to variations in CF (or related factors). An assumption of constant aerosol is reasonable in many cases, especially far from primary sources (Smirnov et al., 2002; Cachorro et al., 2004), but it will not be true in precipitating scenes, where aerosol will be removed from the atmosphere by wet scavenging. Whilst aerosol emissions would also vary AI_{real} over the three hour timestep, emissions processes are not expected to be as regime dependent as wet scavenging.

An estimate of the size of the wet scavenging effect can be calculated by comparing δ_{real}(CF) calculated separately for both Aqua and Terra MODIS. If higher rainrates are correlated with high CF, wet scavenging would be expected to reduce the difference in AI_{real} between the high and low AI populations for Aqua compared to Terra. This would result in a lower δ_{real}(CF) when calculated using Aqua MODIS AI compared to Terra.

The expected reduction is seen in Tab. 4.1, with -δ_{real}(CF)Aqua less than δ_{real}(CF)Terra. The difference is larger in regimes that have a larger precipitation rate (Tab 3.1), especially over land, providing further evidence that this change is the result of wet scavenging. The negative sign allows for a better comparison with δ_{real}(CF)Terra, as δ_{real}(CF)Aqua is determined using an AI retrieval at

Table 4.1: Difference in cloud fraction between high and low AI populations at the end of the timestep (Eq. 4.1). δ_{real}(CF)Terra uses an AI retrieval from the start of the timestep to determine a non-cloud contaminated AI, whereas $\delta_{\text{retrieved}}$(CF) uses a contaminated retrieval performed at the end of the timestep. Both δ_{real}(CF)Terra and $\delta_{\text{retrieved}}$(CF) use the same population of clouds. -δ_{real}(CF)Aqua uses an AI retrieval where the AI-CF correlation is accounted for, determined at the end of the timestep, and uses a different population of clouds, so it is not exactly comparable. It is presented as a negative due to the AI being retrieved at the end of the timestep, and so δ_{real}(CF)Aqua is determined 'backwards' in time compared to the other measurements of δ(CF)

Regime	δ_{real}(CF)Terra	$\delta_{\text{retrieved}}$(CF)	-δ_{real}(CF) Aqua	$\delta_{\text{real}}(\text{CF})\text{Terra} / \delta_{\text{retrieved}}(\text{CF})$
Land				
Shallow Cumulus	2.9	7.1	1.2	0.4
Thick Mid Level	6.1	12.5	-4.4	0.5
Thin Mid Level	6.2	12.7	-2.8	0.5
Transition	2.6	7.4	3.3	0.4
Anvil Cirrus	4.0	9.4	1.7	0.4
Deep Convective	–	–	-7.8	–
Stratocumulus	4.1	9.2	0.9	0.4
Ocean				
Shallow Cumulus	3.9	7.1	1.1	0.6
Thick Mid Level	1.6	11.0	2.8	0.1
Thin Mid Level	5.2	10.7	4.3	0.5
Transition	5.7	10.9	1.2	0.5
Anvil Cirrus	5.7	10.5	4.3	0.5
Deep Convective	–	–	-6.3	–
Stratocumulus	4.6	10.4	3.7	0.4

the end of the timestep, and so δ(CF)Aqua is determined backwards in time.

The exact effect of wet scavenging cannot be determined here, as δ_{real}(CF)Aqua and δ_{real}(CF)Terra cannot be calculated from a single group of clouds. Calculating δ_{real}(CF)Aqua requires setting δ_{real}(CF)Terra to zero (and vice-versa). Using separate populations of clouds (as done here) can only give an indication of the size of the wet scavenging effect.

The difference between $\delta_{\text{retrieved}}$(CF) and δ_{real}(CF) shows the extent of the overestimation of the AI-CF relationship when not accounting for the CF dependent part of the AI retrieval. This links the results from studying the regime transition frequencies to previous 'snapshot' correlation studies.

4.3 Correlation or causation

When considering aerosol effects, it is important to consider possible interactions between the cloud and aerosol properties that could lead to the observed correlation. The strong correlation between AI

and CF may lead to other correlations appearing, such as a CF reduction with increasing AI over the timestep, that are not the result of aerosol effects.

To account for the strong AI-CF relationship, it is removed at the start of the timestep, accounting for meteorological effects on the AI retrieval which are a function of CF (Section 4.1.2). The same process used for CF at the start of the timestep is also used for other meteorological variables that have been suggested to generate correlations between aerosol and cloud properties (Fig. 4.1). The changes in the frequency of transitions between the regimes over the timestep then shows whether the AI-CF relationship returns, and to what extent. Even after these steps are taken to remove meteorological factors and possible biases from satellite retrieval errors, there is still a positive δ(CF) (an increase in CF in with increasing AI) at the end of the timestep (Fig. 4.5). This positive δ(CF), along with changes in cloud optical depth and CTP generates transitions which are consistent with an aerosol effect on CF in stratiform clouds over ocean, and the aerosol invigoration hypothesis in convective clouds over land (Fig. 4.3).

An important issue to note here is the different effects that meteorological covariations can have on correlations between aerosol and cloud properties. These effects are separated based on how they interact with the AI retrieval. Type one meteorological effects modify the aerosol properties so as to change the retrieved AI without changing the number of CCN, and may also modify cloud properties. These type one effects include cloud contamination of the retrieval and humid swelling of aerosols, although they may act as type two effects in certain situations. Given how these are thought to be major contributors to the AI-CF relationship, by accounting for the AI-CF relationship at the start of the timestep, the impact of these type one effects is reduced.

Type two meteorological covariations are much harder to account for. These effects modify cloud properties and the CCN number simultaneously, and so would not be accounted for even with a perfect CCN retrieval. They may occur globally, such as increased windspeed modifying sea salt fluxes (Woodcock, 1953) together with surface heat fluxes resulting in changes cloud properties (Nuijens and Stevens, 2012). More local effects may also play a role, such as Saharan dust outbreaks across the North Atlantic being accompanied by warm dry air (Carlson and Prospero, 1972), influencing cloud properties. Ensuring that the high and low AI populations have the same distribution of certain meteorological parameters should act to reduce these type two errors, but without a control experiment, they cannot be removed completely.

There is some evidence that the observed changes in transitions frequencies (Fig. 4.3) may not be due to an aerosol effect. δ(CF) is remarkably similar between regimes (δ_{real}(CF) column in table 4.1) and in the shallow cumulus regime it shows a much stronger link to LTSS (Fig. 4.6) than to the magnitude of change in AI (Fig. 4.5e). This is emphasised by the lower value of δ(CF) in the Northern Hemisphere, where a larger AI variance (Fig. 4.5e) might be expected to produce a larger δ(CF).

This hemispheric discrepancy over ocean might be explained by the non-linearity of proposed aerosol effects resulting in a stronger interaction in cleaner regions. Over land, where the aerosol perturbation is larger, strong responses to aerosol perturbations are observed, indicating that this non-linearity is perhaps not the main factor. The differing nature of the clouds in the different hemispheres (Wood et al., 2002) probably plays an important role in determining the magnitude of the response to aerosol perturbations. The dependence of δ(CF) on meteorological factors would support this conclusion.

The nature of the re-analysis data used at the start of the timestep to account for meteorological covariations also introduces an uncertainty into these results. If the re-analysis was a perfect representation of the atmosphere, it could be used to sample the results in such a way as to remove the influence of meteorological covariation. The imperfect representation of the atmosphere in reanalysis data, coupled with an inability to sample every possible meteorological variable, suggests that these results provide the upper limit to an aerosol effect, as a better accounting for meteorological covariations might be expected to reduce any apparent aerosol effect on cloud properties.

4.4 Conclusions

This chapter demonstrates a way to investigate aerosol-cloud interactions which allows for the study of aerosol correlations with CF, whilst accounting for the influences of CF and meteorological properties on the aerosol retrieval. This is of particular importance, as hypothesised aerosol effects that modify the CF in some manner cannot easily be separated from CF-related errors in the aerosol retrieval. Investigating the transitions between cloud regimes also allows the direct study of cloud development in different AI environments.

The cloud regimes defined in chapter 3 are used and the change in relative frequency of occur-

rence (RFO) of different cloud regimes with changing AI is studied. By making use of the two time-separated MODIS retrievals, the frequency of transitions between the regimes in high and low AI environments is also investigated.

To ensure the transitions between regimes are not due to the strong AI-CF relationship, each regime is selected such that the CF distribution is the same for the high and low AI populations at the start of the timestep (Fig. 4.1). By accounting for variations in CF with AI, meteorological errors due to the strong AI-CF correlation are reduced. The same method is also applied to other meteorological variables thought to have effects on correlations between aerosol and cloud properties, such as 10 m windspeed and low troposphere static stability. Accounting for CF influences on the AI retrieval increases the confidence that it reflects the actual CCN. By ensuring similar meteorological conditions, the possibility that the observed results are due to differences in the meteorological environment is reduced.

With increasing AI, the RFO of both stratiform cloud types and convective cloud types increases at the expense of the shallow cumulus regime. These results would be consistent with both with an aerosol influence on the transition between open and closed cell stratocumulus clouds, and the convective invigoration hypothesis (Fig. 4.2).

The changes in regime RFOs are probably the result of the strong AI-CF relationship, and so could be considered as primarily the result of meteorological covariation (Quaas et al., 2010; Grandey et al., 2013b). There are also increases in the probability of transitions to higher CF regimes with increased AI, as well as changes in regime transition frequencies consistent with the aerosol invigoration hypothesis (Fig. 4.3). These are less likely to be the result of the same meteorological covariation, as the relationship between CF and AI has been accounted for. With increasing AI there is also an increase in the persistence of marine stratiform types over ocean, contrary to previous studies, which showed an increase in the breakup rate with increasing AOD. The increase in persistence is consistent with an aerosol influence on the open-closed cell transition in marine stratocumulus reducing the rate of dissipation of stratocumulus clouds. Similar changes in regime transition frequency are also found when using the ISCCP cloud product and the AATSR GlobAerosol AOD retrieval, indicating that this effect is not dependent on a single satellite product/retrieval (Fig. A.2).

As AI cannot be retrieved in cloud covered scenes, the ECMWF MACC AOD product is used to investigate possible sampling errors. It suggests that the results in stratiform regions are unlikely

to be significantly influenced by sampling errors. However, the reduced transition frequency into the deep convective regime found when using MACC AOD compared to MODIS AI suggests that the high precipitation rate and corresponding increased wet scavenging in high CF regimes may be important in determining any links between AI and convective cloud development (Fig. 4.3e,f).

To compare the magnitude of these results looking at cloud regime development with previous 'snapshot' studies, the change in regime CF over the timestep is investigated using AI retrieved both at the start and the end of the timestep. This gives one AI retrieval where CF influences are accounted for, and one where they are not, allowing an estimate of the possible overestimates of the AI-CF relationship in 'snapshot' studies. This shows that a simple AI-CF regression overestimates the link between CF and AI by at least a factor of two. The exact amount is uncertain due to wet scavenging processes and uncertainty in the development of the cloud regime properties, so the overestimation by 'snapshot' correlations is probably larger still (Tab. 4.1).

The increases in transitions between regimes with increasing AI (Fig. 4.3) are consistent with previously hypothesised effects of aerosols on cloud development, even after accounting for the influence of CF and meteorological parameters at the time of the AI retrieval. Whilst this study does not rule out meteorological covariation, it does reduce the upper limit on the strength of an aerosol effect on CF by at least a factor of two (Tab. 4.1). This demonstrates the importance accounting for CF and meteorological influences on aerosol retrievals when investigating aerosol-cloud interactions.

The work in this chapter demonstrates the powerful possibilities of studying cloud development, allowing for an accounting of meteorological covariation when studying aerosol-cloud interactions. In the next chapter, this method is extended to study the development of precipitation over a longer time period. In chapter six, the occurrence of cloud regimes and their response to AI perturbations is studied in a GCM, allowing an investigation into the influence of type two meteorological covariations on the relationship between AI and regime transition frequencies seen in this chapter.

Chapter 5

Links between satellite retrieved aerosol and precipitation

Observational studies have often shown an increase in precipitation in increased aerosol environments. Lin et al. (2006) compare MODIS AOD with precipitation from TRMM over the Amazon, stratifying by the cloud work function to reduce meteorological variability. They find an increase in precipitation with increasing AOD, coupled with an increase in cloud top effective radius at -10°C, suggesting an increase in ice formation. Studies using in-situ observations have also suggested a link between CCN and precipitation, with a ten-year record at the ARM Southern Great Plains site showing an increase in precipitation with increasing CCN (Li et al., 2011). At very high aerosol concentrations, opposing effects have been noted. Koren et al. (2008) show that the radiative effect of aerosols may dominate microphysical effects at high AOD, suppressing cloud formation rather than increasing it.

When considering precipitation and aerosol, wet scavenging is also important, as precipitation is expected to remove aerosol from the atmosphere (Seinfeld and Pandis, 1998). A negative relationship between AOD and precipitation might be indicative of this relationship. It is also possible that this negative relationship cannot be observed using satellites, as they cannot sample the aerosol in cloud covered scenes where the wet scavenging is occurring (Grandey et al., 2013b).

A link has been shown between satellite retrieved AOD and precipitation globally, with an almost universal increase in precipitation with increasing AOD, similar to that in Fig. 5.1 (Koren et al.,

The text and figures in this chapter are from a paper in preparation for submission to Atmospheric Chemistry and Physics which I have been working on with Philip Stier and Daniel Partridge. The analysis and manuscript are my own work, with comments and suggestions from co-authors.

2012). Whilst the interpretation of this result has been disputed (Boucher and Quaas, 2012), it shows a strong link between satellite retrieved aerosol and precipitation properties. The cause of this relationship is less clear, and may be due to meteorological covariation, satellite retrieval errors or aerosol influences on precipitation.

In this chapter, the time-dependent method developed in the previous chapter is extended to investigate the relationship between precipitation and retrieved aerosol. The main aim of this chapter is to account for possible meteorological covariation and biases in the retrievals of cloud and aerosol properties to gain a clearer picture of how aerosols might be influencing precipitation properties and development.

5.1 Methods

Both the aerosol effects on precipitation and meteorological influences on the correlation between aerosol and precipitation are expected to be strongly influenced by the cloud type, with aerosol invigoration effects expected primarily in convective regimes. Meteorological covariations, where aerosol and cloud properties are correlated because they are linked to a meteorological parameter (such as relative humidity (Quaas et al., 2010; Grandey et al., 2013b)) are particularly pervasive when considering relationships between aerosol and cloud properties, due to the strong influence of meteorological factors on cloud and aerosol. To attempt to reduce these covariations, the retrievals are again separated by cloud regime, using the regimes determined in chapter 3 and listed in Tab. 3.1. The entire tropics, 30°N – 30°S, 180°W – 180°E, over the period 2003-2007 is used in this study (2003-2009 for the maps of precipitation change).

Given the strong influence of the AI-CF correlation on other correlations between aerosol and cloud properties (see chapter 2), the regimes are again sampled such that the high and low AI populations have the same CF distributions at the time of the AI retrieval for each regime and season (see section 4.1.2). This process is also repeated for ECMWF ERA Interim 850 hPa relative humidity and 500 hPa pressure vertical velocity. As noted in the supplementary information of Koren et al. (2012), removing the link between CF and AI will reduce the vertical extent of the sample of clouds under investigation. This in turn can remove any links between AI and precipitation, including links due to an aerosol effect on precipitation. To avoid this, the diurnal nature of the cloud and precipitation

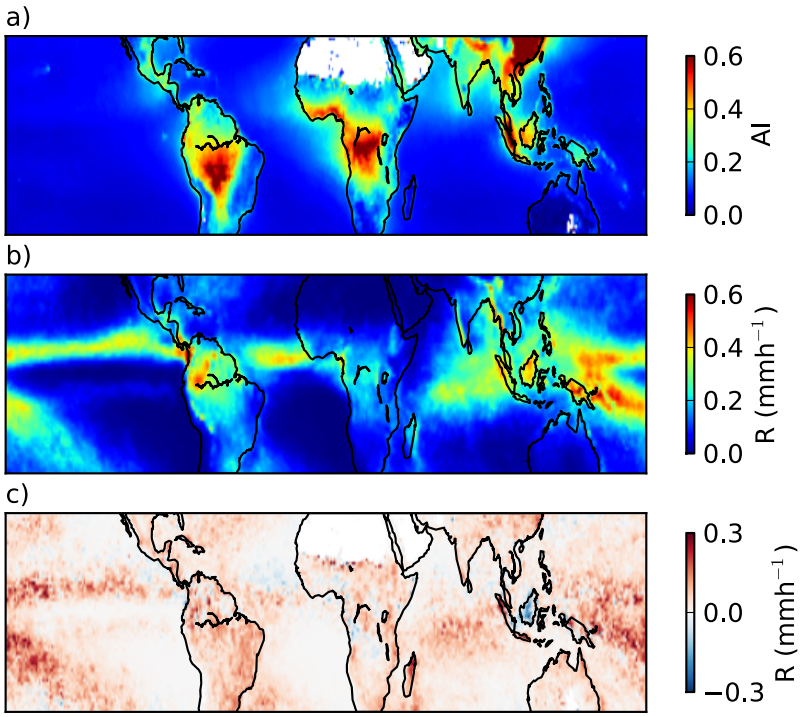

Figure 5.1: a)The annual mean MODIS aerosol index (AI) in the tropics (30°N-30°S) for the years 2005-2007. b) The annual mean TRMM 3B42 merged precipitation rate in the same region. c) The difference in TRMM 3B42 precipitation rate between days in the highest AI quartile and days in the lowest AI quartile, with red indicating an increase in precipitation at high AI (based on Koren et al. (2012))

cycle in the tropics is studied using multiple different satellite retrievals. Retrievals both before and after the AI retrieval are used to determine how aerosol is related to the development of precipitation, rather than the relationship between aerosol and precipitation in 'snapshots' of satellite retrieved properties.

As with chapter 4, MODIS is used for both aerosol and cloud properties. These are both from the collection 5.1 level 3 daily data, at 1° by 1° resolution. High and low aerosol are defined as the highest and lowest AI quartiles respectively, and are defined separately for each 1° by 1° location, regime, and season. This means that the difference in AI between the highest and lowest AI quartiles varies by location and regime, with a large difference between high and low AI in regions with a large AI variation, such as the Bay of Bengal. The mean AI value is strongly influenced by the high values due to the AI distribution being biased towards smaller values. This means that high AI regions typically have a large variation in AI. As precipitation is typically heavier in high cloud fraction regimes, to prevent sampling issues, the spatial interpolation method of Koren et al. (2012) is used. This method interpolates aerosol retrievals into cloud covered pixels that are adjacent to pixels

with a valid AI retrieval.

For precipitation retrievals, the TRMM merged precipitation product (3B42) (Adler et al., 2000; Huffman et al., 2007) is used. In this work, version 7 of the 3B42 product is used, regridded to a 1° by 1° resolution. For each TRMM 3B42 precipitation retrieval, the closest MODIS aerosol and cloud regime retrievals are determined, noting the time offset between the MODIS and the precipitation retrievals. Using the regime determined at the same time as the AI retrieval and the calculated time offset between the AI/regime and the precipitation retrievals, the diurnal cycle of precipitation is determined for each of the regimes. Due to possible missing data and sparse retrievals, the data is not used to track the development of individual clouds, only to infer the development of the regimes.

At 1° by 1° resolution, advection can cause a significant change in the properties of a single 1° by 1° gridbox over a period of 12 hours. To account for this, the HYSPLIT lagrangian trajectory model (Draxler and Rolph, 2013) is used, with NCEP reanalysis providing the meteorological data for the model. The starting altitude is determined separately for each regime (Tab. 3.1), and the model is run forward and backward 12 hours across the tropics to account for the effect of advection on the observed results. The starting altitude is determined based on the cloud regime. It is possible that the aerosols are located at a different height to the clouds and so do not follow the HYSPLIT trajectory determined for the clouds. This should have a minimal impact due to the larger spatial scales of aerosols compared to clouds and the short timescales involved (Engström and Magnusson, 2009). Any errors in the HYSPLIT trajectories should be a random rather than a systematic function of aerosol, so by using several years of data, the impact of errors in the trajectories is reduced.

In addition to these main datasets, several other datasets are also used in a lesser capacity. The TRMM Precipitation Radar (PR) reflectivity product (2A25) is used to provide a semi-independent precipitation retrieval. Whilst data from the TRMM PR is included in the 3B42 rainfall product, it is only a small component of the 3B42 product, which is based primarily on microwave precipitation retrievals (Huffman et al., 2007). The PR reflectivity also provides a vertically resolved view of the precipitation within the regimes.

The TRMM Lightning Imaging Sensor (LIS) also provides a measure of the activity of convective systems (Christian, 2003). By using high frequency optical measurements, the LIS is able to determine the lightning flash rate of storms in a 90 second observation period. An increase in lightning flash rate indicates increased vigour in a convective system. Increases in flash rate with increased

AOD have been previously observed in the West Pacific (Yuan et al., 2011b). The GlobAerosol AATSR aerosol product is again used to provide a independent aerosol retrieval.

Finally, the ISCCP three hourly D1 dataset (Rossow and Schiffer, 1999) is used to provide cloud top temperatures at several times during the day so the effects of cloud top temperature on the precipitation development, and on the possible aerosol-precipitation interactions can be investigated. The ISCCP, AATSR and TRMM LIS data are regridded to a 1° by 1° resolution.

Using the diurnal sampling ability of TRMM merged product, the precipitation development of different regimes in varying aerosol environments is investigated. This can account for the influence of CF and other meteorological properties at the time of the retrieval, whilst still allowing cloud vertical development, and time for any aerosol effects to act on the cloud properties.

5.2 Results

5.2.1 Temporal variations

Aqua MODIS is used to provide the AI and cloud retrievals, defining time zero (T+0) as the satellite overpass time (1330 local solar time (LST)). Without separating the data by regime, a differing diurnal cycle is observed over both land and ocean (Fig. 5.2a,b). Over land (Fig. 5.2b), the peak precipitation rate occurs at approximately T+4 (1730 LST), with a minimum in precipitation around T-2 (1130 LST). Over ocean (Fig. 5.2a), the peak in precipitation is less clearly defined, occurring between around T-12 and T-6 (0130 and 0730 LST). The mean precipitation rate over land is higher than that over ocean, although the mean daily minimum rain rate is similar, at about 0.05 mm h^{-1}.

When separating the data by regimes, the regime is defined at T+0. For example, this means that the deep convective regime (Fig. 5.2m,n) is only guaranteed to be a deep convective cloud at T+0. The cloud regimes transition to other regimes over the observation period; the influence of aerosols on the transition frequencies is investigated in chapter 4. The transitioning between regimes means that it is very unlikely that the clouds in the deep convective regime at T+12 are still deep convective clouds. However, they have all transitioned from the deep convective regime at T+0, so the lifecycle of the regimes can be studied.

As the regime is only guaranteed at T+0, apparent diurnal cycles can be generated in regimes/locations where the real diurnal cycle is weak or where the frequency of occurrence of a regime is particularly

Table 5.1: The mean total TRMM 3B42 merged precipitation (mm) for the six hours following T+0 for the years 2003-2007. These are the mean precipitation rates over the period T+0→+6 for each of the sub-figures in Fig. 5.2.

Regime	Ocean (mm day^{-1}) High AI	Low AI	Land (mm day^{-1}) High AI	Low AI
Total	2.10	0.78	6.13	4.11
Shallow Cumulus	0.58	0.47	2.98	2.20
Thick Mid Level	10.4	9.19	13.8	11.7
Thin Mid Level	2.10	1.87	5.85	4.22
Transition	0.72	0.56	4.11	2.73
Anvil Cirrus	1.63	1.54	4.09	3.01
Deep Convective	28.9	26.7	33.8	29.5
Stratocumulus	1.63	1.44	6.38	4.75

low. The best example of this is the deep convective regime over ocean, which shows a clear peak in precipitation at T+0 (Fig. 5.2m). In contrast to the deep convective clouds found over land (Fig. 5.2n), those found over ocean at 1330 LST are not part of a strong diurnal cycle, and they are as likely to be found early in their lifecycle as they are to be found late in their lifecycle. This makes compositing them less successful, such that their peak precipitation occurs at T+0, and their shape is defined by the timescale for formation/decay of the deep convective regime, as well as decoherence of the HYSPLIT predicted trajectory with the actual storm trajectory. This effect is most significant for deep convective clouds over ocean, but also affects deep convective clouds over land when T+0 is 1030 LST (Fig. 5.3n).

The difference in precipitation rate between the high and low AI populations when not considering regimes is large (Fig. 5.2a,b), especially over ocean (Fig. 5.2a) where there is a strong increase in precipitation with AI. At T+0, the difference in precipitation rates is comparable to those found by Koren et al. (2012), although there are some differences in how the data is prepared (quartiles rather than terciles for determining high and low AI in this study). Without limiting the study to specific cloud regimes or accounting for the AI-CF correlation, the high AI population has a precipitation rate almost three times the low AI population at T+0 over ocean, over land the increase is approximately 50%.

Separating the data into cloud regimes and accounting for CF at the time of the AI retrieval reduces the link between AI and precipitation at T+0 (Fig. 5.2c-p). Over ocean the difference in precipitation between the high and low AI populations is eliminated completely in almost all of the

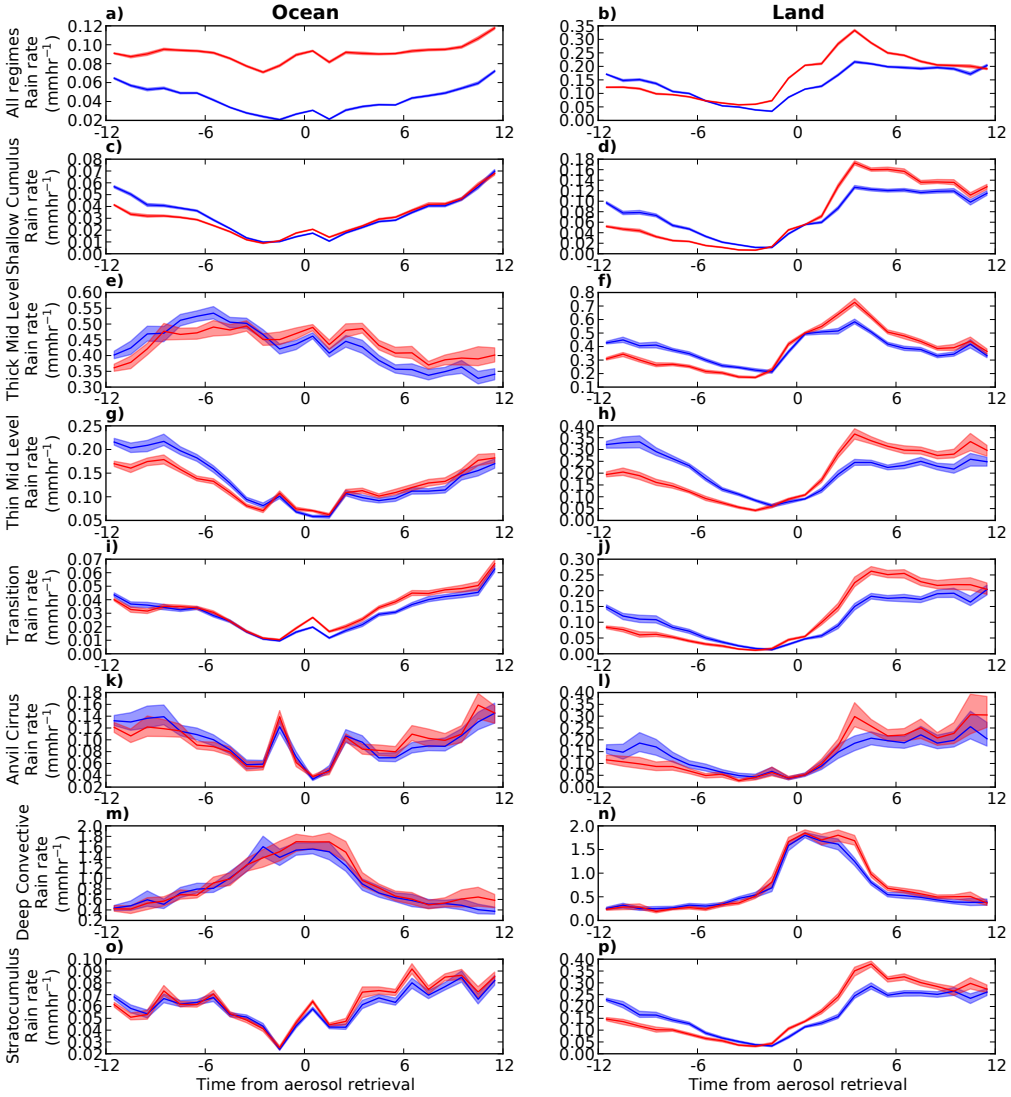

Figure 5.2: Mean precipitation rainrates at times before and after the Aqua MODIS aerosol and cloud retrieval at T+0 (1330 LST) for the region 30°N-30°S. The development in a high AI environment is shown in red and a low AI environment in blue. Statistical errors are shown at 95% significance, the variation in the precipitation rate suggests a larger overall error in some regimes due to other factors. The top row ('All regimes') shows the development of precipitation if cloud regimes and the AI-CF relationship are not accounted for. These plots are created from MODIS L3 cloud and aerosol data and TRMM 3B42 3hr Merged precipitation data over the five years 2003-2007. Numerical values for the mean precipitation between T+0→+6 are given in Tab. 5.1

regimes, with only the transition and shallow cumulus regimes showing a small difference. Over land, only the stratocumulus regime shows a significant difference in precipitation rate between the high and low AI populations at T+0, although the difference is small (Fig. 5.2p). The minimal difference in T+0 precipitation rate between the high and low AI populations is important, as it is not explicitly reduced; only the difference in CF is minimised. This emphasises the strength of

the correlation between CF and precipitation rate, suggesting that CF may act to mediate the AI-precipitation correlation in the same way as the AOD-CTP correlation (chapter 2).

Over ocean, the regimes show similar precipitation development in both the high and low AI populations. The deep convective regime shows little significant difference in mean rainrate between the high and low AI populations and the thick mid-level regime (Fig. 5.2e) shows only a small increase in precipitation in the high AI population compared to the low AI population. The stratiform regimes show slight increases in precipitation at times after the AI retrieval (Fig. 5.2c,i,o). They also show small differences in precipitation rate at T+0, although these are much smaller than those found when not accounting for the effects of CF on the AI retrieval (Fig. 5.2a). It should be noted that although the statistical errors are shown in Fig. 5.2, the variation in the precipitation rate through the day indicates larger errors in some of the regimes, especially those with low precipitation rates and a low RFO, such as marine stratocumulus.

Over land (Fig. 5.2d,f,h,j,l,n,p), the differences in precipitation development are much more striking, with all the regimes showing increased precipitation for the high AI population after T+0. At times before T+0 over land and ocean, many of the regimes show a higher rainrate from the low AI population. This difference in pre-T+0 precipitation is also seen to a lesser extent over land where the data is not separated by regime (Fig. 5.2b). This is likely due to wet scavenging, which removes aerosol from the atmosphere. A higher precipitation rate at times before T+0 would result in more aerosol being removed from the atmosphere and a lower retrieved AI at T+0. This generates an inverse relationship between pre-T+0 precipitation and retrieved AI at T+0.

The time of maximum precipitation and maximum difference in rainrate between the high and low AI populations differs by regime. The deep convective regime (Fig. 5.2n) experiences a maximum in precipitation rate between T+0 and T+2, whilst the thick mid-level regime shows a maximum at around T+3/T+4 and a significant increase in precipitation at T+0 (Fig. 5.2f). The stratiform regimes exhibit a maximum even later, at around T+4/T+5 (Fig. 5.2j,p). This change in the time of peak precipitation is due to the development of the regimes, and transitions between them. Some of the thick mid-level clouds will transition into the deep-convective regime in the hours after T+0, where they will have higher rainrates. The thick mid-level regime can be considered as partially developed deep convective clouds, which only reach their peak rainrate once they have transitioned into the deep convective regime, exhibiting a later precipitation peak. This development is evident in the shallow

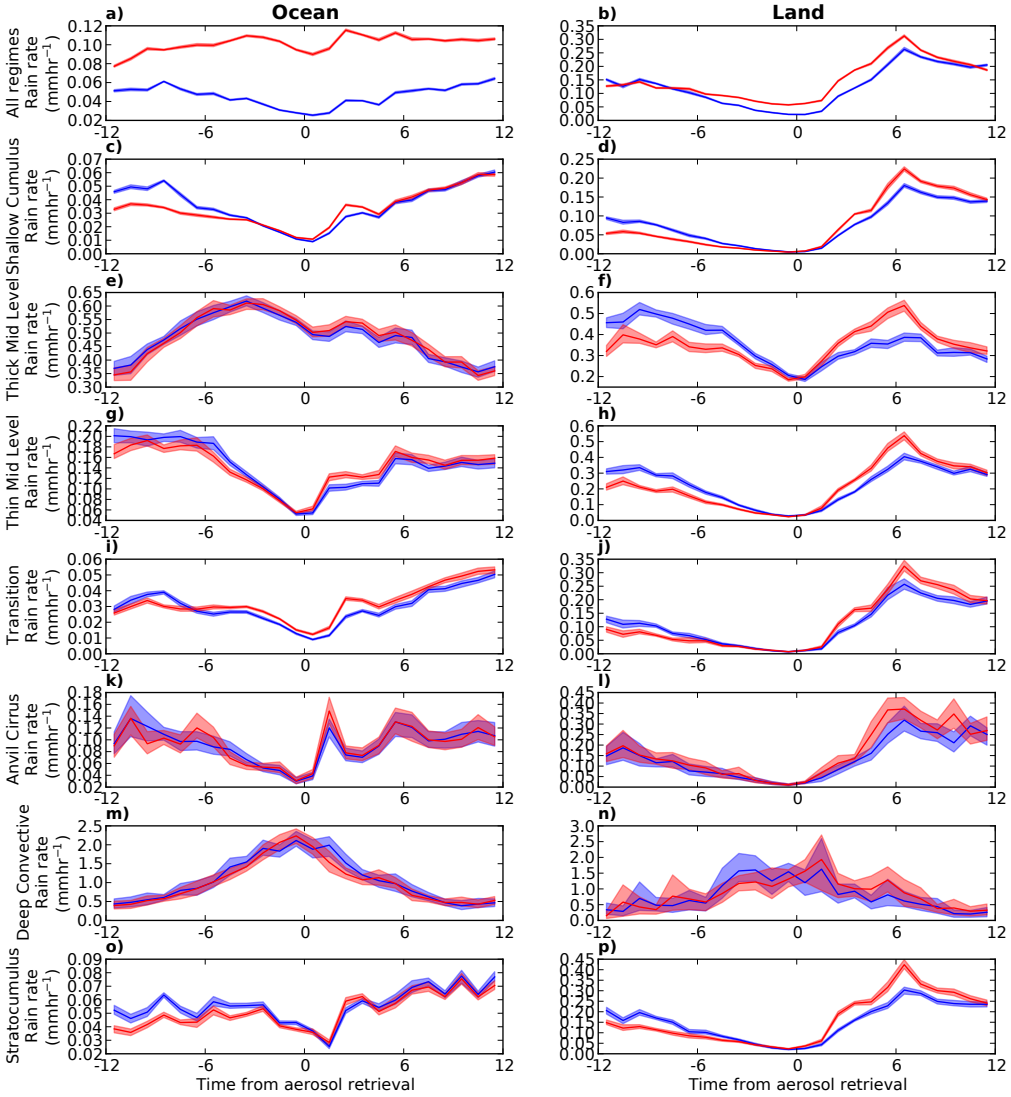

Figure 5.3: As Fig. 5.2, but using Terra MODIS for the cloud and aerosol retrievals, giving a T+0 of 1030 LST.

cumulus regime (Fig. 5.2d), where the peak precipitation rate lasts for a longer period of time and is later in the day, when some of the shallow cumulus clouds have transitioned to the thick mid-level or deep convective regimes. As this could be expected to take longer than the transition from thick mid-level to deep convective, the time of peak precipitation is later. This provides a good example of how the regime based analysis separates out clouds with different properties and at different stages of development.

Due to the timing of the diurnal cycle, many of the convective regimes observed using a T+0 of 1330 LST will have already started to develop. With a T+0 of 1030 LST, Terra MODIS is used to further investigate the precipitation development of these regimes (Fig. 5.3).

The overall patterns are very similar when using Terra AI and a T+0 of 1030 LST (Fig. 5.3) compared to Aqua AI and a T+0 of 1330 LST (Fig. 5.2). The deep convective regime over land now shows similar features to the deep convective regime over ocean, with a peak at T+0 and a steady buildup/decay in rain rate before and after T+0. This is due to the lack of deep convective clouds at this stage in the diurnal cycle over land.

The most notable difference is in the thick mid-level regime over land (Fig. 5.3f), where a much larger fractional increase in precipitation after T+0 is observed in the high AI population compared to the low AI population than is seen when using Aqua MODIS (T+0 at 1330 LST). There is almost a 30% increase in the rainrate of the high AI population over the six hours T+0→+6 compared to the low AI population, but no difference in rainrate at T+0. The increased sensitivity of the precipitation to AI changes when using Terra MODIS compared to Aqua is due to the diurnal cycle. Many of the deep convective regime clouds found when using Aqua MODIS are developing at 1030 LST and so are in the thick mid-level regime. The high AI population thick mid-level clouds are more likely to transition to the deep convective regime over the next three hours than the low AI population (Fig. 4.3). This suggests that for observing convective systems, 1030 LST has advantages for use as T+0, as it catches the systems as they are developing, rather than when they are already in the deep convective regime. However, it does not allow the investigation of developed deep convective regimes due to a low deep convective regime RFO at 1030 LST.

These regime based results show similarities to the results found without using regimes, but they also illustrate the importance of accounting for regimes and the AI-CF correlation. Whilst the restriction of CF reduces the vertical extent of the clouds (due to the strong CF-CTP relationship), not controlling for this effect can result in an overestimation of the AI-CF correlation by at least a factor of two (Tab. 4.1). Investigating the development of the regimes reduces the effect of CF on the AI retrieval, whilst allowing an aerosol influence on cloud vertical development.

5.2.2 Regional variations

As the majority of the precipitation increase with AI occurs in the 6hrs following the aerosol retrieval, the mean rainrate across the period T+0→+6 is examined to investigate regional variations in precipitation development. Due to the sparse nature of the data in some regimes, it is averaged over 5° by 5° regions (Fig. 5.4). For the rest of this chapter, only Aqua MODIS is used to provide the

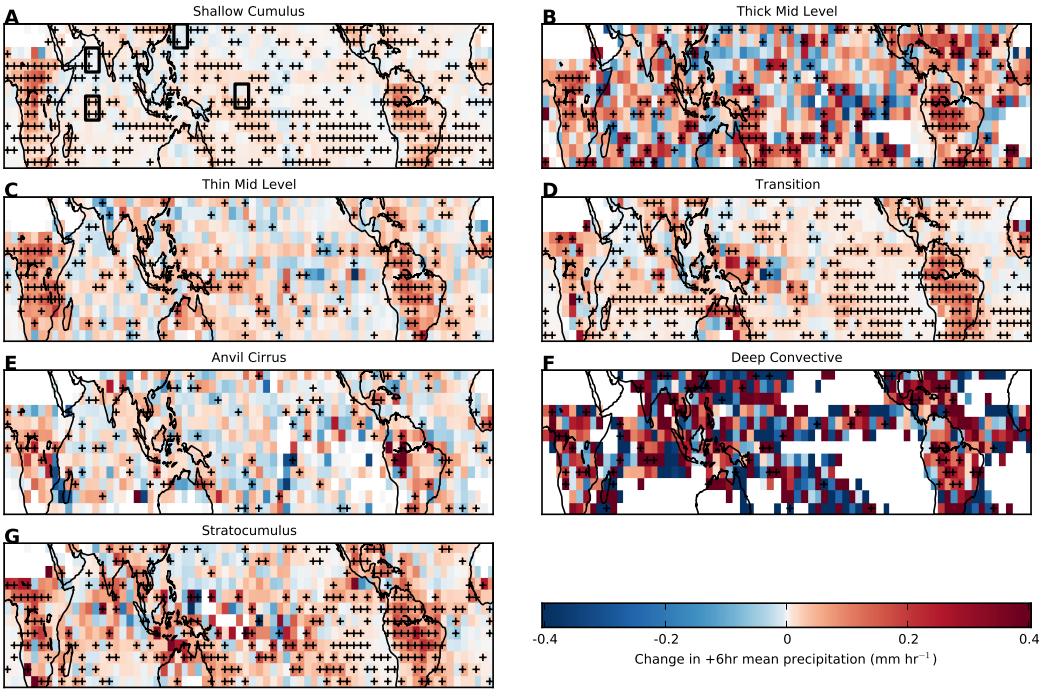

Figure 5.4: The difference in mean precipitation between the high and low AI populations from T+0 to T+6 using Aqua MODIS (T+0 at 1330 LST) for each regime, averaged over 5° by 5° regions for the period 2003-2009. Red indicates an increase in precipitation at high AI. Crosses indicate 95% statistical significance. The boxes on the shallow cumulus plot are the regions selected for further study.

cloud and aerosol properties, giving a T+0 of 1330 LST.

The difference in the regime behaviour is clear, and there are also clear regional variations (Fig. 5.4). The shallow cumulus regime shows an increase in T+0→+6 precipitation for the high AI population over almost all the continental regions (Fig. 5.4a). Also notable is the small decrease in mean precipitation over the Arabian Sea and South China Sea for the high AI population. This decrease in precipitation is confined to the region close to land in the Indian Ocean and West Pacific, with increases in precipitation being observed in the East Pacific and Southern Indian Ocean. There are some anomalous decreases in precipitation with increasing AI in the middle of the Pacific Ocean, which is most obvious in the shallow cumulus regime. These are due to an uncertainty in the Aqua overpass time around the international dateline when using level 3 MODIS data.

There is less data from the convective regimes, making determination of any regional patterns difficult (Fig. 5.4b,f). Although both the thick mid-level (Fig. 5.4b) and deep convective regimes (Fig. 5.4f) show some significant increases in mean precipitation over land, over ocean the results are too noisy to determine the magnitude or sign of any regional effect.

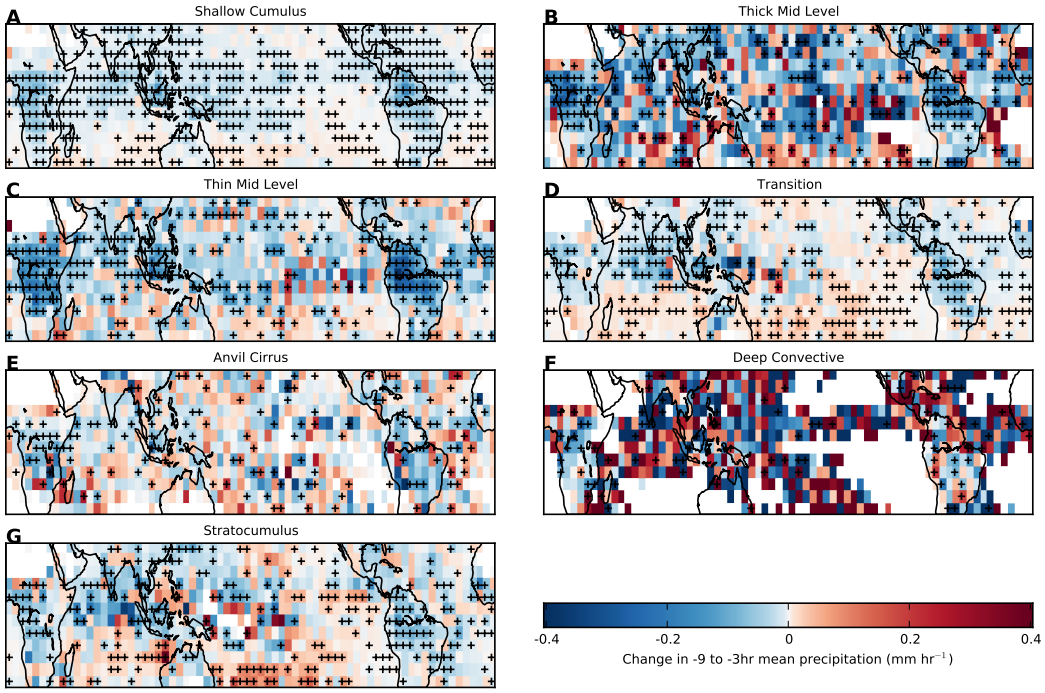

Figure 5.5: Mean precipitation difference between the high and low AI populations from T-9 to T-3 (T+0 at 1330 LST) over the period 2003-2009. Red indicates an increase in precipitation at high AI. Crosses indicate 95% statistical significance.

For the maps of the mean precipitation rate difference between the high and low AI populations between T-9 and T-3 (Fig. 5.5), the expected wet scavenging relationship is observed, with higher mean precipitation rates in the low AI population. This difference is larger in regions with high precipitation rates and occurs over both land an ocean with a similar magnitude. In some very clean regions, there is a slight increase in precipitation over the period T-9→-3 for the high AI population compared to the low AI population. This may indicate wet scavenging of aerosol is less effective or that another process, such as an increase in liquid water path in high aerosol environments, is important in these clean, low precipitation rate regions.

The difference in mean shallow cumulus precipitation rate over the period T+0→+6 between the high and low AI populations shows a clear regional pattern (Fig. 5.4a). Whilst there is an observable change in the regions where there is significant rainfall (Fig. 5.1a), it is not of the same sign globally. The strength of the effect varies with mean AI, with a decrease in precipitation with increasing AI in high AI locations, such as the Bay of Bengal, and an increase in precipitation further south in the Indian Ocean, where the mean AI is lower but there is still a high mean precipitation rate.

The relationship between the mean AI and the T+0→+6 mean precipitation rate for marine shal-

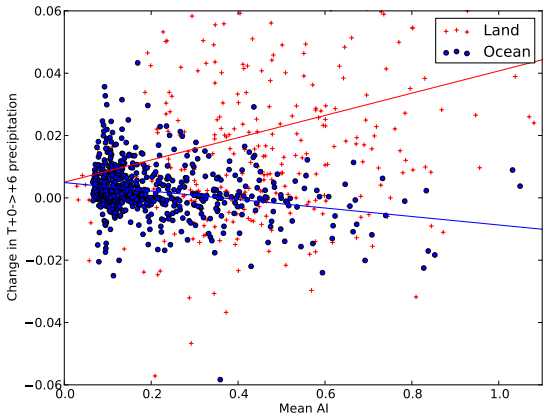

Figure 5.6: The dependence of the mean precipitation rate over the period T+0→+6 on local mean AI for oceanic (blue dots) and continental (red crosses) shallow cumulus. The change in precipitation points are taken from Fig. 5.4a. The straight lines (Kempe, 1877) are linear regressions over land (red) and ocean (blue) respectively.

low cumulus (Fig. 5.6) shows a negative correlation (r = -0.25), with increased AI being correlated with an increase in precipitation in regions with a low mean AI, but a decrease in precipitation in regions with high mean AI. There is a very low correlation between the mean precipitation and the difference in T+0→+6 mean precipitation between the high and low AI populations (r = -0.02). Over land, there is a positive correlation between the difference in T+0→+6 mean precipitation between the high and low AI populations and AI (r = 0.25), but it is smaller than the correlation with local mean precipitation (r = 0.4). Local mean precipitation is even more strongly correlated to the difference in mean T-9→T-3 precipitation between the high and low AI populations (r = -0.5) in the oceanic shallow cumulus regime, providing further evidence that this difference in precipitation between the high and low AI populations at times before T+0 is due to wet scavenging.

5.2.3 Warm and mixed phase clouds

While they depend on CTP, the regimes used in this work do not explicitly separate warm and mixed phase clouds. However, many hypothesised effects of aerosols on precipitation depend on whether the clouds include ice phase hydrometeors. Clouds with tops colder than 273 K are separated out using the ISCCP D1 cloud top temperature retrieval (Rossow and Schiffer, 1999). This is provided on a 3hr timestep, synchronised with the 3B42 precipitation retrievals. Unlike the regime, which is determined only at T+0, the cloud top temperature is required to be above 273 K for all the precipitation

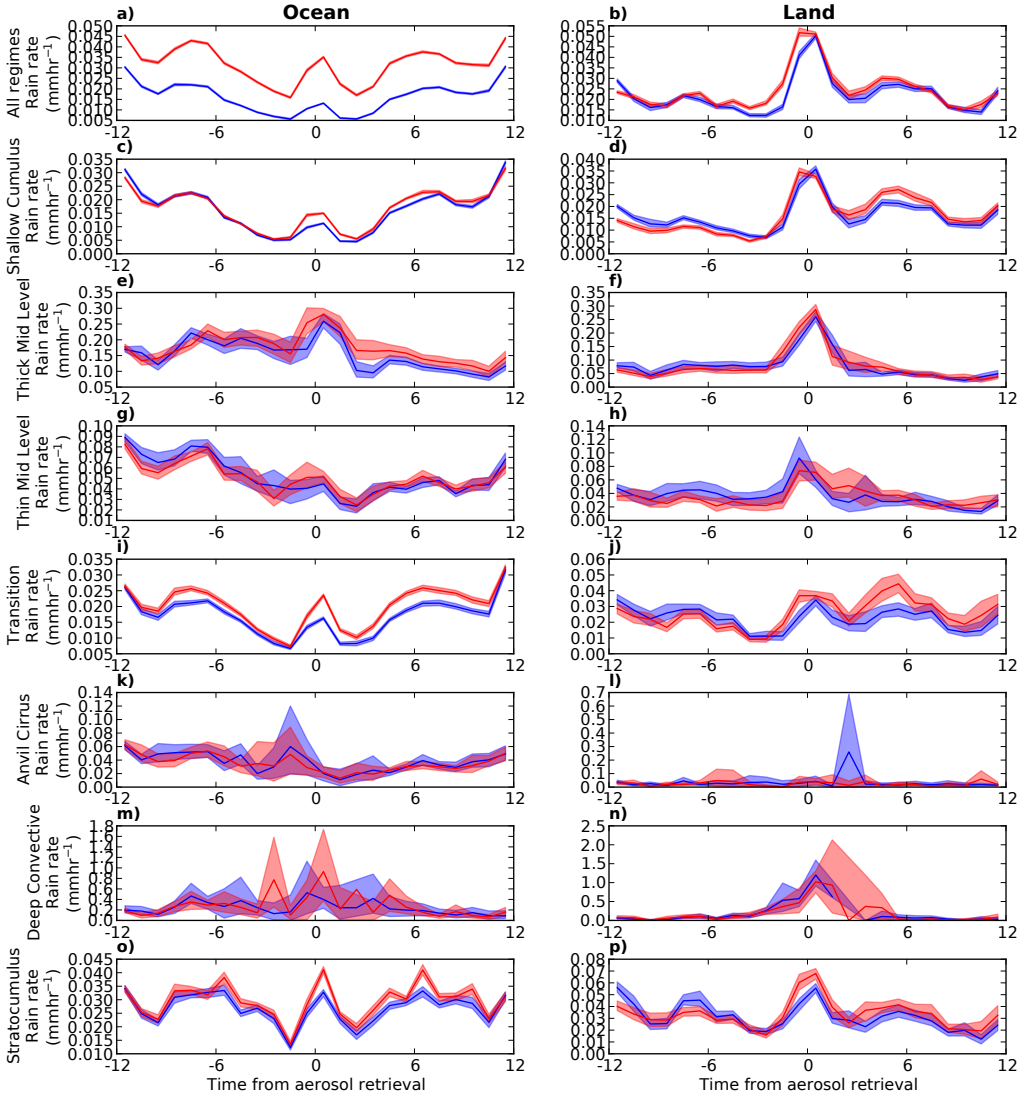

Figure 5.7: As Fig. 5.2, but using ISCCP CTT to remove all clouds with a mean CTT of less then 273K, keeping only liquid phase clouds.

retrievals at all time offsets in the warm case.

Plotting the precipitation development for each regime, both before and after the AI retrieval (Fig. 5.2), shows an increase in precipitation after the AI retrieval for the high AI population compared to the low AI population. When repeated using only clouds with tops warmer than 273 K (Fig. 5.7), a much smaller difference in precipitation development between the high and low AI populations is found. These warm clouds also have a much smaller precipitation rate compared to the mixed-phase clouds. Clouds with mean cloud top temperatures warmer than 273 K contribute about 60% of the total retrievals used, but only 10% of the total retrieved precipitation.

In the warm clouds, the wet scavenging effect (Fig. 5.7), with the high AI populations having

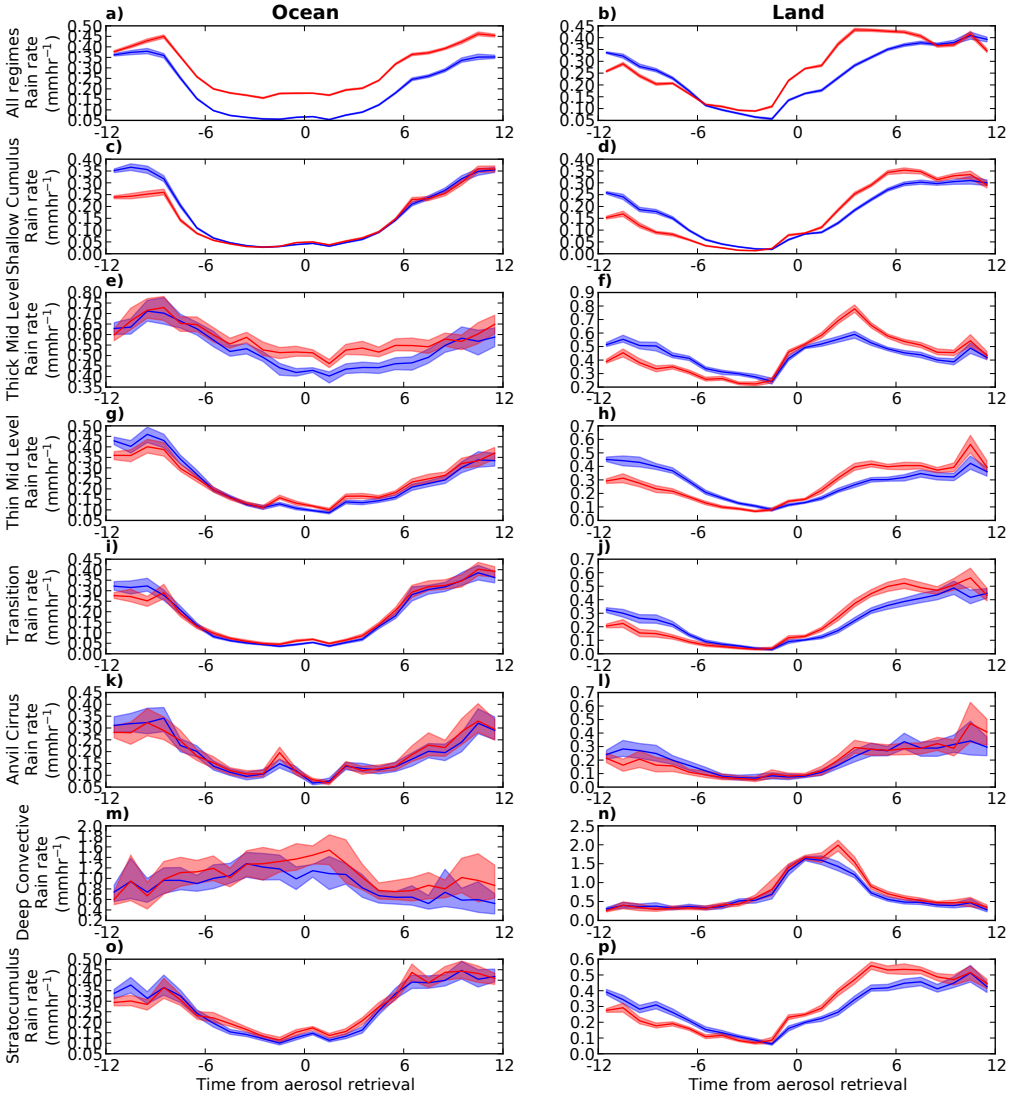

Figure 5.8: As Fig. 5.2, but using ISCCP CTT to remove all clouds with a mean CTT of more than 273K, keeping only mixed and ice phase clouds.

a lower rainrate at times before the AI retrieval is not so clear, although it is visible over land in certain regimes. It is likely that this effect is stronger over land due to the larger AI variance. This indicates that the precipitation from these warm clouds is still removing aerosol from the atmosphere and that the wet scavenging effect exists even when the clouds are ice-free. The reduction of the wet scavenging effect when compared to the 'all-data' case (no separation between warm and mixed/ice phase clouds Fig. 5.2) is most likely due to the lower overall precipitation rate in the warm clouds.

At times after T+0 in the warm clouds (Fig. 5.7), some regimes do show an increase in retrieved precipitation. This increase is observed in the shallow cumulus and transition regimes. As the TRMM 3B42 product may not be able to accurately retrieve very light rain, the occurrence of this difference

in precipitation after T+0 in the warm clouds may indicate an increase in cloud liquid water, rather than a precipitation increase.

In the mixed/ice phase case (Fig. 5.8), the development of the precipitation is very much like the 'all-data' case (Fig. 5.2), with increased precipitation at times after T+0 with increasing AI in many of the regimes, especially over land. This is most likely due to the larger precipitation rate in the clouds with tops colder 273 K, which generate the majority (almost 90%) of the precipitation observed in the 'all-data' case (Fig. 5.2).

Restricting the cloud top temperature restricts the vertical development of the cloud, and prevents the warm clouds growing into higher precipitation rate regimes. The small differences in precipitation rate for the warm clouds (where vertical development is restricted) suggest that the growth into these more highly precipitating regimes is important for generating the difference in precipitation rate between the high and low AI populations. It also suggests that ice processes are likely to be important in an invigoration effect, as increases in precipitation are only observed for the high AI population when clouds tops are allowed to ascend above the freezing level.

5.2.4 Instrument effects

It is possible that the changes in precipitation development observed here are due to limits in the precipitation retrieval. Whilst the 3B42 retrieval includes data from the TRMM precipitation radar, the majority of retrievals are performed using microwave radiometers and IR geostationary satellites (Huffman and Bolvin, 2009). These retrievals make assumptions about the properties of the clouds which may not hold in different aerosol environments, especially if there is a change in cloud properties. The 'HQ' product from the TRMM 3B42 version 7 dataset provides the non gauge-corrected merged microwave–only retrieval, without the IR precipitation retrieval combined. This allows investigation of the role of the IR precipitation retrieval.

The results are very similar to those including the geostationary IR products (Fig. B.1). There are a number of small differences; the spike in precipitation rates at T-2 in the anvil cirrus over ocean regime would appear to be due to the IR precipitation retrieval. The difference in precipitation between the high and low AI populations for the marine stratocumulus is also reduced. Finding similar effects when using the HQ product suggests that the IR retrieval is not the cause of the results in this study.

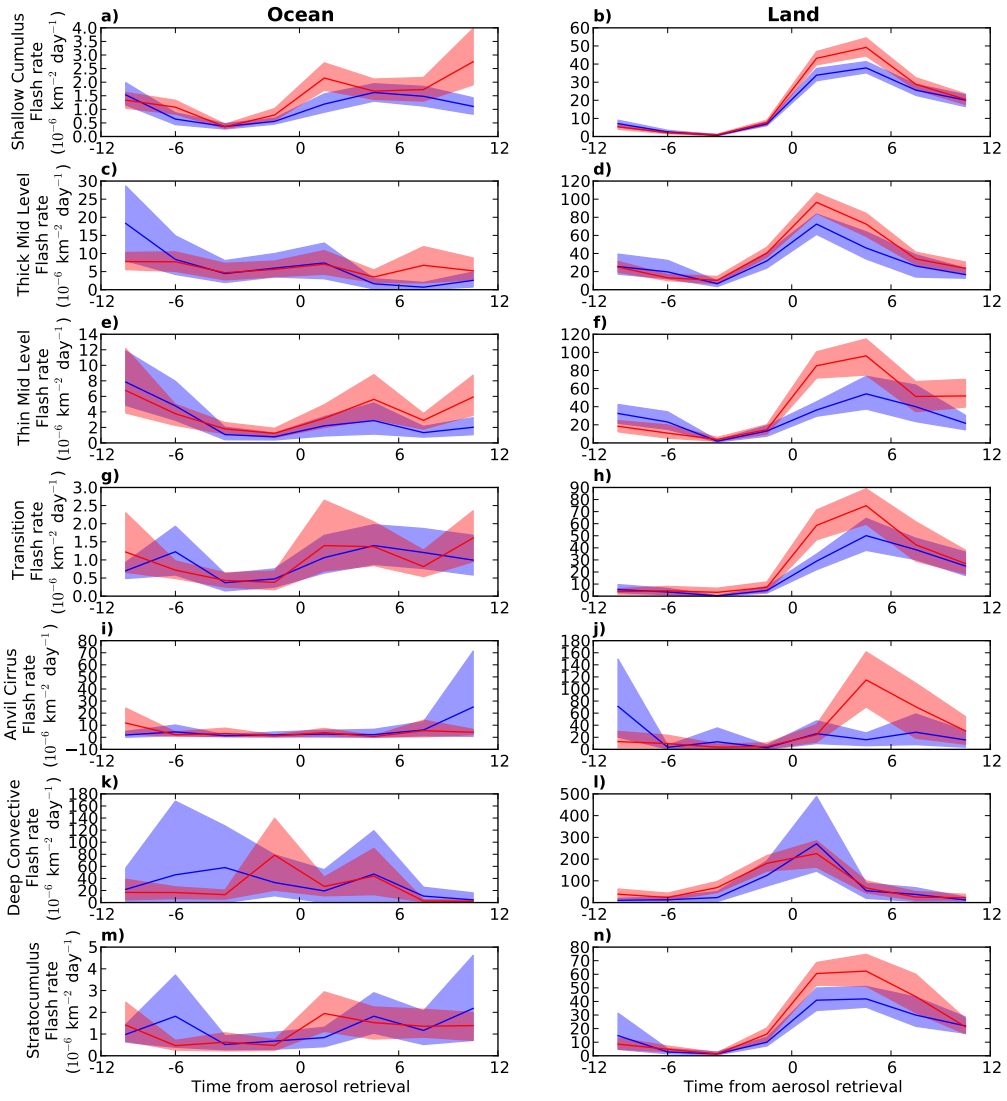

Figure 5.9: The difference in TRMM LIS flash rate for the high and low AI populations for the tropics (30°N – 30°S, 180°W – 180°E) over the period 2003-2007. Red indicates the flash rate development for the high AI population and blue the low AI population.

Lightning flash counts from the Lightning Imaging Sensor (LIS) on-board TRMM are used to provide an independent measure of convective activity, via an increase in flash rate. The LIS flash counts are treated in the same fashion as the 3B42 precipitation data, resulting in a diurnal cycle of flash rates for the high and low AI quartiles in each regime, over both the tropical land and ocean (Fig. 5.9).

There is a large difference between the oceanic and continental flash rates (Fig. 5.9), with flash rates over land being up to ten times larger than over ocean for the same regime. This is believed to be due to an increased vigour of convection over land (Zipser, 1994). The peak flash rates in the

regimes over land are consistent with the expectation of convective activity within the regimes. The deep convective regime exhibits the largest peak flash rates; the other regimes have similar peak flash rates, with the thick mid-level and anvil cirrus regimes having slightly higher flash rates than the other regimes.

The diurnal cycle in flash rate over land is much stronger than that observed over ocean. There are increases in the flash rate for the high AI populations compared to the low AI population after T+0, especially over land. This is similar to the increases in precipitation seen in the high AI population after T+0. In the shallow cumulus regime (Fig. 5.9b), there is a strong increase in the flash rate between T+1 and T+6, with very little difference at T+0. In many of the other regimes, especially over ocean, there is not enough data to draw any significant conclusions about the relationship between AI and the lightning flash rate.

Over both land and ocean, there is little difference between the flash rates of the high and low AI population before T+0. This again is most likely due to a combination of the lack of data from these regimes and the influence of the diurnal cycle. Low flash rates in the morning (T-6 to T+0) over land are due to the lack of convective activity (Liu and Zipser, 2008). Combining this with the sparse nature of lightning flashes makes observing any wet scavenging-like effect very difficult. The significant increase in flash rate for the shallow cumulus regime (Fig. 5.9b) over land in the high AI population would suggest that the increase in precipitation observed using 3B42 is not due to errors in the precipitation retrieval resulting from the aerosol environment.

5.2.5 Reflectivity profiles

Estimates of precipitation rates based on microwave emission are known to suffer from retrieval errors over land, with assumptions about surface emissivity not always being valid (Wilheit, 1986; Greenwald et al., 2007). Microwave instruments are also known to have issues separating cloud water from rain water, such that a change in cloud water may appear as a precipitation change (Berg et al., 2006). Whilst active microwave instruments such as the TRMM PR also suffer from errors in their retrievals, they do not have the same difficulties distinguishing between cloud and rainwater. Both active (such as the TRMM PR) and passive microwave retrievals make assumptions about droplet size, so changes in the TRMM PR reflectivity (which includes comparatively few assumptions) are investigated. Precipitation estimates from the TRMM PR are included in the TRMM 3B42 prod-

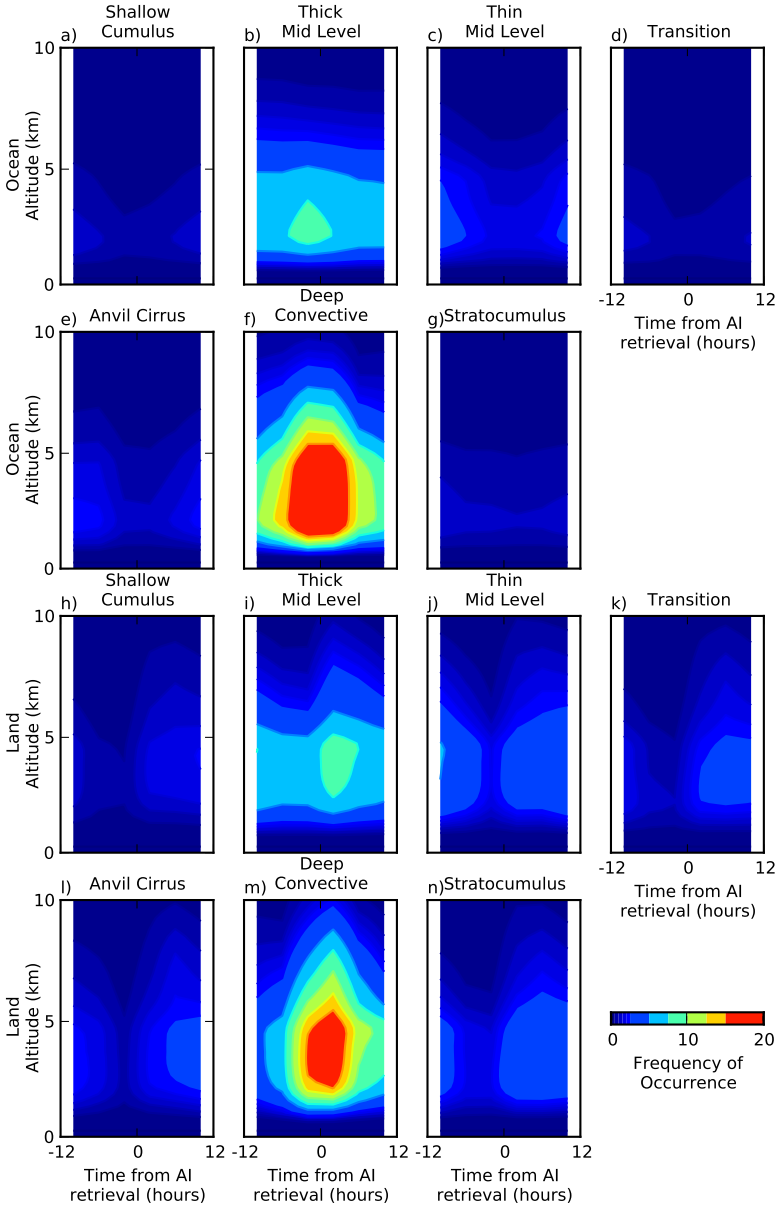

Figure 5.10: The frequency of occurrence of reflectivities above 20 dbZ from the TRMM PR for each regime at times relative to 1330 LST over the period 2003-2007. These are from the TRMM 2A25 PR radar reflectivity product over the tropics 30°N-30°S

uct. However, as the majority of the 3B42 product is determined using passive microwave and IR instruments, the radar reflectivity presents a semi-independent evaluation of precipitation properties.

The TRMM PR cannot detect very light rain, having a minimum detectable signal of about 15 dbZ (Nesbitt et al., 2000). Although it is not able to capture the entire spectrum of rainfall events, it is not sensitive to cloud water, so changes in the PR reflectivity are due to changes in rainfall properties,

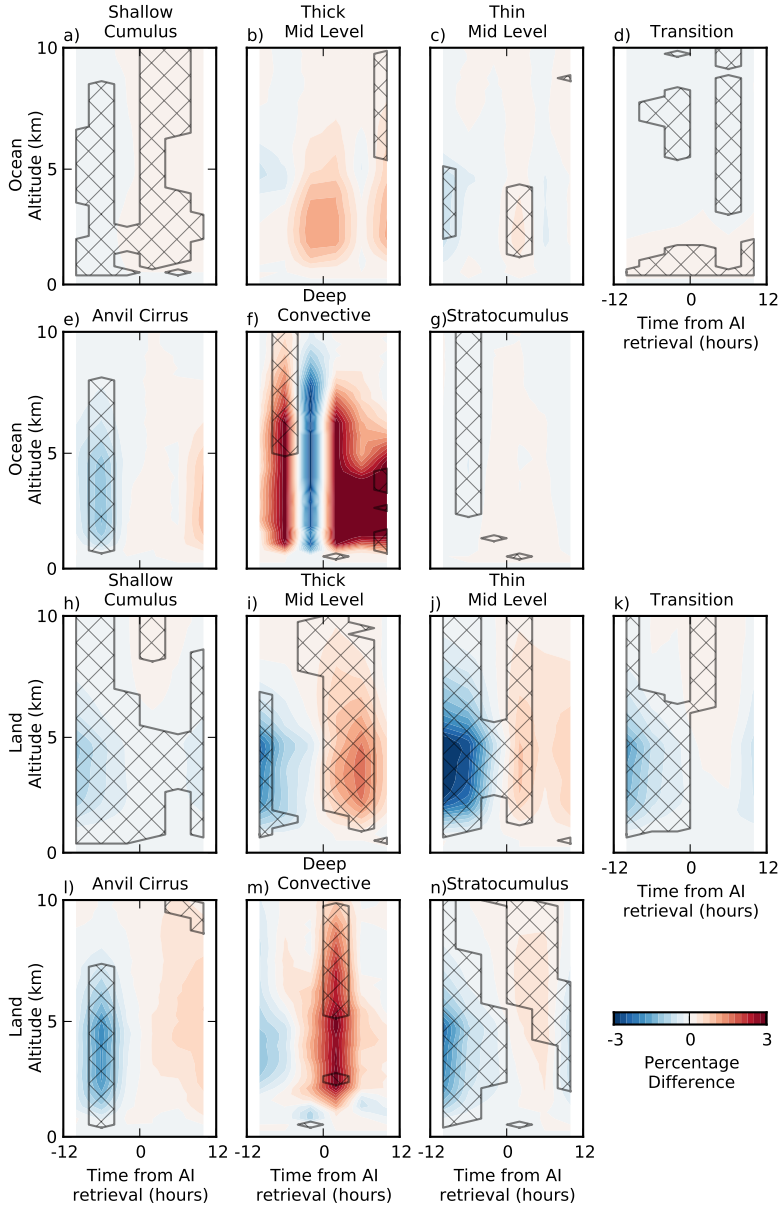

Figure 5.11: The difference in the percentage of reflectivities above 20 dbZ from the TRMM PR between the high and low AI populations over the period 2003-2007. Red indicates an increase in >20 dbZ retrievals at high AI. The hatched areas show 95% significance in the change in frequency of occurrence.

rather than cloud properties.

The TRMM PR reflectivity profiles from the TRMM 2A25 radar reflectivity product are used to investigate the development of radar reflectivity within the cloud regimes and how it changes as a function of retrieved AI, in the same way as with the 3B42 precipitation product. The frequency of

occurrence of reflectivity retrievals above 20 dbZ is used as a proxy for raining pixels. An increase in the occurrence of retrievals above 20 dbZ suggests an increase in precipitation occurrence (eg. Liu and Zipser, 2008).

The diurnal cycle of reflectivity (Fig. 5.10) shows many similar features to the diurnal cycle of precipitation (Fig. 5.2). Over ocean, only the thick mid-level (Fig. 5.10b) and the deep convective regimes (Fig. 5.10f) show a maximum in 20 dbZ occurrence at T+0, with all of the other regimes showing a minimum. This is due to the low frequency of occurrence and weak diurnal cycle over ocean generating an artificial peak in the reflectivity at T+0 for these regimes, a peak also seen in the 3B42 precipitation rate (Fig. 5.2m). Over land (Fig. 5.10h-n), there is a peak in the reflectivity after T+0 for all of the regimes. For each of the regimes over land, the frequency of occurrence of 20 dbZ reflectivities is higher than over ocean.

The regimes dominated by heavy precipitation (Thick mid level and deep convective) show results supporting those found using the 3B42 product (Fig. 5.11i,m). The thick mid-level regime (Fig. 5.11i) and the deep convective regimes over land (Fig. 5.11m) show an increase in high reflectivities in the high AI population at times after T+0, whilst also showing a decrease in reflectivities at times before T+0, which may be due to wet scavenging. Over ocean, the results, especially for the deep convective regime, are noisier and so harder to interpret. Many of the other regimes, especially over land, show lower reflectivities in the high AI population at times before the AI retrieval, consistent with wet scavenging removing more aerosol at higher rainrates.

The stratocumulus (Fig. 5.11n) and transition (Fig. 5.11k) regimes over land do not show a large increase in reflectivity at times after T+0, although there is a small increase in reflectivity in both of these regimes, which is significant at higher altitudes. In the shallow cumulus regime over land, there is a small decrease in the occurrence of reflectivities above 20 dbZ, in apparent contrast to the 3B42 precipitation retrievals, which show an increase in precipitation (which would usually be associated with an increase in reflectivity). It is possible that this lack of reflectivity increase with increasing AI when observed by the radar is due to an increase in very light precipitation, which might be detected by the microwave instruments and not the radar (Kummerow et al., 1998). It is also possible that the increase in precipitation detected by the 3B42 product is due to an increase in cloud water, or some other change in cloud properties, rather than a change in precipitation, although the increase in LIS flash rate (Fig. 5.9) suggests there is still an invigoration. Passive microwave instruments can have

difficulties determining precipitation over land (Bauer et al., 2005), and although the high frequency channels typically used over land are less susceptible to influences from surface properties, the link to precipitation properties is not as direct as with the low frequency channels (Stephens et al., 2008). The extra assumptions made when determining precipitation over land might explain the differences in the effects of aerosols on retrieved precipitation and radar reflectivity.

Although the TRMM PR is not able to retrieve very light precipitation, it can be used to investigate the regional dependence of the T+0→+6 mean precipitation rate for the shallow cumulus regime (Fig. 5.4a). A reflectivity–height histogram (Fig. 5.12a,e,i,m) (eg. L'Ecuyer et al., 2009) is created for each of the four regions highlighted in Fig. 5.4a. These histograms are very similar for each of the regions, suggesting that there is not a fundamental property of the precipitation in the shallow cumulus regime that is different between these regions. The difference in the histograms between the high and low AI populations over the T+0→+6 period (Fig. 5.12b,f,j,n) shows effects supporting the results found when using the 3B42 precipitation product.

The Central Pacific and Seychelles regions show an increase in high reflectivities over the T+0→+6 period and a corresponding reduction in the number of pixels with less than 12 dbZ reflectivities in the high AI population (leftmost column in Figs. 5.12f,j). This suggests that there is an increase in precipitation at high AI after T+0 in these regions, rather than just a modification of the cloud properties. These changes in reflectivity are consistent with the precipitation changes observed in the 3B42 product (Fig. 5.4a). When considering only the pixels with reflectivities above 12 dbZ in these regions (Fig. 5.12h), a shift to higher reflectivities is seen, suggesting that the distribution of precipitation has changed. This indicates not only an increase in the frequency of occurrence of precipitation events, but an increase in the intensity of these events.

The Arabian Sea region shows a decrease in reflectivities with increasing AI over the T+0→+6 period (Fig. 5.12b), suggesting a decrease in precipitation with increasing AI. This reflects the precipitation change seen in the 3B42 product, where there is also a decrease in precipitation with increasing AI over the T+0→+6 period (Fig. 5.4a). Similar effects are observed in the China Sea region (Fig. 5.12n), with a decrease in the occurrence of reflectivities above 12 dbZ in the high AI population compared to the low AI population over this period. The decrease in occurrence in reflectivities above 12 dbZ in the period T-9→-3 for the high AI population (Fig. 5.12o) is sensitive to large scale RH in this region, even after accounting for CF variations with AI (not shown). The

sensitivity to large scale RH is likely due to related variations in column water vapour, which is well correlated to differences between passive microwave and radar precipitation retrievals (Berg et al., 2006).

5.2.6 Development of meteorological properties

Although the influence of meteorological properties is accounted for at the time of the AI retrieval (T+0), reanalysis products are known to not be a perfect representation of the atmosphere (eg. Wang et al., 2011). There is a possibility that the aerosol retrieval is more sensitive to certain meteorological conditions than the reanalysis dataset. If a divergence in the reanalysis meteorology between the high and low AI populations is observed after T+0, this would suggest that the re-analysis data is not as sensitive to the meteorological parameters as necessary for this study.

The 500 hPa vertical velocity (ω_{500}) is investigated, as it is strongly related to precipitation, especially in convective clouds (Koren et al., 2010a; Medeiros and Stevens, 2011). A strong link is observed between AI and ω_{500} (Fig. 5.13a,b), especially over ocean. The effect is similar to the observed relationship between AI and precipitation, with lower values of ω_{500} (rising air) correlated to higher precipitation rates. The expected link between precipitation and ω_{500} is also seen, with the more heavily precipitating regimes having a lower mean ω_{500} at T+0. The strong link between AI and ω_{500}, coupled with the ω_{500}-precipitation correlation could allow ω_{500} to act as a controlling variable in the AI-precipitation correlation, in the same way as CF does in chapter 2. This further emphasises the importance of accounting for the initial cloud fraction and meteorological state.

The majority of regimes show very little difference in the ω_{500} development between the low and high AI populations, once the variance in ω_{500} at T+0 is accounted for (Fig. 5.13). Where a difference is observed, such as for the shallow cumulus (Fig. 5.13d) regime over land, this appears to be due to small errors in the accounting for the variation at T+0, rather than a difference in the environment of the regimes, and so is unlikely to be producing the observed precipitation changes. This suggests that the correlation between AI at meteorological properties at T+0 has been adequately accounted for.

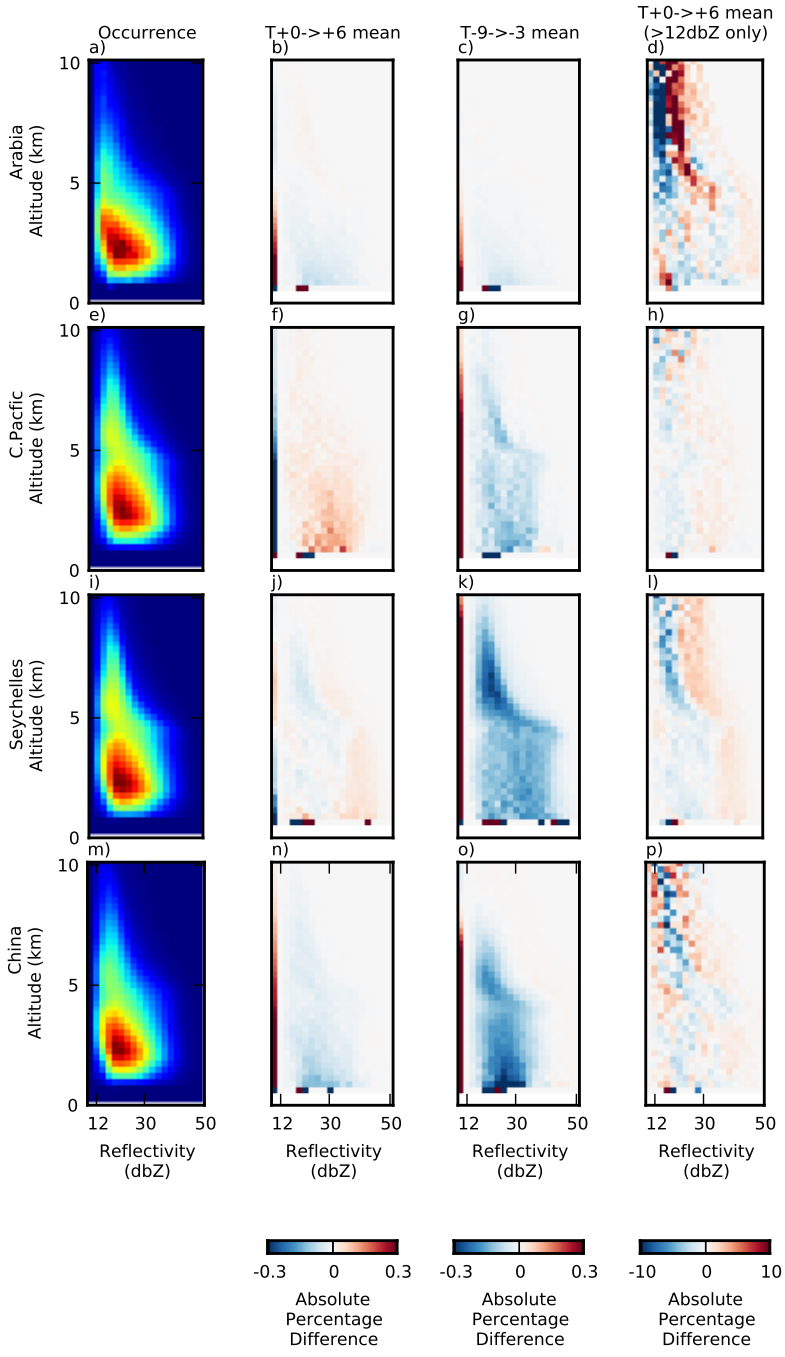

Figure 5.12: (a,e,i,m) TRMM PR reflectivity-height histograms for the regions highlighted in Fig. 5.4a. (b,f,j,n) shows the difference in the histograms for the low and high AI populations over the period T+0→+6. (c,g,k,o) show the difference for the time period T-9→-3. For these histograms, retrievals below 12 dbZ are included in the left-most column of the histogram. (d,h,l,p) show the difference in the histograms only including retrievals greater than 12 dbZ (these histograms are re-normalised). For each of the plots, red indicates an increase with high AI and the difference histograms are normalised such that the changes sum to zero at each altitude.

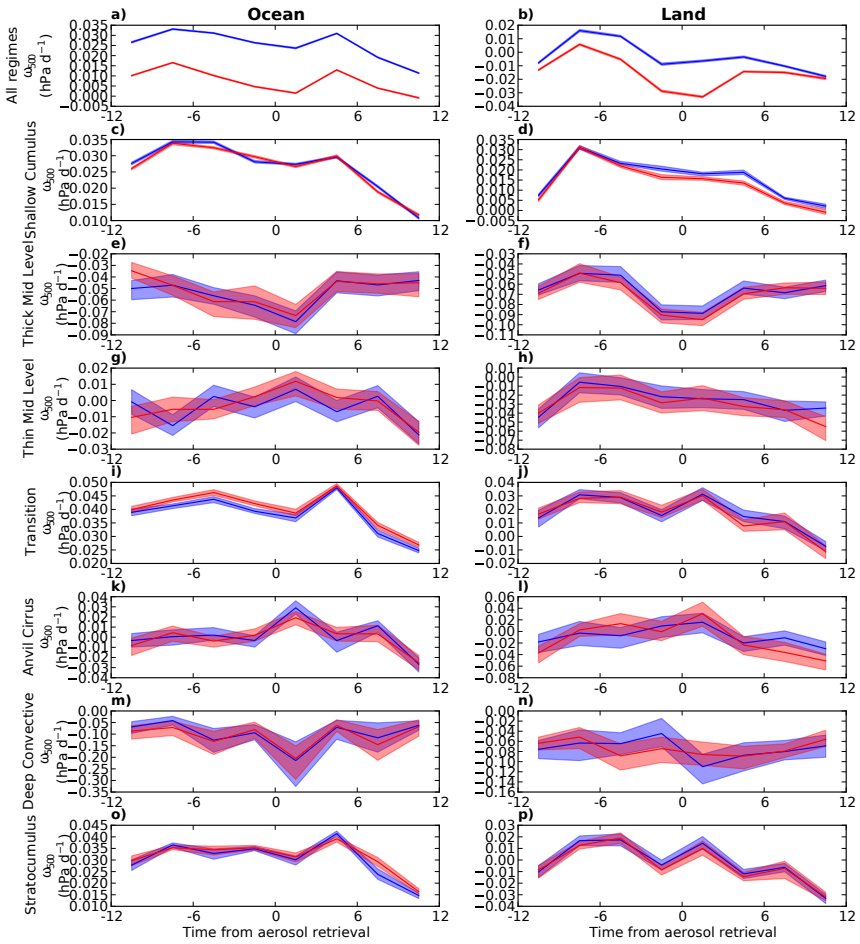

Figure 5.13: The development of ECMWF ERA Interim 500 hPa pressure vertical velocity (ω_{500}) for the high (red) and low (blue) AI populations, for each of the regimes over the period 2003-2007. The error bars show the 95% confidence limits. As in Fig. 5.2, the difference in CF and ω_{500} between the high and low AI populations is removed at T+0.

5.3 Discussion

These results appear to show an increase in precipitation with increasing AI that is not due to the strong AI-CF correlation. There are several possible factors that could be generating the observed results. These can be classified into one of three main types. Firstly, the precipitation retrievals may not be reliable in regions of high aerosol, where the assumptions about the cloud and precipitation properties used in the precipitation retrieval may no longer be valid. Secondly, it is possible that the AI retrieval is not a good retrieval of CCN in certain conditions. Finally, meteorological covariation resulting in a change of CCN (and AI) along with a change in cloud and precipitation properties could possibly generate the observed relationships without an aerosol effect on precipitation. Each of these possibilities is considered in turn in the following section.

5.3.1 Precipitation retrieval errors

Areal precipitation is a notoriously hard quantity to measure, even using surface instruments. While the random errors in the precipitation retrieval may be large, these are reduced by using a large quantity of data. However, possible systematic errors as a function of aerosol could still be generating the observed results. The apparent wet scavenging effect at times before T+0 provides a possible mechanism for systematic errors, especially over land.

Microwave retrievals over land are sensitive to the surface emission properties, which themselves are dependent on soil moisture (Rao et al., 1987; Greenwald et al., 1997). For a given atmospheric profile, a high soil moisture results in a lower brightness temperature and so, if unaccounted for, a lower retrieved precipitation. Recent work has suggested that precipitation in the afternoon is more common over drier soils, in contrast to the naïve expectation (Taylor et al., 2012). Due to the wet scavenging of aerosol, the AI retrieval is correlated to precipitation intensity before T+0. As such, AI might also be an indicator of soil moisture and so perhaps an indicator of errors in the precipitation retrieval due to soil moisture. Changes in the droplet size distribution due to aerosols are also a possible source of errors in the retrieved precipitation. Both the microwave retrievals and the radar retrievals make assumptions about the droplet size distribution when retrieving precipitation, so even though the microwave and radar results agree, they may not be able to account for this effect.

By comparing the precipitation development results from the 3B42 product (Fig. 5.2,B.1) with the

reflectivity results from the TRMM PR (Fig. 5.11) and the flash rates from the TRMM LIS (Fig. 5.9), multiple different measurements of precipitation and convective activity are investigated, reducing the likelihood that the results are due to precipitation retrieval errors. Evidence from chapter 4 (Fig. 4.3), showing increased transitions into the deep convective regime at high AI also provide supporting evidence to the aerosol invigoration hypothesis (Fig. 4.3). There is some variation in the results using the different observational tools, although they all show an increase in precipitation/reflectivity/flash rate for the high AI population at times after T+0, especially over land. This increases the confidence that these results are due to an increase in precipitation in high AI environments.

5.3.2 Aerosol retrieval errors

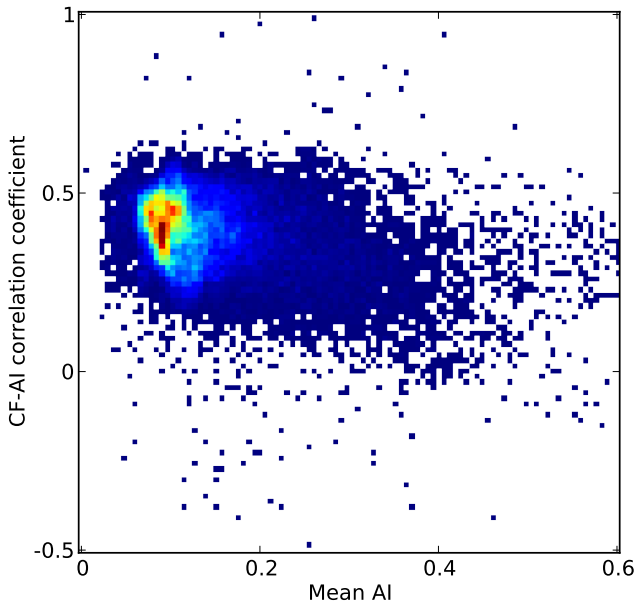

Figure 5.14: The AI-CF correlation in the tropics as a function of local mean AI in Terra MODIS data over the period 2003-2011.

Systematic errors in the aerosol retrieval may also result in a spurious correlations between precipitation and satellite retrieved aerosol properties (type one meteorological covariations). Previous studies have suggested that the AI is well correlated to the CCN concentration (Nakajima et al., 2001). However, a strong correlation with CF still suggests that other effects, such as humid swelling, are important controlling factors on the AI retrieval.

Whilst AI is not perfectly correlated to CCN, using it to select the highest and the lowest quartiles of CCN should be possible, especially in polluted regions where there is a large variance in CCN

concentration. In very clean regions, where there is little difference between high and low AI, its ability to separate out high and low CCN may be compromised. In these clean regions, humid swelling or other meteorological effects may be generating the majority of the difference between high and low retrieved AI. If so, then the results in this chapter may be due to a correlation between precipitation and CF rather than precipitation and AI in these clean regions.

Fig. 5.14a shows AI-CF correlation as a function of local mean AI. This provides a measure of how much of the variance in CF is correlated to AI variations. If the correlation approaches one, then the method of accounting for the CF influence on AI becomes invalid, as fluctuations in AI cannot be distinguished from fluctuations in CF. However, although there is an increase in the correlation at smaller mean AI, only in a few rare cases is it close to one. This suggests that the retrieved AI is not completely correlated to CF, even in very clean regions. Whilst other meteorological variables almost certainly play a role, it does suggest that even in these clean regions, retrieved AI is still able to distinguish between high and low CCN concentrations.

Observations of increased cloud top height with increasing CCN over land using in-situ aerosol measurements (Li et al., 2011), suggest that aerosol retrieval errors are not the primary reason for the observed correlations. Repeated analysis using the AATSR GlobAerosol product (Fig. B.3) show similar results to those seen when using the MODIS, suggesting that these results are not due to the particular details of the aerosol retrieval.

5.3.3 Meteorological covariation

Even with perfect CCN and precipitation retrievals, type two meteorological covariations could still be causing the observed effects. When considering precipitation, wet scavenging is also an important consideration. The development of important ECMWF ERA-Interim variables as a function of AI, shows little evidence to support a meteorological effect as the cause of the observed relationships (Fig. 5.13). However, there is still the possibility of meteorological influences on the results in this study.

Over both land and ocean, there is an increase in precipitation for times after T+0 in the high AI population compared to the low AI population. The regions where decreases in precipitation with increasing AI over ocean are found are also regions where biomass burning is a strong contributor to the total aerosol. It would be reasonable to suggest that fires are suppressed when there is

high precipitation, so this might generate a negative correlation between aerosol and precipitation. Regime–based analysis may help to reduce these errors, by selecting clouds with similar properties at T+0, but the only way to completely determine the influence of these effects is by using a control sample, perhaps demanding the use of a model.

This suggests that the change in precipitation with increasing AI is not solely due to meteorological covariation. If high AI is an indicator of drier atmospheric conditions, a decrease in precipitation should be observed for the high AI population at times after T+0. Whilst a decrease in precipitation with increasing AI is observed in regions of high mean AI over ocean, the same effect is not observed over land. This would suggest that a precipitation influence on emission is not the primary cause of the results in this study.

High AI could also be considered as an indicator of low morning precipitation, given the wet scavenging effect. Low precipitation in the morning may lead to higher precipitation in the afternoon, or perhaps indicate a slight shift in the diurnal cycle, picking out situations where the precipitation rate peaks later. This is unlikely to be the cause of the results in this study, as previous studies suggest that the temporal auto-correlation in precipitation rates would cause a location with higher precipitation before T+0 to be more likely to show a high precipitation after T+0 ((Lee et al., 2013), Fig. B.4). This is opposite to results observed here.

5.4 Conclusions

This chapter has expanded on the work in previous chapters studying the temporal development of cloud regimes, investigating the development of precipitation in these cloud regimes. As before, the data is separated into cloud regimes, with high and low aerosol defined within these regimes by making use of the MODIS AI. To account for CF influences on the AI retrieval the regimes are sampled so that, both the high and low AI populations have the same CF distribution at the time of the AI retrieval for each regime. Whilst this will remove any aerosol effect on CF at the time of the AI retrieval, these effects are thought to be small in comparison to meteorological covariations (Quaas et al., 2010).

To investigate the effects of aerosol on precipitation, the temporal evolution of the satellite retrieved precipitation rate is studied. An increase in precipitation for the high AI population after T+0

is observed in the majority of regimes over land. This increase in precipitation is consistent with the hypothesised aerosol invigoration effect in convective clouds. At times before the aerosol retrieval, a higher precipitation rate is found in the low AI population, consistent with the wet scavenging of aerosols. Over ocean, these effects are present but much smaller, possibly due to the smaller variance in AI.

Over both ocean and land, there is very little difference in precipitation between the low and high AI populations at the time of the aerosol retrieval. This is in contrast to previous work where a strong correlation between AI and precipitation was observed at the time of the aerosol retrieval (Koren et al., 2012) and is likely due to the method of accounting for the AI-CF correlation in this work. The small difference in the precipitation rate at T+0 emphasises the strong correlation between CF and precipitation, which would lead to a strong AI-precipitation correlation via the method shown in chapter 2 if the AI-CF correlation is not accounted for.

The observed increase in precipitation for the 6 hours after the AI retrieval varies by region. In the shallow cumulus regime, an increase in precipitation is found with increasing AI in many regions. However, in regions over ocean with a very high mean AI, a decrease in precipitation is found with increasing AI. This indicates an aerosol suppression of precipitation at very high AI.

The change in precipitation development also depends on cloud top temperature, with the effect being much stronger in clouds with tops colder than 273 K. This may be due to the increased precipitation in these colder clouds, although it might support the hypothesis of ice-phase driven invigoration of convective clouds.

Due to the possible retrieval errors in the TRMM 3B42 precipitation retrieval, other measures of convective activity are also investigated. An increase in TRMM LIS lightning flash rate is observed at times after T+0 in the shallow cumulus regime for the high AI population compared to the low AI one. The high AI population also exhibits an increased occurrence of high TRMM PR radar reflectivities at times after T+0, especially in the convective regimes over land. This suggests that the observed increase in precipitation with increasing AI is not primarily due to precipitation retrieval errors. Whilst it is possible that the observed results are due to either systematic biases in the aerosol retrieval, or that they are the product of remaining meteorological covariation, the largest known meteorological covariations are accounted for in this study.

These results provide a new picture of how tropical precipitation might vary in response to aerosol

perturbations. Accounting for some of the larger known errors reduces the apparent influence of aerosols on precipitation. The results presented in this chapter are consistent with an invigoration of precipitation from tropical convective clouds in the presence of higher aerosol concentrations. This increase in precipitation in high AI environments is consistent with the increase in transitions into the deep convective regime seen in chapter 4. In the next chapter, the occurrence, frequency of transitions between regimes, and precipitation development of cloud regimes is investigated in a GCM coupled to an aerosol model.

Chapter 6

Globally modelled cloud regimes and comparison to observations

Meteorological covariations exert a significant influence on correlations between aerosol and cloud properties. Previous chapters have presented a new method for accounting for these meteorological covariations when investigating aerosol-cloud-precipitation interactions. However, as noted in the previous chapters, there is the possibility of meteorological covariations generating the observed results. Previous studies have acknowledged the possibility of meteorological covariation and have tried to account for it in various ways. Koren et al. (2010a) investigate the correlation between NOAA NCEP-GDAS meteorological variables and retrieved aerosol and cloud properties, finding that although aerosol and cloud properties are strongly correlated to meteorological variables, they are correlated to different variables. They conclude that meteorological factors are not important in generating an apparent invigoration effect. However, Boucher and Quaas (2012) show that the correlation between AOD and precipitation can be reproduced in a model without aerosol effects on precipitation, and that this correlation still exists in this model, even when variations in large scale relative humidity are accounted for. Quaas et al. (2010) and Grandey et al. (2013b) use models with and without aerosol indirect effects to determine how much of the AOD-CF relationship can be attributed to aerosol-cloud interactions in the ECHAM model. They show that even when the model includes no aerosol indirect effects, the model still shows a strong AOD-CF correlation. Chapter 2 showed the importance of the AOD-CF correlation when considering aerosol cloud interactions and

The runs in this chapter were setup and performed by Zak Kipling (Department of Physics, University of Oxford. UK) and Rosalind West (Department of Physics, University of Oxford, UK. Now at the Department for the Environment, Fisheries and Rural Affairs, Westminster, UK.). The analysis and manuscript are my own work.

so have attempted to account for the influence of the AI-CF correlation in the later chapters of this thesis.

A model study provides a way to investigate the roles meteorological and aerosol effects play on the transitions between cloud regimes, as it allows a control simulation to be run without aerosol indirect effects. If an effect observed in the model is no longer present when aerosol indirect effects are excluded, it suggests that aerosol indirect effects are responsible for generating the observed effects in the model.

This chapter investigates how the transitions between cloud regimes and the precipitation development of the regimes is represented in a GCM. The model used includes some explicitly parametrised effects of aerosols on large scale precipitation, but has no explicitly parametrised effects on convective clouds, only feedbacks from the stratiform cloud scheme via the large scale environment. Many GCMs have similar limitations on their parametrised aerosol effects but often show an increase in CF with increased AOD (Quaas et al., 2009). As these parametrisations are designed such that large scale precipitation is suppressed in high aerosol environments, the model might be expected to reproduce the results from previous chapters showing the response of the stratiform pathway to AI variations. The lack of explicit effects on convective clouds may be important. It is possible that a suppression of precipitation in the early stages of cloud formation may be sufficient to invigorate convective clouds through increasing cloud water. However, it is not clear whether a GCM would be able to reproduce the observed effects on convective clouds and precipitation without parametrised aerosol effects on convection.

6.1 Methods

The UK Met Office Hadley Centre HadGEM3 model (v7.3) (Hewitt et al., 2011) is used in this chapter, coupled to the UKCA (United Kingdom Chemistry and Aerosols) module (Bellouin et al., 2013; Mann et al., 2013). The GLOMAP-mode aerosol scheme in UKCA (Mann et al., 2010) is coupled to the HadGEM3 cloud scheme via the Abdul-Razzak and Ghan (2000) aerosol activation scheme (West et al., 2013) which modifies the cloud droplet number concentration (CDNC) in the stratiform cloud scheme. The UKCA aerosol module interacts with the radiation scheme by providing the optical properties of the aerosols to the radiation scheme.

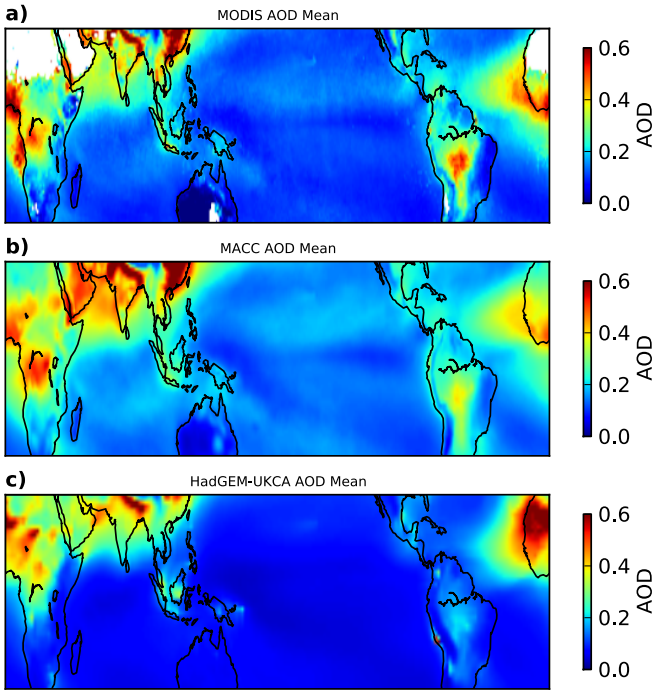

Figure 6.1: Comparison between the annual mean AOD from MODIS (a), MACC (b) and HadGEM-UKCA (c).

HadGEM3 uses the PC2 cloud scheme (Wilson et al., 2008a,b), which treats both cloud fraction and cloud water as prognostic variables. CDNC is treated diagnostically, calculated by the activation scheme at each timestep. The calculated CDNC influences the cloud scheme by modifying the auto-conversion of cloud liquid water to rain in the large scale precipitation scheme (Wilson and Ballard, 1999). This means that aerosol generally acts to suppress precipitation in this model. UKCA aerosol has no direct coupling to the convective cloud and precipitation scheme. As such, the stratiform cloud scheme might be expected to respond to increases in aerosol, but increases in convective cloud with increasing AI would not be expected. HadGEM is known to have a reasonable representation of tropical low clouds (Nam et al., 2012) where indirect effects are expected to be strong.

This model is run in atmosphere-only, non-nudged configuration at N96 resolution (1.25° latitude by 1.875° longitude), for five years with a single month spinup and constant year 2007 emissions. Further details on the model setup can be found in West et al. (2013).

For improved comparisons with observations, an observational simulator is used. This generates a more consistent comparison between the model state and observations by simulating the properties of the retrieval from a specific instrument. This is particularly important for cloud properties due to the strong diurnal cycle of cloudiness and the potential for overlapping cloud layers. The integrated

HadGEM3 ISCCP simulator is used. The regime RFOs and transition frequencies for ISCCP (Figs. A.1, A.2) are very similar to those from MODIS (Figs. 4.2, 4.3), showing the same important features (see section 4.2.6), so the use of ISCCP does not make a large difference to the conclusions. The ISCCP simulator in HadGEM3-UKCA (Bodas-Salcedo et al., 2011) provides mean cloud property data for all sunlit regions, every three hours of model time. The three hourly gridbox mean cloud properties are used to assign the data to the ISCCP cloud regimes determined by Williams and Webb (2009), on which the MODIS regimes are based. To ease comparison with the MODIS results, the regimes named 'tropical congestus' and 'thin cirrus' in ISCCP regimes show similar occurrence and transitions to the 'thick mid-level' and 'thin mid-level' MODIS regimes. The model AI is determined using the 550 nm and 670 nm AODs diagnosed by the model.

This analysis follows the same pattern as that in chapter 4. The change in frequency of occurrence of the regimes with AI is determined using the local AI quartiles, with the highest and the lowest quartiles as the high and low AI respectively. When considering transitions between regimes, the regimes are sampled so that the CF distribution is the same for the high and low AI populations within each regime. This process is also performed for 500 hPa vertical velocity, 10 m windspeed, low troposphere static stability and 850 hPa relative humidity. For a full description of this method, see section 4.1.1.

6.2 Results

6.2.1 Regime RFOs

The frequency of occurrence of the regimes in the model (Fig. 6.2) is similar to that found in the observations (Figs. 4.2, A.1), although there are some important differences. The thin cirrus regime is much more common in the model than in the observations. The shallow cumulus, tropical congestus and transition regimes all show a lower RFO in the model than the observations, quite possibly due to the observations failing to detect some thin high cloud. This would be likely to affect the lower level regimes, where overlying cirrus is more common as regimes with high cloud tops, such as the deep convective regime, are unlikely to have any overlying thin cloud. Although the satellite simulator should account for sub-visible cirrus, ISCCP is known to have difficulties retrieving to correct cloud top height for high thin cloud over lower thick cloud (Marchand et al., 2010). There

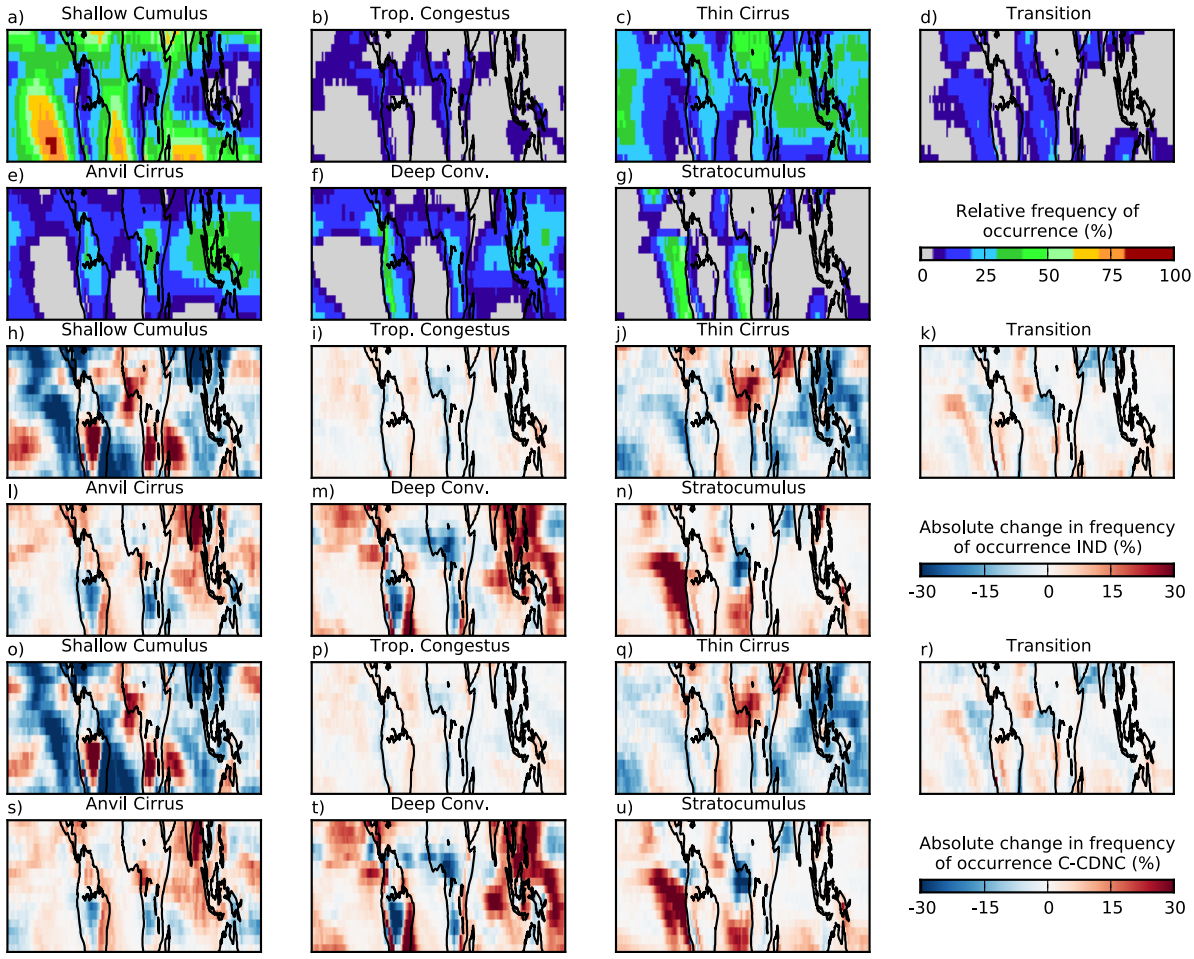

Figure 6.2: (a-g) The frequency of occurrence of each of the ISCCP cloud regimes in the HadGEM3-UKCA run including aerosol indirect effects (IND). (h-n) The absolute difference in frequency of occurrence between the high and low AI populations for the run including aerosol indirect effects (IND). (o-u) as (h-n) except for the run with constant cloud droplet number concentration (C-CDNC). For a comparison with observations, see Figs. 4.2 and A.1.

is also the strong possibility that this is due to the model producing a higher thin cirrus RFO, rather than an error in the ISCCP retrieval. The regime frequencies seen here are similar to those found by Williams and Webb (2009), who used the HadGEM2 model and based their regime RFOs on the daily mean cloud properties, rather than the three hour properties used here. The UK Met Office models simulate regime frequencies of occurrence closer to observations than many other GCMs (Williams and Webb, 2009); these cloud regimes are used as part of the evaluation process for the UM (Bodas-Salcedo et al., 2012).

When looking at the change in regime frequencies with increasing AI (Fig. 6.2h-n), some discrepancies between the model and observations are seen. The most obvious change is the modelled increase in shallow cumulus RFO with increasing AI in some regions (Fig. 6.2h), whereas in the

observations there is a decrease in shallow cumulus with increasing AI globally (Fig. 4.2h). Whilst some of these increases in shallow cumulus RFO are found in regions where there is a strong absorbing aerosol component (Herman et al., 1997), many of these increases are in relatively clean locations (such as over the South Pacific). The shallow cumulus regime appears to grow at the expense of the thin cirrus regime in the southern hemisphere, but it is not possible to determine the origin of this increase from only changes in RFO. The model shows an increase in stratocumulus in the Pacific stratocumulus region with increasing AI, however, decreases are found in regions where absorbing aerosols are common, such as the western coast of equatorial Africa. This decrease is not seen in observations, so may be indicative of retrieval errors in this region, meteorological covariation, or perhaps a stronger influence of absorbing aerosols in the model compared to observations.

The change in regime frequencies with increasing AI when the model is run with a constant CDNC distribution (no aerosol indirect effects, Fig. 6.2o-u) shows a very similar pattern to that seen when aerosol indirect effects are included in the model. This supports the assessment of regime RFOs in chapter 4, that the correlation between regime RFO and AI is controlled primarily by effects other than aerosol-cloud interactions. Correlations between AI and regime RFO are not adequate for assessing the strength of aerosol-cloud interactions.

6.2.2 Regime Transitions

Although there are differences between the regimes transition histograms observed using ISCCP and those found using the model (Fig. 6.3a,b), the model transition histograms reproduce the main transitions seen in the observations (Fig. A.2a,b). The majority of regimes 'transition' into the same regime (i.e. lie on the diagonal of the transition histogram) over the three hour observation period. The frequency of occurrence of these transitions along the diagonal are very similar to those from the observations (Fig. 4.3a,b), suggesting that the regimes exhibit similar persistence.

Over land (Fig. 6.3a), the tropical congestus to thin cirrus transition is much stronger in the model compared to observations, as is the anvil cirrus to thin cirrus transition. This would help to explain the high frequency of thin cirrus in the model compared to observations. Over ocean (Fig. 6.3b), there is a weaker stratocumulus to transition regime transition in the model than in observations. This may indicate slightly more persistent stratocumulus cloud in the model than in observations. The thin cirrus regime is also slightly more persistent in the model compared to observations, contributing to

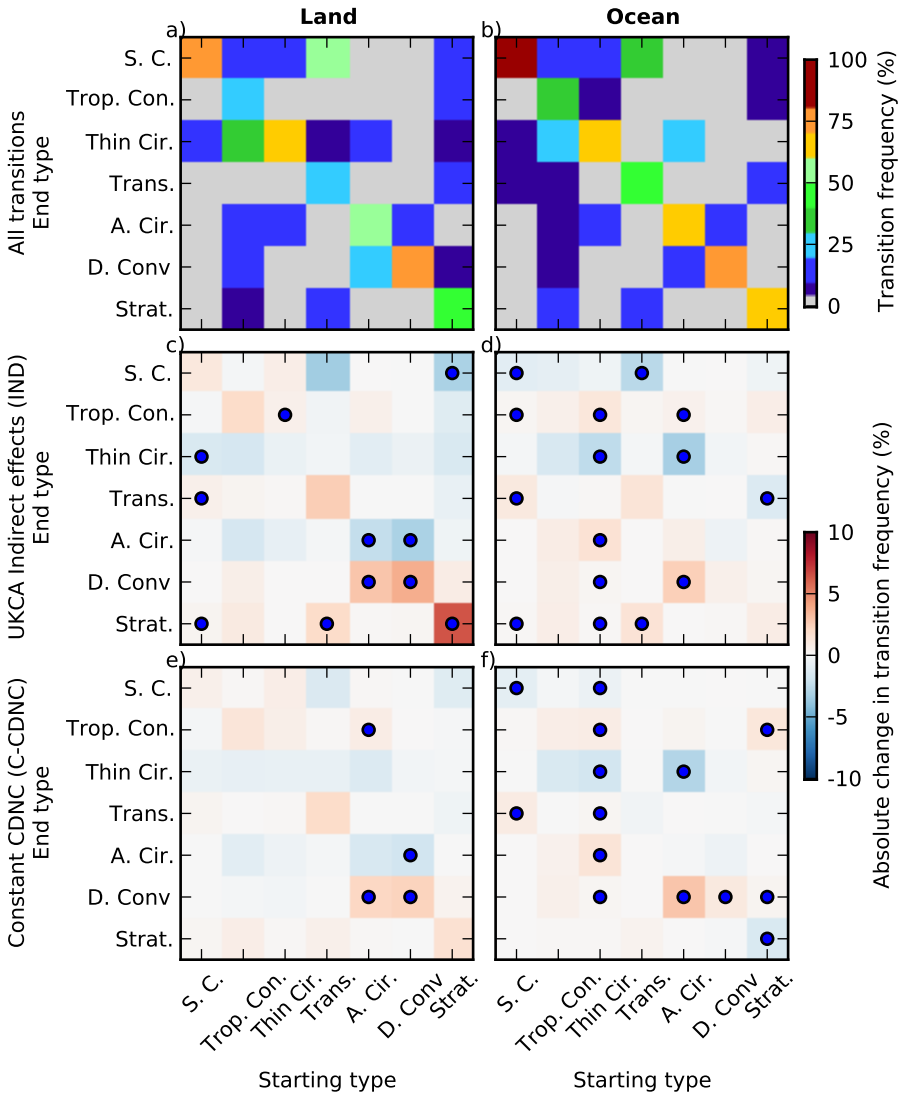

Figure 6.3: Regime transition histograms showing the conditional probability of a given transitions between regimes over (a) land and (b) ocean during the three hour 1030 - 1330 LST period being observed, given each starting regime. Each column sums to 100%. The difference in the histograms between the highest and lowest AI quartile days for the run including indirect effects (IND) over c) land and d) ocean, and without indirect effects (C-CDNC) over e) land and f) ocean. Positive values in the difference plots indicate an increase in the frequency of the transition with increasing AI. Note the non-linear colourbar in a) and b). The dots indicate 95% statistical significance. This plot covers regime transitions for the tropical region (20°N - 20°S) where the ISCCP regimes are defined. For a comparison with observations, see Figs. 4.3 and A.2.

the increased thin cirrus RFO.

The changes in the transition frequencies observed in the model with increasing AI show some similarities to those observed in satellite data. In the model run including aerosol indirect effects (IND), both the model and the observations show a decrease in transitions into the shallow cumulus regime over ocean (Fig. 6.3d). There is a slight increase in transitions into the stratocumulus regime with increasing AI; this increase is stronger over land (Fig. 6.3c). Additionally, over land there

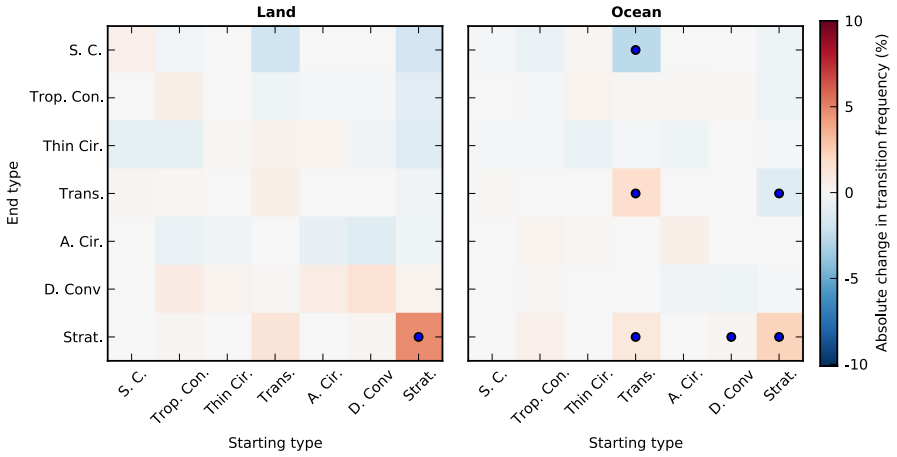

Figure 6.4: The difference in the relationship between transition frequencies and AI for IND and the C-CDNC runs. Red indicates an increase in the strength of the relationship between AI and transition frequency when aerosol effects are activated in the model. Dots indicate 95% significance.

is an increase in stratocumulus to stratocumulus transitions indicating an increase in stratocumulus persistence at higher AI. There is also an increase in transitions into the deep convective regime at the expense of the anvil cirrus regime.

It is notable that several of the most important changes in convective transitions in the observations are not seen in the model. The increase in stratocumulus persistence with increasing AI over ocean is much smaller than that seen in observations and there is no increase in the tropical congestus to deep convective transition with increasing AI over land.

When the runs are repeated with a constant cloud droplet number concentration (C-CDNC, Fig. 6.3e,f), there is a reduction in the strength of the relationship between transition frequencies and AI. There is a much reduced increase in stratocumulus persistence with increased AI over land, and there is a reduction in many of the other related transitions in the stratocumulus pathway. There is little change in the magnitude of the transitions into the deep convective regime. Over ocean, there is a reduction in the change in stratocumulus pathway transitions with increasing AI (Fig. 6.4), although many of the other transitions remain almost unchanged compared to the IND run.

The change in relationship between transition frequencies and AI between the IND and the C-CDNC runs (Fig. 6.4) is small for most of the transitions. The models do show significant differences in the transition frequencies for the stratocumulus to stratocumulus transition over land and ocean, as well as transitions frequencies between the stratocumulus, shallow cumulus and transition regimes over ocean. In the C-CDNC run, some of the transitions show no relationship to AI, where a rela-

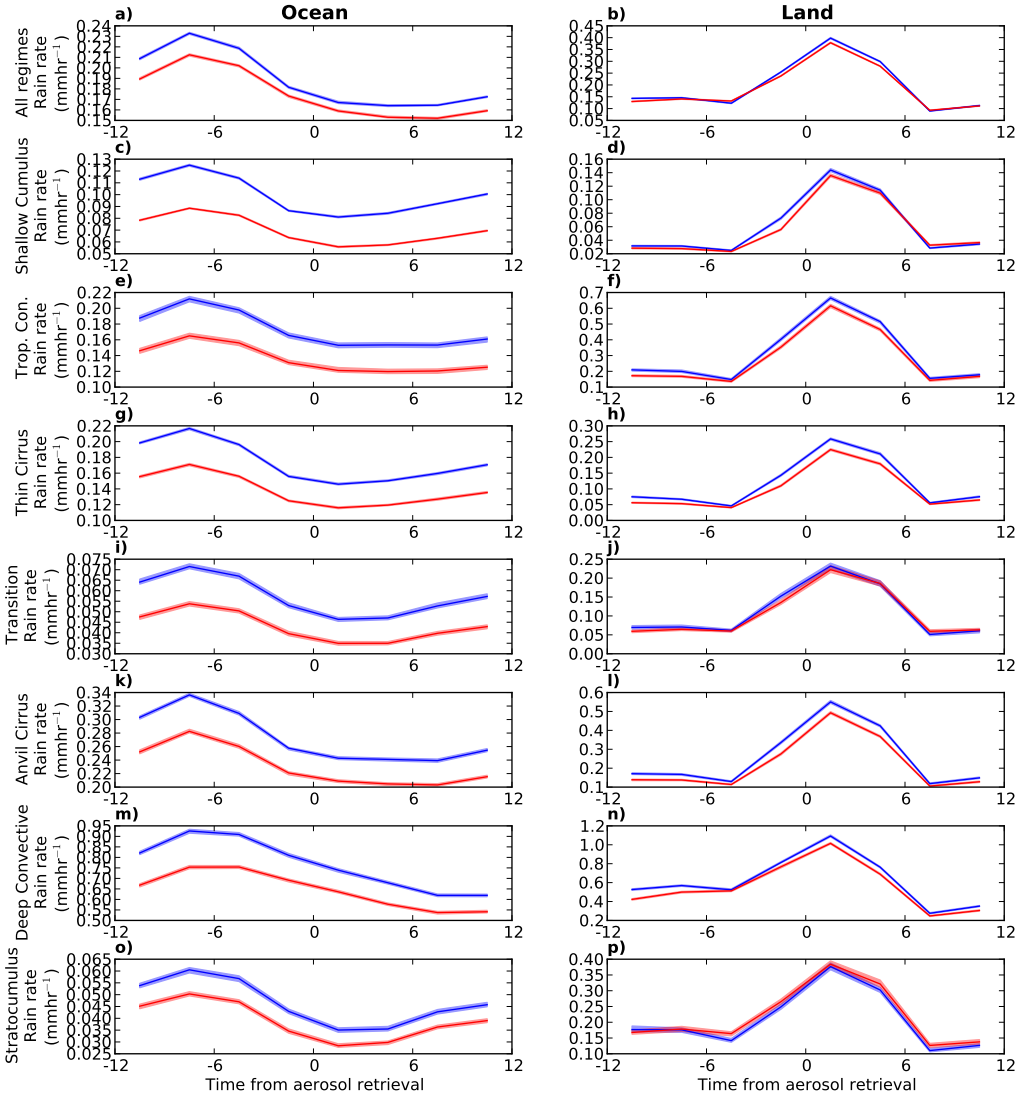

Figure 6.5: Mean precipitation rates at times before and after 1330 LST. The development of the regimes in a high AI environment is shown in red and a low AI environment in blue. Errors are shown at 95% significance. The top row ('All regimes') shows the development of precipitation if cloud regimes and the AI-CF relationship are not accounted for. These plots are created from five years of HadGEM3 data from a run including UKCA aerosol indirect effects (IND). For a comparison with observations, see Fig. 5.2.

tionship is seen in the IND run. However, several of the transitions, especially in convective regimes, still show a small change in frequency with increasing AI in the C-CDNC run, suggesting that there may be unaccounted for meteorological effects influencing the correlation between AI and regime transition frequencies.

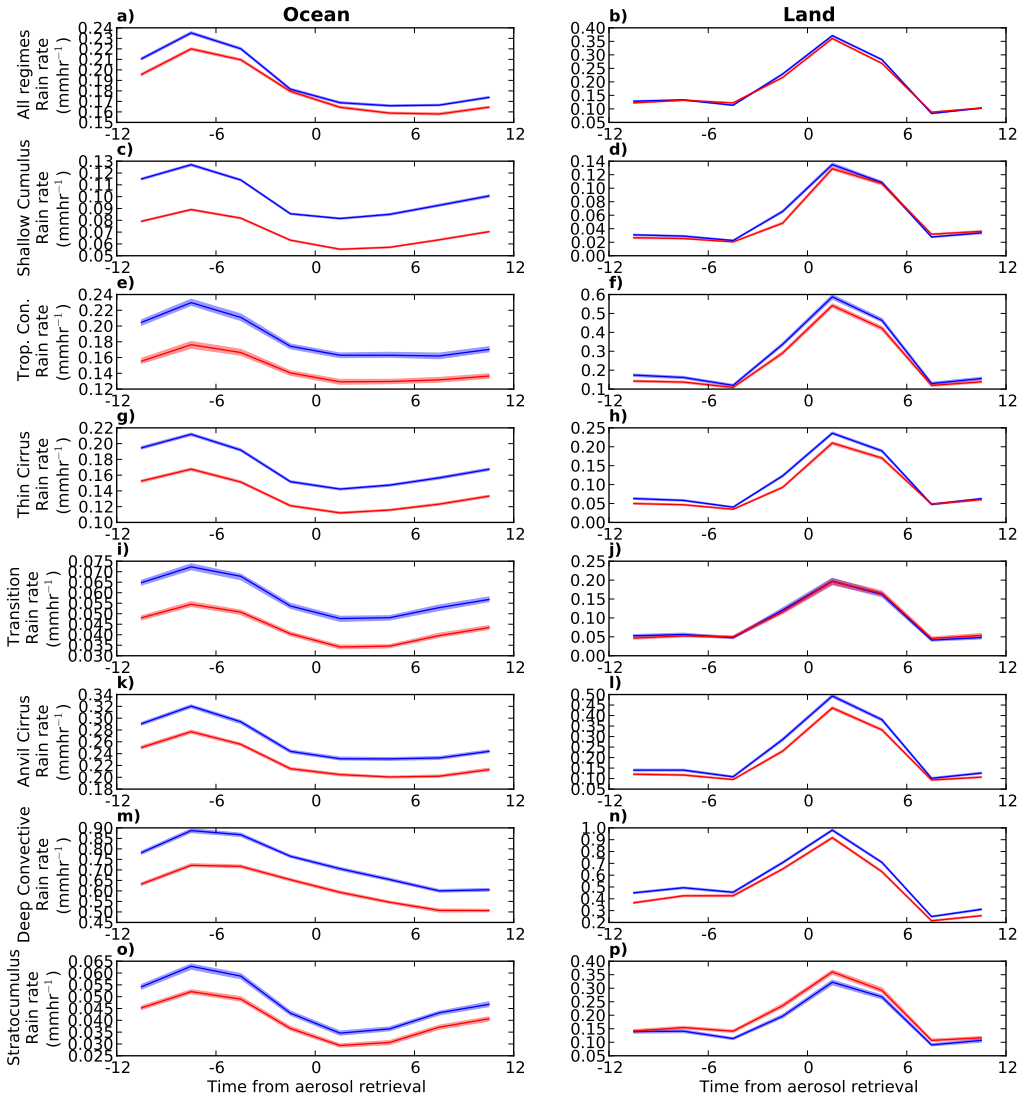

Figure 6.6: As Fig. 6.5 but using five years of HadGEM3-UKCA data from a run excluding UKCA aerosol indirect effects, instead using a constant cloud droplet number concentration (C-CDNC).

6.2.3 Precipitation

The analysis of the precipitation development of the cloud regimes is also replicated in HadGEM3-UKCA. No trajectory following is used, so the results are not a directly comparable to those of chapter 5. However, the trajectory following makes a small enough difference over the 12 hour period that it can be ignored in this case.

The model (Fig. 6.5) reproduces some of the characteristics of the diurnal cycle observed in the observations (Fig. 5.2). The peak precipitation rate over ocean is around T-8 (0530 LST), with a minimum around T+0, similar to the minimum found in observations. Over land, the peak precipitation rate is around T+2 (1530 LST), similar to that found in the 'all regimes' version of the observational

data (Fig. 5.2b). The precipitation rate over land is much larger during the day compared to night, similar but more extreme than the day-night contrast found in observations. The mean precipitation rates for the regimes also show similarities to those found in observations, with the deep convective, anvil cirrus and tropical congestus regimes having the largest precipitation rates. The diurnal cycle over land is strikingly similar between the regimes, with all the regimes showing an peak precipitation time of approximately T+2. This is in contrast to the diurnal cycle found in observations over land (Fig. 5.2), where the less developed regimes at T+0 (eg. shallow cumulus) show a later time of peak precipitation, as they take time to develop.

Over ocean, the model shows a lower precipitation rate in the high AI population than the low AI population at T+0 in the 'all-regime' case, a difference that is reflected in the individual regimes (Fig. 6.5a). This negative relationship at T+0 is similar to that found in other models (Grandey et al., 2013b), although it is unlike the retrieved relationship in the satellite data, where there is very little difference in precipitation rate at T+0 over ocean. Over land, there is a very small difference in the precipitation rate between the high and low AI populations at T+0. This small difference is similar to that found in the observations, where accounting for the variations in CF between the high and low AI populations removes the link between precipitation and AI (Fig. 5.2).

The difference in precipitation rate between the high and low AI populations over ocean at other times varies little from the difference at T+0. This is similar to the observations over ocean, with the high and low AI populations showing a similar cycle of precipitation. However, in the observations, accounting for the difference in CF between the high and low AI populations removes the difference in precipitation rate at T+0. This allows other effects, such as wet scavenging, to be observed. This is not the case in the model, where the strong AI-precipitation relationship at T+0 disguises these effects.

Over land (Fig. 6.5), there is very little difference between the precipitation development for the the high and low AI populations, both at T+0 and at other times. Some regimes (thin cirrus and anvil cirrus) show a negative relationship between precipitation and AI at T+0. Other than a peak in precipitation shortly after T+0, the model results show little similarity to the observations. There is no increase in precipitation for the high AI population at times after T+0, and there is no evidence of wet-scavenging at times before T+0. This lack of a wet-scavenging signature over land is unexpected, as wet-scavenging is a process that is modelled in HadGEM3-UKCA.

When comparing the precipitation development in the IND model run (Fig. 6.5) with the C-CDNC model run (Fig. 6.6), very little difference is found between them. This would suggest that very little of the difference in precipitation between the high and low AI populations in this model is due to aerosol–cloud interactions.

6.3 Discussion

A GCM can be used to test which processes are important to observed aerosol-cloud correlations. As the only difference between the IND and the C-CDNC runs is whether the UKCA aerosol scheme is coupled to the HadGEM3 cloud scheme, the difference between the IND and the C-CDNC runs (Fig. 6.4) shows the strength of the aerosol indirect effects within the model. Where the C-CDNC run shows a relationship between cloud and aerosol properties, this would indicate meteorological covariation influencing the aerosol-cloud correlations. Likewise, if there is no relationship between aerosol and cloud properties in the C-CDNC run, then any relationship in the IND run could be attributed to aerosol effects on clouds in the model. This would provide more evidence that the effects observed in the satellite data are due to an aerosol effect rather than meteorological covariation.

6.3.1 Stratiform clouds

For the stratiform pathway, the model provides some supporting evidence that the differences in transition frequencies between the high and low AI populations in the satellite observations are due to an aerosol effect on clouds. With aerosol effects on clouds included (IND), the stratocumulus to stratocumulus transition in the model shows a strong increase in frequency of occurrence with increased AI, especially over land (Fig. 6.3c). In the run without aerosol effects on clouds (C-CDNC), the strength of the relationship between the model AI and both the stratocumulus-stratocumulus transition and other transitions in the stratiform pathway is reduced compared to the IND run. In some cases the relationship between transition frequency and AI is not reduced to zero in the C-CDNC run. This is likely due to meteorological covariation between cloud and aerosol properties, but could also be due to aerosol influences on cloud via the radiation scheme, as these are active in both the IND and the C-CDNC runs.

Aerosols modify cloud properties in HadGEM3-UKCA by reducing the large scale precipitation

rate (Wilson and Ballard, 1999) and so should have the strongest effect in the stratiform cloud regimes (transition and stratocumulus). Over ocean, the difference in transition frequencies between the high and low AI populations in the model is not nearly as strong as that found in observations. One possible reason for this is the lower AODs in the remote ocean in HadGEM3-UKCA than are seen in observations. This is demonstrated by the low AODs in Fig. 6.1, and results in a smaller difference in AI between the high and low AI populations in the model when compared to observations. The modelled structure of the clouds in the model also leads to uncertainties in the effect of aerosols. Whilst it has been suggested that aerosols influence the transition between open and closed celled stratocumulus, the cell structure of stratocumulus is not represented in the model. This means that the response of stratocumulus to aerosol perturbations in the model does not proceed by the same pathways as in the atmosphere. More confounding effects may be present in the treatment of the CDNC within the model. CDNC is treated diagnostically within HadGEM3-UKCA, which may be important when considering the effect of aerosols on CDNC (Lohmann et al., 2000).

Despite these issues, there is a weaker relationship between transition frequencies and AI along the stratiform pathway in the C-CDNC run (Fig. 6.4e,f). There are also significant differences in the relationship between the transition frequencies and AI when comparing the IND and C-CDNC runs, especially along the stratiform pathway over ocean (Fig. 6.4). This suggests that the changes in the transition frequencies with increasing AI found in the observations of the stratiform regimes may be the result of an aerosol effect on stratiform cloud properties, not meteorological covariation of cloud and aerosol properties.

6.3.2 Convective clouds

The precipitation development and the changes in convective regime transitions indicate the simulated convective regimes do not compare as well to the observations as the stratiform regimes. In both the IND and the C-CDNC runs, there is very little change in convective regime transitions with increasing AI. This is in contrast to the changes in regime transition frequency found when using MODIS AI (Fig. 4.3c,d), although it is similar to that found when using MACC AOD (Fig. 4.3e,f).

The precipitation development as a function of AI also shows some notable differences from the observations. Although there is a negative relationship between precipitation rate and AI at T+0, suggestive of wet scavenging, there is no negative relationship between precipitation rate and AI at

times before T+0 over land. If this relationship between precipitation rate and AI before T+0 in the observations is indicative of wet scavenging, this would then suggest that wet scavenging in the model has different properties to those observed in the atmosphere.

There are several possible reasons for the lack of transitions along the convective pathway in the model. The model has no parametrised effects of aerosol on convective cloud processes. It is possible that suppression of the large-scale precipitation rate may affect convective precipitation in the model. However, the lack of direct aerosol interactions with convective cloud processes is likely to play an important role. If the lack of parametrised aerosol effects on convection is the only reason that the convective transition frequencies in the IND run show a weak relationship with AI, then for convective clouds, the IND run might serve a similar purpose to the C-CDNC run for stratiform clouds. If this is the case, the small change in convective transition frequencies with increasing AI in the model might indicate that meteorological covariations for the convective transitions have been significantly reduced. This in turn might suggest that the effects on convective cloud transitions observed in the satellite data might be due to an aerosol effect. However, it is likely that other issues, such as sampling differences between the model and satellite observations (Grandey et al., 2013b) play a role and so no firm conclusions can be drawn about the effect of aerosols on convective clouds.

6.4 Conclusions

In this chapter, the representation of satellite retrieved relationships between aerosol and cloud properties are investigated in the coupled GCM-aerosol model HadGEM3-UKCA.

The regime relative frequency of occurrence (RFO) in the HadGEM3-UKCA is very similar to that found in the satellite observations, although there are some differences. There is a higher thin cirrus regime RFO in the model compared to observations, possibly due to sub-visible cloud in the model. The relationship between regime RFO and AI in the model shows some significant differences to observations. In some regions there is an increase in shallow cumulus RFO with increasing AI, opposite to the change observed in the observations. The relationship between regime RFO and AI shows very little change when aerosol indirect effects are excluded from the model, still showing a strong relationship between RFO and AI. This emphasises how the strength of the AI-RFO relationship is a poor indicator of the strength of aerosol-cloud interactions in satellite studies.

The frequency of transitions between the regimes in the model is similar to that found in observations. There is an increase in the transitions into the thin cirrus regime compared to those found in the observations, which is to be expected given the increased thin cirrus RFO in the model. The relationship between the regime transition frequencies and AI in the model is similar to observations for the stratiform regimes. In a run repeated with constant CDNC (no parametrised aerosol indirect effects), many of the transitions in the stratocumulus pathway show a much weaker relationship to AI. This reduction in the relationship between AI and transition frequencies in the stratiform regimes suggests that the observed increase in stratocumulus persistence may be the result of an aerosol indirect effect.

However, the model shows no relationship between transition frequencies and AI consistent with an aerosol invigoration of convective clouds in either a run including aerosol indirect effects or a run with a constant CDNC. This suggests that convective transitions are not influenced by aerosols in this model. This is unsurprising, as there is no direct interaction between aerosols and convective cloud microphysics in this model.

The model simulations of precipitation development as a function of AI do not show the increase in precipitation in the high AI population at times after T+0 that is seen in the observations. This is most likely due to the lack of a parametrised effect of aerosols on convective cloud microphysics, as precipitation in the study region is dominated by convective precipitation. Whilst the model produces a diurnal cycle of precipitation that is similar to observations, this cycle does not vary between the regimes. This is in contrast to the observations, where variation in the time of maximum precipitation is seen between the different regimes, especially over land.

The use of the HadGEM3-UKCA model indicates that some of the observed effects in satellite data, especially changes in transitions along the stratocumulus pathway, may be the result of an aerosol indirect effect on clouds properties. The model does not recreate the changes in convective cloud or precipitation seen in observations, which could be due to the lack of a parametrised effect of aerosols on convective cloud microphysics in this model.

Chapter 7

Conclusions

The effect of aerosols on precipitation and cloud properties has been studied for over fifty years, but the recent advent of global satellite datasets and global climate models provides an unprecedented opportunity to make progress into understanding these effects.

Many strong relationships have been observed between aerosols and cloud properties, as well as between aerosol and precipitation properties. The magnitude of the contribution of aerosol-cloud interactions to these relationships is unclear, such that uncertainties related to aerosols and clouds are the largest uncertainties in future climate projections (eg. Forster et al., 2007). Uncertainties related to aerosol effects on cloud fraction are particularly hard to quantify, due to a strong non-causal relationship between aerosol optical depth and cloud fraction. As shown in this thesis, this strong relationship also generates spurious correlations between observed aerosol and cloud properties. Aerosol influences on cloud fraction may be an important component of the total aerosol influence on climate.

Detecting aerosol an influence on precipitation shares many of the same problems. A strong wet scavenging effect links the relationship between aerosol and precipitation properties, but even this is confounded by strong covariation of aerosol and precipitation properties with meteorology. Whilst many studies have investigated a possible aerosol effect on precipitation, the difficulty of determining causality can make it difficult to determine observational constraints on aerosol-precipitation interactions.

This work reduces some of the key issues in determining the influence of aerosols on cloud and precipitation properties. A new time-dependent analysis is demonstrated that reduces the influence of meteorological covariation on the observed relationships between aerosol and cloud properties,

allowing for a better determination of the magnitude of aerosol-cloud-precipitation interactions.

Conclusions

Cloud fraction (CF) has been previously shown to be strongly correlated with aerosol optical depth (AOD). It is suspected that a large part of this relationship is the result of effects other than an aerosol influence on cloud fraction. AOD retrieval errors (such as cloud contamination) and errors due to the use of AOD as a CCN proxy (such as the swelling of aerosol in humid environments) have been suggested as contributing factors to this relationship, along with possible aerosol-cloud interactions.

A strong correlation has also been observed between AOD and cloud top pressure (CTP), a correlation which has been suggested to be evidence of an aerosol invigoration of convective clouds. In chapter 2, the influence of the strong AOD-CF correlation on other correlations between aerosol and cloud properties is examined, demonstrating that much of the AOD-CTP correlation can be attributed to variations in CF as a controlling variable. Using regularly gridded data at a 1° by 1° resolution from the MODIS instrument on-board Terra, these correlations were reproduced globally. When the AOD-CF was relationship multiplied by the CF-CTP relationship, it was shown that a strong correlation between AOD and CTP can be produced. Neither the CF-CTP nor the AOD-CF correlations require an aerosol effect on convection, suggesting that the correlation between AOD and CTP is not evidence of aerosol invigoration of convection. This spurious correlation disguises the AOD-CTP correlation due to aerosol influences, in some regions obscuring a negative relationship between AOD and CTP (at constant CF).

The CF-CTP correlation is unlikely to be due to an error in the cloud properties retrieval, but previous work suggests that the AOD-CF correlation is unlikely to be entirely due to an aerosol effect on cloud. This in turn creates uncertainty about the true effect of aerosols on CTP and cloud vertical development. As a basic attempt to account for the influence of the AOD-CF correlation, the AOD-CTP sensitivity at a constant CF was investigated, showing a significantly decreased sensitivity of CTP to AOD variations. There are some downsides to examining cloud vertical development using a constant CF approach. The main disadvantage is that some of the AOD-CF relationship is thought to be due to aerosol-cloud interactions influencing CF, and so by restricting CF, the response of the CTP (through the CF-CTP correlation) to aerosol perturbations is also restricted. Restricting CF also necessarily removes any ability to investigate the effect of aerosols on CF. The accounting for the

strong AOD-CF relationship whilst allowing cloud development is an important motivator for later parts of this work.

In chapter three, MODIS cloud regimes were determined using a k-means clustering process on MODIS cloud top pressure - cloud optical depth histograms. These regimes represent several distinct cloud types, similar to the ISCCP weather states. These regimes were then used to investigate how the sensitivity of the cloud droplet number concentration (CDNC) to AOD varies by regime. The cloud albedo effect predicts an increase in CDNC with increasing CCN concentrations. MODIS observations of cloud optical depth and effective radius were used to determine the CDNC using the adiabatic approximation.

The sensitivity of CDNC to AOD was found to vary by regime, with only the liquid cloud regimes showing significant sensitivities of CDNC to AOD. Among the liquid cloud regimes over ocean, CDNC in the stratocumulus regime shows a higher sensitivity to AOD than the shallow cumulus regime. This indicates a sampling bias when calculating the sensitivity without accounting for cloud regimes, as the stratocumulus regime is undersampled due to its high cloud fraction and corresponding low AOD retrieval success rate.

A negative sensitivity had previously been found over land in the standard MODIS products, indicating a reduction in CDNC with increasing AOD. This is contrary to the theoretical effect of aerosols on cloud properties. Considering sensitivity by regime showed that this negative relationship is driven by the relationship in the shallow cumulus regime. As the shallow cumulus regime has a much lower CF, this indicates a possible retrieval error for MODIS CDNC at low CF over land. Recombining the regime sensitivities (accounting for the sampling issues), the sensitivity over land increases, becoming positive in many regions. This emphasises the importance of considering cloud properties and aerosol effects by regime.

In chapter four, two temporally spaced MODIS retrievals each day were used to examine the links between MODIS AI and the transitions between the previously determined cloud regimes. The main aim of this chapter was to determine whether aerosols have an influence on cloud development in a way that takes into account the influence of CF, meteorological factors and the importance of regimes.

The frequency of occurrence of the cloud regimes themselves are very strongly linked to the local AOD. This is due to the strong AOD-CF relationship, which as suggested previously is thought to be

mostly the result of non-aerosol influences. This relationship is accounted for whilst still allowing the study of cloud development and the influence of aerosol on cloud fraction, by investigating the changes in transition frequency between the regimes with increasing AI.

Separate transition histograms were generated for high and low AI populations, accounting for the strong AI-CF relationship by ensuring the high and low AI populations have the same distribution of CF and other meteorological parameters at the start of the observation period. The changes in the frequencies of transitions between regimes are consistent with an increase in stratocumulus persistence with increasing AI, resulting in an increase in CF with increasing AI. An increase in transitions into mid-level and deep convective regimes was also found, consistent with an aerosol invigoration of convective cloud. The correlation between AI and CF development in the shallow cumulus regime is dependent on the local meteorology, with AI having a stronger correlation with CF development in regions of higher low tropospheric static stability and higher windspeed.

By using multiple aerosol retrievals, at the start and the end of the observation period, the aerosol effect on cloud fraction was limited to less than half of that found when performing a simple correlation between AI and CF. Determining the exact magnitude of the aerosol influence on CF was prevented due to the uncertainties in the magnitude of the wet scavenging influence on AI over the observation period, but this sets an upper limit to the influence of aerosol on CF.

This methodology was then extended in chapter five to study the changes in precipitation development with increasing AI. The main aim of this chapter was to determine whether aerosols have an influence on precipitation development. Using MODIS AI and cloud property retrievals to provide cloud regime and AI retrievals at a single overpass time, multiple precipitation retrievals were then used to build a picture of the diurnal cycle of precipitation for each regime. By using AI defined at the same time as the cloud regime retrieval, the influence of CF on the AI retrieval is accounted for in the same way as the previous chapter.

Unlike previous studies of the correlation between AOD and precipitation, little evidence of a link between AI and precipitation is found at the time of the aerosol retrieval, as the AI-CF correlation is accounted for. However, there is an increase in precipitation at times after the AI retrieval - consistent with an aerosol invigoration of convective precipitation. This increase in precipitation with increasing AI is stronger in clouds with tops colder than 273 K, suggesting that ice processes are an important factor in a possible aerosol effect on precipitation. An inverse relationship was found

between AI and precipitation at times before the AI retrieval, consistent with wet scavenging. This wet scavenging effect is stronger in regions with a high mean precipitation rate. The increase in precipitation with increasing AI at times after the AI retrieval shows a dependence on the local mean AI. In regions of high mean AI, decreases in precipitation with increasing AI were found, suggesting that although aerosol acts to increase precipitation at low levels, as it reaches a high concentration, it acts to suppress precipitation.

Investigations into the diurnal cycle of other variables related to convective activity also showed a similar effect. The high AI population has a higher lightning flash rate at times after the AI retrieval, particularly over land. This would suggest that the increase in retrieved precipitation with increasing AI is not a retrieval bias in the precipitation retrieval caused by a change in droplet size distribution with increasing AI.

Meteorological covariations can be considered as one of two types. Type one effects are caused by inaccurate determinations of CCN, in many cases due to a breakdown in the AOD-CCN or AI-CCN relationship. Many of the type one errors (such as cloud contamination and humid swelling) are related to the CF within a regime. By making use of the AI and accounting for the AI-CF correlation within the cloud regimes, these errors are reduced. Type two effects, where the cloud and CCN properties vary together, are harder to remove. To reduce them, the high and low AI populations of each regime were sampled so that they had the same distribution of the meteorological properties. However, it is possible that the correlations seen in observations are still the result of covariation between cloud and aerosol properties, caused by unaccounted-for meteorological covariations. Investigations using model data provide one possible way to determine if the observed effects are due to an influence of aerosols on cloud properties, or a remaining meteorological covariation.

Global climate models provide the possibility of investigating the role of individual effects on aerosol-cloud correlations, as these effects can be removed from the model separately. Chapter six made use of the HadGEM3 GCM with the UKCA aerosol module to investigate whether a GCM can reproduce the relationships between aerosol and cloud regime transitions and properties. The studies show that the model is able to represent the frequency of occurrence of the regimes and the frequencies of transitions between the regimes well. Examining the difference between the transition frequencies for the high and low AI populations shows that for the transitions between the stratiform cloud regimes, the model shows similar changes in transition frequencies with increasing AI to those

seen in observations, indicating an increase in stratocumulus persistence with increased AI. Repeating the experiment with a constant CDNC, these transitions between the stratiform cloud regimes show a much smaller difference in occurrence between the high and low AI populations. This suggests that the correlations seen between the transition frequencies and AI in satellite observations may be the result of an aerosol effect on clouds, rather than meteorological covariations of cloud and aerosol properties.

The model does not reproduce the changes in transitions between the convective cloud regimes with increasing AI as well, in many cases showing no change in transition frequency with increased AI. A similar effect was found when investigating precipitation development in the model, with the model showing little difference between the development of the high and low AI populations. It is most likely that this is due to the necessary aerosol interactions with convective cloud microphysics not being parametrised in this model, making it difficult to draw conclusions about the possible aerosol influences on convective clouds in this model.

Summary

This thesis has demonstrated a method by which meteorological and retrieval errors can be reduced when investigating an aerosol effect on precipitation and cloud properties. Results consistent with an aerosol invigoration of convective clouds are observed, although the magnitude of the effect is smaller than that seen in previous studies. Changes in the cloud development consistent with increased stratocumulus persistence in high aerosol environments are also observed. It is not possible to conclusively determine whether these results are due to an aerosol effect on precipitation, although they do provide new upper limits to the effect of aerosols on cloud fraction and precipitation.

Future work

There are several possible avenues for future investigation leading from the work done in this thesis.

CF-CTP relationship in models

The intensification of the AOD-CTP relationship by the AOD-CF and the CF-CTP relationships is also present in climate models and explains the strength of the AOD-CTP correlations within the models of the AeroCom Indirect Effect Experiment. A detailed description of the models and their

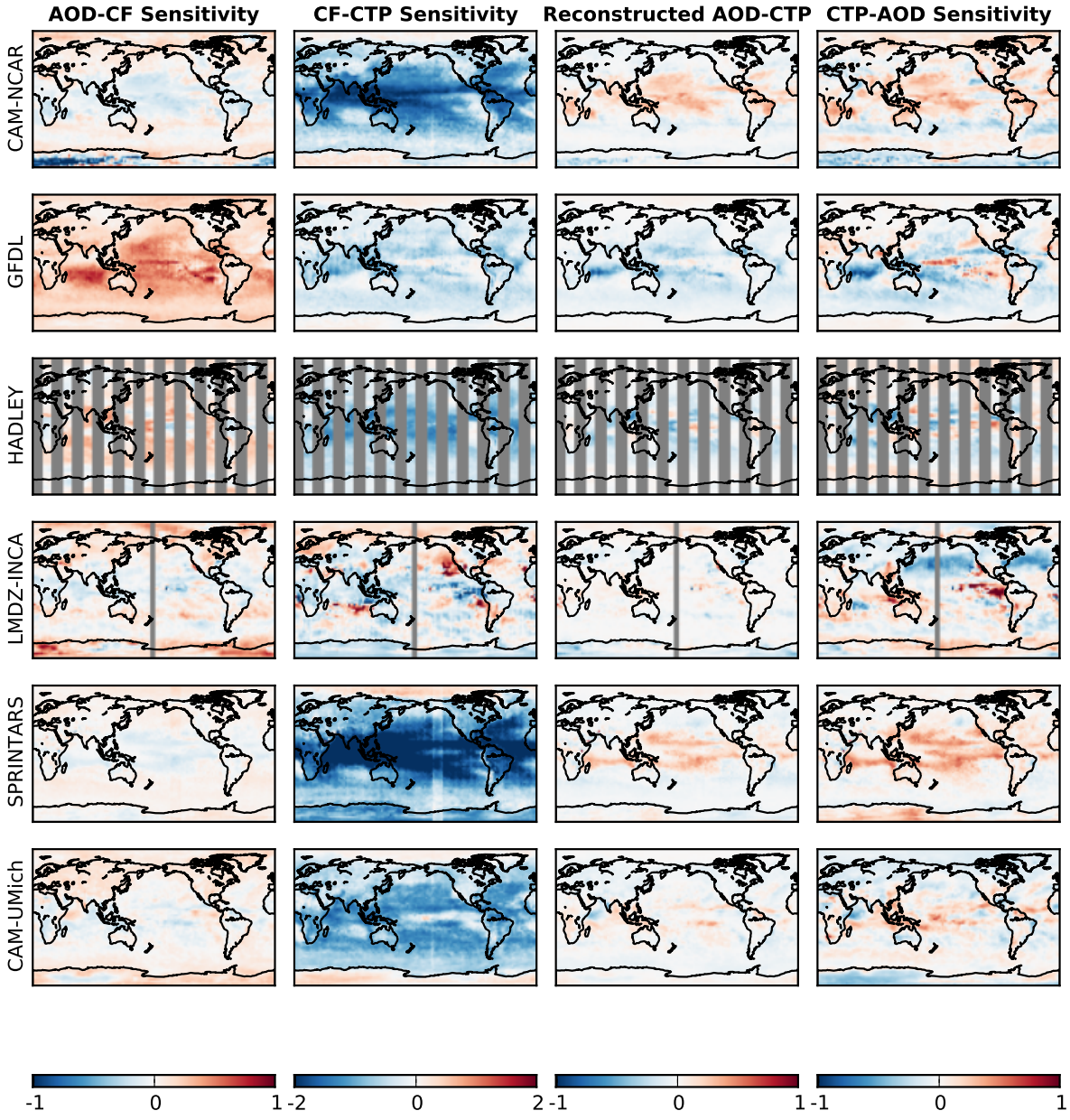

Figure 7.1: The sensitivities of cloud properties to aerosol properties in the AeroCom indirect effect models.

behaviour can be found in (Quaas et al., 2009), here it is important to note that these models include some parametrised effects of aerosols on clouds, but none of them include explicitly parametrised effects of aerosols on convective clouds or ice. Whilst this does not prevent an aerosol invigoration effect, many of the current theories of the aerosol invigoration process depend on an interaction with droplet freezing.

All of the models (Fig. 7.1) apart from the LMDZ model show a negative CF-CTP sensitivity of varying strengths across the globe. Whilst the strength of the AOD-CF and AOD-CTP sensitivities in

the models vary, they are typically anti-correlated. Models with a strong positive AOD-CF sensitivity (eg. GFDL and HadGEM), typically have a strong negative AOD-CTP sensitivity, with a positive AOD-CTP relationship being found in regions where the AOD-CF correlation is negative or the CF-CTP relationship is weak. Models with a negative AOD-CF correlation, such as SPRINTARS or CAM-UMich typically show a positive AOD-CTP sensitivity, which helps to explain the large range of AOD-CTP sensitivities observed in this collection of models.

The models used in the AeroCom Indirect effect experiment are now several years old; these models now include more advanced aerosol and cloud schemes. It would be interesting to know if the AOD-CF relationship is still the primary cause of AOD-CTP correlations in these models, especially in cases where the models include parametrised effects of aerosol on convection.

Determination of total aerosol effect on CF

Previous work has focused on correlations between aerosol and cloud properties retrieved at the same time. These 'snapshot' correlations have a restricted ability to account for the effects of CF on the aerosol retrieval. However, they do allow for the investigation of an 'integrated' effect, where the total effect of the aerosol on the cloud properties can be considered. In contrast, the studies of cloud development in varying aerosol environments presented in this work are unlikely to have reached equilibrium by the end of the observation period.

Some progress has been made towards determining a total effect of aerosols on CF by comparing d(CF) calculated with both an AI retrieval where the AI-CF relationship is accounted for and one where it is not (section 4.2.7). This indicates a relative magnitude between the development and snapshot methods, which may be suitable for determining a total effect of aerosols on cloud fraction. Determining a total effect on precipitation is also challenging, as an increase in precipitation will increase the wet scavenging of aerosol, perhaps resulting in a reduced precipitation rate at later times.

There are other aspects which would need to be addressed to determine the magnitude of a global effect, for which the current methods and data are not suitable. Transition histograms and changes in the histograms with changes in aerosol would need to be investigated at different times of day. Given the important effect of the diurnal cycle, the frequencies of transitions will be different at different times of day. For transitions at night, this will require a new approach, as cloud and aerosol optical depth are not currently retrieved in darkness.

It will also be necessary to determine the applicability of these results in regions outside the tropics, where the diurnal cycle is not such a strong driver of variability.

Sampling in models

Different correlations between aerosol and cloud regime transitions are found when using MODIS AI/AOD and MACC AOD. As MODIS and MACC are designed not to differ in locations where there is a MODIS retrieval, this suggests that there may be a sampling issue in regimes with high cloud cover. MODIS can only sample the aerosol in clear sky regions, whereas MACC can determine an AOD even in cloud covered regions. In these cloud covered regions, there is a strong likelihood of precipitation, which would generate a negative correlation between aerosol and precipitation. This negative correlation would likely be stronger than that found in the clear-sky MODIS aerosol. In regimes with high cloud cover and high precipitation rates (such as the deep convective regime), the strong negative correlation from wet scavenging could disguise an invigoration effect if the all-sky aerosol is sampled. As GCMs in general do not have a separate population of aerosol for clear sky-regions, this might limit comparisons between models and observations.

To investigate the possibility of sampling issues, studies using high resolution models, which resolve aerosol processes in cloud covered and clear sky separately will be needed. These can then investigate the importance of the difference between model and satellite sampling of aerosols, as well as whether using all-sky or clear-sky AOD is more suitable for determining an aerosol influence on precipitation.

Improved satellite assessments

Improved satellite observing systems may provide new insights into cloud and aerosol processes. The Global Precipitation Mission (GPM) is due to be launched in 2014 as a successor to TRMM. It will have a microwave imager on-board, but will also carry a dual frequency precipitation radar. Like TRMM it will be able to retrieve the vertical structure of precipitation, but with a dual frequency radar, it will also be able to retrieve microphysical properties of precipitation. This is particularly important for studies of aerosol effects on precipitation, as it will enable a retrieval of the droplet size distribution. As aerosol processes may modify the droplet size distribution, this would enable a study of whether the changes observed in this work are due to a change in precipitation rate, or droplet size

distribution.

Other satellite due for launch in the next few years will also provide increased insight into aerosol-cloud interactions. EarthCARE will carry a sensitive doppler radar, enabling the retrieval of vertical velocities within convective clouds. MeteoSat Third Generation, due for launch in 2018, will be able to provide full disk image at 1 km resolution, every 30 minutes. This will have many useful applications for investigating cloud development.

Bibliography

Abdul-Razzak, H. and Ghan, S. J.: A parameterization of aerosol activation: 2. Multiple aerosol types, J. Geophys. Res., 105, 6837, doi:10.1029/1999JD901161, 2000.

Ackerman, A. S., Kirkpatrick, M. P., Stevens, D. E., and Toon, O. B.: The impact of humidity above stratiform clouds on indirect aerosol climate forcing, Nature, 432, 1014, doi:10.1038/nature03174, 2004.

Ackerman, S., Toon, O., Stevens, D., Heymsfield, A., Ramanathan, V., and Welton, E.: Reduction of Tropical Cloudiness by Soot, Science, 288, 1042–1047, doi:10.1126/science.288.5468.1042, 2000.

Adler, R. F., Huffman, G. J., Bolvin, D. T., Curtis, S., and Nelkin, E. J.: Tropical Rainfall Distributions Determined Using TRMM Combined with Other Satellite and Rain Gauge Information, J. App. Met., 39, 2007–2023, doi:10.1175/1520-0450(2001)040⟨2007:TRDDUT⟩2.0.CO;2, 2000.

Adler, R. F., Kidd, C., Petty, G., Morissey, M., and Goodman, H. M.: Intercomparison of Global Precipitation Products: The Third Precipitation Intercomparison Project (PIP-3)., Bull. A. Met. Soc., 82, 1377–1396, doi:10.1175/1520-0477(2001)082⟨1377:IOGPPT⟩2.3.CO;2, 2001.

Adler, R. F., Huffman, G. J., Chang, A., Ferraro, R., Xie, P.-P., Janowiak, J., Rudolf, B., Schneider, U., Curtis, S., Bolvin, D., Gruber, A., Susskind, J., Arkin, P., and Nelkin, E.: The Version-2 Global Precipitation Climatology Project (GPCP) Monthly Precipitation Analysis (1979 Present), J. Hydrometeorology, 4, 1147, doi:10.1175/1525-7541(2003)004⟨1147:TVGPCP⟩2.0.CO;2, 2003.

Albrecht, B.: Aerosols, Cloud Microphysics, and Fractional Cloudiness, Science, 245, 1227–1230, doi:10.1126/science.245.4923.1227, 1989.

Allen, M. and Ingram, W.: Constraints on future changes in climate and the hydrologic cycle, Nature, 419, 224–232, doi:10.1038/nature01092, 2002.

Altaratz, O., Koren, I., Reisin, T., Kostinski, A., Feingold, G., Levin, Z., and Yin, Y.: Aerosols' influence on the interplay between condensation, evaporation and rain in warm cumulus cloud, Atmos. Chem. Phys., 8, 15–24, doi:10.5194/acp-8-15-2008, 2008.

Anderberg, M.: Cluster Analysis for Applications, Elsevier, New York, 1973.

Andreae, M.: Correlation between cloud condensation nuclei concentration and aerosol optical thickness in remote and polluted regions, Atmos. Chem. Phys., 9, 543–556, doi:10.5194/acp-9-543-2009, 2009.

Andreae, M. and Rosenfeld, D.: Aerosol cloud precipitation interactions. Part 1. The nature and sources of cloud-active aerosols, Earth Sci. Rev., 89, 13–41, doi:10.1016/j.earscirev.2008.03.001, 2008.

Andreae, M., Rosenfeld, D., Artaxo, P., Costa, A., Frank, G., Longo, K., and Silva-Dias, M.: Smoking Rain Clouds over the Amazon, Science, 303, 1337–1342, doi:10.1126/science.1092779, 2004.

Andreas, E. L.: A new sea spray generation function for wind speeds up to 32 ms^{-1}, J. Phys. Oceanography, 28, 2175–2184, doi:10.1175/1520-0485(1998)028⟨2175:ANSSGF⟩2.0.CO;2, 1998.

Arakawa, A.: The Cumulus Parameterization Problem: Past, Present, and Future, J. Climate, 17, 2493–2525, doi:10.1175/1520-0442(2004)017⟨2493:RATCPP⟩2.0.CO;2, 2004.

Arkin, P. A. and Meisner, B. N.: The Relationship between Large-Scale Convective Rainfall and Cold Cloud over the Western Hemisphere during 1982-84, M. Weather Rev., 115, 51–74, doi:10.1175/1520-0493(1987)115⟨0051:TRBLSC⟩2.0.CO;2, 1987.

Austin, R. and Stephens, G.: Retrieval of stratus cloud microphysical parameters using millimeter-wave radar and visible optical depth in preparation for CloudSat 1. Algorithm formulation, J. Geophys. Res., 106, 28 233–28 242, doi:10.1029/2000JD000293, 2001.

Ayers, G. P. and Gillet, G. W.: DMS and its oxidation products in the remote marine atmosphere: implications for climate and atmospheric chemistry, J. Sea Res., 43, 275–286, doi:10.1016/S1385-1101(00)00022-8, 2000.

Baker, M. B. and Charlson, R. J.: Bistability of CCN concentrations and thermodynamics in the cloud-topped boundary layer, Nature, 345, 142–145, doi:10.1038/345142a0, 1990.

Bauer, P., Moreau, E., and di Michele, S.: Hydrometeor Retrieval Accuracy Using Microwave Window and Sounding Channel Observations., J. App. Met., 44, 1016–1032, doi:10.1175/JAM2257.1, 2005.

Beheng, K. D.: A parameterization of warm cloud microphysical conversion processes, Atmos. Res., 33, 193–206, doi:10.1016/0169-8095(94)90020-5, 1994.

Bell, T., Rosenfeld, D., Kim, K.-M., Yoo, J.-M., Lee, M.-I., and Hahnenberger, M.: Midweek increase in U.S. summer rain and storm heights suggests air pollution invigorates rainstorms, J. Geophys. Res., 113, D02209, doi:10.1029/2007JD008623, 2008.

Bell, T. L. and Rosenfeld, D.: Comment on "Weekly precipitation cycles? Lack of evidence from United States surface stations" by D. M. Schultz et al., Geophys. Res. Lett., 35, L09803, doi:10.1029/2007GL033046, 2008.

Bell, T. L., Rosenfeld, D., and Kim, K.-M.: Weekly cycle of lightning: Evidence of storm invigoration by pollution, Geophys. Res. Lett., 36, L23 805, doi:10.1029/2009GL040915, 2009.

Bellouin, N., Mann, G. W., Woodhouse, M. T., Johnson, C., Carslaw, K. S., and Dalvi, M.: Impact of the modal aerosol scheme GLOMAP-mode on aerosol forcing in the Hadley Centre Global Environmental Model, Atmos. Chem. Phys., 13, 3027–3044, doi:10.5194/acp-13-3027-2013, 2013.

Bennartz, R.: Global assessment of marine boundary layer cloud droplet number concentration from satellite, J. Geophys. Res., 112, D02201, doi:10.1029/2007JD007547, 2007.

Bennartz, R., Fan, J., Rausch, J., Leung, L., and Heidinger, A.: Pollution from China increases cloud droplet number, suppresses rain over the East China Sea, Geophys. Res. Lett., 38, L09704, doi:10.1029/2011GL047235, 2011.

Berg, W., L'Ecuyer, T., and Kummerow, C.: Rainfall Climate Regimes: The Relationship of Regional TRMM Rainfall Biases to the Environment, J. App. Met. Clim., 45, 434–454, doi: 10.1175/JAM2331.1, 2006.

Bodas-Salcedo, A., Webb, M. J., Bony, S., Chepfer, H., Dufresne, J.-L., Klein, S. A., Zhang, Y., Marchand, R., Haynes, J. M., Pincus, R., and John, V. O.: COSP: Satellite simulation software for model assessment, Bull. A. Met. Soc., 92, 1023–1043, doi:10.1175/2011BAMS2856.1, 2011.

Bodas-Salcedo, A., Williams, K. D., Field, P. R., and Lock, A. P.: The Surface Downwelling Solar Radiation Surplus over the Southern Ocean in the Met Office Model: The Role of Midlatitude Cyclone Clouds, J. Climate, 25, 7467–7486, doi:10.1175/JCLI-D-11-00702.1, 2012.

Bollasina, M. A., Ming, Y., and Ramaswamy, V.: Anthropogenic Aerosols and the Weakening of the South Asian Summer Monsoon, Science, 334, 502, doi:10.1126/science.1204994, 2011.

Bond, T. C., Doherty, S. J., Fahey, D. W., Forster, P. M., Berntsen, T., DeAngelo, B. J., Flanner, M. G., Ghan, S., Kärcher, B., Koch, D., Kinne, S., Kondo, Y., Quinn, P. K., Sarofim, M. C., Schultz, M. G., Schulz, M., Venkataraman, C., Zhang, H., Zhang, S., Bellouin, N., Guttikunda, S. K., Hopke, P. K., Jacobson, M. Z., Kaiser, J. W., Klimont, Z., Lohmann, U., Schwarz, J. P., Shindell, D., Storelvmo, T., Warren, S. G., and Zender, C. S.: Bounding the role of black carbon in the climate system: A scientific assessment, J. Geophys. Res., 118, 5380–5552, doi:10.1002/jgrd.50171, 2013.

Bony, S. and Dufresne, J.-L.: Marine boundary layer clouds at the heart of tropical cloud feedback uncertainties in climate models, Geophys. Res. Lett., 32, L20 806, doi:10.1029/2005GL023851, 2005.

Bony, S., Dufresne, J.-L., Le, T. H., Morcrette, J.-J., and Senior, C.: On dynamic and thermodynamic components of cloud changes, Climate Dyn., 22, 71, doi:10.1007/s00382-003-0369-6, 2004.

Borg, L. A., Holz, R. E., and Turner, D. D.: Investigating cloud radar sensitivity to optically thin cirrus using collocated Raman lidar observations, Geophys. Res. Lett., 38, L05 807, doi:10.1029/2010GL046365, 2011.

Boucher, O. and Quaas, J.: Water vapour affects both rain and aerosol optical depth, Nat. Geosci., 6, 4–5, doi:10.1038/ngeo1692, 2012.

Bowman, K. P.: Comparison of TRMM Precipitation Retrievals with Rain Gauge Data from Ocean Buoys, J. Climate, 18, 178–190, doi:10.1175/JCLI3259.1, 2005.

Brenguier, J.-L., Pawlowska, H., Schüller, L., Preusker, R., Fischer, J., and Fouquart, Y.: Radiative Properties of Boundary Layer Clouds: Droplet Effective Radius verses Number Concentration, J. Atmos. Sci., 57, 803–821, doi:10.1175/1520-0469(2000)057⟨0803:RPOBLC⟩2.0.CO;2, 2000.

Brennan, J., Kaufman, Y., Koren, I., and Li, R.: Aerosol Cloud Interaction - Misclassification of MODIS Clouds in Heavy Aerosol, IEEE T. GeoSci. Remote, 43, 911–915, doi:10.1109/TGRS.2005.844662, 2005.

Bréon, F.-M., Tanré, D., and Generoso, S.: Aerosol Effect on Cloud Droplet Size Monitored from Satellite, Science, 295, 834–838, doi:10.1126/science.1066434, 2002.

Cachorro, V., Pomero, P., Toledano, C., Cuevas, E., and de Frutos, A.: The fictitious diurnal cycle of aerosol optical depth: A new approach for 'in situ' calibration and correction of AOD data series, Geophys. Res. Lett., 31, L12106, doi:10.1029/2004GL019651, 2004.

Cappa, C. D., Onasch, T. B., Massoli, P., Worsnop, D. R., Bates, T. S., Cross, E. S., Davidovits, P., Hakala, J., Hayden, K. L., Jobson, B. T., Kolesar, K. R., Lack, D. A., Lerner, B. M., Li, S.-M., Mellon, D., Nuaaman, I., Olfert, J. S., Petäjä, T., Quinn, P. K., Song, C., Subramanian, R., Williams, E. J., and Zaveri, R. A.: Radiative absorption enhancements due to the mixing state of atmospheric black carbon., Science, 337, 1078–1081, doi:10.1126/science.1223447, 2012.

Carlson, T. N. and Prospero, J. M.: The large-scale movement of Saharan air outbreaks over the Northern Equatorial Atlantic, Journal of Applied Meteorology, 11, 283–297, doi:10.1175/1520-0450(1972)011⟨0283:TLSMOS⟩2.0.CO;2, 1972.

Chand, D., Wood, R., Ghan, S. J., Wang, M., Ovchinnikov, M., Rasch, P. J., Miller, S., Schichtel, B., and Moore, T.: Aerosol optical depth increase in partly cloudy conditions, J. Geophys. Res., 117, D17207, doi:10.1029/2012JD017894, 2012.

Chen, S. S. and Houze, R. A.: Diurnal variation and life-cycle of deep convective systems over the tropical pacific warm pool, Q. J. RMetS., 123, 357–388, doi:10.1002/qj.49712353806, 1997.

Chen, Y.-C., Christensen, M. W., Xue, L., Sorooshian, A., Stephens, G. L., Rasmussen, R. M., and Seinfeld, J. H.: Occurrence of lower cloud albedo in ship tracks, Atmos. Chem. Phys., 12, 8223–8235, doi:10.5194/acp-12-8223-2012, 2012.

Christian, H. J.: Global frequency and distribution of lightning as observed from space by the Optical Transient Detector, J. Geophys. Res., 108, D14 005, doi:10.1029/2002JD002347, 2003.

Chu, D. A., Kaufman, Y. J., Ichoku, C., Remer, L. A., Tanré, D., and Holben, B. N.: Validation of MODIS aerosol optical depth retrieval over land, Geophys. Res. Lett., 29, 8007, doi:10.1029/2001GL013205, 2002.

Chung, C. E., Ramanathan, V., and Decremer, D.: Observationally constrained estimates of carbonaceous aerosol radiative forcing., P. Natl. A. Sci., 109, 11 624–11 629, doi:10.1073/pnas.1203707109, 2012.

Coakley, J. A., Bernstein, R. L., and Durkee, P. A.: Effect of Ship-Stack Effluents on Cloud Reflectivity, Science, 237, 1020–1022, doi:10.1126/science.237.4818.1020, 1987.

Costantino, L. and Bréon, F.-M.: Aerosol indirect effect on warm clouds over South-East Atlantic, from co-located MODIS and CALIPSO observations, Atmos. Chem. Phys., 13, 69–88, doi:10.5194/acp-13-69-2013, 2013.

Dai, A.: Precipitation Characteristics in Eighteen Coupled Climate Models, J. Climate, 19, 4605–4630, doi:10.1175/JCLI3884.1, 2006.

Davis, S. M., Avallone, L. M., Kahn, B. H., Meyer, K. G., and Baumgardner, D.: Comparison of airborne in situ measurements and Moderate Resolution Imaging Spectroradiometer (MODIS) retrievals of cirrus cloud optical and microphysical properties during the Midlatitude Cirrus Experiment (MidCiX), J. Geophys. Res., 114, D02 203, doi:10.1029/2008JD010284, 2009.

Dee, D. P., Uppala, S. M., Simmons, A. J., Berrisford, P., Poli, P., Kobayashi, S., Andrae, U., Balmaseda, M. A., Balsamo, G., Bauer, P., Bechtold, P., Beljaars, A. C. M., van de Berg, L., Bidlot, J., Bormann, N., Delsol, C., Dragani, R., Fuentes, M., Geer, A. J., Haimberger, L., Healy, S. B., Hersbach, H., Hlm, E. V., Isaksen, L., Kllberg, P., Khler, M., Matricardi, M., McNally, A. P., Monge-Sanz, B. M., Morcrette, J.-J., Park, B.-K., Peubey, C., de Rosnay, P., Tavolato, C., Thpaut, J.-N., and Vitart, F.: The ERA-Interim reanalysis: configuration and performance of the data assimilation system, Quarterly Journal of the Royal Meteorological Society, 137, 553–597, doi:10.1002/qj.828, 2011.

DeMott, P. J., Sassen, K., Poellot, M. R., Baumgardner, D., Rogers, D. C., Brooks, S. D., Prenni, A. J., and Kreidenweis, S. M.: African dust aerosols as atmospheric ice nuclei, Geophys. Res. Lett., 30, 1732, doi:10.1029/2003GL017410, 2003.

Denman, K. L., Brasseur, G., Chidthaisong, A., Ciais, P., Cox, P., Dickinson, R. E., Hauglustaine, D., Heinze, C., Holland, E., Jacob, D., Lohmann, U., Ramachandran, S., da Silva Dias, P., Wofsy, S., and Zhang, X.: Couplings Between Changes in the Climate System and Biogeochemistry, in: Solomon et al. (2007), chap. 7, 2007.

Dey, S., Di, G. L., Zhao, G., Jones, A. L., and McFarquhar, G. M.: Satellite-observed relationships between aerosol and trade-wind cumulus cloud properties over the Indian Ocean, Geophys. Res. Lett., 38, L01 804, doi:10.1029/2010GL045588, 2011.

Draxler, R. R. and Rolph, G. D.: HYSPLIT (HYbrid Single-Particle Lagrangian Integrated Trajectory) Model access via NOAA ARL READY Website (http://www.arl.noaa.gov/HYSPLIT.php), Tech. rep., NOAA, 2013.

Durkee, P. A., Noone, K. J., Ferek, R. J., Johnson, D. W., Taylor, J. P., Garrett, T. J., Hobbs, P. V., Hudson, J. G., Bretherton, C. S., Innis, G., Frick, G. M., Hoppel, W. A., O'Dowd, C. D., Russell, L. M., Gasparovic, R., Nielsen, K. E., Tessmer, S. A., Öström, E., Osborne, S. R., Flagan, R. C., Seinfeld, J. H., and Rand, H.: The Impact of Ship-Produced Aerosols on the Microstructure and Albedo of Warm Marine Stratocumulus Clouds: A Test of MAST Hypotheses 1i and 1ii., J. Atmos. Sci., 57, 2554–2569, doi:10.1175/1520-0469(2000)057⟨2554:TIOSPA⟩2.0.CO;2, 2000.

Dusek, U., Frank, G., Hildebrandt, L., Curtius, J., Schneider, J., Walter, S., Chand, D., Drewnick, F., Hings, S., Jung, D., Borrmann, S., and Andreae, M.: Size Matters More Than Chemistry for Cloud-Nucleating Ability of Aerosol Particles, Science, 312, 1375–1378, doi:10.1126/science.1125261, 2006.

Efron, B.: Bootstrap methods: Another look at the jackknife, Ann. Stat., 7, 1–26, 1979.

Ellis, T., L'Ecuyer, T., Haynes, J., and Stephens, G.: How often does it rain over the global oceans? The perspective from CloudSat, Geophys. Res. Lett., 36, L03815, doi:10.1029/2008GL036728, 2009.

Engstrom, A. and Ekman, A. M.: Impact of meteorological factors on the correlation between aerosol optical depth and cloud fraction, Geophys. Res. Lett., 37, L18814, doi:10.1029/2010GL044361, 2010.

Engström, A. and Magnusson, L.: Estimating trajectory uncertainties due to flow dependent errors in the atmospheric analysis, Atmos. Chem. Phys., 9, 8857–8867, doi:10.5194/acp-9-8857-2009, 2009.

Evan, A., Heidinger, A., and Vimont, D.: Arguments against a physical long-term trend in global ISCCP cloud amounts, Geophys. Res. Lett., 34, L04 701, 2007.

Evan, A. T., Kossin, J. P., 'Eddy' Chung, C., and Ramanathan, V.: Arabian Sea tropical cyclones intensified by emissions of black carbon and other aerosols, Nature, 479, 94–97, doi:10.1038/nature10552, 2011.

Fan, J., Zhang, R., Li, G., and Tao, W.-K.: Effects of aerosols and relative humidity on cumulus clouds, J. Geophys. Res., 112, D14 204, doi:10.1029/2006JD008136, 2007.

Feingold, G., Eberhard, W., Veron, D., and M, P.: First measurements of the Twomey indirect effect using ground-based remote sensors, Geophys. Res. Lett., 30, 1287, doi:10.1029/2002GL016633, 2003.

Fleming, J. R.: The pathological history of weather and climate modification: Three cycles of promise and hype, Hist. Stud. Phys. Biol., 37, 3, doi:10.1525/hsps.2006.37.1.3, 2006.

Forster, P., Ramaswamy, V., Artaxo, P., Berntsen, T., Betts, R., Fahey, D., Haywood, J., Lean, J., Lowe, D., Myhre, G., Nganga, J., Prinn, R., Raga, G., Schulz, M., and Van Dorland, R.: Changes in Atmospheric Constituents and in Radiative Forcing, in: Solomon et al. (2007), chap. 2, 2007.

Franklin, B.: Meteorological Imaginations and Conjectures, Mem. Manchester Lit. and Phil. Soc., 2, 374–381, 1789.

Frieler, K., Meinshausen, M., Schneider von Deimling, T., Andrews, T., and Forster, P.: Changes in global-mean precipitation in response to warming, greenhouse gas forcing and black carbon, Geophys. Res. Lett., 38, L04 702, 2011.

Gantt, B. and Meskhidze, N.: The physical and chemical characteristics of marine primary organic aerosol: a review, Atmos. Chem. Phys., 13, 3979–3996, doi:10.5194/acp-13-3979-2013, 2013.

Garstang, M., Bruintjes, R., Serafin, R., Orville, H., Boe, B., Cotton, W., and Warburton, J.: Weather Modification: Finding Common Ground., B. Am. Meteorol. Soc., 86, 647, 2005.

Goren, T. and Rosenfeld, D.: Satellite observations of ship emission induced transitions from broken to closed cell marine stratocumulus over large areas, J. Geophys. Res., 117, D17 206, doi:10.1029/2012JD017981, 2012.

Grabowski, W.: Impact of Cloud Microphysics on Convective-Radiative Quasi Equilibrium Revealed by Cloud-Resolving Convection Parameterization., J. Climate, 16, 3463–3475, doi:10.1175/1520-0442(2003)016⟨3463:IOCMOC⟩2.0.CO;2, 2003.

Grandey, B. and Stier, P.: A critical look at spatial scale choices in satellite-based aerosol indirect effect studies, Atmos. Chem. Phys., 10, 11 459–11 470, doi:10.5194/acp-10-11459-2010, 2010.

Grandey, B., Stier, P., Wagner, T., Grainger, R., and Hodges, K.: The effect of extratropical cyclones on satellite-retrieved aerosol properties over ocean, Geophys. Res. Lett., 38, L13805, doi:10.1029/2011GL047703, 2011.

Grandey, B., Stier, P., Grainger, R., and Wagner, T.: The contribution of extratropical cyclones to observed cloudaerosol relationships, Atmos. Chem. Phys. Discuss., 13, 11 971–11 995, doi:10.5194/acpd-13-11971-2013, 2013a.

Grandey, B. S., Stier, P., and Wagner, T. M.: Investigating relationships between aerosol optical depth and cloud fraction using satellite, aerosol reanalysis and general circulation model data, Atmos. Chem. Phys., 13, 3177–3184, doi:10.5194/acp-13-3177-2013, 2013b.

Greenwald, T. J., Combs, C. L., Jones, A. S., Randel, D. L., and Vonder Haar, T. H.: Further Developments in Estimating Cloud Liquid Water over Land Using Microwave and Infrared Satellite Measurements., J. App. Met., 36, 389–405, doi:10.1175/1520-0450(1997)036⟨0389:FDIECL⟩2.0.CO;2, 1997.

Greenwald, T. J., L'Ecuyer, T. S., and Christopher, S. A.: Evaluating specific error characteristics of microwave-derived cloud liquid water products, Geophys. Res. Lett., 34, L22 807, doi:10.1029/2007GL031180, 2007.

Groisman, P. and Legates, D.: The Accuracy of United States Precipitation Data., B. Am. Meteorol. Soc., 75, 215–227, doi:10.1175/1520-0477(1994)075⟨0215:TAOUSP⟩2.0.CO;2, 1994.

Gunn, R. and Phillips, B.: A Experimental Investigation of the Effect of Air Pollution on the Initiation of Rain., J. Atmos. Sci., 14, 272–280, doi:10.1175/1520-0469(1957)014⟨0272:AEIOTE⟩2.0.CO;2, 1957.

Haynes, J., L'Ecuyer, T., Stephens, G., Miller, S., Mitrescu, C., Wood, N., and Tanelli, S.: Rainfall retrieval over the ocean with spaceborne W-band radar, J. Geophys. Res., 114, D00A22, doi:10.1029/2008JD009973, 2009.

Haywood, J. and Shine, K.: The effect of anthropogenic sulfate and soot aerosol on the clear sky planetary radiation budget, Geophys. Res. Lett., 22, 603–606, doi:10.1029/95GL00075, 1995.

Haywood, M. J., Osborne, R. S., and Abel, J. S.: The effect of overlying absorbing aerosol layers on remote sensing retrievals of cloud effective radius and cloud optical depth, Q. J. RMetS., 130, 779–800, doi:10.1256/qj.03.100, 2004.

Hazewinkel, M., ed.: Encyclopedia of mathematics, Springer, New York, 2002.

Henze, D. K. and Seinfeld, J. H.: Global secondary organic aerosol from isoprene oxidation, Geophys. Res. Lett., 33, L09 812, doi:10.1029/2006GL025976, 2006.

Herman, J. R., Bhartia, P. K., Torres, O., Hsu, C., Seftor, C., and Celarier, E.: Global distribution of UV-absorbing aerosols from Nimbus 7/TOMS data, J. Geophys. Res., 102, 16 911, doi:10.1029/96JD03680, 1997.

Hewitt, H. T., Copsey, D., Culverwell, I. D., Harris, C. M., Hill, R. S. R., Keen, A. B., McLaren, A. J., and Hunke, E. C.: Design and implementation of the infrastructure of HadGEM3: the next-generation Met Office climate modelling system, Geosci. Model Dev., 4, 223–253, doi:10.5194/gmd-4-223-2011, 2011.

Heymsfield, A. J. and McFarquhar, G. M.: Microphysics of INDOEX clean and polluted trade cumulus clouds, J. Geophys. Res., 106, D28 653, doi:10.1029/2000JD900776, 2001.

Holben, B., Eck, T., Slutsker, I., Tanre, D., Buis, J., Setzer, A., Vermote, E., Reagan, J., Kaufman, Y., Nakajima, T., Lavenu, F., Jankowiak, I., and Smirnov, A.: AERONET - A federated Instrument Network and Data Archive for Aerosol Characterisation, R. Sensing Env., 66, 1–16, doi:10.1016/S0034-4257(98)00031-5, 1998.

Hoose, C. and Möhler, O.: Heterogeneous ice nucleation on atmospheric aerosols: a review of results from laboratory experiments, Atmos. Chem. Phys., 12, 9817–9854, doi:10.5194/acp-12-9817-2012, 2012.

Hsu, K.-L., Gao, X., Sorooshian, S., and Gupta, H.: Precipitation Estimation from Remotely Sensed Information Using Artificial Neural Networks., J. App. Met., 36, 1176–1190, doi:10.1175/1520-0450(1997)036⟨1176:PEFRSI⟩2.0.CO;2, 1997.

Huang, J., Zhang, C., and Prospero, J.: African aerosol and large-scale precipitation variability over West Africa, Env. Res. Lett., 4, 015 006, doi:10.1088/1748-9326/4/1/015006, 2009a.

Huang, J., Zhang, C., and Prospero, J.: Aerosol-Induced Large-Scale Variability in Precipitation over the Tropical Atlantic, J. Climate, 22, 4970–4988, doi:10.1175/2009JCLI2531.1, 2009b.

Huang, J., Hsu, N., Tsay, S.-C., Jeong, M.-J., Holben, B., Berkoff, T., and Welton, E.: Susceptibility of aerosol optical thickness retrievals to thin cirrus contamination during the BASE-ASIA campaign, J. Geophys. Res., 116, D08214, doi:10.1029/2010JD014910, 2011.

Hubanks, P. A., King, M. D., Platnick, S. A., and Pincus, R. A.: MODIS Atmosphere L3 Gridded Product Algorithm Theoretical Basis Document No. ATBD-MOD-30, Tech. rep., National Aeronautics and Space Administration, 2008.

Huffman, G. and Bolvin, D.: TRMM and Other Data Precipitation Data Set Documentation, Tech. rep., Laboratory for Atmospheres, NASA Goddard Space Flight Center and Science Systems and Applications Inc., 2009.

Huffman, G., Adler, R., Morrissey, M., Bolvin, D., Curtis, S., Joyce, R., McGavock, B., and Susskind, J.: Global Precipitation at One-Degree Daily Resolution from Multisatellite Observations, J. Hydrometeorology, 2, 36–50, doi:10.1175/1525-7541(2001)002⟨0036:GPAODD⟩2.0.CO;2, 2001.

Huffman, G. J., Bolvin, D. T., Nelkin, E. J., Wolff, D. B., Adler, R. F., Gu, G., Hong, Y., Bowman, K. P., and Stocker, E. F.: The TRMM Multisatellite Precipitation Analysis (TMPA): Quasi-Global, Multiyear, Combined-Sensor Precipitation Estimates at Fine Scales, J. Hydrometeorology, 8, 38–55, doi:10.1175/JHM560.1, 2007.

Huffman, G. J., Adler, R. F., Bolvin, D. T., and Gu, G.: Improving the global precipitation record: GPCP Version 2.1, Geophys. Res. Lett., 36, L17 808, doi:10.1029/2009GL040000, 2009.

Iguchi, T. and Meneghini, R.: Intercomparison of Single-Frequency Methods for Retrieving a Vertical Rain Profile from Airborne or Spaceborne Radar Data, J. Atmos. Ocean Tech., 11, 1507–1516, doi:10.1175/1520-0426(1994)011⟨1507:IOSFMF⟩2.0.CO;2, 1994.

Inness, A., Baier, F., Benedetti, A., Bouarar, I., Chabrillat, S., Clark, H., Clerbaux, C., Coheur, P., Engelen, R. J., Errera, Q., Flemming, J., George, M., Granier, C., Hadji-Lazaro, J., Huijnen, V., Hurtmans, D., Jones, L., Kaiser, J. W., Kapsomenakis, J., Lefever, K., Leitão, J., Razinger, M., Richter, A., Schultz, M. G., Simmons, A. J., Suttie, M., Stein, O., Thépaut, J.-N., Thouret, V., Vrekoussis, M., Zerefos, C., and the MACC Team: The MACC reanalysis: an 8 yr data set of atmospheric composition, Atmos. Chem. Phys., 13, 4073–4109, doi:10.5194/acp-13-4073-2013, 2013.

Jacobson, M. Z.: Fundamentals of atmospheric modeling, Cambridge University Press, Cambridge, UK, 2005.

Jiang, H., Xue, H., Teller, A., Feingold, G., and Levin, Z.: Aerosol effects on the lifetime of shallow cumulus, Geophys. Res. Lett., 33, L14 806, doi:10.1029/2006GL026024, 2006.

Jones, T. A., Christopher, S. A., and Quaas, J.: A six year satellite-based assessment of the regional variations in aerosol indirect effects, Atmos. Chem. Phys., 9, 4091–4114, doi:10.5194/acp-9-4091-2009, 2009.

Joyce, R. J., Janowiak, J. E., Arkin, P. A., and Xie, P.: CMORPH: A Method that Produces Global Precipitation Estimates from Passive Microwave and Infrared Data at High Spatial and Temporal Resolution, J. Hydrometeorology, 5, 487–503, doi:10.1175/1525-7541(2004)005⟨0487:CAMTPG⟩2.0.CO;2, 2004.

Kapustin, V. N., Clarke, A. D., Shinozuka, Y., Howell, S., Brekhovskikh, V., Nakajima, T., and Higurashi, A.: On the determination of a cloud condensation nuclei from satellite: Challenges and possibilities, J. Geophys. Res., 111, D4202, doi:10.1029/2004JD005527, 2006.

Kaufman, Y., Koren, I., Remer, L., Rosenfeld, D., and Rudich, Y.: The effect of smoke, dust, and pollution aerosol on shallow cloud development over the Atlantic Ocean, P Natl. A. Sci., 102, 11 207, doi:10.1073/pnas.0505191102, 2005.

Kaufman, Y. J. and Koren, I.: Smoke and pollution aerosol effect on cloud cover., Science, 313, 655–658, doi:10.1126/science.1126232, 2006.

Kaufman, Y. J., Wald, A. E., Remer, L. A., Gao, B.-C., Li, R.-R., and Flynn, L.: The MODIS 2.1-μm channel-correlation with visible reflectance for use in remote sensing of aerosol, IEEE T. GeoSci. Remote, 35, 1286–1298, doi:10.1109/36.628795, 1997.

Kaufman, Y. J., Gobron, N., Pinty, B., Widlowski, J.-L., and Verstraete, M. M.: Relationship between surface reflectance in the visible and mid-IR used in MODIS aerosol algorithm - theory, Geophys. Res. Lett., 29, 2116, doi:10.1029/2001GL014492, 2002.

Kempe, A. B.: How to Draw a Straight Line, Nature, 16, 65–67, doi:10.1038/016065a0, 1877.

Kerminen, V.-M., Virkkula, A., Hillamo, R., Wexler, A. S., and Kulmala, M.: Secondary organics and atmospheric cloud condensation nuclei production, J. Geophys. Res., 105, 9255–9264, doi:10.1029/1999JD901203, 2000.

Khain, A.: Notes on state-of-the-art investigations of aerosol effects on precipitation: a critical review, Env. Res. Lett., 4, 5004, 2009.

Khain, A., Benmoshe, N., and Pokrovsky, A.: Factors Determining the Impact of Aerosols on Surface Precipitation from Clouds: An Attempt at Classification, J. Atmos. Sci., 65, 1721, 2008.

Kientzler, C. F., Arons, A. B., Blanchard, D. C., and Woodcock, A. H.: Photographic Investigation of the Projection of Droplets by Bubbles Bursting at a Water Surface, Tellus, 6, 1–7, doi:10.1111/j.2153-3490.1954.tb01085.x, 1954.

King, M. D., Kaufman, Y. J., Menzel, W. P., and Tanre, D.: Remote sensing of cloud, aerosol, and water vapor properties from the moderate resolution imaging spectrometer (MODIS), IEEE T. GeoSci. Remote, 30, 2, doi:10.1109/36.124212, 1992.

King, M. D., Radke, L. F., and Hobbs, P. V.: Optical properties of marine stratocumulus clouds modified by ships, J. Geophys. Res., 98, D2729, doi:10.1029/92JD02082, 1993.

Kittaka, C., Winker, D., Vaughan, M., Omar, A., and Remer, L.: Intercomparison of column aerosol optical depths from CALIPSO and MODIS-Aqua, Atmos. Meas. Tech., 4, 131–141, doi:10.5194/amt-4-131-2011, 2011.

Klein, S. and Hartmann, D.: The seasonal cycle of low stratiform clouds, J. Climate, 6, 1587–1606, doi:10.1175/1520-0442(1993)006⟨1587:TSCOLS⟩2.0.CO;2, 1993.

Koch, D. and Del Genio, A. D.: Black carbon semi-direct effects on cloud cover: review and synthesis, Atmos. Chem. Phys., 10, 7685–7696, doi:10.5194/acp-10-7685-2010, 2010.

Kohler, H.: The nucleus in and the growth of hygroscopic droplets, Trans. Faraday Soc., 32, 1152–1161, 1936.

Koren, I. and Feingold, G.: Aerosol-cloud-precipitation system as a predator-prey problem., Proc Natl Acad Sci U S A, 108, 12 227–12 232, doi:10.1073/pnas.1101777108, 2011.

Koren, I., Kaufman, Y., Rosenfeld, D., Remer, L., and Rudich, Y.: Aerosol invigoration and restructuring of Atlantic convective clouds, Geophys. Res. Lett., 32, L14828, doi:10.1029/2005GL023187, 2005.

Koren, I., Remer, L. A., Kaufman, Y. J., Rudich, Y., and Martins, J. V.: On the twilight zone between clouds and aerosols, Geophys. Res. Lett., 34, L08 805, doi:10.1029/2007GL029253, 2007.

Koren, I., Martins, J., Remer, L. A., and Afargan, H.: Smoke Invigoration Versus Inhibition of Clouds over the Amazon, Science, 321, 946–949, doi:10.1126/science.1159185, 2008.

Koren, I., Feingold, G., and Remer, L.: The invigoration of deep convective clouds over the Atlantic: aerosol effect, meteorology or retrieval artifact?, Atmos. Chem. Phys., 10, 8855–8872, doi:10.5194/acp-10-8855-2010, 2010a.

Koren, I., Remer, L., Altaratz, O., Martins, J., and Davidi, A.: Aerosol-induced changes of convective cloud anvils produce strong climate warming, Atmos. Chem. Phys., 10, 5001–5010, doi:10.5194/acp-10-5001-2010, 2010b.

Koren, I., Altaratz, O., Remer, L. A., Feingold, G., Martins, J. V., and Heiblum, R. H.: Aerosol-induced intensification of rain from the tropics to the mid-latitudes, Nature Geosci., 5, 118, doi:10.1038/ngeo1364, 2012.

Krishna Moorthy, K., Suresh Babu, S., Manoj, M. R., and Satheesh, S. K.: Buildup of aerosols over the Indian Region, Geophys. Res. Lett., 40, 1011–1014, doi:10.1002/GRL.50165, 2013.

Krüger, O. and Graßl, H.: Southern Ocean phytoplankton increases cloud albedo and reduces precipitation, Geophys. Res. Lett., 38, L08 809, doi:10.1029/2011GL047116, 2011.

Kummerow, C., Barnes, W., Kozu, T., Shiue, J., and Simpson, J.: The Tropical Rainfall Measuring Mission (TRMM) Sensor Package, J. Atmos. Ocean Tech., 15, 809–817, doi:10.1175/1520-0426(1998)015⟨0809:TTRMMT⟩2.0.CO;2, 1998.

Kummerow, C., Simpson, J., Thiele, O., Barnes, W., Chang, A., Stocker, E., Adler, R., Hou, A., Kakar, R., Wentz, F., Ashcroft, P., Kozu, T., Hong, Y., Okamoto, K., Iguchi, T., Kuroiwa, H., Im, E., Haddad, Z., Huffman, G., Ferrier, B., Olson, W., Zipser, E., Smith, E., Wilheit, T., North, G., Krishnamurti, T., and Nakamura, K.: The Status of the Tropical Rainfall Measuring Mission (TRMM) after Two Years in Orbit, J. App. Met. Clim., 39, 1965–1982, doi:10.1175/1520-0450(2001)040⟨1965:TSOTTR⟩2.0.CO;2, 2000.

Kummerow, C., Hong, Y., Olson, W. S., Yang, S., Adler, R. F., McCollum, J., Ferraro, R., Petty, G., Shin, D.-B., and Wilheit, T. T.: The Evolution of the Goddard Profiling Algorithm (GPROF) for Rainfall Estimation from Passive Microwave Sensors., J. App. Met. Clim., 40, 1801, doi:10.1175/1520-0450(2001)040⟨1801:TEOTGP⟩2.0.CO;2, 2001.

Kummerow, C. D., Ringerud, S., Crook, J., Randel, D., and Berg, W.: An Observationally Generated A Priori Database for Microwave Rainfall Retrievals, J. Atmos. Ocean Tech., 28, 113–130, doi:10.1175/2010JTECHA1468.1, 2011.

Lebo, Z. and Seinfeld, J.: Theoretical basis for convective invigoration due to increased aerosol concentration, Atmos. Chem. Phys., 11, 5407–5429, doi:10.5194/acp-11-5407-2011, 2011.

Lebsock, M., Stephens, G., and Kummerow, C.: Multisensor satellite observations of aerosol effects on warm clouds, J. Geophys. Res., 113, D15 205, doi:10.1029/2008JD009876, 2008.

L'Ecuyer, T. and Jiang, J.: Touring the atmosphere aboard the A-Train, Physics Today, 63, 36, doi: 10.1063/1.3463626, 2010.

L'Ecuyer, T., Berg, W., Haynes, J., Lebsock, M., and Takemura, T.: Global observations of aerosol impacts on precipitation occurrence in warm maritime clouds, J. Geophys. Res., 114, D09 211, doi:10.1029/2008JD011273, 2009.

Lee, D., Oreopoulos, L., Huffman, G. J., Rossow, W. B., and Kang, I.-S.: The Precipitation Characteristics of ISCCP Tropical Weather States, J. Climate, 26, 772–788, doi:10.1175/JCLI-D-11-00718.1, 2013.

Lee, S.-S. and Feingold, G.: Precipitating cloud-system response to aerosol perturbations, Geophys. Res. Lett., 37, L23 806, doi:10.1029/2010GL045596, 2010.

Lee, S. S., Penner, J. E., and Saleeby, S. M.: Aerosol effects on liquid-water path of thin stratocumulus clouds, J. Geophys. Res., 114, D07 204, doi:10.1029/2008JD010513, 2009.

Lehahn, Y., Koren, I., Altaratz, O., and Kostinski, A. B.: Effect of coarse marine aerosols on stratocumulus clouds, Geophys. Res. Lett., 38, L20 804, doi:10.1029/2011GL048504, 2011.

Levin, Z. and Cotton, W.: Aerosol Pollution Impact on Precipitation, Springer, 2009.

Levy, R., Remer, L., Kleidman, R., Mattoo, S., Ichoku, C., Kahn, R., and Eck, T.: Global evaluation of the Collection 5 MODIS dark-target aerosol products over land, Atmos. Chem. Phys., 10, 10 399–10 420, doi:10.5194/acp-10-10399-2010, 2010.

Li, Z., Niu, F., Fan, J., Liu, Y., Rosenfeld, D., and Ding, Y.: Long-term impacts of aerosols on the vertical development of clouds and precipitation, Nat. Geosci., 4, 888, doi:10.1038/ngeo1313, 2011.

Liepert, B., Feichter, J., Lohmann, U., and Roeckner, E.: Can aerosols spin down the water cycle in a warmer and moister world?, Geophys. Res. Lett., 31, L06 207, doi:10.1029/2003GL019060, 2004.

Lin, J., Matsui, T., Pielke, R., and Kummerow, C.: Effects of biomass-burning-derived aerosols on precipitation and clouds in the Amazon Basin: A satellite-based empirical study, J. Geophys. Res., 111, D19 204, doi:10.1029/2005JD006884, 2006.

Liou, K. N.: An Introduction to Atmospheric Radiation, Academic Press, San Diego, USA, 2002.

Liu, C. and Zipser, E. J.: Diurnal cycles of precipitation, clouds, and lightning in the tropics from 9 years of TRMM observations, Geophys. Res. Lett., 35, L04 819, doi:10.1029/2007GL032437, 2008.

Liu, J. and Li, Z.: Estimation of cloud condensation nuclei concentration from aerosol optical quantities: influential factors and uncertainties, Atmos. Chem. Phys. Discuss., 13, 23 023–23 056, doi: 10.5194/acpd-13-23023-2013, 2013.

Loeb, N. G. and Schuster, G. L.: An observational study of the relationship between cloud, aerosol and meteorology in broken low-level cloud conditions, J. Geophys. Res., 113, D14 214, doi:10.1029/2007JD009763, 2008.

Lohmann, U. and Feichter, J.: Global Indirect Aerosol Effects: A review, Atmos. Chem. Phys., 5, 715–737, doi:10.5194/acp-5-715-2005, 2005.

Lohmann, U., Feichter, J., Penner, J., and Leaitch, R.: Indirect effect of sulfate and carbonaceous aerosols: A mechanistic treatment, J. Geophys. Res., 105, 12 193, doi:10.1029/1999JD901199, 2000.

Lohmann, U., Koren, I., and Kaufman, Y. J.: Disentangling the role of microphysical and dynamical effects in determining cloud properties over the Atlantic, Geophys. Res. Lett., 33, L09 802, doi: 10.1029/2005GL024625, 2006.

Lu, M.-L., Sorooshian, A., Jonsson, H., Feingold, G., Flagan, R., and Seinfeld, J.: Marine stratocumulus aerosol-cloud relationships in the MASE-II experiment: Precipitation susceptibility in eastern Pacific marine stratocumulus, J. Geophys. Res., 114, D24 203, doi:10.1029/2009JD012774, 2009.

Lynn, B., Khain, A., Rosenfeld, D., and Woodley, W.: Effects of aerosols on precipitation from orographic clouds, J. Geophys. Res., 112, D10 225, doi:10.1029/2006JD007537, 2007.

Machado, L. A. T., Laurent, H., and Lima, A. A.: Diurnal march of the convection observed during TRMM-WETAMC/LBA, J. Geophys. Res., 107, 8064, doi:10.1029/2001JD000338, 2002.

Maddux, B. C., Ackerman, S. A., and Platnick, S.: Viewing Geometry Dependencies in MODIS Cloud Products, J. Atmos. Ocean Tech., 27, 1519–1528, doi:10.1175/2010JTECHA1432.1, 2010.

Mahowald, N. and Kiehl, L.: Mineral aerosol and cloud interactions, Geophys. Res. Lett., 30, 28, doi:10.1029/2002GL016762, 2003.

Mann, G., Johnson, C., Bellouin, N., Dalvi, M., Abraham, L., Carslaw, K. S., Boucher, O., Stier, P., Rae, J., Spraklen, D. V., Telford, P., Pyle, J., O'Connor, F., Carver, G., Pringle, K. J., and Woodhouse, M. T.: Evaluation of the new UKCA climate composition model. Part 3:Tropospheric aerosol properties, in preparation, 2013.

Mann, G. W., Carslaw, K. S., Spracklen, D. V., Ridley, D. A., Manktelow, P. T., Chipperfield, M. P., Pickering, S. J., and Johnson, C. E.: Description and evaluation of GLOMAP-mode: a modal global aerosol microphysics model for the UKCA composition-climate model, Geosci. Model Dev., 3, 519–551, doi:10.5194/gmd-3-519-2010, 2010.

Marchand, R., Ackerman, T., Smyth, M., and Rossow, W.: A review of cloud top height and optical depth histograms from MISR, ISCCP, and MODIS, J. Geophys. Res., 115, D16 206, doi:10.1029/2009JD013422, 2010.

Matsui, T., Masunaga, H., Kreidenweis, S., Pielke, R., Tao, W.-K., Chin, M., and Kaufman, Y.: Satellite-based assessment of marine low cloud variability associated with aerosol, atmospheric stability, and the diurnal cycle, J. Geophys. Res., 111, D17204, doi:10.1029/2005JD006097, 2006.

Mauger, G. and Norris, J.: Meteorological bias in satellite estimates of aerosol-cloud relationships, Geophys. Rev. Lett., 34, D16824, doi:10.1029/2007GL029952, 2007.

Mauger, G. and Norris, J.: Assessing the impact of meteorological history on subtropical cloud fraction, J. Climate, 23, 2926, doi:10.1175/2010JCLI3272.1, 2010.

McComiskey, A. and Feingold, G.: The scale problem in quantifying aerosol indirect effects, Atmos. Chem. Phys., 12, 1031, doi:10.5194/acp-12-1031-2012, 2012.

Medeiros, B. and Stevens, B.: Revealing differences in GCM representations of low clouds, Climate Dyn., 36, 385–399, doi:10.1007/s00382-009-0694-5, 2011.

Menzel, W., Frey, R., Zhang, H., Wylie, D., Moeller, C., Holz, R., Maddux, B., Baum, B., Strabala, K., and Gumley, L.: MODIS Global Cloud-Top Pressure and Amount Estimation: Algorithm Description and Results, J. App. Met. Clim., 47, 1175–1198, doi:10.1175/2007JAMC1705.1, 2008.

Meskhidze, N., Remer, L., Platnick, S., Negron Juarez, R., LichtenBerger, A., and Aiyyer, A.: Exploring the differences in cloud properties observed by the terra and Aqua MODIS sensors, Atmos. Chem. Phys., 9, 3461–3475, doi:10.5194/acp-9-3461-2009, 2009.

Ming, Y., Ramaswamy, V., and Persad, G.: Two opposing effects of absorbing aerosols on global-mean precipitation, Geophys. Rev. Lett., 37, L13 701, doi:10.1029/2010GL042895, 2010.

Minnis, P., Sun-Mack, S., Young, D. F., Heck, P. W., Garber, D. P., Chen, Y., Spangenberg, D. A., Arduini, R. F., Trepte, Q. Z., Smith, W. L., Ayers, J. K., Gibson, S. C., Miller, W. F., Hong, G., Chakrapani, V., Takano, Y., Liou, K.-N., Xie, Y., and Yang, P.: CERES Edition-2 Cloud Property Retrievals Using TRMM VIRS and Terra and Aqua MODIS Data—Part I: Algorithms, 49, 4374–4400, doi:10.1109/TGRS.2011.2144601, 2011.

Muller, C. and O'Gorman, P.: An energetic perspective on the regional response of precipitation to climate change, Nature Climate Change, 1, 266–271, doi:10.1038/nclimate1169, 2011.

Murphy, D. M.: Little net clear-sky radiative forcing from recent regional redistribution of aerosols, Nat. Geosci., 6, 258–262, doi:10.1038/ngeo1740, 2013.

Myhre, G., Stordal, F., Johnsrud, M., Kaufman, Y., Rosenfeld, D., Storelvmo, T., Kristjansson, J., Berntsen, T., Myhre, A., and Isaksen, I.: Aerosol-cloud interaction inferred from MODIS satellite data and global aerosol models, Atmos. Chem. Phys., 7, 3081–3101, doi:10.5194/acp-7-3081-2007, 2007.

Myhre, G., Samset, B. H., Schulz, M., Balkanski, Y., Bauer, S., Berntsen, T. K., Bian, H., Bellouin, N., Chin, M., Diehl, T., Easter, R. C., Feichter, J., Ghan, S. J., Hauglustaine, D., Iversen, T., Kinne, S., Kirkevåg, A., Lamarque, J.-F., Lin, G., Liu, X., Lund, M. T., Luo, G., Ma, X., van Noije, T., Penner, J. E., Rasch, P. J., Ruiz, A., Seland, Ø., Skeie, R. B., Stier, P., Takemura, T., Tsigaridis, K., Wang, P., Wang, Z., Xu, L., Yu, H., Yu, F., Yoon, J.-H., Zhang, K., Zhang, H., and Zhou, C.: Radiative forcing of the direct aerosol effect from AeroCom Phase II simulations, Atmos. Chem. Phys., 13, 1853–1877, doi:10.5194/acp-13-1853-2013, 2013.

Nakajima, T., Higurashi, A., Kawamoto, K., and Penner, J.: A possible correlation between satellite-derived cloud and aerosol microphysical parameters, Geophys. Res. Lett., 28, 1171–1174, doi:10.1029/2000GL012186, 2001.

Nam, C., Bony, S., Dufresne, J.-L., and Chepfer, H.: The 'too few, too bright' tropical low-cloud problem in CMIP5 models, Geophys. Res. Lett., 39, L21 801, doi:10.1029/2012GL053421, 2012.

National Research Council, ed.: Critical Issues in Weather Modification Research, The National Academies Press, Washington D.C., 2003.

Nesbitt, S. W., Zipser, E. J., and Cecil, D. J.: A Census of Precipitation Features in the Tropics Using TRMM: Radar, Ice Scattering, and Lightning Observations., J. Climate, 13, 4087–4106, doi:10.1175/1520-0442(2000)013⟨4087:ACOPFI⟩2.0.CO;2, 2000.

Niu, F. and Li, Z.: Systematic variations of cloud top temperature and precipitation rate with aerosols over the global tropics, Atmos. Chem. Phys., 12, 8491–8498, doi:10.5194/acp-12-8491-2012, 2012.

Nuijens, L. and Stevens, B.: The influence of Wind Speed on Shallow Marine Convection, J. Atmos. Sci., 69, 168–184, doi:10.1175/JAS-D-11-02.1, 2012.

O'Dell, C. W., Wentz, F. J., and Bennartz, R.: Cloud Liquid Water Path from Satellite-Based Passive Microwave Observations: A New Climatology over the Global Oceans, J. Climate, 21, 1721, doi: 10.1175/2007JCLI1958.1, 2008.

O'Gorman, P. A., Allan, R. P., Byrne, M. P., and Previdi, M.: Energetic Constraints on Precipitation Under Climate Change, Surv. Geophys., p. 111, doi:10.1007/s10712-011-9159-6, 2011.

Pearl, J.: Causality, Cambridge University Press, Cambridge, 2009.

Penner, J. E., Quaas, J., Storelvmo, T., Takemura, T., Boucher, O., Guo, H., Kirkevåg, A., Kristjánsson, J. E., and Seland, Ø.: Model intercomparison of indirect aerosol effects, Atmos. Chem. Phys., 6, 3391–3405, doi:10.5194/acp-6-3391-2006, 2006.

Peters, K., Quaas, J., and Bellouin, N.: Effects of absorbing aerosols in cloudy skies: a satellite study over the Atlantic Ocean, Atmos. Chem. Phys., 11, 1393–1404, doi:10.5194/acp-11-1393-2011, 2011.

Phillips, V., Pokrovsky, A., and Khain, A.: The Influence of Time-Dependent Melting on the Dynamics and Precipitation Production in Maritime and Continental Storm Clouds, J. Atmos. Sci., 64, 338–359, doi:10.1175/JAS3832.1, 2007.

Pincus, R., Baker, M. B., and Bretherton, C. S.: What controls Stratocumulus Radiative Properties? Lagrangian Observations of Cloud Evolution, J. Atmos. Sci., 54, 2215–2236, doi: 10.1175/1520-0469(1997)054⟨2215:WCSRPL⟩2.0.CP:2, 1997.

Platnick, S., King, M., Ackerman, S., Menzel, W., Baum, B., Riedi, J., and Frey, R.: The MODIS cloud products: algorithms and examples from Terra, IEEE T. GeoSci. Remote, 41, 459, doi: 10.1109/TGRS.2002.808301, 2003.

Pruppacher, H. R. and Jaenicke, R.: The processing of water vapor and aerosols by atmospheric clouds, a global estimate, Atmos. Res., 38, 283–295, doi:10.1016/0169-8095(94)00098-X, 1995.

Pruppacher, H. R. and Klett, J. D.: Microphysics of Clouds and Precipitation, D. Reidel, Dordrecht, Holland, 1978.

Quaas, J., Boucher, O., and Lohmann, U.: Constraining the total aerosol indirect effect in the LMDZ and ECHAM4 GCMs using MODIS satellite data, Atmos. Chem. Phys., 6, 947, doi:10.5194/acp-6-947-2006, 2006.

Quaas, J., Boucher, O., Bellouin, N., and Kinne, S.: Satellite-based estimate of the direct and indirect aerosol climate forcing, J. Geophys. Res., 113, D05204, doi:10.1029/2007JD008962, 2008.

Quaas, J., Ming, Y., Menon, S., Takemura, T., Wang, M., Penner, J., Gettelman, A., Lohmann, U., Bellouin, N., Boucher, O., Sayer, A., Thomas, G., McComiskey, A., Feingold, G., Hoose, C., Kristjnsson, J., Liu, X., Balkanski, Y., Donner, L., Ginoux, P., Stier, P., Grandey, B., Feichter, J., Sednev, I., Bauer, S., Koch, D., Grainger, R., Kirkevg, A., Iversen, T., Seland, Ø., Easter, R., Ghan, S., Rasch, P., Morrison, H., Lamarque, J.-F., Iacono, M., Kinne, S., and Schulz, M.: Aerosol indirect effects - general circulation model intercomparison and evaluation with satellite data, Atmos. Chem. Phys., 9, 8697–8717, doi:10.5194/acp-9-8697-2009, 2009.

Quaas, J., Stevens, B., Stier, P., and Lohmann, U.: Interpreting the cloud cover - aerosol optical depth relationship found in satellite data using a general circulation model, Atmos. Chem. Phys., 10, 6129–6135, doi:10.5194/acp-10-6129-2010, 2010.

Radke, L. F., Coakley, J. A., and King, M. D.: Direct and Remote Sensing Observations of the Effects of Ships on Clouds, Science, 246, 1146–1149, doi:10.1126/science.246.4934.1146, 1989.

Ramanathan, V., Chung, C., Kim, D., Bettge, T., Buja, L., Kiehl, J., Washington, W., Fu, Q., Sikka, D., and Wild, M.: Atmospheric brown clouds: Impacts on South Asian climate and hydrological cycle, P Natl. A. Sci., 102, 5326–5333, doi:10.1073/pnas.0500656102, 2005.

Rao, K. S., Chandra, G., and Rao, P. V. N.: The relationship between brightness temperature and soil moisture Selection of frequency range for microwave remote sensing, Int. J. Remote Sens., 8, 1531–1545, doi:10.1080/01431168708954795, 1987.

Remer, L., Kaufman, Y., Tanré, D., Matto, S., Chu, D., Martins, J., Li, R.-R., Ichoku, C., Levy, R., Kleidman, R., Eck, T., Vermote, E., and Holben, B.: The MODIS aerosol algorithm, products, and validation, J. Atmos. Sci., 62, 947–973, doi:10.1175/JAS3385.1, 2005.

Remer, L. A., Kaufman, Y. J., and Kleidman, R. G.: Comparison of Three Years of Terra and Aqua MODIS Aerosol Optical Thickness Over the Global Oceans, IEEE GeoSci. Remote S. Lett., 3, 537, doi:10.1109/LGRS.2006.879562, 2006.

Reynolds, O.: On the Formation of Hailstones, Raindrops, and Snowflakes, Nature, 17, 207–209, doi:10.1038/017207a0, 1878.

Roeckner, E., Buml, G., Bonaventura, L., Brokopf, R., Esch, M., Giorgetta, M., Hagemann, Sand Kirchner, I., Kornblueh, L., Manzini, E., Rhodin, A., Schlese, U., Schulzweida, U., and Tompkins, A.: The Atmospheric General Circulation Model ECHAM 5 - Model desciption, Tech. rep., Max Planck Institute for Metorology, 2003.

Roesler, E. and Penner, J.: Can global models ignore the chemical composition of aerosols?, Geophys. Res. Lett., 37, L24 809, doi:10.1029/2010GL044282, 2010.

Rogers, R. and Yau, M.: A short course in cloud physics - 3rd ed., Pergamon Press, 1989.

Rosenfeld, D.: TRMM Observed First Direct Evidence of Smoke from Forest Fires Inhibiting Rainfall, Geophys. Res. Lett., 26, 3105–3108, doi:10.1029/1999GL006066, 1999.

Rosenfeld, D.: Suppression of Rain and Snow by Urban and Industrial Air Pollution, Science, 287, 1793–1796, doi:10.1126/science.287.5459.1793, 2000.

Rosenfeld, D. and Bell, T. L.: Why do tornados and hailstorms rest on weekends?, J. Geophys. Res., 116, D20 211, doi:10.1029/2011JD016214, 2011.

Rosenfeld, D. and Gutman, G.: Retrieving microphysical properties near the tops of potential rain clouds by multispectral analysis of AVHRR data, Atmos. Res., 34, 259–283, doi:10.1016/0169-8095(94)90096-5, 1994.

Rosenfeld, D., Lahav, R., Khain, A., and Pinsky, M.: The Role of Sea Spray in Cleansing Air Pollution over Ocean via Cloud Processes, Science, 297, 1667–1670, doi:10.1126/science.1073869, 2002.

Rosenfeld, D., Kaufman, Y., and Koren, I.: Switching cloud cover and dynamical regimes from open to closed Benard cells in response to the suppression of precipitation by aerosols, Atmos. Chem. Phys., 6, 2503–2511, doi:10.5194/acp-6-2503-2006, 2006.

Rosenfeld, D., Lohmann, U., Raga, G., O'Dowd, C., Kulmala, M., Fuzzi, S., Reissell, A., and Andreae, M.: Flood or Drought: How Do Aerosols Affect Precipitation?, Science, 321, 1309–1313, doi:10.1126/science.1160606, 2008.

Rossow, W. and Schiffer, R.: Advances in Understanding Clouds from ISCCP., B. Am. Meteorol. Soc., 80, 2261–2287, doi:10.1175/1520-0477(1999)080⟨2261:AIUCFI⟩2.0.CO;2, 1999.

Rossow, W. B. and Schiffer, R. A.: ISCCP Cloud Data Products., B. Am. Meteorol. Soc., 72, 2–20, doi:10.1175/1520-0477(1991)072⟨0002:ICDP⟩2.0.CO;2, 1991.

Rossow, W. B., Tselioudis, G., Polak, A., and Jakob, C.: Tropical climate described as a distribution of weather states indicated by distinct mesoscale cloud property mixtures, Geophys. Rev. Lett., 32, L21812, doi:10.1029/2005GL024584, 2005.

Rotstayn, L. and Lohmann, U.: Tropical Rainfall Trends and the Indirect Aerosol Effect., J. Climate, 15, 2103–2116, doi:10.1175/1520-0442(2002)015⟨2103:TRTATI⟩2.0.CO;2, 2002.

Sanchez-Lorenzo, A., Laux, P., Hendricks Franssen, H.-J., Calbó, J., Vogl, S., Georgoulias, A. K., and Quaas, J.: Assessing large-scale weekly cycles in meteorological variables: a review, Atmos. Chem. Phys., 12, 5755–5771, doi:10.5194/acp-12-5755-2012, 2012.

Sandu, I., Brenguier, J.-L., Geoffory, O., Thouron, O., and Masson, V.: Aerosol impacts on the diurnal cycle of marine stratocumulus, J. Atmos. Sci., 65, 2705–2718, doi:10.1175/2008JAS2451.1, 2008.

Sayer, A. M., Thomas, G. E., and Grainger, R. G.: A sea surface reflectance model for (A)ATSR, and application to aerosol retrievals, Atmos. Meas. Tech., 3, 813–838, doi:10.5194/amt-3-813-2010, 2010a.

Sayer, A. M., Thomas, G. E., Palmer, P. I., and Grainger, R. G.: Some implications of sampling choice on comparisons between satellite and model aerosol optical depth fields, Atmos. Chem. Phys., 10, 10 705–10 716, doi:10.5194/acp-10-10705-2012, 2010b.

Schaap, M., Timmermans, R. M. A., Koelemeijer, R. B. A., de, L. G., and Builtjes, P. J. H.: Evaluation of MODIS aerosol optical thickness over Europe using sun photometer observations, Atm. Meas. Tech., 42, 2187–2197, doi:10.1016/j.atmosenv.2007.11.044, 2008.

Schmetz, J., Pili, P., Tjemkes, S., Just, D., Kerkmann, J., Rota, S., and Ratier, A.: Supplement to An Introduction to Meteosat Second Generation (MSG)., Bull. A. Met. Soc., 83, 992–992, doi:10.1175/BAMS-83-7-Schmetz-2, 2002.

Schnell, R. C. and Vali, G.: Biogenic Ice Nuclei: Part I. Terrestrial and Marine Sources., J. Atmos. Sci., 33, 1554–1564, doi:10.1175/1520-0469(1976)033⟨1554:BINPIT⟩2.0.CO;2, 1976.

Schreier, M., Mannstein, H., Eyring, V., and Bovensmann, H.: Global ship track distribution and radiative forcing from 1 year of AATSR data, Geophys. Res. Lett., 34, L17 814, doi:10.1029/2007GL030664, 2007.

Schultz, D., Mikkonen, S., Laaksonen, A., and Richman, M.: Weekly precipitation cycles? Lack of evidence from United States surface stations, Geophys. Res. Lett., 34, L22 815, doi:10.1029/2007GL031889, 2007.

Schumacher, C. and Houze, R. A.: Stratiform Rain in the Tropics as Seen by the TRMM Precipitation Radar, J. Climate, 16, 1739–1756, doi:10.1175/1520-0442(2003)016⟨1739:SRITTA⟩2.0.CO;2, 2003.

Seethala, C. and Horvath, A.: Global assessment of AMSR-E and MODIS cloud liquid water path retrievals in warm oceanic clouds, J. Geophys Res., 115, D13202, doi:10.1029/2009JD012662, 2010.

Seinfeld, J. H. and Pandis, S. N.: Atmospheric Chemistry and Physics, Wiley-Interscience, New-York, 1998.

Sekiguchi, M., Nakajima, T., Suzuki, K., Kawamoto, K., Higurashi, A., Rosenfeld, D., Sano, I., and Mukai, S.: A study of the direct and indirect effects of aerosols using global satellite data sets of aerosol and cloud parameters, J. Geophys. Res., 108, 4699, doi:10.1029/2002JD003359, 2003.

Shenk, W. E. and Salomonson, V. V.: A Simulation Study Exploring the Effects of Sensor Spatial Resolution on Estimates of Cloud Cover from Satellites, J. App. Met., 11, 214–220, doi:10.1175/1520-0450(1972)011⟨0214:ASSETE⟩2.0.CO;2, 1972.

Shi, Y., Zhang, J., Reid, J. S., Holben, B., Hyer, E. J., and Curtis, C.: An analysis of the collection 5 MODIS over-ocean aerosol optical depth product for its implication in aerosol assimilation, Atmos. Chem. Phys., 11, 557–565, doi:10.5194/acp-11-557-2011, 2011.

Small, J. D., Jiang, J. H., Su, H., and Zhai, C.: Relationship between aerosol and cloud fraction over Australia, Geophys. Res. Lett., 38, L23 802, doi:10.1029/2011GL049404, 2011.

Smirnov, A., Holben, B., Eck, T., Slutsker, I., Chatenet, B., and Pinker, R.: Diurnal variability of aerosol optical depth observed at AERONET sites, Geophys. Res. Lett., 29(23), 2115, doi:10.1029/2002GL016305, 2002.

Solomon, S., Qin, D., Manning, M., Chen, Z., Marquis, M., Averyt, K. B., Tignor, M., and Miller, H., eds.: Climate Change 2007: The Physical Science Basis. Contribution of Working Group I to the Fourth Assessment Report of the Intergovernmental Panel on Climate Change, Cambridge University Press, Cambridge, United Kingdom and New York, NY, USA, 2007.

Sorooshian, A., Feingold, G., Lebsock, M., Jiang, H., and Stephens, G.: On the precipitation susceptibility of clouds to aerosol perturbations, Geophys. Res. Lett., 36, L13 803, doi:10.1029/2009GL038993, 2009.

Sorooshian, A., Feingold, G., Lebsock, M., Jiang, H., and Stephens, G.: Deconstructing the precipitation susceptibility construct: Improving methodology for aerosol-cloud precipitation studies, J. Geophys. Res., 115, D17 201, 2010.

Sorooshian, S., Hsu, K., Gao, X., Gupta, H., Imam, B., and Braithwaite, D.: Evaluation of PERSIANN System Satellite-Based Estimates of Tropical Rainfall., Bull. A. Met. Soc., 81, 2035–2046, doi:10.1175/1520-0477(2000)081⟨2035:EOPSSE⟩2.3.CO;2, 2000.

Stephens, G. and Kummerow, C.: The Remote Sensing of Clouds and Precipitation from Space: A Review, J. Atmos. Sci., 64, 3742–3765, doi:10.1175/2006JAS2375.1, 2007.

Stephens, G., Vane, D., Tanelli, S., Im, E., Durden, S., Rokey, M., Reinke, D., Partain, P., Mace, G., Austin, R., L'Ecuyer, T., Haynes, J., Lebsock, M., Suzuki, K., Waliser, D., Wu, D., Kay, J., Gettelman, A., Wang, Z., and Marchand, R.: CloudSat mission: Performance and early science after the first year of operation, J. Geophys. Res., 113, D00A18, doi:10.1029/2008JD009982, 2008.

Stephens, G., L'Ecuyer, T., Forbes, R., Gettlemen, A., Golaz, J.-C., Bodas-Salcedo, A., Suzuki, K., Gabriel, P., and Haynes, J.: Dreary state of precipitation in global models, J. Geophys. Res., 115, D24 211, doi:10.1029/2010JD014532, 2010.

Stevens, B. and Feingold, G.: Untangling aerosol effects on clouds and precipitation in a buffered system, Nature, 461, 607–613, doi:10.1038/nature08281, 2009.

Stevens, B., Ackerman, A. S., Albrecht, B. A., Brown, A. R., Chlond, A., Cuxart, J., Duynkerke, P. G., Lewellen, D. C., Macvean, M. K., Neggers, R. A. J., Sánchez, E., Siebesma, A. P., and Stevens, D. E.: Simulations of Trade Wind Cumuli under a Strong Inversion, J. Atmos. Sci., 58, 1870–1891, doi:10.1175/1520-0469(2001)058⟨1870:SOTWCU⟩2.0.CO;2, 2001.

Stier, P., Feichter, J., Kinne, S., Kloster, S., Vignati, E., Wilson, J., Ganzeveld, L., Tegen, I., Werner, M., Balkanski, Y., Schulz, M., Boucher, O., Minikin, A., and Petzold, A.: The aerosol-climate model ECHAM5-HAM, Atmos. Chem. Phys., 5, 1125, 2005.

Stier, P., Seinfeld, J., Kinne, S., and Boucher, O.: Aerosol absorption and radiative forcing, Atmos. Chem. Phys., 7, 5237–5261, doi:10.5194/acp-7-5237-2007, 2007.

Stjern, C.: Weekly cycles in precipitation and other meteorological variables in a polluted region of Europe, Atmos. Chem. Phys., 11, 4095, doi:10.5194/acp-11-4095-2011, 2011.

Tao, W.-K., Li, X., Khain, A., Matsui, T., Lang, S., and Simpson, J.: Role of atmospheric aerosol concentration on deep convective precipitation: Cloud-resolving model simulations, J. Geophys. Res., 112, D24S18, doi:10.1029/2007JD008728, 2007.

Taylor, C. M., de Jeu, R. A. M., Guichard, F., Harris, P. P., and Dorigo, W. A.: Afternoon rain more likely over drier soils., Nature, 489, 423–426, doi:10.1038/nature11377, 2012.

Taylor, J. P., Glew, M. D., Coakley, J. A. J., Tahnk, W. R., Platnick, S., Hobbs, P. V., and Ferek, R. J.: Effects of Aerosols on the Radiative Properties of Clouds., J. Atmos. Sci., 57, 2656, doi:10.1175/1520-0469(2000)057⟨2656:EOAOTR⟩2.0.CO;2, 2000.

Textor, C., Schulz, M., Guibert, S., Kinne, S., Balkanski, Y., Bauer, S., Berntsen, T., Berglen, T., Boucher, O., Chin, M., Dentener, F., Diehl, T., Easter, R., Feichter, H., Fillmore, D., Ghan, S., Ginoux, P., Gong, S., Grini, A., Hendricks, J., Horowitz, L., Huang, P., Isaksen, I., Iversen, I., Kloster, S., Koch, D., Kirkevg, A., Kristjansson, J., Krol, M., Lauer, A., Lamarque, J., Liu, X., Montanaro, V., Myhre, G., Penner, J., Pitari, G., Reddy, S., Seland, Ø., Stier, P., Takemura, T., and Tie, X.: Analysis and quantification of the diversities of aerosol life cycles within AeroCom, Atmos. Chem. Phys., 6, 1777–1813, doi:10.5194/acp-6-1777-2006, 2006.

Thomas, G., Poulsen, C., Siddans, R., Sayer, A., Carboni, E., Marsh, S., Dean, S., Grainger, R., and Lawrence, B.: Validation of the GRAPE single view aerosol retrieval for ATSR-2 and insights into the long term global AOD trend over the ocean, Atmos. Chem. Phys., 10, 4849–4866, doi:10.5194/acp-10-4849-2010, 2010.

Thomas, G. E., Chalmers, N., Harris, B., Grainger, R. G., and Highwood, E. J.: Regional and monthly and clear-sky aerosol direct radiative effect (and forcing) derived from the GlobAEROSOL-AATSR satellite aerosol product, Atmos. Chem. Phys., 13, 393–410, doi:10.5194/acp-13-393-2013, 2013.

Tompkins, A. M. and Adebiyi, A. A.: Using CloudSat Cloud Retrievals to Differentiate Satellite-Derived Rainfall Products over West Africa, J. Hydrometeorology, 13, 1810–1816, doi:10.1175/JHM-D-12-039.1, 2012.

Torres, O., Jethva, H., and Bhartia, P. K.: Retrieval of Aerosol Optical Depth above Clouds from OMI Observations: Sensitivity Analysis and Case Studies, J. Atmos. Sci., 69, 1037–1053, doi:10.1175/JAS-D-11-0130.1, 2012.

Twohy, C., Coakley, J., and Tahnk, W.: Effect of changes in relative humidity on aerosol scattering near clouds, J. Geophys. Res., 114, D05 205, doi:10.1029/2008JD010991, 2009.

Twomey, S.: Pollution and the Planetary Albedo, Atm. Env., 8, 1251–1256, doi:10.1016/0004-6981(74)90004-3, 1974.

Twomey, S.: The Influence of Pollution on the Shortwave Albedo of Clouds., J. Atmos. Sci., 34, 1149–1152, doi:10.1175/1520-0469(1977)034⟨1149:TIOPOT⟩2.0.CO;2, 1977.

UK Meteorological Office: Met Office Integrated Data Archive System (MIDAS) Land and Marine Surface Stations Network (1853-current), URL `http://badc.nerc.ac.uk/view/badc.nerc.ac.uk__ATOM__dataent_ukmo-midas`, 2012.

Várnai, T. and Marshak, A.: MODIS observations of enhanced clear sky reflectance near clouds, Geophys. Res. Lett., 36, L06 807, doi:10.1029/2008GL037089, 2009.

Vonnegut, B.: The Nucleation of Ice Formation by Silver Iodide, J. App. Phys., 18, 593–595, doi:10.1063/1.1697813, 1947.

Wang, H. and Feingold, G.: Modeling Mesoscale Cellular Structures and Drizzle in Marine Stratocumulus. Part I: Impact of Drizzle on the Formation and Evolution of Open Cells, J. Atmos. Sci., 66, 3237–3256, doi:10.1175/2009JAS3022.1, 2009a.

Wang, H. and Feingold, G.: Modeling Mesoscale Cellular Structures and Drizzle in Marine Stratocumulus. Part II: The Microphysics and Dynamics of the Boundary Region between Open and Closed Cells, J. Atmos. Sci., 66, 3257–3275, doi:10.1175/2009JAS3120.1, 2009b.

Wang, W., Xie, P., Yoo, S.-H., Xue, Y., Kumar, A., and Wu, X.: An assessment of the surface climate in the NCEP climate forecast system reanalysis, Climate Dyn., 37, 1601–1620, doi:10.1007/s00382-010-0935-7, 2011.

Warner, J.: A Reduction in Rainfall Associated with Smoke from Sugar-Cane Fires—An Inadvertent Weather Modification?, J. App. Met., 7, 247–251, doi:10.1175/1520-0450(1968)007⟨0247:ARIRAW⟩2.0.CO;2, 1968.

Wen, G., Marshak, A., Cahalan, R., Remer, L., and Kleidman, R.: 3-D aerosol-cloud radiative interaction observed in collocated MODIS and ASTER images of cumulus cloud fields, J. Geophys. Res., 112, D13204, doi:10.1029/2006JD008267, 2007.

West, R. E. L., Stier, P., Jones, A., Johnson, C. E., Mann, G. W., Bellouin, N., and Kipling, Z.: The importance of vertical velocity variability for estimates of the indirect aerosol effects, Atmos. Chem. Phys. Discuss., 13, 27 053–27 113, doi:10.5194/acpd-13-27053-2013, 2013.

Wilcox, E.: Stratocumulus cloud thickening beneath layers of absorbing smoke aerosol, Atmos. Phys. Chem., 10, 11 769–11 777, doi:10.5194/acp-10-11769-2010, 2010.

Wild, M. and Liepert, B.: The Earth radiation balance as driver of the global hydrological cycle, Env. Res. Lett., 5, 025 203, doi:10.1088/1748-9326/5/2/025203, 2010.

Wilheit, T. T.: Some Comments on Passive Microwave Measurement of Rain., Bull. A. Met. Soc., 67, 1226–1232, doi:10.1175/1520-0477(1986)067⟨1226:SCOPMM⟩2.0.CO;2, 1986.

Williams, E., Rosenfeld, D., Madden, N., Gerlach, J., Gears, N., Atkinson, L., Dunnemann, N., Frostrom, G., Antonio, M., Biazon, B., Camargo, R., Franca, H., Gomes, A., Lima, M., Machado, R., Manhaes, S., Nachtigall, L., Piva, H., Quintiliano, W., Machado, L., Artaxo, P., Roberts, G., Renno, N., Blakeslee, R., Bailey, J., Boccippio, D., Betts, A., Wolff, D., Roy, B., Halverson, J., Rickenbach, T., Fuentes, J., and Avelino, E.: Contrasting convective regimes over the Amazon: Implications for cloud electrification, J. Geophys. Res., 107, 8082, doi:10.1029/2001JD000380, 2002.

Williams, K. and Webb, M.: A quantitative performance assessment of cloud regimes in climate models, Climate Dyn., 33, 141–157, doi:10.1007/s00382-008-0443-1, 2009.

Wilson, D. R. and Ballard, S. P.: A microphysically based precipitation scheme for the UK meteorological office unified model, Q. J. RMetS., 125, 1607–1636, doi:10.1002/qj.49712555707, 1999.

Wilson, D. R., Bushell, A. C., Kerr-Munslow, A. M., Price, J. D., and Morcrette, C. J.: PC2: A prognostic cloud fraction and condensation scheme. I: Scheme description, Q. J. RMetS., 134, 2093–2107, doi:10.1002/qj.333, 2008a.

Wilson, D. R., Bushell, A. C., Kerr-Munslow, A. M., Price, J. D., Morcrette, C. J., and Bodas-Salcedo, A.: PC2: A prognostic cloud fraction and condensation scheme. II: Climate model simulations, Q. J. RMetS., 134, 2109–2125, doi:10.1002/qj.332, 2008b.

Winker, D., Hunt, W., and McGill, M.: Initial performance assessment of CALIOP, Geophys. Res. Lett., 34, L19 803, doi:10.1029/2007GL030135, 2007.

Wood, R.: Cancellation of Aerosol Indirect Effects in Marine Stratocumulus through Cloud Thinning, J. Atmos. Sci., 64, 2657–2669, doi:10.1175/JAS3942.1, 2007.

Wood, R.: Stratocumulus Clouds, M. Weather Rev., 140, 2373–2423, doi:10.1175/MWR-D-11-00121.1, 2012.

Wood, R., Bretherton, C. S., and Hartmann, D. L.: Diurnal cycle of liquid water path over the subtropical and tropical oceans, Geophys. Res. Lett., 29(23), 2092, doi:10.1029/2002GL015371, 2002.

Woodcock, A.: Salt nuclei in marine air as a function of altitude and wind force, J. Meteorology, 10, 362–371, doi:10.1175/1520-0469(1953)010⟨0366:SNIMAA⟩2.0.CO;2, 1953.

Woodruff, S., Worley, S., Lubker, S., Ji, Z., Eric, F., Berry, D., Brohan, P., Kent, E., Reynolds, R., Smith, S., and Wilkinson, C.: ICOADS Release 2.5: extensions and enhancements to the surface marine meteorological archive, Int. J. Climatology, 31, 951–967, doi:10.1002/joc.2103, 2011.

Xia, X.: Significant overestimation of global aerosol optical thickness by MODIS over land, Ch. Sci. Bull., 23, 2905–2912, doi:10.1007/s11434-006-2157-2, 2006.

Xia, X., Eck, T. F., Holben, B. N., Phillippe, G., and Chen, H.: Analysis of the weekly cycle of aerosol optical depth using AERONET and MODIS data, J. Geophys. Res., 113, D14 217, doi:10.1029/2007JD009604, 2008.

Xiong, X., Wu, A., and Cao, C.: On-orbit calibration and inter-comparison of Terra and Aqua MODIS surface temperature spectral bands, Int. J. Remote Sens., 29, 5347–5359, doi:10.1080/01431160802036300, 2008.

Xue, H. and Feingold, G.: Large-Eddy Simulations of Trade Wind Cumuli: Investigation of Aerosol Indirect Effects., J. Atmos. Sci., 63, 1605–1622, doi:10.1175/JAS3706.1, 2006.

Yang, G.-Y. and Slingo, J.: The Diurnal Cycle in the Tropics, M. Weather Rev., 129, 784–801, 2001.

Yu, H., Chin, M., Remer, L. A., Kleidman, R. G., Bellouin, N., Bian, H., and Diehl, T.: Variability of marine aerosol fine-mode fraction and estimates of anthropogenic aerosol component over cloud-free oceans from the Moderate Resolution Imaging Spectroradiometer (MODIS), J. Geophys. Res., 114, D10 206, doi:10.1029/2008JD010648, 2009.

Yuan, T., Remer, L., and Yu, H.: Microphysical, macrophysical and radiative signatures of volcanic aerosols in trade wind cumulus observed by the A-Train, Atmos. Chem. Phys., 11, 7119–7132, doi:10.5194/acp-11-7119-2011, 2011a.

Yuan, T., Remer, L. A., Pickering, K. E., and Yu, H.: Observational evidence of aerosol enhancement of lightning activity and convective invigoration, Geophys. Res. Lett, 38, L04 701, doi:10.1029/2010GL046052, 2011b.

Zhang, J. and Reid, J. S.: MODIS aereosol product analysis for data assimilation: Assessment of over-ocean level 2 aerosol optical thickness retrievals, J. Geophys. Res., 111, D22 207, doi:10.1029/2005JD006898, 2006.

Zhang, J. and Reid, J. S.: A decadal regional and global trend analysis of the aerosol optical depth using a d ata-assimilation grade over-water MODIS and Level 2 MISR aerosol products, Atmos. Chem. Phys., 10, 10 949–10 963, doi:10.5194/acp-10-10949-2010, 2010.

Zhang, J., Reid, J., and Holben, B.: An analysis of potential cloud artifacts in MODIS over ocean aerosol optical thickness products, Geophys. Res. Lett., 32, L15803, doi:10.1029/2005GL023254, 2005.

Zhang, R., Khalizov, A. F., Pagels, J., Zhang, D., Xue, H., and McMurry, P. H.: Variability in morphology, hygroscopicity, and optical properties of soot aerosols during atmospheric processing, P. Natl. A. Sci., 105, 10 291, doi:10.1073/pnas.0804860105, 2008.

Zhao, T. X. P., Laszlo, I., Guo, W., Heidinger, A., Cao, C., Jelenak, A., Tarpley, D., and Sullivan, J.: Study of long-term trend in aerosol optical thickness observed from operational AVHRR satellite instrument, J. Geophys. Res., 113, D07 201, doi:10.1029/2007JD009061, 2008.

Zipser, E. J.: Deep Cumulonimbus Cloud Systems in the Tropics with and without Lightning, M. Weather Rev., 122, 1837–1851, doi:10.1175/1520-0493(1994)122⟨1837:DCCSIT⟩2.0.CO;2, 1994.

Zuidema, P., Westwater, E., Fairall, C., and Hazen, D.: Ship-based liquid water path estimates in marine stratocumulus, J. Geophys. Res., 110, D20206, doi:10.1029/2005JD005833, 2005.

Zuidema, P., Painemal, D., de Szoke, S., and Fairall, C.: Stratocumulus Cloud-Top Height Estimates and Their Climatic Implications, J. Climate, 22, 4652–4666, doi:10.1175/2009JCLI2708.1, 2009.

Appendix A

Changes in regime transition frequencies

This appendix includes plots repeating those in chapter 4, but using the ISCCP D1 cloud product and the GlobAerosol AATSR AOD product for the cloud and aerosol properties. It also includes a repeat of the analysis in chapter 4 including transitions to and from a 'clear-sky' regime.

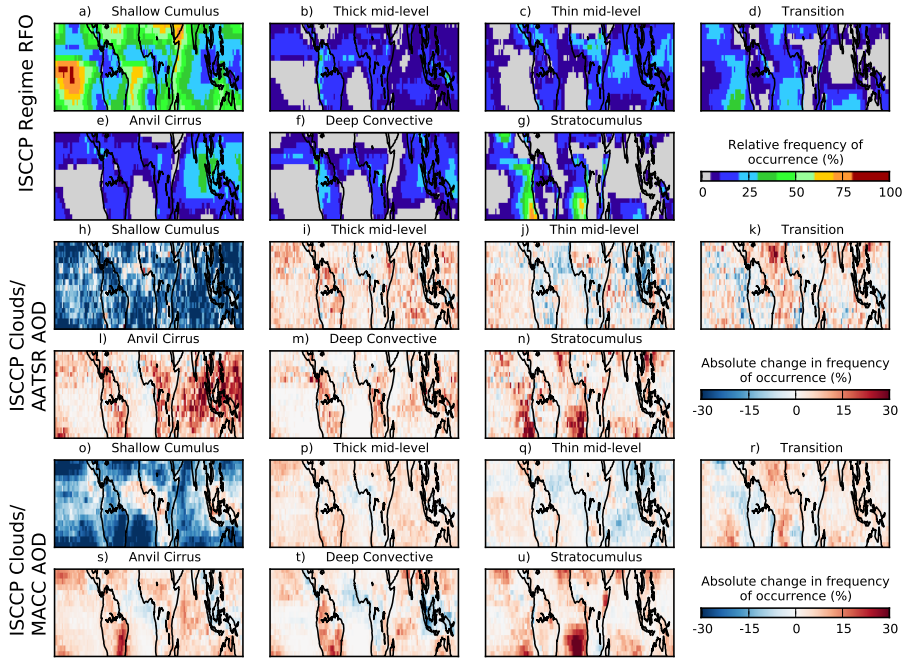

Figure A.1: a)Relative frequency of occurrence (RFO) of each of the ISCCP cloud regimes (Williams and Webb, 2009) from ISCCP (2003-2007). The RFO is defined such that the sum of the RFOs for all of the regimes is 100%. b) Shows the difference in frequency of occurrence of the regimes between the lowest and the highest GlobAerosol AATSR AOD quartiles. c) As b but using MACC AOD instead of AATSR AOD as the aerosol product.

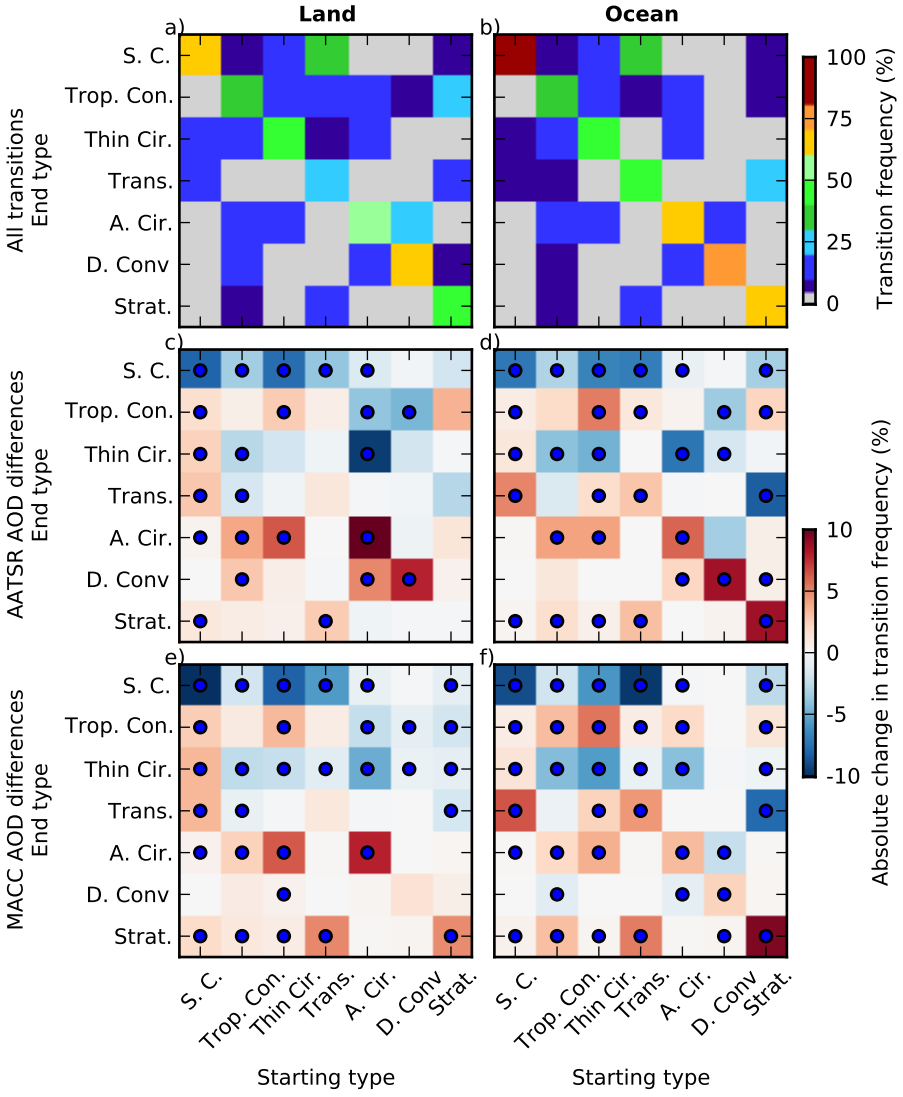

Figure A.2: Regime transition histogram showing the conditional probability of a given transitions between regimes over (a) land and (b) ocean during the three hour afternoon period being observed, given each starting regime. As such, each column sums to 100%. This plot covers regime transitions for the tropical region (20°N - 20°S). The difference in the histograms between the highest and lowest Globaerosol AATSR AOD quartile days over c) land and d) ocean, and using MACC AOD over e) land and f) ocean. Positive values indicate an increase in the frequency of the transition with increasing AOD. Note the non-linear colourbar in a) and b). The dots indicate statistical significance. The properties of the regimes used here are described in Williams and Webb (2009)

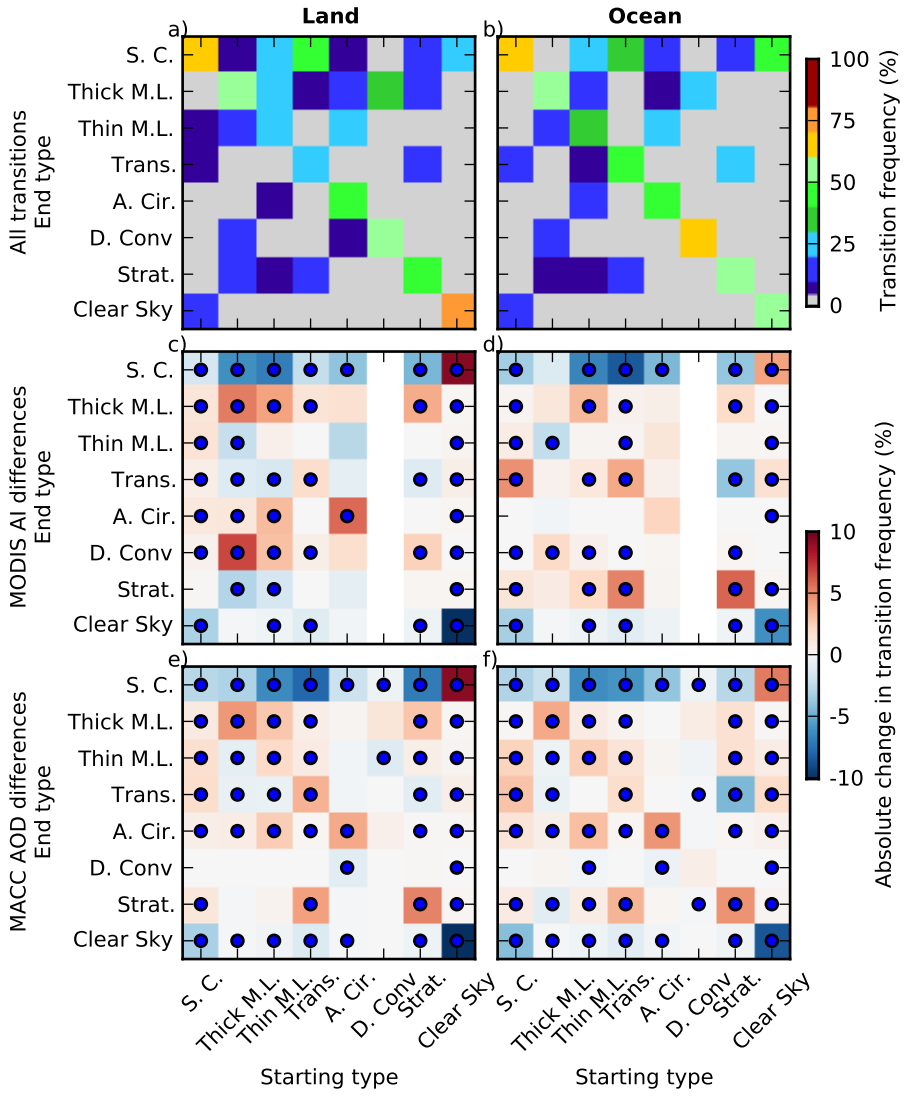

Figure A.3: As Fig. A.2 but using the MODIS AI, cloud regimes and a 'clear-sky' regime. The clear sky regime is defined at locations where MODIS finds a cloud fraction of zero, and so does not retrieve a cloud top pressure or cloud optical depth. Each column sums to 100 %. The 'clear-sky' regime has not had the influence of the AI-CF correlation accounted for, so the changes in transition frequency from the 'clear-sky' regime are not reliable. This plot covers regime transitions for the tropical region (20°N - 20°S). Positive values indicate an increase in the frequency of the transition with increasing AOD. Note the non-linear colourbar in a) and b). The dots indicate statistical significance.

Appendix B

Precipitation development

Additional satellite products

As the 3B42 retrieval includes some IR precipitation data, the analysis is repeated using the 3B42 HQ' product, which includes only the non-gauge adjusted microwave data (Fig. B.1).

This analysis is also repeated excluding points where the retrieved precipitation is zero (Fig. B.2). The analysis excluding non-precipitating points is not included in the main analysis, as it removes the ability to study the complete lifecycle of clouds. It shows a similar increase in precipitation after T+0 to that seen when using the complete 3B42 product, suggesting that the increase in precipitation is found in an increased precipitation rate for precipitating clouds, rather than a simple increase in precipitation initiation (although that is still likely to be important).

The precipitation development analysis repeated using GlobAerosol AATSR daily AOD data (Fig. B.3). As AATSR is flown on the Envisat satellite, T+0 is shifted to 1030 LST, making Fig. 5.3 the most suitable comparison. The plots using AATSR AOD are noisier than those using MODIS data, due to a smaller swath reducing the available data. Only the all data and the shallow cumulus regime precipitation development plots are shown.

To demonstrate that the observed increase in precipitation observed at times after T+0 for the high AI population is not a consequence of a reduced precipitation rate at times before T+0 in the high AI population, the precipitation development of each regime where the regimes are separated by the precipitation rate at T-3 is also shown (Fig. B.4). The red line shows the precipitation development within each regime of the quartile with the highest precipitation rate and the blue line in the lower precipitation rate quartile at T-3. It is clear that a low precipitation rate at times T-3 is not

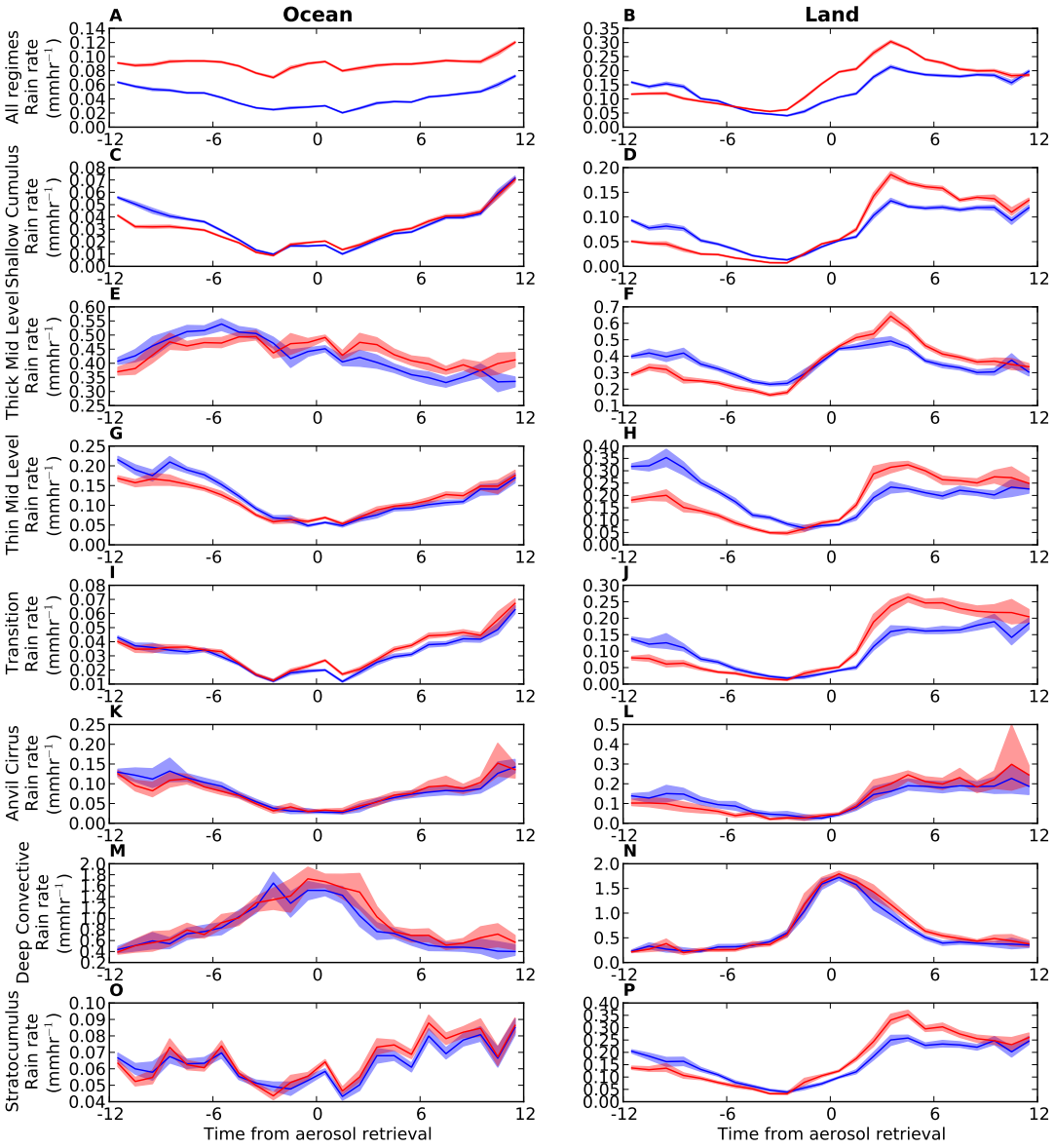

Figure B.1: As Figure 5.2 but using the 'HQ' product, which is restricted to the microwave precipitation retrievals.

correlated with a high precipitation rate at times after T+0. The CF distributions for the high and low precipitation rate quartiles have been sampled so that they are the same at T+0 (see section 4.1.2.

Surface precipitation

To compare these results against a 'ground-truth' precipitation product, precipitation retrievals from the UK Met. Office MIDAS database (UK Meteorological Office, 2012) are also used. This includes precipitation data from multiple rain-gauges at a time resolution of three hours or lower. The total

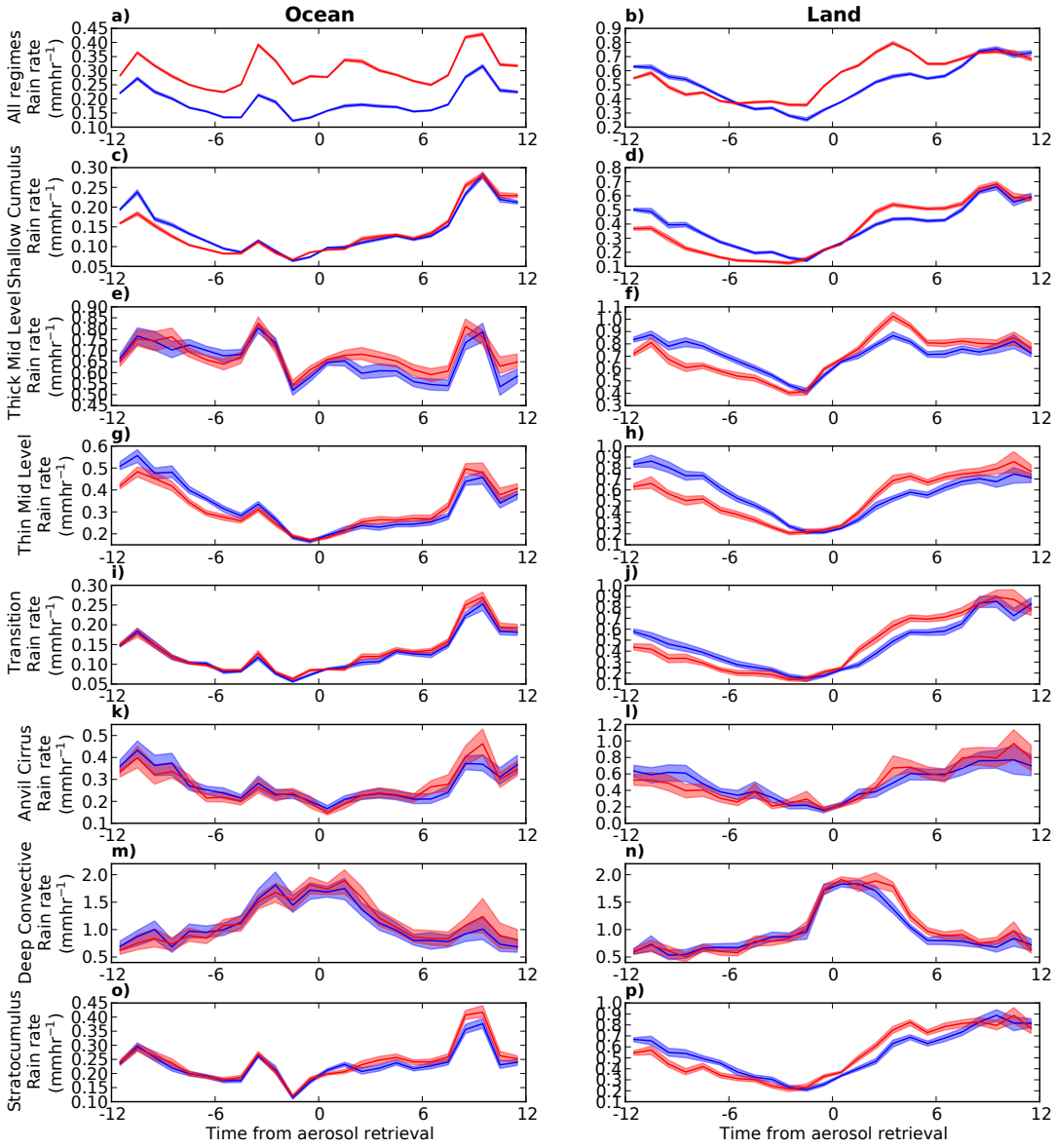

Figure B.2: As Figure 5.2 but restricting the precipitation retrievals used to only those where precipitation is detected by the 3B42 precipitation product.

number of sites available is restricted by the need to use a sub-daily temporal resolution, which is not commonly supplied in gauge datasets.

Both the TRMM PR and the merged product require assumptions about the droplet size distribution to determine the precipitation rate,especially over land (Iguchi and Meneghini, 1994; Stephens et al., 2008). As one possible effect of aerosols is to modify the droplet size distribution, an increase in retrieved precipitation is not necessarily due to a increased precipitation rate. A shift in the droplet size distribution towards larger droplets without an increase in the total precipitation amount could be interpreted by both active and passive microwave instruments as an increase in precipitation.

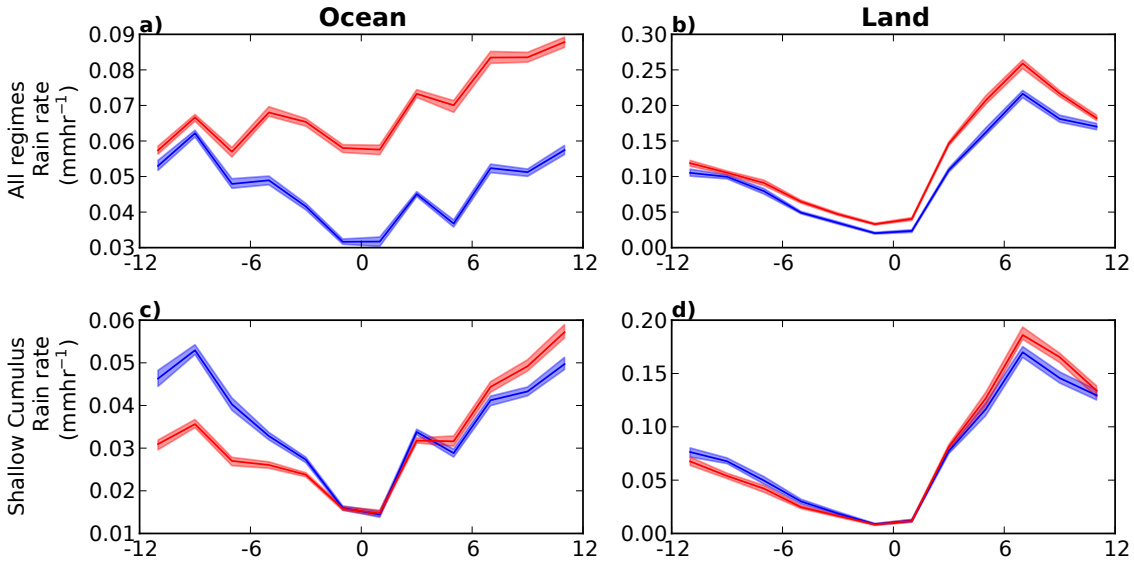

Figure B.3: As Figure 5.2 for the shallow cumulus regime and the regimes combined, but using the GlobAerosol AATSR AOD product over the years 2003-2007.

The only way to sure of an increase in precipitation is to use a surface measurement of precipitation. Unfortunately surface rain gauges are limited in their sampling compared to satellite instruments.

The UK Met Office MIDAS database of surface station data is used here, which includes surface data from the tropics, with precipitation data from a subset of stations at a temporal resolution of 3 or 6 hours. The data is averaged over three hour periods, rather than the single hour periods used for the merged precipitation product. Unfortunately, there is not enough rain gauge data available to make a determination about whether the satellite studies are seeing a change in surface precipitation. Although there are hints of effects, they are not significant.

The main issue appears to be the shortage of data for the rain gauges, ideally there would be a greater number of rain gauges than satellite datapoints so that the gauge data might be closer to the areal mean precipitation rate. The lack of sampling in regions with a particularly strong response in the satellite data (Fig. B.5a) is unfortunate.

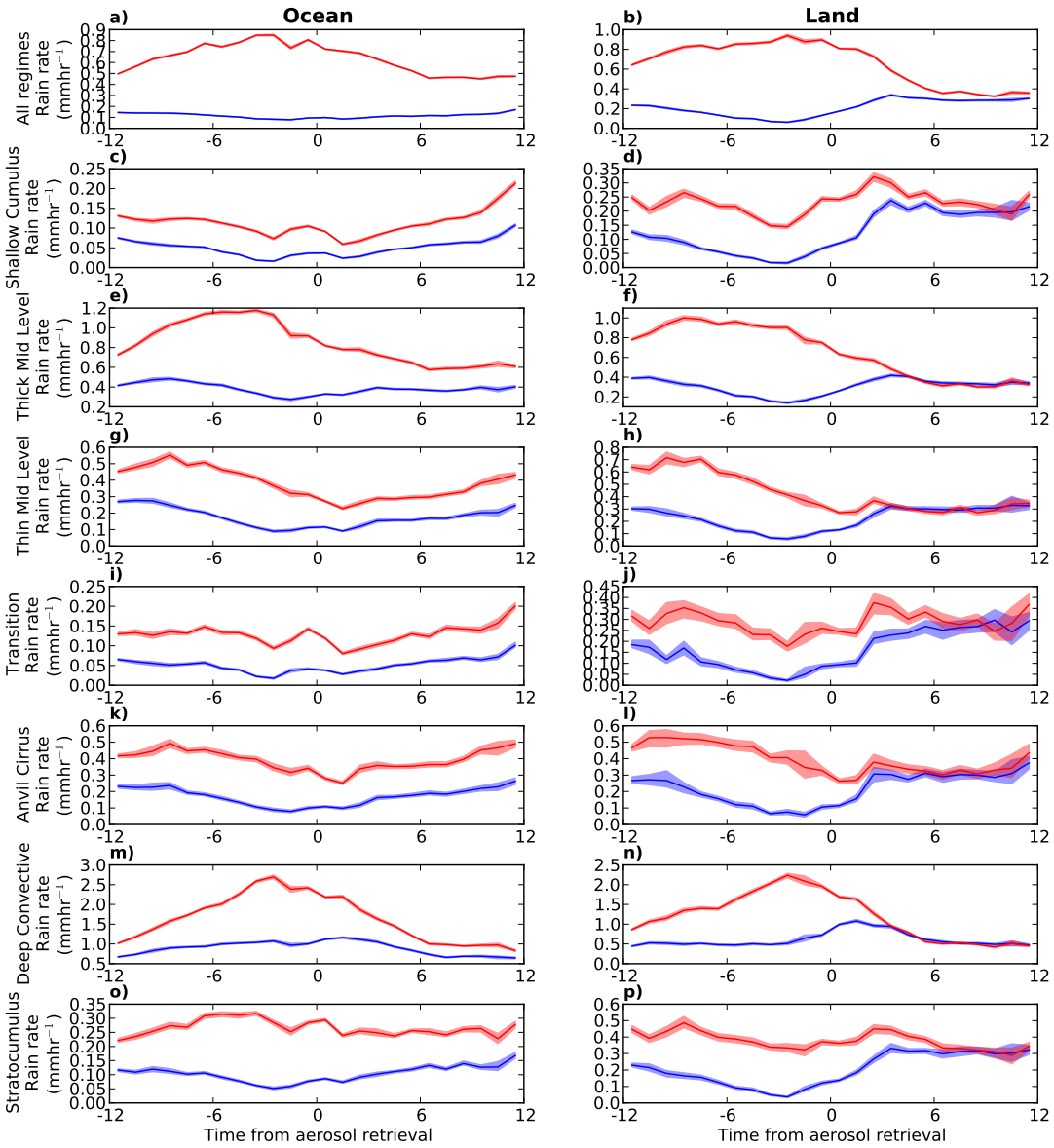

Figure B.4: As Figure 5.2 but using the precipitation rate at T-3 to define the high and low populations. The red line shows the precipitation rate of the highest quartile of precipitation rates at T-3 and blue the lowest quartile. The CF and meteorological property distributions are the same at T+0 for the high and low populations.

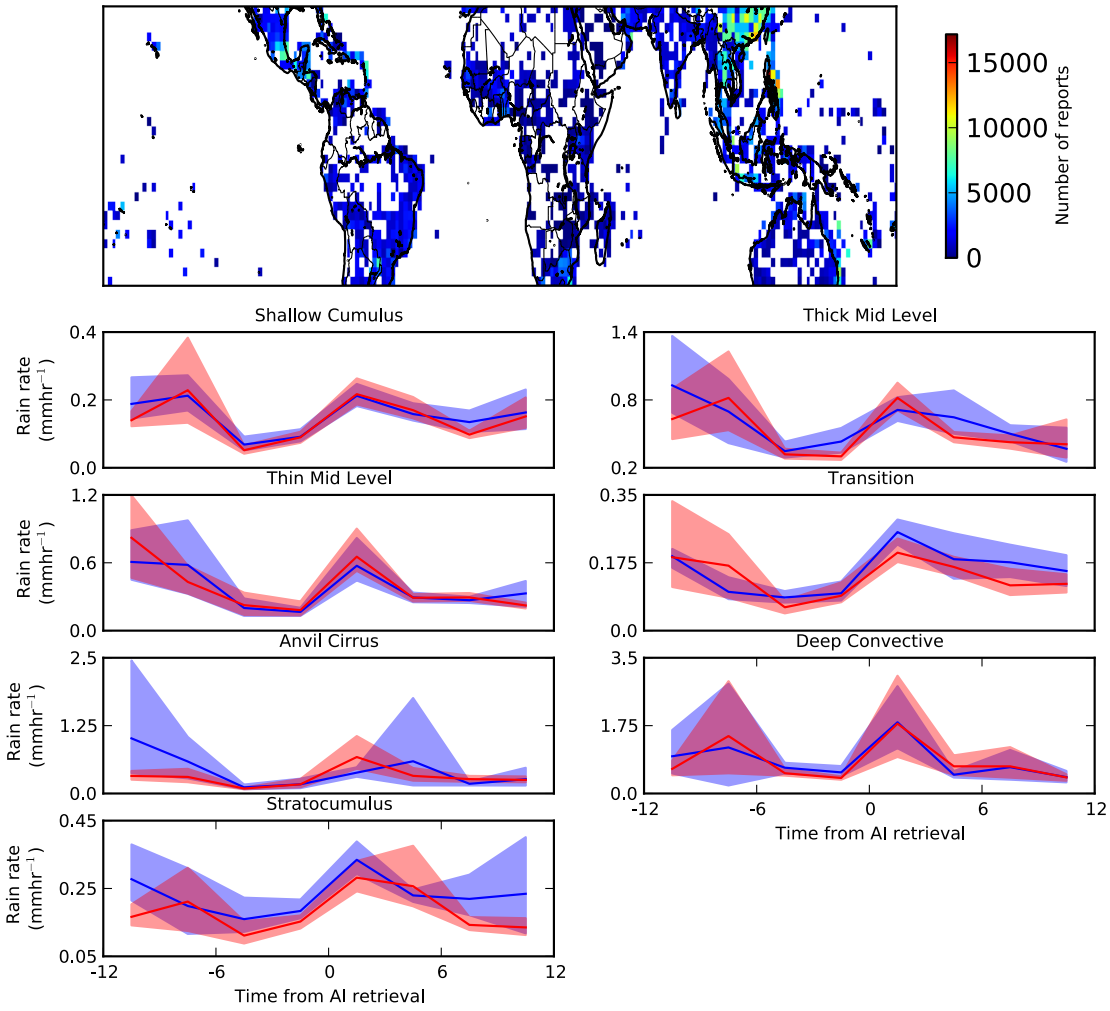

Figure B.5: a) The number of surface station precipitation reports over the period 2003-2011 from the UK Met. Office MIDAS database. For comparison, the 3B42 product would generate 12,000 reports per year for each of the 2° by 2° location shown here. b-h) Precipitation rates for each of the regimes at times before and after the Aqua MODIS AI retrieval (1330 LST). Red is the precipitation rate from the high AI population.